

Aus dem Institut für Bioinformatik  
*Direktor Univ.-Prof. Dr. Lars Kaderali*  
der Universitätsmedizin der Universität Greifswald

---

# Mathematical Modeling of Plus-Strand RNA Virus Replication

Inaugural – Dissertation

*zur*

Erlangung des akademischen Grades

Doktor der Wissenschaften in der Medizin

(Dr. rer. med.)

*der*

Universitätsmedizin

*der*

Universität Greifswald

2023

vorgelegt von: Zitzmann, Carolin  
geb. am: 19.01.1987  
in: Neuhaus am Rennweg



Dekan: Prof. Dr. Karlhans Endlich  
1. Gutachter: Prof. Dr. Lars Kaderali  
2. Gutachter: Prof. Dr. Marc Thilo Figge  
Ort, Raum: Greifswald, 0.52 C\_FunGene  
Tag der Disputation: 23. Oktober 2023



*Dedicated to my Grandpa*



## Abstract

Plus-strand RNA [(+)RNA] viruses are the largest group of viruses, medically highly relevant human pathogens, and are a socio-economic burden. The current global pandemic of the severe acute respiratory syndrome coronavirus 2 (SARS-CoV-2) shows how a virus has been rapidly spreading around the globe and that – without an antiviral treatment – virus transmission is solely dependent on human behavior. However, other (+)RNA viruses such as rhino-, noro-, dengue- (DENV), Zika, and hepatitis C virus (HCV) are constantly spreading and expanding geographically. As in the case of hepatitis C, since its first identification in the 1970s, it took more than 30 years to understand the HCV structure, genome organization, life cycle, and virus-host interplay leading to the cure of a chronic and life-threatening disease. However, no vaccination or antiviral treatment exists for most (+)RNA viruses. Consequently, a precise and comprehensive analysis of the viruses, their life cycles, and parasitic interactions with their hosts remains an important field of research.

In the presented thesis, we use mathematical modeling to study the life cycles of (+)RNA viruses. We analyze replication strategies of closely related (+)RNA viruses, namely HCV, DENV, and coxsackievirus B3 (CVB3), to compare their life cycles in the presence and absence of the host's immune response and antiviral drug treatment and consider different viral spreading mechanisms. Host dependency factors shape the viral life cycle, contributing to permissiveness and replication efficiency. Our mathematical models predicted that host dependency factors, such as ribosomes, and thus the virus' ability to hijack the host cell's translation machinery play an essential role in the viral genome replication efficiency. Furthermore, our mathematical model suggested that the availability of ribosomes in the viral life cycle is a crucial factor in disease outcome: the development of an acute or chronic disease. Even though the host developed strategies to attack the virus, e.g., by degrading the viral genome, blocking the viral protein production, and preventing viral spread, viruses found strategies to countermeasure those so-called host restriction factors derived from the immune system. Our mathematical models predicted that DENV might be highly effective in blocking the cell's attempts to recognize the invader. Moreover, we found ongoing HCV RNA replication even with highly effective antiviral drugs that block processes in the viral life cycle. Furthermore, we found alternative pathways of infection spread, e.g., by HCV RNA carrying exosomes, which may be a possible explanation for reported plasma HCV RNA at the end of treatment, found in a subset of patients.

Hence, the mathematical models presented in this thesis provide valuable tools to study the viral replication mechanism in detail. Even though being a simplification of reality, our model predictions confirm and explain known and suggest novel biological mechanisms. In the presented thesis, I will summarize and discuss key findings and contextualize model predictions in the broader scientific literature to improve our understanding of the viral dynamics and the virus-host interplay.





## Zusammenfassung

Plusstrang RNA [(+)RNA] Viren gehören zu der größten Virengruppe. Sie sind medizinisch höchst relevante Humanpathogene und eine starke Belastung für die Gesellschaft und die Wirtschaft. Die derzeitige globale Severe Acute Respiratory Syndrome Coronavirus 2 (SARS-CoV-2)-Pandemie zeigte, wie rasant sich ein Virus auf der Welt ausbreiten kann und dass die Virusverbreitung ohne antivirale Behandlung alleinig vom menschlichen Verhalten anhängig ist. Allerdings gibt es andere (+)RNA Viren, wie zum Beispiel Rhino-, Noro-, Dengue- (DENV), Zika- und das Hepatitis C Virus (HCV), welche sich ständig verbreiten und geografisch weiter ausbreiten. Wie im Falle von Hepatitis C brauchte es seit der Identifizierung in den 1970ern mehr als 30 Jahre, um die Struktur, Genomorganisation, Lebenszyklus und Virus-Wirts-Interaktion vom HCV zu verstehen, welches zu der Heilung einer chronischen und lebensbedrohlichen Krankheit geführt hat. Für die meisten (+)RNA Viren gibt es jedoch keinen Impfstoff oder medikamentöse Behandlung. Eine genaue und umfangreiche Analyse der Viren, ihrer Lebenszyklen und parasitäre Interaktion mit dem Wirt ist daher ein wichtiger Forschungsbereich.

In der von mir vorgestellten Dissertation wenden wir mathematische Modelle an, um die Lebenszyklen von (+)RNA Viren zu studieren. Wir analysieren Replikationsmechanismen von nahe verwandten (+)RNA Viren wie HCV, DENV und Coxsackievirus B3 (CVB3) und vergleichen deren Lebenszyklen in An- und Abwesenheit der Wirtsimmunantwort, antiviralen Behandlungsmöglichkeiten und berücksichtigen verschiedene virale Verbreitungsmechanismen. Zelluläre Wirtsfaktoren tragen zu Zellpermissivität und Replikationseffizienz in vielen viralen Lebenszyklen bei. Unsere mathematischen Modelle sagten vorher, dass Wirtsfaktoren, wie zum Beispiel Ribosomen und damit die virale Fähigkeit, die zelluläre Translationsmaschinerie zu übernehmen, eine wesentliche Funktion in der Replikationseffizienz des Virusgenoms annehmen. Außerdem zeigten unsere Modelle, dass die Verfügbarkeit von Ribosomen im Lebenszyklus der Viren eine ausschlaggebende Rolle im Krankheitsausgang spielen kann: die Entwicklung einer akuten oder chronischen Erkrankung. Auch wenn der Wirt Strategien zur Bekämpfung des Virus entwickelt hat, zum Beispiel durch Abbau des Virusgenoms, durch die Blockierung der viralen Proteinproduktion und Verhinderung der Virusverbreitung, fanden die Viren Strategien, um diese vom Immunsystem produzierten inhibierenden Wirtsfaktoren entgegenzuwirken. Unsere entwickelten Modelle sagten vorher, dass DENV höchst effizient den Versuch der Zelle, den Eindringling zu erkennen, blockiert. Außerdem fanden wir, dass auch mit effektiven antiviralen Medikamenten, welche die Prozesse im viralen Lebenszyklus blockieren, die HCV RNA Replikation nicht gestoppt wird. Wir fanden zudem eine alternative Route der Virusverbreitung, zum Beispiel durch Exosomen, die HCV RNA in sich tragen. Diese könnten eine mögliche Erklärung für die berichtete Plasma HCV RNA zu Behandlungsende bei einigen Patienten sein.

Die präsentierten mathematischen Modelle in meiner Dissertation bieten wertvolle Werkzeuge, um die viralen Replikationsmechanismen im Detail zu studieren. Auch wenn die vorgestellten Modelle die Realität stark vereinfachen, haben diese bekanntes Wissen bestätigt und neue biologische Mechanismen vorhergesagt. In der von mir vorgelegten Dissertation werde ich die wichtigsten Ergebnisse zusammenfassen und diskutieren und unsere Modellvorhersagen in die breitere wissenschaftliche Literatur kontextualisieren, um zum Verständnis der Virusdynamiken und Virus-Wirts-Interaktionen beizutragen.



# Contents

<b>Contents</b>	<b>ix</b>
<b>List of Figures</b>	<b>xi</b>
<b>List of Abbreviations</b>	<b>xiii</b>
<b>1 INTRODUCTION</b>	<b>1</b>
<b>2 BIOLOGICAL BACKGROUND</b>	<b>5</b>
2.1 Virus structure and genome organization . . . . .	5
2.2 Plus-strand RNA virus life cycle . . . . .	6
2.3 Host factors . . . . .	10
2.4 Immune response to viral infection . . . . .	11
2.5 Antiviral treatment . . . . .	16
<b>3 MATERIALS AND METHODS</b>	<b>21</b>
<b>4 RESULTS</b>	<b>23</b>
4.1 Article I: Plus-strand RNA virus replication . . . . .	23
4.2 Article II: Dengue virus replication and host cell response . . . . .	24
4.3 Article III: Hepatitis C replication, exosome secretion, and virus release . . . . .	25
<b>5 DISCUSSION</b>	<b>27</b>
5.1 Virus replication and host factors . . . . .	28
5.2 The intrinsic immune response to viral infection . . . . .	30
5.3 The controversy of exosomes . . . . .	31
5.4 Broad-spectrum antivirals . . . . .	32
5.5 Limitations and outlook . . . . .	33
<b>6 CONCLUSION</b>	<b>35</b>
<b>PUBLICATIONS</b>	<b>37</b>
Literature review: Viral replication dynamics models . . . . .	37
Article I: Plus-strand RNA virus replication . . . . .	56
Article II: Dengue virus replication and host cell response . . . . .	95
Article III: Hepatitis C replication, exosome secretion, and virus release . . . . .	115
<b>APPENDIX</b>	<b>143</b>
Supplementary material . . . . .	143
Eidesstattliche Erklärung . . . . .	144
<b>REFERENCES</b>	<b>145</b>



# List of Figures

2.1	Virus structure and genome organization . . . . .	6
2.2	Plus-strand RNA virus life cycle . . . . .	9
2.3	Immune defense systems . . . . .	12
2.4	Intrinsic immune response pathways . . . . .	14



# List of Abbreviations

(+)RNA	Plus-strand RNA
ABM	Agent-based model
ADE	Antibody-dependent enhancement
AIR	Adaptive immune response
COVID-19	Coronavirus disease 2019
CTL	Cytotoxic T lymphocytes
CVB3	Coxsackievirus B3
DAA	Direct-acting antiviral
DAMP	Damage-associated molecular pattern
DC	Dendritic cells
DHF	Dengue hemorrhagic fever
DMV	Double membrane vesicle
dsRNA	double stranded RNA
DSS	Dengue shock syndrome
DENV	Dengue virus
EV	Extracellular vesicle
HAV	Hepatitis A virus
HBV	Hepatitis B virus
HCV	Hepatitis C virus
HIV	Human immunodeficiency virus
hpi	hours post infection
IFIT	IFN-induced protein with tetratricopeptide repeats
IFN	Interferon
Ig	Immunoglobulin
IIR	Innate immune response
IL	Interleukin
IRES	Internal ribosomal entry site

IRF	Interferon-regulatory factors
ISG	Interferon-stimulated genes
JAK	Janus kinase
LGP2	Laboratory of genetics and physiology 2
MAPK	Mitogen-activated protein kinases
MAVS	Mitochondrial antiviral signaling protein
MDA5	Melanoma differentiation-associated antigen 5
MERS-CoV	Middle east respiratory syndrome coronavirus
MHC	Major compatibility complex
mRNA	messenger RNA
NK	Natural killer cells
NK- $\kappa$ B	Nuclear factor $\kappa$ -light-chain-enhancer of activated B cells
NOD	Nucleotide-binding oligomerization domain-containing
NLR	NOD-like receptors
NS	Non-structural
OAS	2'-5'-oligoadenylate synthase
ODE	Ordinary differential equation
ORF	Open reading frame
PAMP	Pathogen-associated molecular pattern
PDE	Partial differential equation
peg-IFN	pegylated interferon
PI4K	phosphatidylinositol 4-kinases
PRR	Pattern-recognition receptors
rER	rough endoplasmic reticulum
RIG-I	Retinoic acid-induced gene I product
RNAi	RNA interference
RLR	RIG-I like receptors
RO	Replication organelle
SARS-CoV-1	Severe acute respiratory syndrome coronavirus 1
SARS-CoV-2	Severe acute respiratory syndrome coronavirus 2
siRNA	small interfering RNA
SMV	Single membrane vesicle
ssRNA	single stranded RNA
STAT	Signal transducer and activator of transcription



---

STING	Stimulator of IFN genes
SVR	Sustained virologic response
TH	T helper cells
TLR	Toll-like receptors
TNF $\alpha$	Tumor necrosis factor $\alpha$
vRNA	viral RNA



Plus-strand RNA [(+)RNA] viruses are the largest group of viruses consisting of eight virus families – *Astro-*, *Arteri-*, *Calci-*, *Corona-*, *Hepe-*, *Flavi-*, *Picorna-* and *Togaviridae* –, which differ in their characteristics of viral genes, polyprotein(s), and viral envelope existence. One key feature of (+)RNA viruses is the self-initiation of translation; hence, the viral RNA (vRNA) genome serves as messenger RNA (mRNA) and synthesizes one or more viral polyproteins, which are subsequently cleaved into viral proteins [115].

(+)RNA viruses cause seasonal and non-seasonal infections and caused multiple infectious disease outbreaks in the past. For example, human rhinoviruses of the family *Picornaviridae* are responsible for 40% of acute respiratory tract infections and cause annually one to three common cold-like infections per individual [115]. Re-emerging viruses such as the Zika virus, a member of the family *Flaviviridae*, caused a large outbreak in Brazil and other countries from 2015 to 2016, with more than 940,000 infections in The Americas alone from 2015 until today (as of April 2023) [128, 51]. Newly emerging viruses have been an additional human health concern. For example, the severe acute respiratory syndrome coronavirus 1 (SARS-CoV-1) caused an outbreak in 2003 in China with 8,098 infections and 774 deaths. Another example is the Middle East respiratory syndrome coronavirus (MERS-CoV), which has been causing infections in 27 countries, with the largest outbreak in the United Arab Emirates, Saudi Arabia, and the Republic of Korea, with 2,494 infections and 858 MERS-related deaths since 2012 [177]. Since 2019, a new SARS-coronavirus strain (SARS-CoV-2) has been spreading around the globe. It has been responsible for more than 670 million confirmed coronavirus disease (COVID-19) cases and more than 6.8 million deaths (as of April 2023) [38, 169]. Coronaviruses are zoonotic viruses, having their natural reservoir in animals, and were passed from animals to humans; civet cats and raccoon dogs in the case of SARS-CoV-1 [23] or dromedary camels in the case of MERS-CoV [8]. The zoonotic origin of SARS-CoV-2 is yet not fully understood. However, pangolins and bats are speculated to be the origin of animal-to-human transmission [34, 174].

Those annual virus infections and new or re-emerging outbreaks have been a health concern in the past and may represent a human health threat in the future due to increasing globalization, air travel, and climate change. Three representatives of (+)RNA viruses were of significant interest for this thesis, namely hepatitis C virus (HCV), dengue virus (DENV), and coxsackievirus B3 (CVB3).

**Hepatitis C virus:** HCV is one of the best-studied (+)RNA viruses belonging to the family *Flaviviridae* and genus *Hepacivirus*. HCV is transmitted through blood, e.g., HCV-contaminated blood transfusion or insufficient sterilized or unsterilized and re-used injection devices in health care. Moreover, 23% of new HCV infections are caused by drug use, while tattooing, body piercing, and sexual transmission may also occur less frequently [127]. Once infected, the blood-borne HCV usually causes asymptomatic acute hepatitis C. If untreated, it may develop into a chronic disease with life-threatening liver cirrhosis and, ultimately, hepatocellular carcinoma. It is estimated that 15 – 45% of HCV-positive patients clear the infection spontaneously without treatment, while 55 – 85% of untreated HCV-positive patients develop chronic disease. In 2015, 1% of the world population (71 million) was living with chronic hepatitis C, with 1.75 million new infections. With the development of direct-acting antivirals (DAA), hepatitis C can be cured in more than 95% of cases [127, 133, 130].

**Dengue virus:** DENV is a rapidly spreading mosquito-borne virus belonging to the *Flaviviridae* family with the *Flavivirus* genus. Within the past 50 years, the dengue incidence has increased 30-fold, with approximately 50 – 100 million dengue infections annually. Infection with DENV causes a flu-like acute disease but is occasionally associated with severe dengue symptoms such as dengue hemorrhagic fever (DHF) or dengue shock syndrome (DSS). The fatality rate of dengue infections is between 1% and 5% but with proper treatment below 1% [145]. Once the infection is cleared, it provides a serotype-specific, lifelong immunization. Subsequent infections with another serotype, however, may then result in severe dengue disease. Treatment options are limited to symptomatic ailment. No antiviral treatment is available against DENV, and a recently approved vaccine showed only limited efficacy [126].

**Coxsackievirus B3:** CVB3 of the family *Picornavirus* and genus *Enterovirus* is transmitted from human to human. Due to fecal-oral transmission, symptoms are often flu-like, associated with fever, sore throat, and gastroenteritis. However, CVB3 also targets cardiac tissue and is the leading cause of viral myocarditis. However, CVB3 may also replicate in pancreas cells leading to pancreatitis and diabetes-like diseases [138]. Acute infection with the mainly cardiotropic CVB3 leads to viral myocarditis, pericarditis, and – in the worst case – sudden death. Furthermore, a CVB3 infection may persist and possesses the ability to develop chronic heart failure [53, 147]. There is no antiviral treatment available for a CVB3 infection [53].

Despite being related, with variations in their key features, such as transmission routes, cellular tropism, and clinical manifestations, (+)RNA viruses share remarkable similarities in their viral replication mechanisms. For example, following virus internalization with subsequent genome release into a susceptible cell, the viral RNA genome serves as mRNA, which is translated into a polyprotein that is co- and post-translationally cleaved into viral proteins. A subset of viral proteins initiate intracellular membrane rearrangements and form replication organelles (ROs) which serve as a protective and favorable environment for viral RNA amplification. Those ROs are the hallmark of the (+)RNA virus life cycle, contain high concentrations of components necessary

---

for viral RNA synthesis, and hide viral genomes from potential intracellular immune recognition and degradation [157, 115].

Experimentally, studying the viral life cycle in detail and quantifying intracellular processes is challenging; e.g., the need for a reliable *in vitro* cell culture system is one of many hurdles [105]. Especially the quantitative characterization and comparison of the life cycles of different (+)RNA viruses may not yet be experimentally feasible. Therefore, we aimed to quantify pan-viral similarities, identify components the viruses critically depend on, and evaluate possible broad-spectrum treatment strategies. Mathematical modeling and systems biology are helpful tools to study and quantify the virus-host interplay and may contribute to understanding the circumstances leading to viral clearance, i.e., cure or complications.

Early mathematical models based on the growth of one population, simplified interactions of two populations, or one single biochemical process [83, 179, 93], e.g., the famous enzyme kinetics equation published by Leonor Michaelis and Maud Leonora Menten in 1913 [83]. Considering the experimental and computational limitations at that time, the field of mathematical biology developed into a considerable part of medical and political decision-making more than 100 years later during the global pandemic of COVID-19. The most prominent model that studies viral dynamics is the target cell limited model. This simple population-based model has been successfully applied to a plethora of viruses such as HCV, human immunodeficiency virus (HIV), Zika, dengue, ebola, and influenza A virus [188].

However, modeling the intracellular life cycle of viruses in detail remains an exception, and the knowledge about intracellular viral kinetics is limited [188]. Therefore, we dedicated our research to contribute to the understanding of intracellular viral dynamics. Our main questions addressed pan-viral similarities and virus-specific differences in the life cycles of selected (+)RNA viruses, as well as the dependency of viruses on cellular co-factors determining or restricting viral replication efficiency. We were further interested in perturbations of the viral life cycles by the immune response and antiviral drug intervention, with a particular interest in studying the feasibility of broad-spectrum antiviral treatment strategies.

Following this introduction, I present a biological background in chapter 2, including virus structure and genome organization, a detailed description of the (+)RNA virus life cycle and involved host cell dependency or restriction factors, as well as the immune response to viral infection and antiviral treatment strategies. Subsequently, I will give a short overview of modeling techniques in chapter 3. In chapters 4 and 5, I will present and discuss our key findings and model predictions, followed by a conclusion in chapter 6.



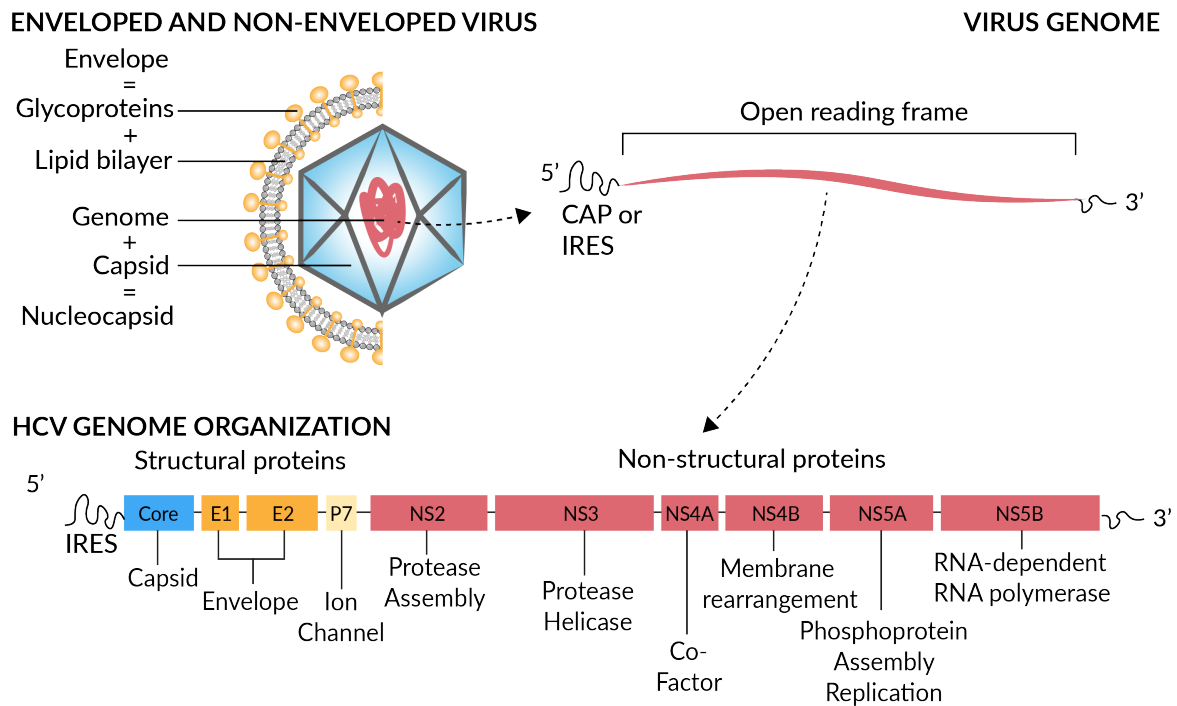
## 2.1 Virus structure and genome organization

The particles of (+)RNA viruses are 30 to 180 nm in diameter and may be categorized by the existence of a viral envelope (non-enveloped are 28 – 39 nm versus enveloped 40 – 180 nm in diameter). While *Flavi-*, *Toga-*, *Arteri-*, and *Coronaviridae* are enveloped, members of the *Picorna-*, *Astro-*, *Calci-*, and *Hepeviridae* families do not possess a viral envelope. The viral envelope is a lipid-bilayer membrane – derived from the host cell membrane – and contains membrane proteins and glycoproteins responsible for viral attachment to a susceptible cell (Figure 2.1). Regardless of a viral envelope, all viruses possess a protein coat, the nucleocapsid, that protects the vRNA genome and viral proteins. However, non-enveloped viruses attach to a susceptible cell with proteins in the nucleocapsid [47, 115, 49].

The genome of (+)RNA viruses is single-stranded RNA of positive polarity that is ribosome ready and, thus, possesses the same polarity as mRNA. The vRNA genome is 6,800 to 32,000 nucleotides long and possesses one or more coding regions or open reading frames (ORF) for all viral proteins. Additionally, (+)RNA viruses are categorized by possessing a 5'-cap structure, which functions similarly to eucaryotic mRNA as a ribosomal binding site. However, *Picornaviridae* and some *Flaviviridae* do not possess the 5'-cap; rather than an internal ribosomal entry site (IRES) that serves the same functionality independent of the 5'-cap structure. Mutations in IRES influence the ability to get translated and determine infectivity and the ability to replicate. The viral genome consists of non-structural and structural proteins; and accessory proteins, as in the case of *Coronaviridae*. Non-structural (NS) proteins have various tasks in the virus life cycle, e.g., polyprotein cleavage (enzymatic activity), intracellular membrane rearrangements, and the viral genome synthesis mediated by the RNA-dependent RNA polymerase. Structural proteins are packaged together with the viral genome into virions, forming the capsid and the envelope (if existing). The accessory proteins are not necessary for replication but virus-host interactions and infectivity. However, their functions are mostly unknown [47, 115, 49].

## 2. BIOLOGICAL BACKGROUND

Figure 2.1: Schematic structure of an enveloped and non-enveloped virus, a capped and non-capped viral genome consisting of one open reading frame, and the HCV genome organization coding for structural and non-structural proteins with its primary functions.



## 2.2 Plus-strand RNA virus life cycle

Despite their varying clinical manifestation, (+)RNA viruses share similarities in their viral replication strategy. The (+)RNA virus life cycle can be summarized in eight main steps: (1) Viral attachment to surface receptors of a susceptible cell, (2) internalization of the virus, (3) fusion of the viral and host cell membrane leading to the release of the viral genome, (4) translation of vRNA into one or more polyprotein(s) that are subsequently cleaved into viral proteins, (5) formation of ROs and vRNA replication within the ROs, (6) assembly of viral proteins and the viral genome to virions, (7) maturation of the virions, and subsequent (8) secretion of the newly produced virus (Figure 2.2) [115].

**Attachment:** The virus attaches to the surface receptors of a susceptible cell. The virus uses different host cell receptors for entry depending on the host cell tropism and the viral surface proteins. In the case of HCV, envelope glycoproteins (E1 and E2), apolipoproteins (apoE and apoC), and other viral surface proteins bind to CD81 and scavenger receptor class B member 1 (SR-B1) at hepatocytes [151, 109]. All picornaviruses use host cell receptors of the immunoglobulin superfamily for entry. For example, CVB3 uses the coxsackievirus adenovirus receptor (CAR) and co-receptor CD55 (also known as decay accelerating factor). The latter receptor protects cells from lysis by the immune system, such as the complement system [115, 53]. In the case of DENV, several receptor candidates have been found to mediate virus entry, such as heparan sulfate, the adhesion molecule of dendritic cells (DC-SIGN), and the mannose receptor of



macrophages. However, a specific receptor has not been identified [33]. Interestingly, DENV may use a second way of host cell attachment: virus-specific antibodies and non-neutralizing cross-reacting immunoglobulins. In the presence of antibodies and immunoglobulins, antibodies bind to virus-serotype-specific epitopes or the DENV envelope (E) protein of other serotypes. While virus-serotype-specific binding leads to viral degradation, the binding to other serotypes leads to viral infection; the Fc portion of immunoglobulins may mediate viral entry and infection in Fc $\gamma$  receptor-expressing cells, e.g., monocytes and macrophages [115, 180].

**Internalization:** The subsequent virus internalization is mediated by the tight-junction factors claudin-1, occludin, and possibly other molecules, such as claudin-6 and -9, and the epidermal growth factor receptor (EGFR) and results in clathrin-dependent endocytosis as in the case of HCV [151, 109]. The internalization of DENV depends on the cell type, DENV serotype, and virus strain. DENV uses clathrin-dependent pathways for internalization in most cell lines, such as A549, Huh7, and HeLa cells. However, non-classical dynamin-dependent endocytosis, independent of clathrin and lipid rafts, has also been described as in the case of the Vero cell line [33]. While CVB3 internalizes via clathrin-dependent endocytosis, the dynamin dependence for CVB3 may be strain-specific [29, 74].

**Fusion:** The late virus uptake step is associated with viral and endosomal membrane fusion and the release of the viral nucleocapsid into the cytosol. ATP-dependent proton pumps are common to HCV, DENV, and CVB3, anchored in the endosome membrane, and mediate acidification within the endosome. However, little is known about the uncoating process that leads to the viral genome release into the cytoplasm [115]. In DENV, it has been found that upon internalization, uncoating is mediated by a ubiquitination process, which inhibition leads to protected vRNA within the endosome, suggesting that ubiquitination is a crucial step [20]. For picornaviruses, however, the uncoating process has been heavily studied. The viral capsid undergoes structural rearrangement leading to the formation of pores that serve as releasing points of the viral RNA genome into the cytoplasm [115].

**vRNA translation:** The following step is associated with protein translation and polyprotein synthesis. Compared to cellular mRNA, the viral (+)RNA genome of *Flaviviridae* and *Picornaviridae* is not capped, which is crucial for correct ribosome binding. Nonetheless, the viral RNA genome possesses an IRES structure that serves as ribosome binding and translation initiation site. Upon correct binding of the ribosomal units, the whole polyprotein is synthesized and co- and post-translational processed by viral and host proteases [115]. However, in the case of *Coronaviridae*, the viral (+)RNA genome possesses a cap structure that serves as a ribosomal binding sites. Coronaviruses possess at least six ORFs, which give rise to multiple polyproteins [139]. For example, SARS-CoV-1 has two large ORFs for the non-structural viral proteins involved in replication and several small ORFs for structural proteins associated with virus assembly and accessory proteins, which are unnecessary for replication but virus-host interaction like immune system modulation [104]. Polyprotein synthesis is associated with ribosomal frameshifts, skipping the stop codons, and synthesizing all proteins [115].

## 2. BIOLOGICAL BACKGROUND

---

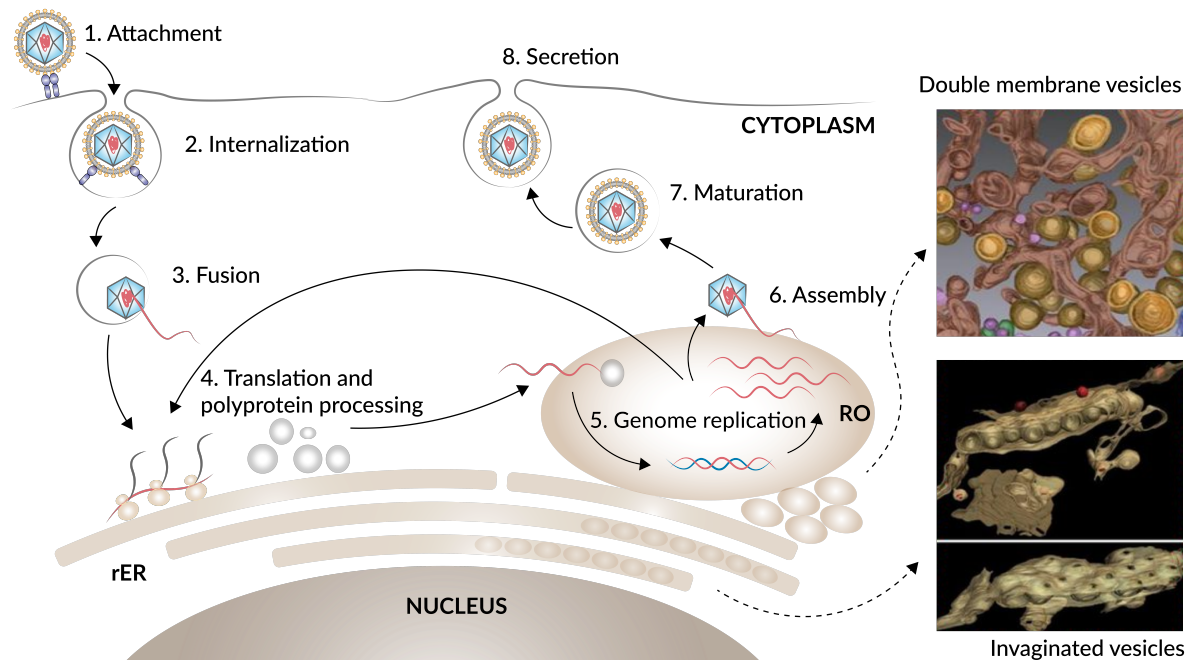
**vRNA replication:** As soon as the non-structural proteins are available, intracellular remodeling events are initiated to establish ROs and, thus, a favorable environment for vRNA synthesis and replication (see BOX 1 for more details). Within the ROs, the viral (+)RNA genome is synthesized into multiple copies mediated by the RNA-dependent RNA polymerase, which is probably the most essential non-structural viral protein. The viral (+)RNA genome is used for complementary negative-strand synthesis to generate an intermediate double-strand RNA molecule that serves as a template to produce multiple copies of the viral (+)RNA genome. As in the case of *Picornaviridae*, five to eight (+)RNA copies are synthesized from one (-)RNA molecule leading to an average amount of 5 to 10% of (-)RNA molecules of the total intracellular vRNA amount. The newly synthesized (+)RNA molecules can either be used for vRNA translation in the cytoplasm or virus packaging [115].

### BOX 1: REPLICATION ORGANELLES

(+)RNA viruses remodel the architecture of an infected cell by forming replication organelles, which serve as a favorable environment with high concentrations of viral RNA, proteins, and nucleotides for efficient viral genome replication. Derived from host membranes, such as the rough endoplasmic reticulum (rER) and Golgi (or peroxisomes, endosomes, mitochondria, plasma membrane), ROs represent a barrier to the cytosol and shield viral components from degradation and the host's immune response [157]. However, within the group of (+)RNA viruses, two distinct, evolutionary conserved classes of ROs have been found: invagination/spherule-type and protrusion-type vesicles such as single, double, and multi-membrane vesicles (SMV/DMV/MMV) and multi-membrane tubes, which appear in a time-dependent manner [120, 15]. It is believed that in the case of invaginations, viral genome replication occurs on the inner membrane surface within the RO connected with the cytosol through a pore that exchanges nucleotides and newly synthesized vRNA [15]. In DENV and Zika virus, the vRNA genome replicates in invaginated vesicles, derived from the rER, and is transported to the opposite side of the pore, where the virions bud. However, the protrusion-type ROs carry their replication machinery on the external membrane surface, thus facing the cytoplasm [15]. Multiple ROs form a tight membranous web, which is further associated with the sites of virion assembly, as in the case of HCV [65]. Especially in the case of Picornaviruses, e.g., poliovirus or CVB3, different RO structures occur at different time points: 2-3 hours post-infection (hpi) tubular SMVs probably derived from the Golgi dominate, four hpi DMV occur, and with an increasing number of DMVs, SMVs disappear [65].

**Assembly:** The production of infectious viruses includes correct virus packaging and maturation for successful infectivity spread. The self-assembly process starts as soon as sufficient structural proteins and vRNA are available. Viral capsid proteins shell around the nucleocapsid, forming the capsomere, while cell membrane and glycoproteins form the envelope. For example, in non-enveloped enteroviruses of the family *Picornaviridae*, the three structural proteins VP0, VP1, and VP3 form a promoter, five promoters form a pentamer, and 12 pentamers assemble to the capsid. The structural proteins assemble around the viral genome, or the capsid is genome-free, and the viral genome is inserted, resulting in the nucleocapsid [156]. As in the case of *Flaviviridae*, virus

Figure 2.2: Schematic illustration of the plus-strand RNA virus life cycle as an example of an enveloped virus. (1) The plus-strand RNA virus attaches to the surface of a susceptible cell. (2 – 3) The virus internalizes and releases its genome into the cytoplasm. (4) The viral genome is translated into a polyprotein that is cleaved into viral proteins. (5) A subset of viral proteins mediates the formation of replication organelles (RO) derived from the rough endoplasmic reticulum (rER). Within replication organelles, the viral genome is replicated. (6 – 8) The newly synthesized viral genome is packaged into virions that mature and are released from the cell. Electron tomography and 3D reconstructions for double membrane and invaginated vesicles are shown as examples of replication organelles (RO) (taken from [25]).



assembly occurs close to the membrane of the rER and, thus, close to ROs [49, 47, 95]. As an enveloped virus, HCV recruits structural proteins, such as the Core protein, to sites of cytosolic lipid droplets. The Core proteins coat the lipid droplet surface and encapsidate the viral genome.

**Maturation:** Newly packaged virions are non-infectious and mature into infectious virus particles by rearrangement and cleavage processes of the capsid. In DENV, the E proteins are glycosylated, and the enzyme furin mediates PrM into M protein cleavage, which is associated with the transport through the Golgi apparatus. E and PrM dissolve, and E forms heterodimers leading to mature virus particles. In enteroviruses, VP0 is a precursor protein that is cleaved into VP2 and VP4 to mature into the infectious virus [115, 49]. In HCV, virions assemble on the ER membrane but mature within the ER lumen, where the virus receives its envelope, glycoproteins (E1 and E2), and apoE, increasing HCV infectivity [95].

**Secretion:** In the case of *Flaviviridae*, the mature virus particles fuse with the cytoplasmic membrane and release the virus [115]. *Picornaviridae* release virions by cell lysis [53]. However, it becomes increasingly evident that virions are released pre-lytic as extracellular vesicles [171].

### 2.3 Host factors

Successful viral infection depends on the viral ability to actively reprogram and gain control over the host cell in order to support viral replication and escape the host's control mechanisms, which suppresses efficient viral replication. Due to the limiting viral coding capacity, viruses hijack cellular components such as membranes, proteins, lipids, and metabolites – so-called host factors – for their benefit.

Host factors are essential for all steps in the (+)RNA life cycle [118]. For example, hundreds of host factors have been identified as being involved in the life cycles of HCV [143, 98, 99] and DENV [108, 62, 6] (see BOX 2 for host factor identification techniques). Those host dependency factors may interact with proteins of all cellular processes and pathways, such as cell cycle, lipid metabolism, stress response, mRNA translation, and apoptosis [143]. Knocking down or out a particular host dependency factor that positively regulates the viral life cycle may shut down the viral replication machinery and represent a potential treatment strategy. Nevertheless, the host induces host restriction factors such as immune system compounds, which inhibit various processes in the viral life cycle. For example, C19orf66 is an interferon-stimulated gene (ISG) that restricts the HCV replication by interfering with the membranous web [91], or viperin (also an ISG) has antiviral properties in – among others – HCV, DENV, West Nile virus, HIV, chikungunya virus, and Zika virus [69, 36]. Interestingly, several host restriction factors have been identified that balance the viral life cycle; a knockdown shifts the viral life cycle from, e.g., vRNA translation to replication or from viral replication to virus particle production [187]. For example, a knockdown of YB-1 has been shown to inhibit HCV RNA replication and increases HCV particle production [27, 26]. Therefore, silencing a particular host factor that blocks viral replication completely without being cytotoxic or stimulating other processes in the viral life cycle may be an interesting challenge for the future.

#### BOX 2: HOST FACTOR IDENTIFICATION TECHNIQUES

Numerous host factors have been identified regulating negatively or positively the viral life cycle by restricting or enhancing viral replication [2]. Inhibiting the host factor expression, e.g., by RNA interference (RNAi), allows grouping these host factors into those functional categories: host dependency factors (positive regulators) or restriction factors (negative regulators). RNAi is also known as post-transcriptional gene silencing. It uses small interfering RNAs (siRNAs) or small non-coding micro RNAs (miRNAs) with a 21 to 25 RNA nucleotide length that target mRNA for degradation and thus silencing or knocking down the target gene transiently [64, 18]. However, a complete gene knockout may be achieved by CRISPR-Cas9 (clustered regularly interspaced short palindromic repeats-CRISPR-associated protein 9) that modifies the target sequence in the nucleus [11]. Since its gene editing application in 2012 [82], CRISPR-Cas9 has grown in popularity as a promising tool to cure various diseases, such as sickle cell disease [52]. It has been further proposed to eliminate the integrated HIV-1 genome in infected CD4+ T cells [85].

## 2.4 Immune response to viral infection

The course of a viral infection can have life-threatening consequences for the host and is mainly determined by the virus-host-interplay: the efficiency of the immune system and the virus' ability to countermeasure the immune response. The immune defense is initiated almost immediately and becomes more and more complex and intense by recruiting many cells to fight the invader. Thus, resisting the viral invader quickly and efficiently is crucial. However, the strength of the immune response must also be critically controlled. Otherwise, cellular damage or, in the worst case, host death may be the result. Nevertheless, successful viruses developed strategies to countermeasure the immune response, resulting in an immune defense versus virus offense situation (Figure 2.3) [56, 49].

**The virus meets the host:** The host's physical and chemical defense systems are pathogens' primary barrier. For example, commensal microorganisms on dead skin cells inactivate pathogens by producing acids and inhibitors [57]. Cuts and punctuations expose living cells and represent entry sites of pathogens into the host [49]. For example, it has been shown that SARS-CoV-2 survives on human skin for about 9 hours, while the influenza A virus remains intact for about 2 hours. However, mechanical and chemical skin cleaning with ethanol killed both viruses after about 15 seconds [72]. Plus-strand RNA viruses use different transmission routes to enter a host, e.g., air droplets (rhinovirus, SARS-CoV-1 and -2), fecal-oral (polio, hepatitis A and E virus), sexual (hepatitis B and C virus), or vector-borne transmission (dengue, Zika, West Nil, and yellow fever virus) [28]. Once the virus encounters a susceptible cell, the first hours are crucial and dictate disease outcome. The virus needs to be recognized and eliminated quickly.

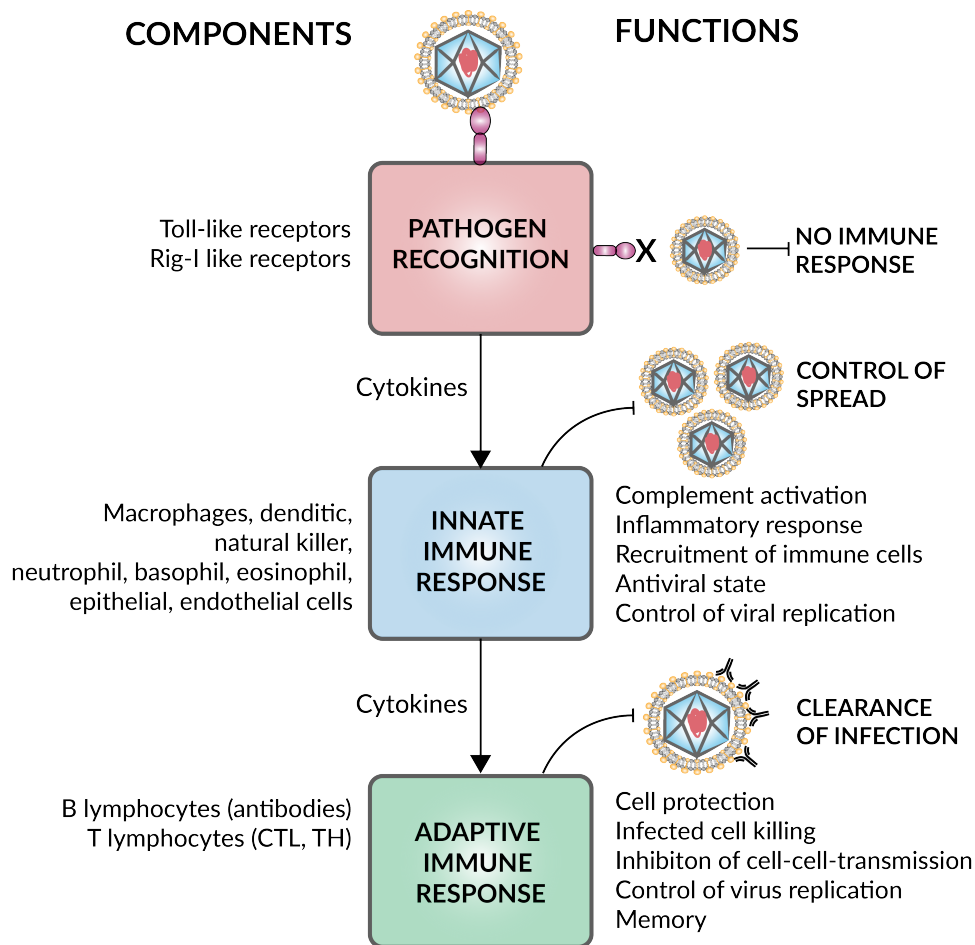
**Recognition of the invader:** Following the successful invasion of the host, so-called pathogen-associated molecular patterns (PAMPs), e.g., viral genome or proteins, are recognized by pattern recognition receptors (PRRs) of the innate immune response (IIR) such as the membrane-bound toll-like receptors (TLR). The ten human TLR family members are expressed on the extracellular cell membrane (TLR1, -2, -4, -5, -6, and -10) and in intracellular components such as endosomes (TLR3, -7, -8, and -9) [39]. Especially TLR2, -3, -4, -7, and -8 are key receptors in recognizing components of RNA viruses, e.g., single-stranded RNA (ssRNA), double-stranded RNA (dsRNA), mall-interfering (siRNA), and viral proteins, while TLR9 detects unmethylated DNA with CpG motifs of viral origin (Figure 2.4) [39, 136, 67, 165, 162, 56, 79]. However, the ligand and precise role of TLR10 are yet unknown and remain to be determined [48].

Following virus detection, TLRs activate three signaling pathways: (1) mitogen-activated protein kinases (MAPKs), (2) interferon-regulatory factors (IRFs, especially IRF3 and -7), and (3) nuclear factor kappa-light-chain-enhancer of activated B cells (NK- $\kappa$ B). They initiate the induction of interferons (IFN), the expression of pro-inflammatory genes, and genes that activate the adaptive immune response (AIR) [67, 79].

Once the virus enters the cell, intracellular receptors recognize viral ssRNA and dsRNA, e.g., RIG-I-like receptors (RLRs), which are expressed by most human cells. The three RLR members

## 2. BIOLOGICAL BACKGROUND

Figure 2.3: Simplified illustration of the integration of immune response systems consisting of pathogen recognition, innate, and adaptive immune response. Successful virus detection results in cytokine production and secretion that activates immune components and recruits immune cells aiming to control and clear the infection—failure of virus recognition results in an immune response absence (adapted from [49]).



are retinoic acid-induced gene I product (RIG-I), melanoma differentiation-associated antigen 5 (MDA5), and laboratory of genetics and physiology 2 (LGP2). While RIG-I recognizes viral dsRNA, 5'triphosphate ssRNA, and stem-loop structures (such as the HCV IRES element), MDA5 detects long dsRNA (> 2kbp). Those RNA motifs are usually not present in uninfected cells and thus discriminate self (e.g., mRNA) from non-self RNA (vRNA). Furthermore, vRNA is usually uncapped, while self-RNA is capped with a 5'-7-methylguanosine cap that underlies 2'O-methylation. Thus, vRNA without 2'O-methylation is sensed and inhibited by ISGs (e.g., IFIT1) [76].

RIG-I and MDA5 activate the mitochondrial antiviral signaling protein (MAVS) located at the mitochondrial membrane, down streaming the signal to IRFs and NF- $\kappa$ B, resulting in the production of pro-inflammatory cytokines and IFN [67]. Unlike RIG-I and MDA5, LGP2 is not a PRR. However, its precise function is controversial. Most recent studies found that LGP2 may facilitate MDA5 recognition and, thus, may be a positive regulator of the IFN signaling pathway [66].

However, this first step of virus recognition is crucial since, without recognizing pathogens, there will be no immune response; the invader can reproduce itself, damage cells and organs, release

substances toxic to the host, and may lead to host death.

**Intrinsic or single-cell defense:** If virus replication continues, cytokines released from infected cells activate a local and global immune response. Cytokines are regulatory proteins promoting the production, activation, differentiation, and regulation of immune cells and constitute, among others, interleukins (IL), IFN, and tumor necrosis factors (TNF) [176, 49, 167]. Pro-inflammatory and anti-inflammatory cytokines and chemokines are crucial in regulating the immune response. Pro-inflammatory cytokines (e.g., IL-4, IL-6, and -9) promote B and T cell activation, differentiation, and growth. Anti-inflammatory cytokines inhibit the production of pro-inflammatory cytokines (e.g., IL-13), inhibit antibody synthesis (e.g., IL-14), or stimulate cell survival and proliferation (e.g., IL-22). Chemokines recruit immune cells to infection sites (e.g., IL-8). Especially IFNs are crucial in viral infections, inhibiting the replication of viruses and inducing an antiviral state in uninfected cells carrying IFN receptors (IFN-R) (see BOX 3 for a description of IFN types and their antiviral activity) [176, 49, 167].

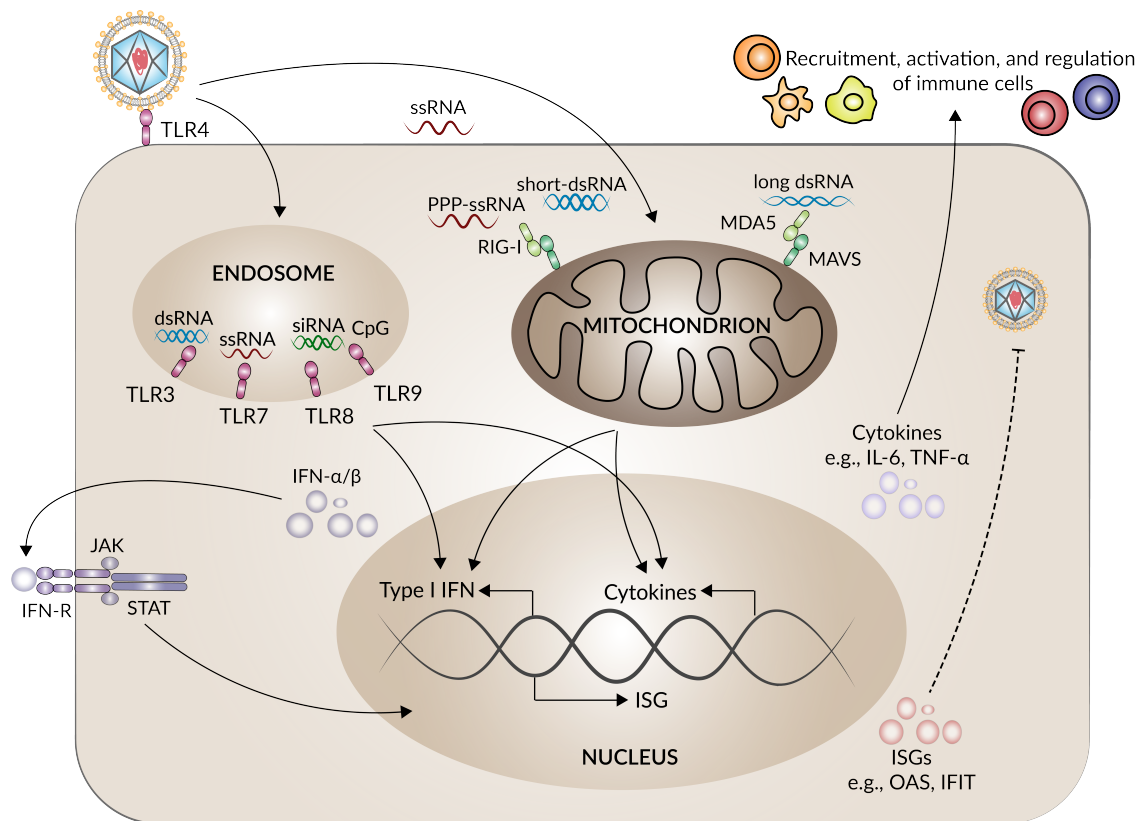
### BOX 3: TYPES OF IFN

There are three classes of IFN: type I IFN (IFN- $\alpha/\beta$ ), type II IFN (IFN- $\gamma$ ), and type III IFN (IFN- $\lambda$ ), which induce the expression of ISGs. While type I and III IFN are produced from virtually all cells in the human body via PRR stimulation (TLRs, RLRs, and NLRs), type II IFN is mainly produced from T cells, natural killer cells, and macrophages [111, 160]. Type I and III IFN show a broad antiviral activity on infected and uninfected cells, stimulating the IIR and AIR. Type II IFN shows antiviral and immunomodulatory activity [160]. Many of the signaling pathways of type I and III IFN are similar. However, while type I IFN is induced by MAVS located at the mitochondrial membrane, type III IFN is preferentially induced by MAVS located at peroxisomes and Ku70 (a cytosolic DNA sensor) [94]. Furthermore, the effector cells of type III IFN are mainly epithelial cells such as cells of the liver, respiratory tract, and gastrointestinal tract [94]. Especially in human hepatocytes, it has been shown that HCV-infected cells induce rather IFN- $\lambda$  (type III IFN) more than type I IFN and may be the key to HCV recognition in hepatocytes through peroxisome-associated MAVS. Furthermore, a single nucleotide polymorphism (SNP) of an IFN- $\lambda$  subgroup (IFN- $\lambda$ -4) seems to have beneficial effects on HCV clearance and disease outcome [78, 94, 40]. However, a different SNP in IFN- $\lambda$ 4  $\Delta$ G seems to be connected with the development of chronic and persisting HCV [40]. Interestingly, early treatment with IFN- $\alpha$  in HCV patients showed only a limited response, similar to the IIR-produced type I IFN, which suggests an HCV resistance to the IFN system or an immune system tolerance to HCV [40].

Extracellular receptor binding of IFN activates the JAK/STAT (Janus kinase/signal transducer and transcription activator) pathway, which transmits the signal via activating STAT proteins and IRF-9 to the nucleus and results in the expression of ISGs (Figure 2.4). ISGs have broad-spectrum antiviral activity and act on different steps in the viral life cycle. For example, by inhibiting viral entry/fusion (IFITM1 and IFITM3), blocking IRES-mediated vRNA translation (ISG56), degrading intracellular RNA (RNase L that OAS1 and OAS2 activate), or restricting the formation of ROs (C19orf66) [40, 121, 170, 91]. ISGs in dendritic cells (DCs) and macrophages (so-called sentinel cells) directly affect T and B cell activation to control the AIR and clear the virus [121].

## 2. BIOLOGICAL BACKGROUND

Figure 2.4: Extracellular and intracellular virus recognition and its components, e.g., ssRNA, dsRNA, siRNA, and DNA with CpG motifs, mediated by TLRs and signaling pathways, such as RIG-I, MAVS, and MDA5. Successful recognition results in the production of IFN and other cytokines, e.g., IL-6 and TNF- $\alpha$ , which recruit, activate, and regulate cells of the innate and adaptive immune response. Extracellular IFN binding to the IFN-receptor (IFN-R) activates the JAK/STAT pathway resulting in the expression of ISGs, e.g., OAS or IFIT, inhibiting steps in the viral life cycle.



However, since the virus uses host cell resources and remodels intracellular components for its translation, transcription, and replication, the infected cell responds to this type of cellular stress by apoptosis (programmed cell suicide) or autophagy (programmed self-eating). These self-destruction processes can be induced by cell surface receptor binding, cell membrane alterations and damage, virus-induced host translation shut-off, nutrient deprivation, as well as degradation of DNA, cell cycle interruption, and gene expression alteration [184, 49]. DCs can also trigger apoptosis in uninfected cells surrounded by infected cells by producing cytokines (e.g., TNF $\alpha$ ) [49]. However, suppose the intrinsic steps in immune defense do not stop viral replication and spread. In that case, the global immune defense system turns to a more aggressive way of fighting the invader: the IIR and AIR.

**Innate immune response:** The IIR is non-specific and rapid but also damaging. It comprises cytokines, DCs and macrophages, the complement system, natural killer (NK), and other white blood cells. DC and macrophages classify the pathogen, induce a local intrinsic response by producing cytokines (IFN) and communicate with AIR cells. Thus, these cells act as a bridge or mediator between IIR and AIR.



DCs exist in two states: immature and mature DCs. Immature DCs carry TLRs and RLRs (RIG-I and MDA5) and, thus, release cytokines in order to trigger the intrinsic immune defense system. Moreover, they endocytose dead cell debris, virus, or viral proteins and process the internalized debris that migrates to the cell surface where it is presented. Mature DCs migrate to the lymph node, present the antigens and stimulate AIR cells. The pro-inflammatory cytokines released from mature DCs dictate the type of AIR, for example, whether a bacterial or viral infection causes the infection. Consequently, the AIR must prepare for a bacterial or viral immune defense [49]. Thus, as professional antigen-presenting cells, DCs dictate the immune response and infection outcome.

NK cells recognize infected cells and mediate infected cell killing. The self-nonsel-discrimination is based on the major compatibility complex (MHC) receptor (so-called self-antigens); the presence of MHC blocks the killing activation, while a missing or altered MHC activates the killing process [49]. Furthermore, NK cells release cytokines (e.g., IFN and  $TNF\alpha$ ), contribute to local inflammation, promote DC maturation and stimulate AIR cells by releasing chemokines. The critical function of NK cells is mediated by IFN- $\gamma$  production, which triggers a T helper cell 1 (TH1) inflammatory response. IFN- $\gamma$  activates an antiviral response in the liver that inhibits viral replication but without killing infected hepatocytes, thus promoting cell survival [40].

Another component of the IIR, the complement system, initiates a broad-spectrum antiviral defense. Complement components are to 90% produced by hepatocytes. They polymerize and build pores in the virus envelope, disrupting the virus. Furthermore, complement proteins bind to the virus surface and coat the virus particle, which is recognized and destroyed by immune cells (so-called opsonization). Additionally, complement proteins stimulate inflammation, enhance the immune response, and clear immune (antibody-antigen) complexes [136, 44, 49, 170].

**Adaptive immune response:** The highly specific AIR differentiates infected from uninfected cells. It consists of the humoral response mediated by antibodies (B cell-derived) and the cell-mediated response mediated by plasma lymphocytes (NK, T, and B cells). B and T cells are both produced in the bone marrow. However, T cells migrate to the thymus, where they mature. The maturation process is selective and ensures that only T cells interacting appropriately with surface molecules via the T cell receptor get selected. In contrast, T cells that recognize self-peptides are killed [49].

A mature DC presents an antigen in the lymph node that triggers the differentiation of T cells into cytotoxic T lymphocytes (CTL), which kill infected cells, T helper (TH) cells, which stimulate antibody production, T memory cells, that respond when encountered with a known pathogen, or regulatory T cells, which control and shut down the T cell response. T cells are differentiated by their surface proteins: TH cells (CD4+) and CTL (CD8+). Depending on the type of pathogen, TH cells differentiate into TH1 or TH2 cells, which secrete different cytokines and stimulate different functions. Viral infections induce the production of the cytokine IL-12, which differentiates immature TH cells into TH1 cells and stimulates the secretion of IFN and pro-inflammatory cytokines. In contrast, bacterial infections induce the production of IL-4 (as well as IL-18 and IL-27

[40]), which differentiates immature TH cells into TH2 cells and stimulates an antibody response. Nevertheless, TH2 is critical for controlling the infection and clearing the vast amount of virus particles from the blood [175].

Similar to DCs, B cells are also antigen-presenting cells. Following antigen encountering in the lymph node, B cells present the antigen via MHC to TH2 cells promoting a TH2-B-cell interaction resulting in B cell differentiation and antibody synthesis [49]. Antibodies – the immunoglobulins IgG, IgA, and IgM – are directed against viral epitopes such as structural and non-structural proteins. IgG remains detectable for years due to the B cell memory [49]. Only a small fraction of the antibodies neutralize, inhibiting the early steps in the viral life cycle [68, 163]. The mechanism of neutralizing antibodies is binding and blocking viral surface receptors and thus preventing entry or binding and interfering with the structural changes necessary for viral entry (see BOX 4 for an example of antibody-mediated disease progression). Additionally, the AIR has a memory function that responds when encountered with a known pathogen with a strong response that stops the infection. Both B and T cells constitute the immunological memory. B-cell-derived antibodies bind to virus particles, and T cells actively recognize and destroy infected cells.

### BOX 4: ANTIBODY-DEPENDENT ENHANCEMENT

The presence of virus-specific antibodies is not always beneficial. A serotypic DENV infection leads to a serotypic long-term immunity and a heterotypic immunity for a short time [60]. Pre-existing antibodies that have been passively or actively acquired during a primary acute dengue infection can cause a so-called antibody-dependent enhancement (ADE), leading to more severe forms of dengue, such as DHF or DSS. First described by Halstead and O'Rourke in 1977 [63], ADE "may be a special case of the opsonization phenomenon [with] non-neutralizing antibodies providing a specific molecular 'ride' for an infectious dengue virion into the interior of a receptive phagocytic cell." More specifically, DENV binds to the Fc Receptor on susceptible cells facilitated by antibodies, resulting in a higher chance of cell entry and, thus, more infected virus-producing cells. However, alterations to the intrinsic cell response have also been described [114], primarily the suppression of type I IFN and pro-inflammatory cytokine production by an up-regulation of RIG-I/MDA-5 signaling pathway inhibitors [24, 168]. The antibody-mediated entry via the Fc receptor may decrease the expression of TLR3, -4, -7, and TLR signaling molecules (activating signaling pathway antagonists), leading to decreased IFN- $\beta$  production. This has also been shown in DHF patients showing suppression of mentioned TLRs (TLR3, -4, and -7) [114]. However, ADE seems to be a unique condition among viral infections and is not universal across all DENV secondary infections and may be mainly determined by a certain antibody-virus ratio [149, 182, 60].

## 2.5 Antiviral treatment

**Direct-acting antiviral agents:** The cure of HCV, and thus a potentially life-threatening and chronic disease, has an almost 30-year history. In 1989, 13 years after the discovery of the once referred to as non-A-non-B-hepatitis virus, the first treatment strategy comprised an IFN-based therapy, which became the backbone of hepatitis C treatment. Having significant side effects,

the sustained virologic response (SVR) was only 10 – 25%. The SVR is defined as the absence (or undetectable) of HCV RNA 3 to 6 months post-treatment cessation [158]. A slightly higher SVR rate of 38% was achieved by combining IFN and ribavirin in 1998. Ribavirin is a nucleoside analog with broad-spectrum antiviral activity, which inhibits the RNA-dependent RNA polymerase and leads to RNA mutagenesis and, thus, unfit virus strains [164]. With pegylated IFN (peg-IFN), which constitutes a higher half-life and better pharmacokinetics, SVR rates of 55% were achieved in combination with ribavirin in 2001. However, the introduction of first-generation direct-acting antivirals (DAA) in 2011, such as the HCV NS3/4A protease inhibitors telaprevir and boceprevir, increased the SVR rates further to 65 – 75% (in combination with peg-IFN and ribavirin). The development of HCV NS5B (RNA-dependent RNA polymerase) inhibitors was a game changer and increased SVR rates to 90% and higher after 12 weeks of treatment and in combination with peg-IFN and ribavirin in 2013. From 2014 on, IFN-free treatment regimens based solely on a combination of DAAs have led to SVR rates of >95% and are well tolerable with a short duration of treatment. Today, several DAAs exist inhibiting non-structural HCV proteins such as NS3/4A (voxilaprevir; FDA approved in 2017), NS5A (pibrentasvir; FDA approved in 2017), as well as NS5B inhibitors such as nucleotide/nucleoside (sofosbuvir; FDA approved 2013) and non-nucleotide/nucleoside inhibitors (dasabuvir; FDA approved 2014).

Even though the cure of hepatitis C is a success story and HCV and DENV are both closely related (+)RNA viruses, there is no treatment available for dengue. *In vitro* compounds have been identified with promising results, which have not been successful in clinical trials. For example, tomatidine has been shown effective against DENV-2 *in vitro* in the human hepatocarcinoma cell line Huh7 and inhibits virus particle production with a suggested mode of action on DENV assembly and maturation. However, the time window of efficient treatment is relatively short, with being effective pre-infection and up to 12 hpi (no antiviral effect after 16 hpi) [37]. Sofosbuvir, which has shown good SRV rates in hepatitis C, has not been effective against DENV replication or the DENV NS5 polymerase [96]. However, in an *in vivo* mouse model, 2'-C-methylcytidine (a sofosbuvir analog) has shown promising results against DENV NS5 polymerase [96]. Balapiravir, another DENV NS5 polymerase inhibitor initially developed for HCV, has reached clinical trials but did not alter the viral kinetics [122]. R1479 (2'-C-methylcytidine analog) also failed to reduce viral load in plasma in clinical trials [96].

Enteroviruses, the most common viruses from the *Picornaviridae* family, usually cause mild infections and only require symptom management. However, enterovirus infections can also lead to more severe symptoms and complications, such as polio, which has a risk of paralysis in 1 in 200 to 1 to 2000 infected people [14, 124]. For enteroviruses, no antiviral treatment exists to date. However, several DAAs have been tested in clinical trials with mixed outcomes. For example, pleconaril, a so-called "capsid binder", is a DAA designed to prevent viral attachment and uncoating. Even though pleconaril increased survival in neonates with enterovirus sepsis in a clinical trial, "capsid binders" are often associated with the emergence of resistance and, thus, are not recommended [14, 1].

## 2. BIOLOGICAL BACKGROUND

---

**Vaccination:** The best antiviral strategy is preventing viral infection or severe disease by vaccination, which is an excellent example of the successful and vital antibody-mediated antiviral response. For six (+)RNA viruses, vaccines are available and in use: polio, yellow fever, dengue, hepatitis A and E, Japanese encephalitis virus, and SARS-CoV-2 [132], as well as promising vaccine candidates for chikungunya [54], enterovirus 71 [146], and norovirus [110] preparing to enter clinical trials. Nevertheless, developing a safe, well-tolerable, and effective vaccine is challenging, evident by the low number of available vaccines (see BOX 5 for the poliovirus vaccine as an example of a successful disease eradication by vaccination).

There are three main approaches to vaccine development. (1) The inactivated vaccine, e.g., for polio, Japanese encephalitis, and hepatitis A virus, eliminates or inactivates the infectivity from the virus but keeps the ability to activate the immune system and induces an immune response. (2) Live attenuated vaccines, e.g., for dengue, polio, and yellow fever virus, contain manipulated virus that is replication competent without spreading and induces mild disease symptoms, thus stimulating the immune system. (3) Subunit vaccines contain purified components of the virus that are recognized by the immune system and induce an immune response. For example, the hepatitis B protein gene is integrated into a non-pathogenic vector (bacterium or yeast), which produces the viral proteins and assembles them into virus-like particles [49, 3, 61]. (4) The mRNA vaccine – a revolutionary vaccine technology that plays an essential role in controlling the SARS-CoV-2 spread. This new vaccine approach delivers the nucleic acid of the SARS-CoV-2 surface spike protein, the primary antigen, that is translated from the host cell. Hence, the host produces the antigen, which triggers an immune response [45].

However, developing a safe and well-tolerable vaccine is challenging, as is evident in the case of dengue. To date, one dengue vaccine is licensed: Dengvaxia or CYD-TDV. The tetravalent live attenuated vaccine consists of a yellow fever 17D backbone (chimeric vaccine) where two yellow fever structural proteins (membrane and envelope [prM and E]) are replaced by those of the four DENV serotypes. The vaccine efficacy depends on age, pre-vaccine serostatus, and infection serotype. It has been shown that Dengvaxia increases the risk of severe dengue in seronegative individuals showing comparable symptoms and severity as a natural secondary infection, i.e., the vaccine leads to a silent primary-like infection. In contrast, a natural post-vaccine infection with the (first) wild type may lead to a secondary, more severe dengue infection. Hence, the vaccine issues safety concerns for seronegative individuals. Nevertheless, the vaccine is recommended for seropositive individuals (individuals with a wild-type dengue infection) and suggests a pre-vaccine serostatus screening. However, other second-generation vaccines are currently in clinical trials, e.g., LATV, TAK-003, TDEN, and DPIV, using DENV strains as a backbone, where DENV non-structural proteins are integrated and, thus, may generate and support T cell response and antibody production against DENV non-structural proteins [126, 141, 181].

**BOX 5: POLIO VACCINE**

The most successful vaccine story against (+)RNA viruses is the vaccine against poliovirus serotypes, which was developed and first licensed in 1955. The three serotypes of poliovirus cause poliomyelitis, and in about 0.5% of the cases, paralytic poliomyelitis, which leads to permanent disability in children if it enters the central nervous system. Since there are no antiviral drugs available, the best protection against poliomyelitis is the vaccine (trivalent intravenous and trivalent or bivalent oral; bivalent contains only type 1 and 3) that led to a decrease in paralytic poliomyelitis by more than 99% (from more than 350,000 cases in >125 countries in 1988 to 359 reported cases in only two countries in 2015). However, the oral vaccine may lead to a "vaccine-associated paralytic poliomyelitis" mainly associated with the type 2 poliovirus serotype compound in 2-4 cases/million births per year. Due to this vaccine-derived poliomyelitis, the WHO suggests switching from the trivalent oral vaccine, which contains all three serotype compounds, to the bivalent oral vaccine, which contains only type 1 and 3 serotype compounds. Nevertheless, the vaccination program and the fight against polio successfully eradicated the type 2 and 3 wild poliovirus serotypes [125, 131].



---

A model is an abstract and simplified mathematical representation of a complex process that helps to gain a system-level understanding and predict a system behavior that changes over time. In general, mathematical models may serve three purposes: (1) developing a scientific understanding, (2) testing the system for changes, and (3) aiding the decision-making process. However, mathematical models are sets of equations representing rules; they simplify and reduce the system reality to the most necessary features [77, 92, 71]. Based on the underlying scientific question to answer, there are different modeling types and techniques [4]:

**Mechanistic versus empirical models:** *Mechanistic* models are hypothesis-driven and aim to understand a particular phenomenon based on the underlying data. However, *empirical* models are data-driven and aim to identify patterns in the data.

**Discrete versus continuous models:** *Discrete* and *continuous* models are discriminated whether the model's state variables change at a finite or infinite number of points in time where the points are the state changes.

**Deterministic versus stochastic:** The type of predicted output can be discriminated in *deterministic* with a determined output based on the input versus *stochastic* that takes randomness into account and predicts a distribution of the predicted outcome. However, a (hybrid) mixture of both is possible where stochasticity and deterministic processes are approached on different scales, e.g., deterministic rules defined for individuals of a stochastic population.

**Static versus dynamic:** Whether the system describes a steady state behavior (one time point) or allows time-dependent changes in model states, models can be further categorized into *static* or *dynamic* models, respectively.

Every model serves a particular purpose to study a specific biological phenomenon or process. To do so, modelers make use of different mathematical modeling techniques, such as ordinary differential equations (ODEs), to study time dynamics, or partial differential equations (PDEs) and agent-based models (ABMs) in the case of additional spatial considerations. ODEs with only one independent variable – time – are the most straightforward representation of complex processes. Therefore, they are used as the modeling technique of choice due to their well-studied and known behavior. Nevertheless, the central assumptions of ODE systems are a well-mixed

### 3. MATERIALS AND METHODS

---

compartment (e.g., blood) and model species are homogeneous and uniformly distributed, which is not always the biologically realistic assumption. In such a case, models formulated as PDEs or ABM, which consider more than one independent variable – time and space – make it possible to formulate rules (or a particular behavior) about how species or agents interact over time and in space. Additionally, biological processes fluctuate, and quantitative data is noisy. Adding a certain stochastic probability to capture fluctuations may be a more realistic representation of biological phenomena but is computationally more expensive [13, 159, 31]. Therefore, to capture the biological reality and answer a specific biological question, there may be multiple different modeling techniques or a combination.

Mathematical modeling has a long history and has been applied to a variety of biological questions in – among others – cancer research [161, 5], immunology [172, 43], and infectious diseases [188]. For example, modeling the virus-host dynamics helped to gain insights into disease origin and progression, pathogenesis, interactions with the immune system, and the prediction of treatment strategies. In virus dynamics modeling, the ODE-based target cell-limited model represents a well-established mathematical model applied to various viruses to study viral spread, the interplay with the immune system, and the effect and modes of action of antiviral drugs. A comprehensive description of model types and techniques and how mathematical modeling contributed to understanding virus-host interactions can be found in our literature review [188].



---

This chapter consists of three publications. In the first publication, we modeled the life cycle of (+)RNA viruses to identify pan-viral similarities and virus-specific differences, which may help to develop broad-spectrum antiviral treatment strategies. In the second publication, we modeled the DENV life cycle coupled to the host cell immune response to identify host dependency and restriction factors determining cell line permissiveness, replication efficiency, and perturbations of the viral replication machinery. Finally, in the third publication, we compare intracellular HCV models toward viral spread uncovering an unconventional viral transmission mechanism via exosomes. This chapter will summarize their main findings, laying the ground for the Discussion in chapter 5.

#### 4.1 Mathematical modeling of plus-strand RNA virus replication to identify broad-spectrum antiviral treatment strategies

This section summarizes the main findings of the following publication:

**Carolin Zitzmann**, Christopher Dächert, Bianca Schmid, Hilde van Tongeren-van der Schaar, Alessia Ruggieri, Martijn van Hemert, Alan S. Perelson, Frank van Kuppeveld, Ralf Bartenschlager, Marco Binder, Lars Kaderali (2023) *Mathematical modeling of plus-strand RNA virus replication to identify a broad-spectrum antiviral treatment strategy*. PLoS computational biology 19(4): e1010423.

##### Highlights

- We studied and identified pan-viral and virus-specific processes in the life cycle of closely related (+)RNA viruses.
- We found that ribosomes involved in viral RNA translation may be key players in vRNA replication efficiency, and the virus' ability to suppress the host's mRNA translation may determine acute or chronic infection outcomes.
- We showed that targeting viral proteases involved in polyprotein cleavage and viral RNA replication may represent promising drug targets with broad-spectrum antiviral activity.

**Description:** Studying the (+)RNA viral life cycle in detail is experimentally challenging. This project aimed to quantitatively study and compare the life cycles of different (+)RNA viruses. Here, we focussed on studying pan-viral similarities and virus-specific differences among the core processes of the (+)RNA virus life cycle. For that, we developed a detailed intracellular (+)RNA virus replication model that has been fit to *in vitro* dynamics of extracellular infectious virus, intracellular vRNA, and viral protein of three (+)RNA virus members (HCV, DENV, and CVB3).

Our mechanistic model identified viral entry and the subsequent release of the viral genome as virus-specific, which may determine cell line permissiveness. Furthermore, our model predicted virus-specific dynamics of the RO formation, where DMVs may be more favorable than invaginations. Interestingly, our modeling also predicted a disadvantage for viruses using different intracellular compartments for vRNA translation and RO formation/vRNA amplification, where the viral genome may get damaged in the trafficking process. Furthermore, our model suggested a correlation between the number of ribosomes involved in vRNA translation and the vRNA replication efficiency: The higher the number of ribosomes, the higher the concentration of intracellular vRNA. Our model predicted virus-specific abilities to suppress the host mRNA translation based on the number of ribosomes involved in the vRNA translation. Consequently, our model suggested that the ability to suppress the host's mRNA translation may determine viral replication efficiency and, ultimately, infection outcomes – an acute or self-limited chronic infection.

With *in silico* drug intervention studies, we tested the efficacy by blocking single steps of the (+)RNA virus life cycle and thus simulating the effect of DAAs. Our model confirmed vRNA synthesis as the most promising drug target that may be conserved among (+)RNA viruses. We also found that vRNA translation-associated processes (formation of the translation complex, vRNA translation, and polyprotein cleavage) may represent promising drug targets.

### 4.2 A coupled mathematical model of the intracellular replication of dengue virus and the host cell immune response to infection

This section summarizes the main findings of the following publication:

**Carolin Zitzmann, Bianca Schmid, Alessia Ruggieri, Alan S Perelson, Marco Binder, Ralf Bartenschlager, Lars Kaderali (2020)** *A coupled mathematical model of the intracellular replication of dengue virus and the host cell immune response to infection.* *Frontiers in microbiology* 11:725.

#### Highlights

- We studied the DENV life cycle in the absence and presence of the intrinsic (innate) immune response.
- We found that the intrinsic immune response targets vRNA translation initiation, degrades cytosolic vRNA, and inhibits DENV spread.

- We showed that DENV efficiently countermeasures the intrinsic immune response by inhibiting the JAK/STAT pathway.

**Description:** The intrinsic immune response represents the first line of defense, and its efficiency may determine disease severity and outcome. In this project, we studied and quantified the DENV replication in the absence and presence of the intrinsic immune response. To do so, we developed a detailed mechanistic model of the intracellular DENV replication coupled to the activation and antiviral effect of the host cellular immune response, i.e., the recognition of the virus, the subsequent IFN response, and ISG expression. The model has been fit to intracellular measurements of DENV (+)RNA, protein, and extracellular infectious virus measured in two cell lines: immuno-competent A549 cells and immuno-compromised Huh7.

Against our expectations, we observed a supported viral genome replication in the presence of the intrinsic immune response suggesting cell line-specific host dependency factors involved in the replicase complex formation that may positively regulate the viral replication. We further found that host dependency factors involved in virion assembly may limit the virus production, which was independent of the immune response. Nevertheless, our model predicted that the intrinsic immune response targets the viral life cycle at multiple steps: by interfering with vRNA translation initiation, actively degrading the vRNA and, thus, preventing its availability for vRNA translation and synthesis, as well as by establishing an antiviral state through the inhibition of infection spread to naive cells.

However, viruses developed many mechanisms to countermeasure the immune response, mainly by inhibiting the IFN induction and the JAK/STAT signaling pathway. Considering both processes, we observed that DENV efficiently targets the JAK/STAT pathway. The RLR-mediated IFN induction seemed to be a highly potent antiviral defense mechanism. To support the early immune response, DAAs targeting processes associated with DENV RNA synthesis and virion assembly/release represent promising drug targets, as our *in silico* drug intervention study suggested.

### 4.3 Modeling of hepatitis C replication, exosome secretion, and virus release

This section summarizes the main findings of the following publication:

**Carolin Zitzmann, Lars Kaderali, Alan S Perelson\*** (2020) *Modeling of hepatitis C replication, exosome secretion and virus release*. PLoS computational biology 16(11):e1008421

#### Highlights

- We studied different HCV transmission routes.
- We found that HCV assembly and release may be limited by host dependency factors leading to decreasing infectivity over time.
- We showed that if virus assembly and release are inhibited, e.g., by DAAs, HCV replication is ongoing and HCV RNA may be secreted as exosomes.

**Description:** Packaging infectious virions is a crucial step in the viral life cycle, usually consisting of hundreds of components such as the viral genome, viral proteins, and host factors. We developed a series of mathematical models describing the intracellular HCV replication with virus assembly/release with and without HCV RNA secretion. The models have been fit to *in vitro* measurements of intracellular vRNA and extracellular infectious virus.

We found that a decreasing virus assembly and release rate over time best described the extracellular HCV dynamics. The decrease in the virus packaging process suggests that the virus assembly and release process may critically depend on and be limited by host dependency factors, which may be responsible for a decreasing *in vitro* infectivity over time.

However, viral spread via extracellular vesicles has been observed in various viruses. HCV-derived exosomes (or EVs) may support the transmission of infection, especially under a disturbed virus assembly and release – either by a limitation in host cellular resources or by inhibition by DAAs. In the presence of DAAs such as daclatasvir, which efficiently blocks HCV RNA replication and HCV assembly and release *in vivo*, we found ongoing HCV RNA replication and secretion as EVs, even though at low levels. We further found that the secreted HCV RNA was (+)RNA, while the secretion of replicative intermediates was negligible. Interestingly, the secretion of newly synthesized vRNA from the RO started later in infection (3 days post-infection), where vRNA is used for vRNA translation early in infection. Our model predictions suggested that detectable plasma HCV levels may be associated with HCV RNA-carrying exosomes.

The presented thesis aimed to investigate viral replication strategies and the interaction of (+)RNA viruses with the host in order to contribute to the understanding of (1) cell line permissiveness and perturbations by host cellular factors, (2) viral trafficking and transmission, and (3) virus-specificity and pan-viral treatment opportunities.

As a starting point, we wrote a comprehensive literature review about the state of the art of mathematical modeling of virus-host interactions [188]. The review describes the well-established target cell-limited model and its extensions to antiviral therapy and the immune response. Furthermore, we highlight how these within-host models have been applied to different viruses, e.g., HIV, HCV, and influenza A virus, and different research questions, most notably the circumstances leading to viral clearance and its pattern following the initiation of antiviral drugs [188]. However, our literature review demonstrates that little is known about the intracellular kinetics of viral replication. Therefore, we dedicated our research to quantifying the (+)RNA virus life cycle.

Building upon a published model of the HCV life cycle from our lab [17], we studied the intracellular replication mechanisms of three viruses – HCV, DENV, and CVB3. To describe the dynamics of the three studied (+)RNA viruses, we identified the most important virus-specific differences, most notably the crucial role of host cellular ribosomes for efficient viral RNA replication and clinical disease outcomes. Furthermore, we predicted broad-spectrum antiviral treatment strategies and the most promising drug targets [191]. Furthermore, we studied the intracellular DENV replication and cell line permissiveness in the absence and presence of the intrinsic immune response. We identified host factors DENV is critically dependent on and host cellular immune factors restricting the efficient intracellular DENV replication [190]. Using a series of intracellular HCV replication models, we analyzed different routes of HCV transmission by considering viral spread through mature HCV particles and the secretion of HCV RNA-containing exosomes. Our models predicted exosomal HCV RNA as an essential key player in viral spread even under antiviral treatment. We further found that HCV critically depends on host factors for virus assembly and that a limitation of host cellular resources leads to a decreased release of infectious virus, possibly contributing to an increased HCV RNA secretion [189].

This chapter will present key findings and contextualize our model predictions in the broader scientific literature. I will discuss the central biological topics predicted by our mathematical models:

virus-specificity and the viral dependency on the living host, the intrinsic immune response to viral infections, the controversy of exosomes, and the feasibility of broad-spectrum antivirals. Finally, I will close this chapter by highlighting the strengths and limitations of our single research projects and will give an overview of possible future research directions and challenges.

### 5.1 Virus-specific replication mechanisms and the dependency on the living host

Viruses depend on their living host for reproduction by hijacking cellular host factors. Host factors are RNAs, proteins, lipids, or membranes, that regulate the viral life cycle positively (proviral) or negatively (antiviral) and are categorized as host dependency or restriction factors, respectively [118, 187, 117]. Host dependency factors are crucial helper molecules and proteins involved in virtually every step of the viral life cycle [155]. However, the first hurdle to overcome for a virus is cell entry and the release of its genome into the cytoplasm, a highly regulated and complex process [30]. Our modeling identified viral entry and the subsequent release of the viral genome as virus-specific processes, which determine cell line permissiveness [191]. Several host factors have been identified to promote virus attachment and internalization, e.g., EGFR and Ras, which contribute to the surface receptor functionality and promote HCV attachment and entry [30, 103]. Furthermore, Cyclophilin A (Cyp A) has been shown to participate among others in the correct host protein folding but also regulates the uncoating process in enterovirus 71 (family *Picornaviridae*) by interacting with and rearranging the viral capsid [142, 101].

Considering viruses' limited gene coding capacity, it is unsurprising that viruses developed strategies to use cellular compounds for their benefit [155]. Over the last years, hundreds of host dependency and restriction factors have been identified that are virus-specific such as for HCV [143, 98, 99], DENV [108, 62, 6], or CVB3 [138, 134, 90]. However, the big challenge is identifying host factors conserved among multiple or a whole group of viruses, e.g., (+)RNA viruses. One of the most conserved host dependency factors is probably ribosomes, which are part of the cellular mRNA translation machinery. Therefore, independent of the virus and its tropism, viruses rely on the availability of ribosomes to produce viral proteins, including the components necessary for viral replication, such as the RNA-dependent RNA polymerase [100]. Our modeling suggested a correlation between the number of ribosomes involved in vRNA translation and the vRNA replication efficiency. Furthermore, ribosomes seem critical for acute or chronic infection outcomes [191], where the optimal usage of ribosomes in combination with suppressing the host's mRNA translation may be responsible for an acute infection. In contrast, viruses with a sub-optimal usage of cellular resources replicate their genetic material at a low level. They may remain mostly undetected by cellular immune response recognition, contributing to a chronic infection.

However, a hallmark of (+)RNA viruses is the membranous web, with ROs providing an environment rich in nucleotides and proteins necessary for vRNA replication. ROs (DMVs or invagina-

tions) derive from cellular membranes sequestered by the virus and serve as the site of vRNA replication [137, 7, 112]. The replication machinery, i.e., the replicase complexes, are anchored in the RO membrane either within the RO or outside, facing the cytoplasm. Our modeling suggested that the formation of replicase complexes associated with DMVs may be more favorable compared to invaginations [191]. Interestingly, it has been shown that various membranous organelles can form invaginations, while the membranes that form DMVs seem to be limited to a secretory pathway origin [183]. Consequently, the virus' ability to utilize various organelles to form ROs as invaginations may possess an evolutionary advantage. That observation may also be explained by cell line permissiveness, the utilization of host factors involved in the formation process, and thus a better adaptation to the host cell. A well-known host dependency factor involved in forming ROs and, thus, the remodeling process of intracellular host cell membranes is phosphatidylinositol 4-kinases (PI4K). PI4K is hijacked by various (+)RNA viruses such as HCV and CVB3, which enriches host cell membranes with phosphatidylinositol 4-phosphate, a binding partner of the viral RNA-dependent RNA polymerase [119, 75]. Interestingly, silencing PI4K seems to affect viral replication negatively in HCV. However, the knockdown of PI4K does not show any negative effect in the DENV life cycle [35], suggesting PI4K may not be crucial for the DENV replicase complex formation and possibly the formation of invaginations.

Previous research in our lab found that host dependency factors involved in the formation of the replicase complex were responsible for cell line permissiveness and cell line-specific replication efficiency in HCV [17]. Consistent with our previous HCV research, our modeling suggested that a higher availability of host dependency factors involved in the replicase complex formation may positively regulate viral replication in DENV [190]. However, the positive or negative association of host factors with viral replication efficiency has been demonstrated in different cell lines and sub-types of the same cell line. For example, the Huh7 cell line and its sub-clones show variations in the replication efficiency, i.e., permissiveness, mainly controlled by host factors. While intrinsic immunity as a viral replication restricting factor has been ruled out [16], several host dependency factors have been found to enhance HCV production by overexpression, such as overexpression of the transcriptional repressor THAP7 [41].

The (+)RNA virus life cycle is a tightly connected and coordinated process. For that purpose, (+)RNA viruses establish their micro-environment where the vRNA replication core processes occur in close proximity. ROs and the membranous web protect vRNA and proteins from damaging cytoplasmic nucleases and the recognition by the immune system [25]. Therefore, minimizing the trafficking distances of viral components and their exposure to the cytoplasm is crucial for producing tens of thousands of infectious viruses. Interestingly, our modeling suggested that the trafficking process from the site of vRNA translation to replication and vice versa may be a critical and sensitive process for non-enveloped viruses [191]. Strikingly, non-enveloped viruses use only a fraction of structural proteins for their nucleocapsid assembly, which may be a possible adaptation to overcome the trafficking shortcoming. Nevertheless, minimizing the distance between vRNA translation and replication sites is as crucial as the proximity of vRNA replication and virus assembly. Furthermore, the bottleneck in the last stage of the viral life cycle may be

the availability of viral proteins and host dependency factors for virus assembly, maturation, and release. Our modeling suggested a limitation in virus assembly-associated host dependency factors leading to a decrease in infectious virus production over time [189]. For example, apoE is essential for HCV assembly and mediates HCV attachment and entry into the cell through its interaction with cell-surface receptors [21, 185]. Furthermore, a decreasing apoE concentration over time has been described as a possible reason for decreasing infectivity [88].

### 5.2 The intrinsic immune response to viral infection

A viral infection is characterized by a battle between a virus and the host's immune system. While the host evolved to recognize and fight the pathogen, the invader developed strategies to countermeasure the immune response [49]. Characterizing key players of the complex virus-host interplay is crucial to understanding infection mechanisms, the host's contribution to fighting the infection, and disease outcome.

The production of viral proteins necessary for vRNA replication and virus assembly is essential to the viral life cycle. Viral proteins carry out various functions in the viral life cycle, most notably the formation of ROs and vRNA synthesis [60]. Therefore, blocking the vRNA translation initiation, as suggested by our modeling [190, 191], may be a critical barrier to infection, and several ISGs have been identified targeting the vRNA translation [56, 152]. For example, ISGs such as members of the IFIT family, ZAP, and PKR have been identified to block and repress the formation of the vRNA translation initiation complex by targeting the eukaryotic initiation factors (eIF) such as eIF3 [153, 152, 56, 144, 81]. However, considering that the availability of ribosomes bound to the viral genome may determine the efficiency of vRNA replication and clinical outcomes (acute versus chronic infection), as suggested by our modeling [191], it is not surprising that the intrinsic immune response aims to interfere with the vRNA translation. Furthermore, a complete host mRNA translation shut off, and thus the prevention of the production of antiviral compounds has a dramatic contribution to the undisturbed vRNA production and, thus, pathogenesis [73]. However, increasing the vRNA degradation, as suggested by our modeling [190], may be another mechanism to minimize the availability of vRNA for its translation or replication. Enhanced vRNA or viral protein degradation may be achieved by the members of the OAS family (ISGs), which activate RNase L-mediated vRNA degradation, or TRIM69 that blocks viral replication by DENV NS3 degradation, which interacts with the RNA-dependent RNA polymerase (DENV NS5) [102, 178].

Inhibiting vRNA replication via ISGs is the autocrine mechanism carried out by IFN. IFNs also act in a paracrine manner by protecting naive cells from infection [97]. However, even though suggested by our modeling, the rate of naive cell protection and, thus, the establishment of a paracrine antiviral state was relatively negligible [190]. Due to a high MOI infection experiment, achieving a high cell infection rate with virtually every cell being infected, second rounds of a cell infected are probably the exception.



Interestingly, viruses developed many highly effective countermeasure strategies, such as inhibiting their recognition and blocking IFN signaling pathways. For example, DENV blocks RLR and TLR signaling and thus type I IFN production, specifically 2'-O-methylation of the 5' untranslated region, which prevents DENV from being recognized, where 2'-O-methylation mimics host mRNA that is not getting recognized by the IIR [170, 166]. Furthermore, several DENV non-structural proteins also countermeasure the JAK/STAT pathway. For example, DENV non-structural proteins NS2A, -4A, and -4B inhibit STAT1, while NS5 blocks STAT2. STAT1 and STAT2, both essential proteins in the JAK/STAT pathway, together with IRF-9, induce the expression of ISGs, highly potent antiviral effector proteins [166]. However, considering those countermeasure strategies, our modeling correctly predicted DENV's ability to target the JAK/STAT pathway more efficiently compared to RLR-mediated IFN induction [190], which has been shown experimentally [116].

### 5.3 The controversy of exosomes as “Trojan horses”

Exosomes are small (30 – 100 nm) membrane vesicles secreted from virtually every cell type. Exosomes have been found in, among others, blood, saliva, semen, urine, cerebrospinal fluid, breast milk, and cell culture supernatant [9, 22, 186, 32]. Extracellular vesicles (EV) serve different functions, such as intracellular communication and transmission of host cell macromolecules. Several databases exist listing molecules and substances found in exosomes (Vesiclepedia, EVpedia, and Exocarta) [87, 135, 89]. However, since they carry proteins, lipids, and genetic material of intracellular origin, exosomes derived from virus-infected cells may transmit viral components and thus possibly contribute to disease spread and progression [42]. This additional path of viral spread by EVs has been found in, among others, hepatitis B/C/E virus, HIV, human T-cell lymphotropic virus (HTLV), DENV, enteroviruses, and SARS-CoV-2 [22, 9, 59, 171].

In the presence of efficient antiviral treatment, e.g., DAAs, our modeling suggested ongoing vRNA replication and secretion at low levels [189]. The presence of plasma viral RNA after treatment, reported in some HCV patients [123, 70], may result from HCV RNA-carrying exosomes. Nevertheless, HCV EVs have been found to transmit replication-competent HCV between hepatocytes in a virion-independent manner, generating a “typical” infection [106, 19]. In dengue, it has been shown that DENV-infected arthropod cells (derived from DENV vectors *Aedes albopictus/aegypti*) secrete exosomes, which contain infectious DENV genome and proteins. Those exosomes could infect naive arthropod and mammalian cells and thus serve as a (virus-free) transmission strategy from arthropods to mammals. Additionally, DENV-derived exosomes had a low pH and carried an autophagy marker (LC3 II) supporting the maturation of assembled virions within the exosome and protecting DENV from neutralizing antibodies, respectively [173, 113].

Nevertheless, the biological function of exosomes is not to harm the host but to support biological processes and functions and establish and recreate a biological equilibrium. For example, it has been shown that exosomes may prevent an infection with HIV-1, where seminal plasma-

derived exosomes block the Tat protein recruitment and, consequently, the early HIV-1 transcription. Furthermore, in poliovirus, human cytomegalovirus, and herpes simplex virus 1, exosomes may induce autophagy and defense against these viruses [84]. Therefore, exosomes participate in the antiviral immune response through immune stimulation and pathogenicity inhibition. The former may be achieved by activating immune cells, e.g., macrophages, NK, T, and B cells, where exosomes function as antigen-presenting cells or by transporting cytokines that trigger the activation of immune cells. The latter may be achieved by the exosomal transport of miRNAs, which act as host restriction factors with the ability to block viral replication. It has been shown that exosomes are enriched with miRNAs and that 60% of miRNAs are passively released from cells [140, 10, 55, 58]. Upon dengue infection, the miRNA profiling changes, influencing immune regulatory pathways and endothelial junction proteins, which may lead to a so-called “cytokine storm” and hyper-permeability [154, 192, 113]. Both phenomena are associated with dengue pathogenesis and severity and thus DHF.

Pathogens hijack the exosomal pathway for their benefit. The most likely critical function of exosomes following pathogen infection may be hiding from the immune system and thus promoting viral transmission. In hepatitis A infections, HAV-carrying exosomes may promote viral spread in the liver through intercellular communication and by escaping neutralizing antibodies [46]. On the one hand, viruses exist as “pseudo-enveloped” viruses within exosomes that may promote viral entry and spread. On the other hand, it is suggested that the exosomal secretion of viruses may prevent inflammation and cell lysis and thus promote virus survival. Furthermore, a diseased cell may promote the secretion of exosomes by activating and supporting the immune reaction to the disease. Viruses seem to have found a way to hijack the exosomal pathway for their spread and transmission as “Trojan horses”. However, exosomes and their possible contribution to viral spread are controversial and under debate and need more investigation in the future.

### 5.4 How realistic are broad-spectrum antivirals?

From the 1990s on, several highly effective drugs have been developed to treat viral infections. The most successful story may be the cure of hepatitis C. Even though the treatment of hepatitis C with DAAs has cured the disease in the majority, a subset of patients report treatment failure, side effects, or DAAs are not available or expensive in developing countries [129, 12, 150]. Furthermore, DAAs are highly specific to a single virus-specific protein, and thus DAAs do usually not have the potential to be re-purposed for other viruses. Furthermore, DAAs possess a low barrier of resistance, and selective pressure thrives the development of mutants and treatment-resistant variants [80]. Another treatment option with a high resistance barrier may be host-directed therapy. Viruses depend on host factors for their replication and, thus, may be potential targets for antiviral therapy. Thus, targeting a particular host dependency factor necessary for completing the viral life cycle may inhibit viral replication and possess a high resistance barrier. In addition, several viruses may hijack a particular host dependency factor, and its inhibition may possess a broad-spectrum antiviral activity [80, 86]. However, silencing host proteins may be cytotoxic

and thus damaging to the cell. If cytotoxicity can be excluded, drug re-purposing becomes an option.

*In silico*, our modeling predicted vRNA translation and synthesis as the most promising drug target found that may be conserved among (+)RNA viruses [191]. Considering our theoretical experiment, where a decreased ribosome availability lowered viral replication, it is unsurprising that vRNA translation has been selected as a sensitive process with drug-targeting potential. However, targeting vRNA translation or inhibiting the formation of the translation complex or even ribosomes seems particularly challenging. However, an eIF2- $\alpha$  inhibitor, nitazoxanide, may be an interesting host factor targeting candidate. Nitazoxanide is FDA-approved and developed initially as an antiparasitic [50]. Nitazoxanide has shown a broad-spectrum antiviral effect in hepatitis C, where nitazoxanide, in combination with IFN- $\alpha$ , achieved SVR rates of 79%. However, its further investigation as an antiviral agent has been terminated due to the development and approval of DAAs [80]. Furthermore, in hepatitis B patients, nitazoxanide leads to a loss of serum HBsAg, the hepatitis B surface antigen, in a subset of patients, which is the challenge of the current hepatitis B standard of care [148]. *In vitro*, nitazoxanide inhibits the viral replication of various viruses such as influenza A and B, coronaviruses (including SARS-CoV-2), chikungunya, dengue, yellow fever, Japanese encephalitis, noro-, Ebola, and other viruses [107]. Furthermore, the efficacy and safety of other host factor-targeting drugs with broad-spectrum antiviral activity are currently tested in clinical trials. For example, iminosugars interact with the folding of envelope proteins of HIV, HCV, DENV, ebola, and influenza viruses. Another example is geldanamycin derivatives, which are also involved in the folding of viral proteins necessary for viral replication in, e.g., HIV, HCV, DENV, influenza, ebola, herpes simplex, chikungunya, and Zika virus [80].

Nevertheless, targeting a particular host factor may even promote viral replication. Our modeling suggested that targeting vRNA trafficking may promote viral growth [191]. Furthermore, considering the possible infectivity of vRNA-carrying exosomes *in vivo*, targeting host dependency factors that, for example, intervene with the infectivity of a virus, as in the case of apoE in HCV or misfolding of envelope proteins, may result in increased cell-to-cell transmission. Nevertheless, host-directed therapy is in its infancy but has vast potential.

## 5.5 Limitations and future research

Even though our models were most suited to describe the dynamics of various viruses and gave valuable insights into different aspects of virus-host interactions, several limitations may be addressed in the future. The developed mathematical models were of a high degree of detail and based exclusively on ODE systems. Since we analyzed the time dynamics of the early phase post-virus infection and studied the viral life cycle in detail within an average infected cell, spatial considerations were neglected. However, our intracellular models may contribute to understanding the intracellular viral replication process, serve as a starting point for model extensions, and promote the development of biological experiments. Advanced and improved experimental

techniques such as single-cell analysis and high-resolution microscopy may help to gain a more comprehensive understanding of spatial-temporal processes within a host cell and the disease spread to naive cells. Nevertheless, measuring intracellular viral replication processes, e.g., the density of bound ribosomes to one single viral genome, the kinetics of the virion assembly process, or the number of virions a single cell produces, is challenging. To date, our model predictions still need to be experimentally validated. In general, a lack of experimentally validated knowledge of intracellular spatial-temporal processes that serve as the basis for the development of mathematical models, the quality and quantity of the underlying data the models are fit to, over-fitting, and uncertainty are only a few pitfalls in mathematical modeling. Nevertheless, without suitable biological experiments, mathematical modeling remains a valuable tool to suggest experimental design and generate predictions. Despite the high degree of freedom and uncertainty, the mathematical models developed in this thesis were suited to describe the experimental measurements of the intracellular viral genome translation and replication processes and confirmed biological knowledge. Furthermore, they were consistent in their predictions: host dependency and restriction factors shape the life cycles and replication efficiency of (+)RNA viruses.

Nevertheless, our mathematical models were developed for (+)RNA viruses containing one ORF. In the future, the models may be extended to the life cycle of (+)RNA viruses with more than one ORF and thus the presence of sub-genomic viral RNA, as in the case of SARS-CoV-2 or chikungunya virus. The logical next step may be adapting our mathematical models to the replication mechanisms of other virus groups. However, due to the involvement of the nucleus or the integration of the viral genome in the host genome, developing intracellular virus replication models for the viral life cycles of other virus groups, such as DNA or reverse transcribing viruses, e.g., HBV and HIV, may be an interesting future challenge. Furthermore, host factors are universal in the viral replication cycle. Whether host factors support or restrict viruses in their replication, viruses with a different life cycle depend on host factors like (+)RNA viruses. Furthermore, the degree to which host factors may determine the clinical outcome, as suggested by our models, needs further research and may be highly important in the clinical treatment of viral infectious diseases. However, studying and comparing host factors of different virus groups may promote the development of broad-spectrum antiviral drugs. Nevertheless, broad-spectrum antiviral drugs may be unable to silence the viral life cycle altogether, and viruses may find alternative ways to spread the infection. Our research emphasized the importance of understanding cell-to-cell communication, e.g., via exosomes, in more detail. Detailed knowledge of viral replication strategies within a host cell is as necessary as understanding infection spread to naive cells. The infection spread via exosomes is controversial. However, more future research is needed to solve this controversy, and our model predictions may serve as a starting point for the design of experiments. Thus, our research contributes to understanding virus disease dynamics and pathogenesis. However, several unanswered questions remain for future research.

---

Quantifying intracellular processes related to viral replication strategies, pathogenesis, and treatment opportunities remain experimentally challenging. A mathematical model, however, represents the tool of choice to study viral dynamics and kinetics, especially in the case of expensive experiments or those that must be designed. In the presented thesis, we successfully developed and applied mathematical models with great detail to fascinating questions concerning the (+)RNA virus life cycle:

- Our mathematical models shed light on pan-viral and virus-specific replication mechanisms and *in silico* predicted broad-spectrum antiviral treatment opportunities.
- Our mathematical models predicted that the cellular immune response blocks the viral life cycle at multiple steps and suggested viral strategies to countermeasure the immune system's recognition.
- Our mathematical models suggested a possible explanation of cell-to-cell communication via exosomes as an alternative infection spread pathway in patients with measurable plasma HCV at the end of treatment.

Interestingly, in every research project, host factors have been identified as critical players in shaping the viral life cycle, highlighting the importance of future research. The presented thesis aimed to develop mathematical models to study and shed light on the (+)RNA virus replication mechanisms and may help develop broad-spectrum antiviral drugs. Especially the global SARS-CoV-2 pandemic has proven that without vaccines or antiviral drugs, the fight against infectious diseases solely depends on human behavior. Our mathematical models contribute to understanding viral dynamics and provide a foundation for future research in the fight against infectious diseases.



# PUBLICATIONS

**Literature review: Mathematical analysis of viral replication dynamics and antiviral treatment strategies: From basic models to age-based multiscale modeling.**

**Carolin Zitzmann\***, Lars Kaderali (2018) *Mathematical analysis of viral replication dynamics and antiviral treatment strategies: From basic models to age-based multiscale modeling*. *Frontiers in microbiology* 9:1546.

I contributed to conceptualization, visualization, and writing—original draft, review & editing.

\* Corresponding author



# Mathematical Analysis of Viral Replication Dynamics and Antiviral Treatment Strategies: From Basic Models to Age-Based Multi-Scale Modeling

Carolin Zitzmann\* and Lars Kaderali

*Institute of Bioinformatics and Center for Functional Genomics of Microbes, University Medicine Greifswald, Greifswald, Germany*

## OPEN ACCESS

### Edited by:

Thomas Dandekar,  
Universität Würzburg, Germany

### Reviewed by:

Marc Thilo Figge,  
Leibniz-Institut für  
Naturstoff-Forschung und  
Infektionsbiologie, Hans Knöll Institut,  
Germany

Larance Ronsard,  
Ragon Institute of MGH, MIT and  
Harvard, Massachusetts Institute of  
Technology, United States

### \*Correspondence:

Carolin Zitzmann  
carolin.zitzmann@uni-greifswald.de

### Specialty section:

This article was submitted to  
Infectious Diseases,  
a section of the journal  
Frontiers in Microbiology

**Received:** 08 January 2018

**Accepted:** 21 June 2018

**Published:** 11 July 2018

### Citation:

Zitzmann C and Kaderali L (2018)  
Mathematical Analysis of Viral  
Replication Dynamics and Antiviral  
Treatment Strategies: From Basic  
Models to Age-Based Multi-Scale  
Modeling. *Front. Microbiol.* 9:1546.  
doi: 10.3389/fmicb.2018.01546

Viral infectious diseases are a global health concern, as is evident by recent outbreaks of the middle east respiratory syndrome, Ebola virus disease, and re-emerging zika, dengue, and chikungunya fevers. Viral epidemics are a socio-economic burden that causes short- and long-term costs for disease diagnosis and treatment as well as a loss in productivity by absenteeism. These outbreaks and their socio-economic costs underline the necessity for a precise analysis of virus-host interactions, which would help to understand disease mechanisms and to develop therapeutic interventions. The combination of quantitative measurements and dynamic mathematical modeling has increased our understanding of the within-host infection dynamics and has led to important insights into viral pathogenesis, transmission, and disease progression. Furthermore, virus-host models helped to identify drug targets, to predict the treatment duration to achieve cure, and to reduce treatment costs. In this article, we review important achievements made by mathematical modeling of viral kinetics on the extracellular, intracellular, and multi-scale level for Human Immunodeficiency Virus, Hepatitis C Virus, Influenza A Virus, Ebola Virus, Dengue Virus, and Zika Virus. Herein, we focus on basic mathematical models on the population scale (so-called target cell-limited models), detailed models regarding the most important steps in the viral life cycle, and the combination of both. For this purpose, we review how mathematical modeling of viral dynamics helped to understand the virus-host interactions and disease progression or clearance. Additionally, we review different types and effects of therapeutic strategies and how mathematical modeling has been used to predict new treatment regimens.

**Keywords:** mathematical modeling, viral kinetics, viral replication, human immunodeficiency virus, Hepatitis C virus, Influenza A virus, antiviral therapy, immune response

## INTRODUCTION

Viruses are small obligate intracellular parasites that are unable to reproduce independent of their host. Outbreaks of infectious viral diseases are a major global health concern, a circumstance that is evident by recent large epidemics of influenza, zika fever, Ebola virus disease, and the Middle East Respiratory Syndrome (MERS). According to the United Nations, the recent zika outbreak



caused socio-economic costs of approximately US\$7-18 billion in Latin America and the Caribbean from 2015 to 2017 (United Nations, 2017). A recent study estimated the socio-economic costs for symptomatic dengue cases (58.40 million) with US\$8.9 billion in 141 countries in 2013 (Shepard et al., 2016). This number is expected to rise further in the coming years. Factors such as climate change and increasing air travel are furthermore increasing the risk of global pandemic infections; examples are recent global influenza outbreaks as much as the emergence of tropical infections such as Dengue Virus infections in previously unaffected regions in the United States and Europe (Mackey et al., 2014). To control this global threat, novel therapeutic and antiviral treatment approaches are urgently needed. To amplify the development of such novel drugs and to optimize treatment strategies, a comprehensive understanding of the viral infection dynamics, their parasitic interaction with their host, as well as host defense strategies against the invader are of major importance. In recent years, targeting viral agents that are essential for the viral replication has proven highly effective (Asselah et al., 2016). However, the emergence of resistance against these direct acting antiviral compounds leads more and more to treatment failure and multi-drug resistant viral strains (Poveda et al., 2014). In order to circumvent drug-resistance, novel antiviral strategies focus on the host by supporting the immune response or targeting host factors required for the viral life cycle. The advantage of these methods are higher barriers for the development of resistance and novel opportunity of broad-spectrum antivirals (Zeisel et al., 2013).

Mathematical modeling has proven to be a powerful tool to study viral pathogenesis and has yielded insights into the intracellular viral infection dynamics, the effect of the immune system, the evaluation of treatment strategies, and the development of drug resistance (Bonhoeffer et al., 1997; Perelson, 2002; Rong and Perelson, 2009; Perelson and Ribeiro, 2013; Boianelli et al., 2015; Perelson and Guedj, 2015; Ciupe and Heffernan, 2017). Modeling can deepen our understanding on different scales: From the molecular scale of intracellular virus-host interactions, extracellular cell-to-cell infection at the population scale, to virus spread within organs or whole organisms (Kumberger et al., 2016). In order to quantitatively study the viral growth at a molecular level and to investigate host requirements and limitations, first intracellular models have been developed for bacteriophages (Buchholz and Schneider, 1987; Eigen et al., 1991; Endy et al., 1997), Baculovirus (Dee and Shuler, 1997), and Semliki Forest Virus (Dee et al., 1995). By studying cell-to-cell infection, early models for Human Immunodeficiency Virus (HIV) (Ho et al., 1995; Wei et al., 1995; Perelson et al., 1996, 1997; Stafford et al., 2000) provided insights into the

**Abbreviations:** AIR, Adaptive Immune Response; ART, Antiretroviral Therapy; CTL, Cytotoxic T lymphocytes; DAA, Direct-Acting Antiviral; DENV, Dengue Virus; EBOV, Ebola Virus; HAART, Highly Active Antiretroviral Therapy; HCV, Hepatitis C Virus; HIV, Human Immunodeficiency Virus; IAV, Influenza A Virus; IFN, Interferon; IIR, Innate Immune Response; NS, Nonstructural Protein; ODE, Ordinary Differential Equation; SVR, Sustained Virologic Response; WHO, World Health Organization; ZIKV, Zika Virus.

pathogenesis, treatment strategies, and virus control by the immune system.

On the population scale, the target cell-limited model (Nowak and Bangham, 1996; Nowak et al., 1996; Bonhoeffer et al., 1997; Perelson, 2002; Wodarz and Nowak, 2002) has been extensively used to investigate the virus-host interaction of HIV, Hepatitis C Virus (HCV), and Influenza A Virus (IAV), which will be explained in this review in more detail. Furthermore, we describe the latest achievements made by modeling the dynamics of Ebola Virus (EBOV), Dengue Virus (DENV), and Zika Virus (ZIKV) that caused the most recent viral outbreaks. In addition, we give an introduction into the target cell-limited model with its extensions and applications to investigate the effects of direct antiviral therapy and immune response and highlight the most important achievements made by viral modeling of the intracellular, extracellular and the integration of both, the multi-scale level.

## THE TARGET CELL-LIMITED MODEL AND ITS EXTENSIONS

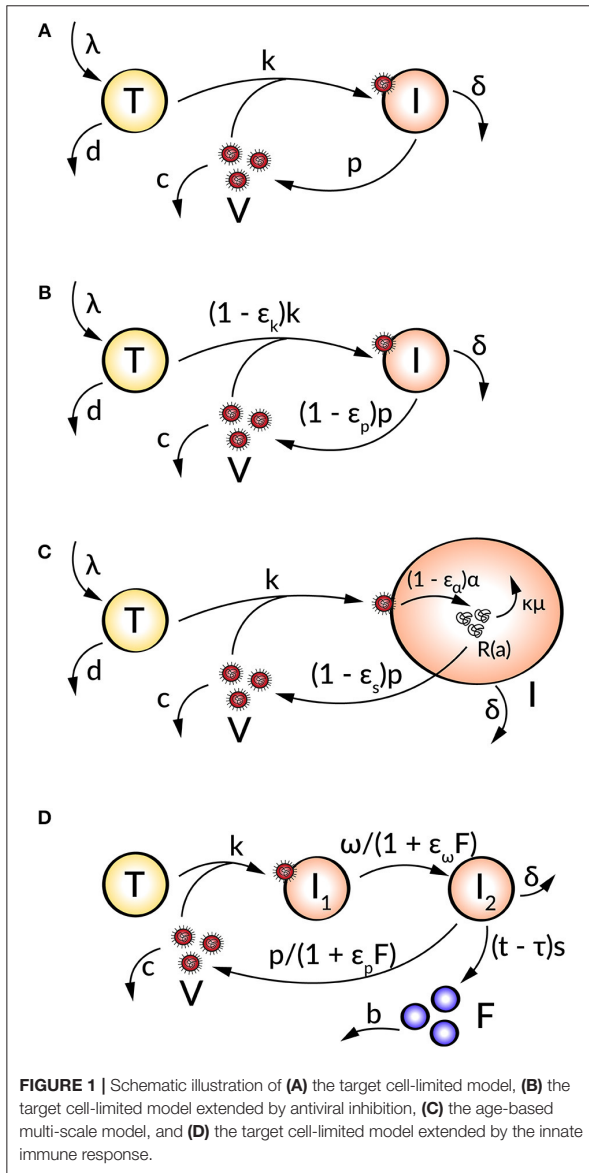
### Target Cell-Limited Model

The first mathematical models described the HIV progression by neglecting intracellular processes and taking only the key players of the virus-host interaction into account (Perelson et al., 1993, 1996, 1997; Ho et al., 1995; Bonhoeffer et al., 1997). The target cell-limited model (**Figure 1A**) includes three species: uninfected susceptible target cells ( $T$ ), infected virus-producing cells ( $I$ ), and the virus load ( $V$ ) and is formulated by the following system of nonlinear ordinary differential equations (ODEs):

$$\begin{aligned}\frac{dT}{dt} &= \lambda - dT - kVT, \\ \frac{dI}{dt} &= kVT - \delta I, \\ \frac{dV}{dt} &= pI - cV.\end{aligned}\tag{1}$$

Uninfected target cells ( $T$ ) are produced at a constant rate  $\lambda$  and die at rate  $d$ , corresponding to a target cell half-life of  $t_{T1/2} = \frac{\ln(2)}{d}$ . By the interaction of virus ( $V$ ) with uninfected target cells ( $T$ ) at a constant infectivity rate  $k$ , the target cells become infected cells ( $I$ ), which in turn produce infectious virus ( $V$ ) with production rate  $p$ . Due to viral cytopathicity, immune elimination and/or apoptosis, infected cells ( $I$ ) die at a rate  $\delta$  [resulting in an infected cell half-life  $t_{I1/2} = \frac{\ln(2)}{\delta}$ ]. Virus is cleared at rate  $c$  from the cells [virion half-life  $t_{V1/2} = \frac{\ln(2)}{c}$ ] per virion by mechanisms such as immune elimination (Nowak and Bangham, 1996; Nowak et al., 1996; Bonhoeffer et al., 1997; Perelson, 2002; Wodarz and Nowak, 2002).

With average lifetimes of  $1/d$ ,  $1/\delta$ , and  $1/c$  for uninfected target cells, infected cells, and virus, respectively, the total number of virus particles  $N$  produced by one infected cell during



its lifetime is calculated by  $p/\delta$ . Therefore, the production rate  $p$  of one infected cell is  $p = N\delta$ . Without a viral infection ( $I = 0$  and  $V = 0$ ), target cells are in equilibrium with  $\lambda/d$  (Nowak and May, 2001; Perelson, 2002; Wodarz and Nowak, 2002).

The ability of a virus to develop an infection or to be cleared is given by the basic reproductive ratio  $R_0 = \frac{\lambda kp}{d\delta c}$ .  $R_0$  represents the number of productively infected cells newly generated by one productively infected cell. With  $R_0 > 1$  the infection grows due to an increase in virus-producing infected cells while  $R_0 < 1$  refers to a decrease in productively infected cells and viral clearance (Nowak and May, 2001).

### Target Cell-Limited Model and Antiviral Therapy

To analyze the effect of antiviral drugs that either block infection ( $\epsilon_k$ ) and/or production of viral particles ( $\epsilon_p$ ), the target cell-limited model is modified as follows (Figure 1B):

$$\begin{aligned} \frac{dT}{dt} &= \lambda - dT - (1 - \epsilon_k)kVT, \\ \frac{dI}{dt} &= (1 - \epsilon_k)kVT - \delta I, \\ \frac{dV}{dt} &= (1 - \epsilon_p)pI - cV, \end{aligned} \tag{2}$$

with  $0 \leq \epsilon_{k,p} \leq 1$  (Neumann, 1998). Here,  $\epsilon_{k,p} = 0$  describes no drug effect while  $\epsilon_{k,p} = 1$  refers to the case of a 100% effective treatment—a perfect drug. Note that before treatment  $\epsilon_{k,p} = 0$ . In simulating treatment, one assumes that the system is in steady state at treatment initiation, at which point the infection and/or production rates are modified depending on the type of antiviral drug used ( $\epsilon_k > 0$  and/or  $\epsilon_p > 0$ ). The overall drug efficacy  $\epsilon_{tot}$  may be calculated as  $\epsilon_{tot} = 1 - (1 - \epsilon_k)(1 - \epsilon_p)$ , while the critical drug efficacy  $\epsilon_c$  is given by  $\epsilon_c = 1 - \frac{d\delta c}{\lambda kp}$  and determines the transition from viral eradication to viral persistence. A successful drug therapy would clear the virus with  $\epsilon_{tot} > \epsilon_c$  while the infection becomes chronic when  $\epsilon_{tot} < \epsilon_c$  (Dahari et al., 2007a).

The relationship between a certain drug dose and the resulting response can be integrated into the target cell-limited model by the simple time-dependent pharmacodynamic equation

$$\epsilon(t) = \frac{\epsilon_{max} \cdot C(t)^n}{EC_{50}^n + C(t)^n}, \tag{3}$$

where  $\epsilon_{max}$  describes the maximum of the drug effect,  $EC_{50}$  the drug concentration with 50% efficacy, and  $C(t)$  the drug concentration or dose applied (Holford and Sheiner, 1982). Depending on the shape and steepness of the underlying drug effect, the Hill coefficient  $n$  describes either a sigmoidal curve for  $n > 1$  or a hyperbolic curve otherwise. By substituting  $C(t)$  by  $C(t - \tau)$ , a pharmacodynamic delay  $\tau$  for the drug effect can be taken into account for  $t > \tau$  (Holford and Sheiner, 1982; Guedj et al., 2010; Canini and Perelson, 2014).

### Age-Based Multi-Scale Model for Direct Acting Antivirals

Age-based multi-scale models have been used in order to study the modes of action of antivirals within a virus-infected cell (Nelson et al., 2004; Guedj et al., 2013; Heldt et al., 2013; Clausznitzer et al., 2015). To include the effect of direct acting antivirals (DAAs), the target cell-limited model can be further extended by more detailed intracellular processes of the viral life cycle (Figure 1C). These multi-scale models that take the age of infected cells into account allow a biologically more realistic representation of intracellular processes with age-dependent reaction rates (Quintela et al., 2017). The target cell-limited model coupled to intracellular processes and an age-dependency is formulated as follows:

$$\begin{aligned} \frac{dT}{dt} &= \lambda - dT - kTV, \\ \frac{\partial I}{\partial a} + \frac{\partial I}{\partial t} &= \delta I(a, t), \\ \frac{\partial R}{\partial a} + \frac{\partial R}{\partial t} &= (1 - \varepsilon_\alpha)\alpha - \kappa\mu R - (1 - \varepsilon_s)\rho R, \\ \frac{dV}{dt} &= (1 - \varepsilon_s)\rho \int_0^\infty R(a, t) I(a, t) da - cV, \end{aligned} \tag{4}$$

with boundary and initial conditions  $I(0, t) = kVT$ ,  $I(a, 0) = I_0(a)$ ,  $R(0, a) = 1$ , and  $R(a, 0) = R_0(a)$  (Guedj et al., 2013). Here, the intracellular viral genome ( $R$ ) is produced at constant rate  $\alpha$  and degraded at constant rate  $\mu$ . The progeny virions are assembled and secreted at constant rate  $\rho$ . The drug effects regard intracellular processes or the viral genome replication: blocking viral RNA production  $\varepsilon_\alpha$  and virion assembly/secretion  $\varepsilon_s$ , as well as increasing viral RNA degradation  $\kappa$  for  $\kappa > 1$ . Note that the intracellular viral genome  $[R(a)]$  and infected cells  $[I(a)]$  are dependent on the age  $a$  of the cell, measured as time elapsed since infection, and viral RNA levels increase with the age of the infected cell (Guedj et al., 2013; Canini and Perelson, 2014; Perelson and Guedj, 2015).

### Extended Target Cell-Limited Model by the Immune Response

The innate and adaptive immune response provide various mechanisms in fighting a viral infection. The innate immune response (IIR) represents the first line of defense that recognizes the virus and triggers the adaptive immune response (AIR) (Braciale et al., 2013; Iwasaki and Medzhitov, 2013). In order to study the effect of the immune response on the viral dynamics, mathematical models incorporate key players of the immune response which inhibit processes in the viral life cycle. A further modification of the target cell-limited model has been developed to take the effect of the cell's IIR into account (Figure 1D). This is done by including the effect of interferon (IFN) into the model:

$$\begin{aligned} \frac{dT}{dt} &= -kTV, \\ \frac{dI_1}{dt} &= kTV - \frac{\omega}{1 + \varepsilon_\omega F} I_1, \\ \frac{dI_2}{dt} &= \frac{\omega}{1 + \varepsilon_\omega F} I_1 - \delta I_2 - sI_2(t - \tau) F, \\ \frac{dV}{dt} &= \frac{p}{1 + \varepsilon_p F} I_2 - cV, \\ \frac{dF}{dt} &= sI_2(t - \tau) - bF. \end{aligned} \tag{5}$$

Herein, two populations of infected cells  $I_1$  and  $I_2$  describe a time delay. Infected but not yet virus producing cells ( $I_1$ ) in the eclipse phase become productively virus producing cells ( $I_2$ ) with average transition time  $1/\frac{\omega}{1+\varepsilon_\omega F}$ . Note that  $I_1$  are not dying before the transition into  $I_2$ . Following a time delay  $\tau$  for the IIR, IFN ( $F$ ) is secreted by  $I_2$  at constant rate  $s$  and degrades at constant rate  $b$ .

The effect of IFN has been modeled by decreasing the transition rate  $\omega$  and/or the virus production rate  $p$  and effectiveness  $\varepsilon_\omega$  and  $\varepsilon_p$  (Baccam et al., 2006).

Moreover, the effect of the IIR and the AIR can be coupled with the target cell-limited model by simple assumptions:

$$\begin{aligned} \frac{dT}{dt} &= rD - kTV, \\ \frac{dI_1}{dt} &= kTV - \omega I_1, \\ \frac{dI_2}{dt} &= \omega I_1 - \delta I_2, \\ \frac{dD}{dt} &= \delta I_2 - rD, \\ \frac{dV}{dt} &= \frac{p}{1 + \varepsilon_p R_{IIR}} I_2 - cV - \gamma kTV - hVR_{AIR}, \\ \frac{dR_{IIR}}{dt} &= \psi V - bR_{IIR}, \\ \frac{dR_{AIR}}{dt} &= fV + \beta R_{AIR}. \end{aligned} \tag{6}$$

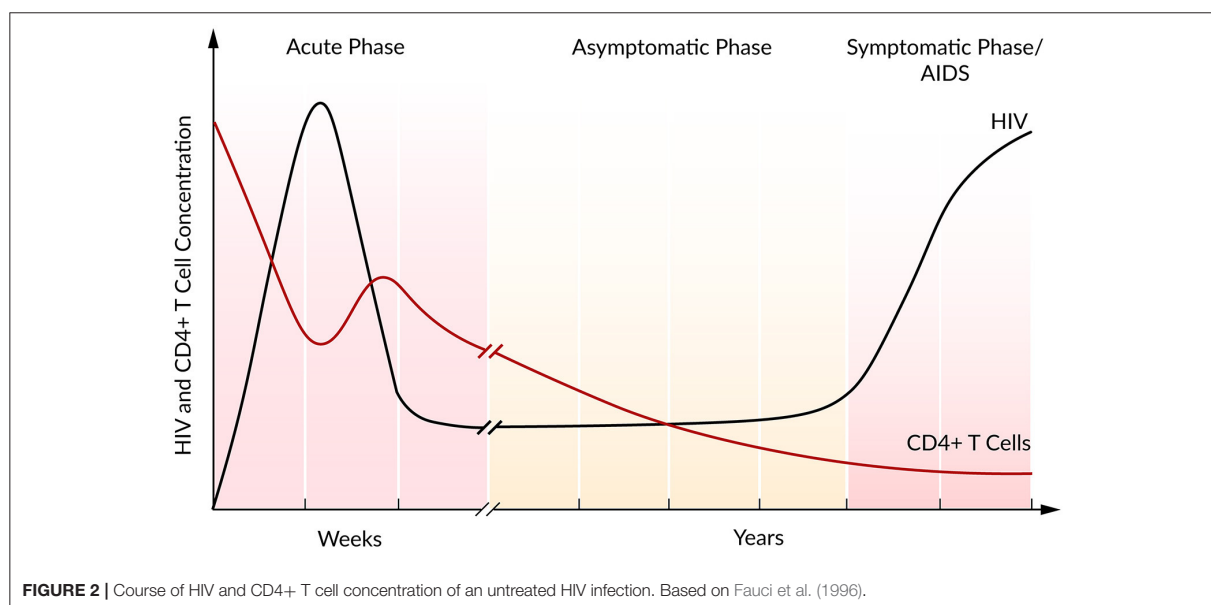
In this model, the IIR ( $R_{IIR}$ ) represent cytokines and recruited cells of the IIR, e.g., neutrophils and macrophages while the AIR ( $R_{AIR}$ ) is represented as humoral immune response via B-cells and antibodies. With the free virus, the  $R_{IIR}$  expands at constant rate  $\psi$  and dies at constant rate  $b$ . Herein, the effect of the IIR is modeled by blocking the virus production rate  $p$ . The  $R_{AIR}$  is triggered by the virus and recruited at constant rate  $f$ . By clonal expansion at rate constant  $\beta$ , the  $R_{AIR}$  is activated and neutralizes the virus with constant rate  $h$ . Note that in this coupled model the dead cells  $D$  are replaced by new target cells at constant rate  $r$  that represents the regeneration of susceptible cells (Handel et al., 2010).

## MODELING HIV INFECTIONS

HIV infects cells of the immune system and causes AIDS within 2–15 years post infection. In 2016, the World Health Organization (WHO) estimated that globally 36.7 million people were living with HIV with 1.8 million new infections in 2016. More than 19.5 million of these were treated with a lifelong antiretroviral therapy (ART), the current standard of care. Nowadays, the replication of HIV can be controlled and suppressed by the combination of at least three antiretroviral drugs, e.g., by reverse transcriptase inhibitors and protease inhibitors (World Health Organization, 2017b). These drugs have to be taken live-long and treatment regimens need to be adapted regularly to keep the infection under control. To date, no curative drugs and no vaccine against HIV are available.

### Viral Dynamics

In the majority of cases, the infection with HIV follows a typical pattern of three different phases (Figure 2) (Simon and Ho, 2003; Munier and Kelleher, 2007). The first weeks post infection, the acute phase, are characterized by an exponential increase in viral load accompanied by a rapid depletion of CD4+ T cells,



the target cells of HIV. Soon after the infection, the immune response kicks in and initiates a decrease in viral load until a constant level, the so-called set point, is reached (Ho, 1996). Within this second asymptomatic phase, the virus persists for years while CD4+ T cells continuously and slowly decline. The third and final phase is characterized by a gradual depletion in CD4+ T cells that is correlated with a strong increase in the viral plasma concentration leading to AIDS (Alizon and Magnus, 2012; Maartens et al., 2014).

During the asymptomatic phase, the viral set point is maintained by a balance in viral clearance and the total virion production rate ( $p_{total} = cV$ ). Therefore, a strong increase in viral load that is associated with a lower viral clearance rate indicates a stronger total viral production rate  $p_{total} > cV$ , while a decrease in viral load refers to a higher clearance rate,  $p_{total} < cV$ . Perturbations of this system equilibrium, e.g., by blocking viral production, lead to information on the rate constants and insights into the course of the viral infection and the potential of antiviral interventions (Perelson, 2002). At steady state and in the absence of ART, it has been estimated that HIV is a rapidly replicating virus that produces  $10^{10}$  virions per day. Furthermore, a rapid virus replication also requires strong viral clearance to maintain the equilibrium (Perelson et al., 1996; Ramratnam et al., 1999).

HIV replicates in CD4+ T cells, which are represented by the target and infected cells in the target cell-limited model. With a modified target cell-limited model, Ribeiro et al. (2010) investigated the very early plasma viremia post exposure to HIV in 47 HIV-positive patients. After a time delay of 24 h where the virus became detectable ( $>50$  RNA copies per mL), simulations have shown an initial viral doubling time of 0.65 days. Viral load peaked at  $10^6$  HIV RNA copies per mL after 14 days. The subsequent viral decline was characterized by a virion half-life

of 1.2 days ( $c = 0.6 \text{ day}^{-1}$ ). Moreover, for this early infection stage, the authors calculated the basic reproductive ratio of  $R_0 \sim 8$ , indicating rapid viral spread and the necessity of an early intervention in order to reduce viral spread and to prevent development of chronicity (Ribeiro et al., 2010). By measuring the viral load in 10 HIV-positive patients for on average the first 100 days during primary infection, Stafford et al. (2000) have shown that the target cell-limited model is able to reproduce the interpatient variability within the highly dynamic initial phase post infection. The model simulations provided strong evidence that the initial viral load decline is due to a limitation in target cells with an estimated lifetime of 2.5 days ( $\delta = 0.39 \text{ day}^{-1}$ ) for infected virus-producing cells. However, the target cell-limited model was not able to mimic the data in all the patients equally well. Therefore, the authors suggested that processes not included in the model, such as an involvement of the immune response by CD8+ T cells or destruction of infected cells by cytotoxic T lymphocytes (CTL), might be associated with the stronger than predicted decrease of viral load observed in some patients (Stafford et al., 2000).

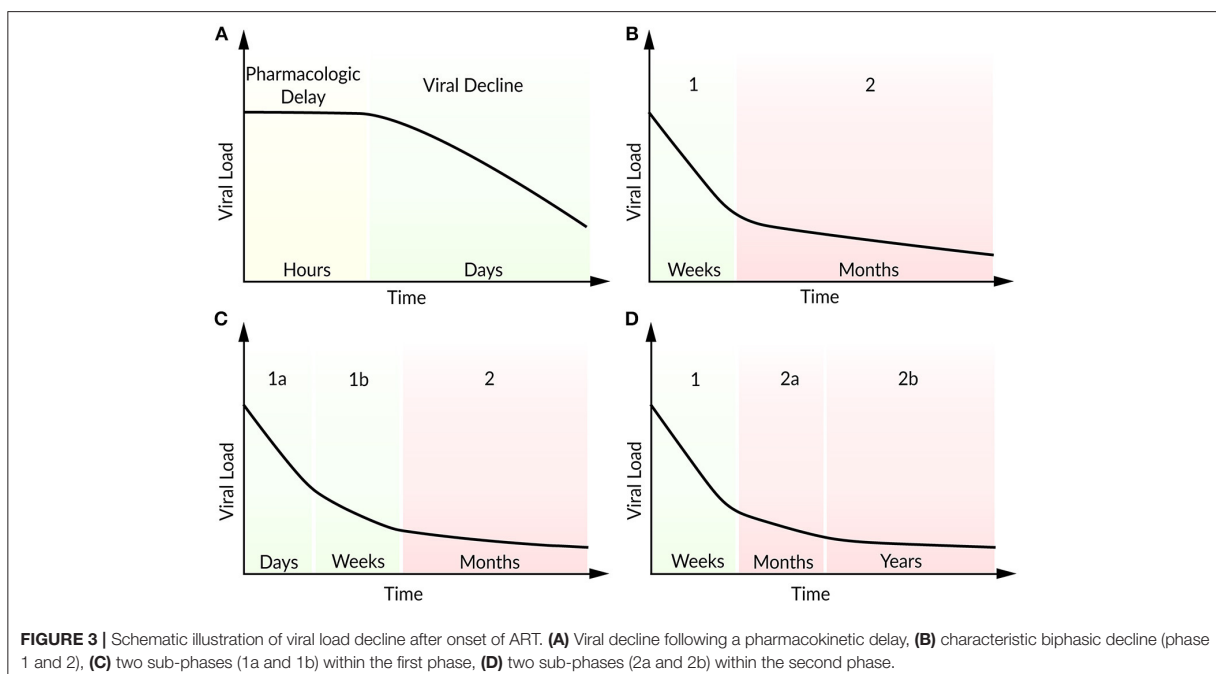
### Antiretroviral Therapy

For more than 20 years, HIV-positive patients are treated with a combination of antiretroviral drugs. To analyze the effects of an antiviral treatment regimen, the target cell-limited model can be modified to include the effects of reverse transcriptase inhibitors ( $\varepsilon_k$ ) that block viral infectivity ( $k$ ) and protease inhibitors ( $\varepsilon_p$ ) which reduce viral production ( $p$ ) (Neumann, 1998). The effect of a protease inhibitor has been investigated within the first 7 days after the oral administration of Ritonavir (Perelson et al., 1996). Following a pharmacokinetic delay, the patients responded well to the Ritonavir treatment with a continuous decline in plasma viral load. In order to study the viral decline under ART,

Perelson et al. (1996) modified the target cell-limited model by the assumption that by the time of drug administration newly produced virions are non-infectious. After a pharmacokinetic delay of about 1.25 days, the model reproduced the strong decline in plasma viremia according to the Ritonavir-treated patients (**Figure 3A**). The model predicted lifetimes of 2.2 days for virus-producing infected cells and 0.3 days for virions (Perelson et al., 1996). Note that at the onset of ART, the system is assumed to be in steady state. By studying the long-term combination therapy of the protease inhibitor Nelfinavir and the reverse transcriptase inhibitors Zidovudine and Lamivudine, all the patients responded in a similar viral decline pattern (**Figure 3B**). After initiation of ART, a biphasic viral decline has been observed: a rapid initial reduction in viral load and productively infected cells (phase 1) followed by a slower decrease (phase 2). Perelson et al. (1997) integrated long-lived CD4+ T cells and latently infected lymphocytes that become productively virus-producing cells upon activation as second sources of virus into the target cell-limited model. The authors identified long-lived infected CD4+ T cells with a half-life of 14.1 days (compared to a half-life of 1.1 days of short-lived infected cells) and the continuous release of trapped virus as the main contributors for the second phase (Perelson et al., 1997). Subsequent studies have found more accurate estimates for the virion half-life with 28–110 min in HIV-positive patients under plasma apheresis (Ramratnam et al., 1999) and productively-infected CD4+ T cell half-life of 0.7 days under combination therapy (Markowitz et al., 2003). The continuous viral replication upon activation that is associated with viral persistence represents the challenge in finding a cure for HIV. Even highly active antiretroviral therapy (HAART)

does not stop viral production completely, but can achieve a suppression of the viral load in plasma below levels of detection (<50 RNA copies per mL). It is assumed that the main reason for failure to achieve a cure is viral latency. At the same time, the transmission of drug-resistant virus strains is increasing, resulting in increasing treatment failure rates (Little et al., 2002).

In patients with multi-drug resistant virus, Raltegravir represents a promising new antiviral drug that inhibits integrase and hence prevents the strand transfer of proviral DNA into the host-cell genome (Steigbigel et al., 2008). Andrade et al. (2015) analyzed the effect of Raltegravir in monotherapy and in combination with the reverse transcript inhibitors Emtricitabine and Tenofovir Disoproxil Fumarate by an extended target cell-limited model that discriminates between infected cells with and without integrated viral DNA. The authors found a biphasic decline within the first phase during the first 10 days after onset of ART (**Figure 3C**). A loss in infected cells with integrated viral DNA and a half-life of ~0.8 days (in agreement with 0.7 days in Markowitz et al., 2003) has been identified as the main contributor to the first sub-phase (phase 1a). Cell loss and in addition the integration of provirus into pre-integrated infected cells have been identified as key contributors to the slower decay in the second sub-phase (phase 1b). Interestingly, the half-life of unintegrated infected cells depended strongly on the provirus integration rate and has been estimated to lie between 4 and 7 days (Andrade et al., 2015). Cardozo et al. (2017) generalized the model of Andrade et al. (2015) by taking long-lived infected cells and the effect of protease inhibitor into account in order to investigate the viral decay in presence or absence of Raltegravir therapy (Cardozo et al., 2017). Herein, the therapy containing



the integrase strand transfer inhibitor Raltegravir replaced as well the first phase by two sub-phases. The traditional therapy regimen without Raltegravir has shown the typical biphasic decline in viral load. Under Raltegravir therapy, the first phase was associated with the loss of short-lived cells while the second phase corresponded to the loss of long-lived cells with a half-life of  $\sim 33$  days. The decline of the short-lived cell population within the first phase can be further separated by a loss of productively virus-producing cells with a half-life of  $\sim 0.8$  days in sub-phase 1a and by pre-integration cells that showed a half-life of  $\sim 1.8$  days. Furthermore, long-lived cells showed a shorter viral integration rate ( $0.05 \text{ day}^{-1}$ ) compared to short-lived cells with a viral integration rate of  $2.6 \text{ day}^{-1}$  (Cardozo et al., 2017).

Moreover, in patients under long-term ART, Palmer et al. (2008) studied a second biphasic decline within the second phase referring to two sources of viremia with persisting virus for more than 7 years (Figure 3D) (Palmer et al., 2008). Kim and Perelson (2006) introduced a model extended by the proliferation of latently infected CD4+ T cells without being activated (bystander proliferation) and explained the persistence of a latent reservoir (Kim and Perelson, 2006). Chomont et al. (2009) observed these results experimentally and identified two different memory T cells contributing to the long-lasting reservoir and thus the persistence of HIV for decades (Chomont et al., 2009). Therefore, an early antiretroviral intervention is necessary to limit the size of the latent reservoir.

However, to understand the effect of ART within the host cell, a comprehensive investigation of the viral life cycle is necessary. Reddy and Yin (1999) described a detailed model of the intracellular viral growth starting with reverse transcription to particle production and maturation. Their simulation results and sensitivity analysis predicted a higher monotherapeutic effect of reverse transcription inhibitors ( $\epsilon_k$ ) than protease inhibitors ( $\epsilon_p$ ). A 10-fold decrease in viral reverse transcriptase reduced the overall viral replication to  $<1\%$ . Moreover, they found that the 10-fold inhibition of Rev—a regulator protein of virion production—increased the viral production, whereas a 100-fold inhibition decreased the production of virions (Reddy and Yin, 1999). These results indicate that incomplete inhibition might be compensated that might lead to adverse and unwanted effects.

As with other RNA viruses, the HIV genome is highly variable, posing its own challenges to treatment. For example, the trans-activating regulatory protein Tat controls gene expression and activates viral transcription by binding at the trans-activating response element TAR (Karn and Stoltzfus, 2012). It has been shown that point mutations in Tat may lead to more virulent HIV strains with higher stability and transcription efficiency which aggravate the development of novel antiretroviral drugs (Ronsard et al., 2014, 2017a; Ronsard, 2017b). On the other hand, Tat might be a promising vaccine candidate and has shown potential in the reduction of HIV plasma viremia associated with a reduced immune activation (Gray et al., 2016). Taking genomic variability and genetic drift of HIV under treatment into account is an important issue, and several authors have modeled the within-host evolution of HIV under selective pressure, see for example (Ribeiro and Bonhoeffer, 2000; Wodarz and Lloyd, 2004; Ball et al., 2007; Rong et al., 2007a,b; Xiao et al., 2013).

## Role of CD8+ T Cells and the Latent Reservoir

Interestingly, within HIV cohort studies [VISCONTI (Goujard et al., 2012; Sáez-Cirión et al., 2013) and SPARTAC (Salgado et al., 2011)] patients have been identified who were able to control HIV infection ( $<50$  RNA copies per mL) after ART cessation, so-called post-treatment controllers. Moreover, there are HIV infected patients (elite controllers) which are able to control and suppress plasma viral load ( $<50$  RNA copies per mL) naturally without ART. In HIV long-term non-progressors, significantly stronger and more complex CD8+ T cell responses associated with higher HIV directed CD8+ proliferation and more effective killing of infected CD4+ T cells have been observed (O'Connell et al., 2009). Recently, Conway and Perelson (2015) extended the target cell-limited model by CTL and latently infected CD4+ cells. Herein, for a very strong immune response, the same dynamics as in elite controllers has been observed. With respect to the size of the latent reservoir, an insufficient CTL response resulted either in viral rebound or post-treatment control. Therefore, post-treatment control after ART cessation depends strongly on a small latent reservoir. The authors suggested therapeutic vaccination to increase the strength of the CTL killing rate and latent reversing agents to decrease the size of the latent reservoir (Conway and Perelson, 2015).

Promising advances in the treatment of latent HIV have been made by an induction and clearing strategy of the latent reservoir, so-called “kick and kill.” Kick refers to the activation of the HIV provirus replication of the latent reservoir, while kill refers to the clearance of reactivated cells by the immune system and/or ART (Barton et al., 2013). For example, vaccinating HIV-positive patients under HAART has shown a transient increase of CD4+ T cell killing and thus a temporary decrease of the latent reservoir (Persaud et al., 2011). Another possibility to activate HIV in latent CD4+ T cells may be achieved by Vorinostat, a histone deacetylase inhibitor. Vorinostat has been shown to be very effective in the induction of HIV transcription in resting memory CD4+ T cells in patients under ART (Archin et al., 2012). To understand the effect of Vorinostat on resting CD4+ cells and the whole latent reservoir, Ke et al. (2015) have developed mathematical models of latency under Vorinostat therapy. They could show that Vorinostat transiently activates HIV transcription but does not reduce the reservoir itself, indicating the necessity of a combination therapy (Ke et al., 2015). In 2015, HIV/AIDS disappeared from the list of the top 10 causes of deaths, indicating that substantial progress has been made by extensively investigating HIV, both experimentally and theoretically. Moreover, from 2000 to 2015 the number of people receiving ART increased from 770,000 to 18.2 million, with a projection of 30 million people on ART in 2020 (Boerma et al., 2015).

## HEPATITIS C VIRUS

The blood-borne HCV is a plus-strand RNA virus that causes the acute hepatitis C infection, as well as life-threatening chronic hepatitis C-related diseases like liver cirrhosis or hepatocellular

carcinoma. Worldwide, ~80 million people live with chronic hepatitis C with annually 400,000 deaths. For decades, the therapy of choice was based on standard or pegylated interferon (IFN/peg-IFN) and achieved a sustained virologic responses (SVR) between 30 and 60% for IFN and 40–65% for peg-IFN, depending on the HCV genotype and disease progression. Recently, DAAs were introduced to HCV treatment, and increased cure rates to over 90% (World Health Organization, 2016b).

### Viral Dynamics

During an acute HCV infection, the viral load increases in a biphasic manner, reaching a peak of  $10^5$ - $10^7$  IU per mL and is then cleared by the host immune response. However, 55–85% of HCV patients develop chronic hepatitis C with persisting virus (Hoofnagle, 2002). Thimme et al. (2001) found that the outcome of an acute infection and its correlation with HCV control is associated with a sustained CD4+ and CD8+ T cell response (Thimme et al., 2001). The biphasic increase in the plasma viral load has been characterized by a rapid viral rise followed by a slower increase, with viral doubling times in the two phases of 0.5 and 7.5 days, respectively (Major et al., 2004). In between these two phases, Dahari et al. (2005) observed a transient reduction in viremia and introduced a generalized model that allows the inhibition of virus production. Model simulations suggest that during that transient decrease of plasma viral load, the endogenous type I IFN response blocks virion production, but without controlling the HCV replication completely (Dahari et al., 2005).

### Antiviral Treatment

To estimate the absolute efficacy of IFN therapy, Neumann (1998) integrated the effect of IFN- $\alpha$  into the target cell-limited model by inhibiting the virus production rate ( $p$ ) or the *de novo* infection rate ( $k$ ). After initiation of IFN- $\alpha$  therapy, plasma viral load declined in a similar biphasic manner as has been observed in HIV patients, with a strong first followed by a slower second decrease, resulting in persistence of HCV. Following a pharmacokinetic delay of ~9 h, this biphasic viral decline could be reproduced in the model by partial blocking of the viral production rate with  $\varepsilon_p < 1$ . Furthermore, the clearance of free virions ( $c$ ) and therapy efficacy ( $\varepsilon$ ) led to the initial rapid decline while the loss of infected cells ( $\delta$ ) represented the second slower phase. Due to a dose-dependent virus reduction, the authors suggested to increase IFN dosage in treatment for a better antiviral effect early in the infection. They estimated the virion half-life to be ~2.7 h ( $c = 6.2 \text{ day}^{-1}$ ) and the infected cell half-life of 1.7–70 days ( $\delta = 0.14 \text{ day}^{-1}$ ). Before the initiation of therapy, the estimated virion production and clearance rates were  $10^{12}$  virions per day (Neumann, 1998).

In some patients, a triphasic decline with a more rapid third phase has been observed under treatment with pegylated IFN- $\alpha$  in monotherapy or in combination with Ribavirin. Herrmann et al. (2003) suggested the possibility that the third phase decline could be the result of an infected cell loss enhanced by immune-mediated clearance of Ribavirin (Herrmann et al., 2003). In some patients with the triphasic decline, the second phase

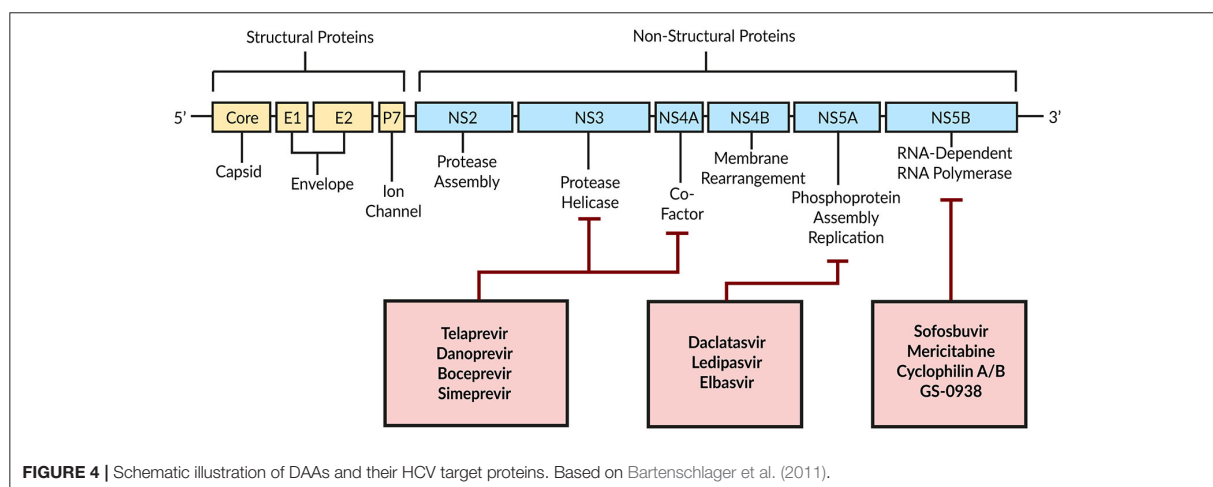
represented a 4–28 days lasting shoulder phase where HCV was slowly decreasing or remained constant. With a modified model concerning the proliferation of uninfected and infected cells, Dahari et al. (2007b) could reproduce this triphasic pattern only if the majority of hepatocytes were assumed infected. Furthermore, an uninfected hepatocyte proliferation rate higher than the rate of infected cell loss resulted in that almost balanced shoulder phase. According to model simulations, the shoulder phase or even a biphasic viral decline are not observed if Ribavirin effects infected cell loss ( $\delta$ ) or inhibits the viral production rate ( $\varepsilon_p$ ). The authors suggested that the rapidly decreasing third phase in patients with combination therapy of peg-IFN and Ribavirin might be explained by a mutagenic effect (Dahari et al., 2007b).

### Direct Acting Antivirals

Combination therapy of peg-IFN with Ribavirin achieves a SVR in only around 50% of patients with HCV genotype 1 (Manns et al., 2001; Fried et al., 2002). With DAAs a new era began by targeting HCV-encoded proteins that are directly involved in the viral life cycle (Figure 4; Scheel and Rice, 2013). A combination of peg-IFN plus Ribavirin with the DAA Telaprevir—an HCV NS3/4A serine protease inhibitor—increased the SVR to around 70% (Jacobson et al., 2011). By modeling the antiviral effect of Telaprevir, Guedj and Perelson (2011) found a 4-fold higher viral decline during the second phase of the biphasic decline with Telaprevir ( $\delta = 0.58 \text{ day}^{-1}$ ) compared to the IFN-based therapy [ $\delta = 0.14 \text{ day}^{-1}$ ; Neumann, 1998]. The authors suggested a higher infected cell death as well as intracellular degradation of viral RNA as modes of action for Telaprevir (Guedj and Perelson, 2011).

### Age-Based Multi-Scale Modeling

In 2010, a promising HCV NS5A inhibitor BMS-790052 (Daclatasvir; Kim et al., 2016) has been associated with a 3-log(10) reduction in viremia within the first 24 h, thus offering a highly potent drug (Gao et al., 2010). To understand and compare the mechanisms of action of Daclatasvir and IFN, Guedj et al. (2013) introduced an age-based multi-scale model by integrating intracellular processes, i.e., the antiviral effect on viral RNA replication and particle assembly/secretion, into the target cell-limited model (Equation 4, Figure 2C). For Daclatasvir, the model predicted a 99.0% effective blocking of viral RNA replication ( $\varepsilon_a$ ) and 99.8% effective inhibition of assembly/secretion ( $\varepsilon_s$ ). The viral clearance rate has been estimated as  $c = 22.3 \text{ day}^{-1}$ , corresponding to an HCV half-life of 45 min, while the intracellular viral RNA had a half-life of on average 11 h. Compared to Daclatasvir, IFN showed a dose-dependent efficacy of 77–96% in blocking intracellular viral replication and only 39% in blocking assembly/secretion, which confirmed the IFN-mediated viral replication inhibition as the main mode of action. Interestingly, the strong antiviral effect of Daclatasvir has been observed only when efficiently blocking both, intracellular viral replication and assembly/secretion. If Daclatasvir was assumed to inhibit only the intracellular viral replication, the kinetics was comparable with that of IFN monotherapy (Guedj et al., 2013). With a similar age-based multi-scale model including intracellular viral RNA replication, viral



RNA degradation, and assembly/secretion, Rong et al. (2013) investigated the antiviral effect of the HCV protease inhibitor Danoprevir. They found that Danoprevir was more efficient in inhibiting viral RNA replication (97%) and enhancing viral RNA degradation than inhibiting assembly/secretion (57%). However, for the Danoprevir monotherapy the viral clearance rate has been estimated with  $c = 10.4 \text{ day}^{-1}$ , corresponding to a virion half-life of 1.6 h (Rong et al., 2013). The age-based multi-scale modeling strategy has shown huge potential in comparing treatment regimens and identifying modes of action of new DAAs.

### IFN-Free Therapy

Regarding the severe side effects that have been reported with IFN-based therapy (Heim, 2013) and the improved therapeutic response to DAAs, an IFN-free therapy became more and more desirable. Patients treated with the DAA Mericitabine, a nucleoside NS5B HCV polymerase inhibitor, have shown a slower initial viral decline (phase 1) compared to, e.g., the IFN-based therapy, NS5A or non-nucleoside NS5B inhibitors. However, in 40% of the patients, a slow but monophasic viral decline has been observed within the 14 days of Mericitabine treatment. Model predictions have shown that Mericitabine blocks effective viral production whereas the efficacy increases with the accumulation of intracellular phosphates (Guedj et al., 2012). However, a faster initial decline compared to Mericitabine but slower than for other DAAs has been found by evaluating the efficacy of single and co-treatment with the nucleoside HCV NS5B polymerase inhibitors Sofosbuvir and GS-0938. By comparing mono and combination therapy of DAAs of the same family, it was shown that both drugs alone were highly effective and only minor more effective in combination, suggesting an antiviral combination therapy with DAAs of different families (Guedj et al., 2014).

Clinical trials investigating the combination of Sofosbuvir with Ledipasvir (an HCV NS5A inhibitor) with and without Ribavirin have proven highly effective and safe with a SVR

>90% (Afdhal et al., 2014a,b; Kowdley et al., 2014). Using a mathematical model, Dahari et al. (2016) analyzed the curing time of Sofosbuvir in combination with either Daclatasvir, Simeprevir, or Ledipasvir within a 12-week treatment duration in 58 patients with chronic hepatitis C. Their simulations show that 98% of patients achieved a SVR with less than one remaining hepatitis C virion. Interestingly, after 6 weeks of treatment, 100% of patients have shown viral loads <15 IU per mL and no detectable virions in 91% of patients. Additionally, the model predicted that therapy could be shortened in more than 80% of the patients, resulting in a reduce in medication costs by 16–20% (Dahari et al., 2016).

### Host Factor Targeting and Intracellular Models

A limitation of the DAA-based therapy is the possibility of developing viral resistance, i.e., emergence of drug-escaping variants dependent on patient groups, HCV genotype, and treatment regimen (Pawlotsky, 2016). In patients treated with Telaprevir over a period of 14-days, Kieffer et al. (2007) found not only an increase in plasma viral load, but also an increase in drug-resistant variants, which replaced the wild-type HCV almost completely at day 15 (Kieffer et al., 2007). Therefore, attention must be paid to finding an effective therapy regimen so that development of drug resistance is avoided. Another alternative treatment strategy is to not directly target the virus, but rather aim for cellular co-factors, since the virus depends strongly on the living host cell for efficient replication. As an example, Cyclophilin B has been identified as a cellular factor modulating the RNA binding activity to HCV NS5B polymerase and thus regulating the HCV replication (Watashi et al., 2005). Liu et al. (2009) reported an interaction of Cyclophilin A and the HCV NS5B polymerase, and predicted that Cyclophilin A as a major key host factor for an active replicase (Liu et al., 2009). Cyclophilin inhibitors such as Alisporivir (Gallay and Lin, 2013), SCY-635 (Hopkins et al., 2012), and NIM 88 (Lawitz et al., 2011) have confirmed the potential in disrupting the HCV



replication. This and other findings on host factors have proven how important a detailed understanding of the HCV life cycle and the host interaction is.

To characterize the intracellular viral replication in more detail, Dahari et al. (2007c) developed a detailed mathematical model investigating the single steps of intracellular RNA replication. The model with cytoplasmic translation and RNA replication within a replication compartment has shown that HCV regulates the plus-strand to the minus-strand relation by a strand-specific affinity of HCV NS5B polymerase. Additionally, the authors have shown that the virus benefits from encapsulating its genome replication inside membranous replication sites (Dahari et al., 2007c). Using an extended model and based on detailed measurements of the initial replication kinetics, Binder et al. (2013) mimicked the highly dynamic initial phase within the first hours post infection until steady state of minus-strand RNA, plus-strand RNA, and protein activity. An important finding of this model is the role of the protective replication compartment in which HCV replicates its genome. On the one hand, this compartment appears to protect the virus from antiviral mechanisms and is required for the establishment of a successful replication, on the other hand, this compartment also seems to limit viral growth and thus exerts tight control over the viral dynamics. By the integration of host factors into the model, the authors showed that cellular co-factors that are involved in the formation of the membranous replication sites and the initiation of minus-strand synthesis are responsible for differences in replication efficacy in different cell lines (Binder et al., 2013).

Recently, Benzine et al. (2017) have estimated the half-lives of the replicase complex (a complex of viral and cellular proteins associated with viral genome synthesis) in slowly and rapidly replicating HCV strains. Their mathematical model distinguishes between different viral plus-strand RNA genomes—RNA associated with translation, RNA responsible for RNA synthesis in the membranous web and the replicase complex, as well as RNA that is assembled and packed into virions. The authors estimated replicase complex half-lives of 3.5 h for the fast replicating strain and 9.9 h for the slow replicating strain and speculated that differences in the amino-acids in non-structural (NS) proteins that are responsible for replicase complex formation as well as the interactions with each other or host proteins are underlying the observed differences in half-lives. Furthermore, the antiviral efficacy has been integrated by the effect of the NS5A inhibitor Elbasvir, the NS5B inhibitor Sofosbuvir, and Compound 23. Sofosbuvir inhibits the plus- and minus-strand synthesis, Elbasvir blocks the formation of new replicase complexes and the viral assembly while Compound 23 inhibits the formation of replicase complexes. For the slowly replicating strains, the model predicted that by blocking viral assembly, the RNA is increasingly used for translation while that redirection was very low in fast replicating viral strains (Benzine et al., 2017).

Clausznitzer et al. (2015) developed a multi-scale model combining the target cell-limited model with detailed intracellular replication to investigate the specific effect of Daclatasvir that targets HCV NS5A within the first 2 days

post drug administration. For Daclatasvir, the exact mode of action is still unknown. The authors compared different putative mechanisms concerning the initial and long-term dynamics. Blocking viral replication affected the long-term dynamics, while blocking viral assembly/secretion had an effect on the initial and the long-term dynamics. Interestingly, a complete inhibition of viral assembly/secretion did not eradicate the virus. Additionally, it has been shown that the host factor affected the long-term dynamics and represented the main parameter in individual differences in the viral replication efficacy (Clausznitzer et al., 2015).

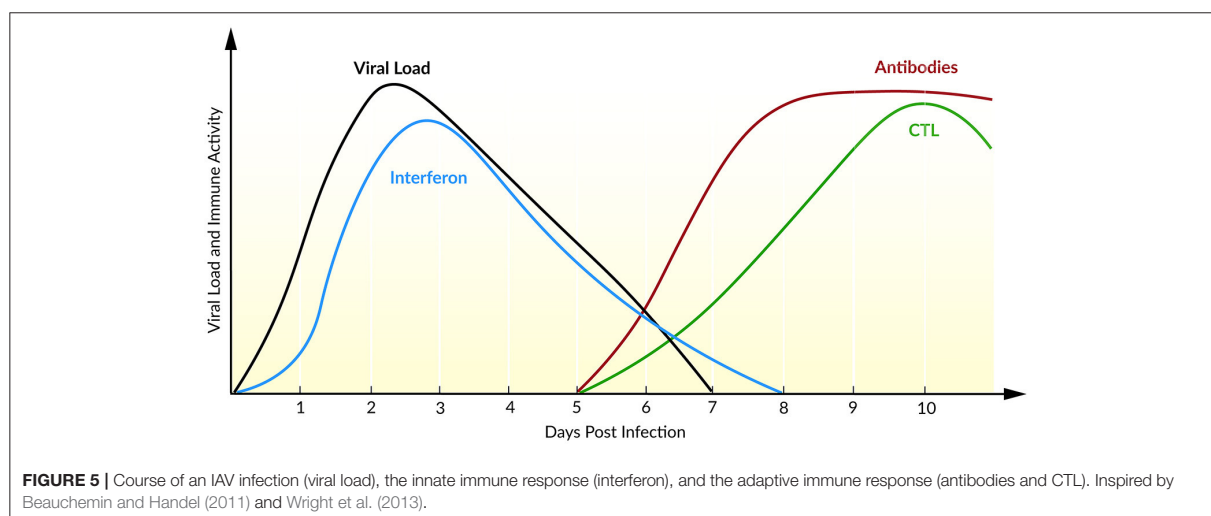
In a mouse model, Mailly et al. (2015) have shown that the inhibition of Claudin1-mediated viral entry by Claudin1-specific monoclonal antibodies has shown highly effective in preventing HCV infection without the emergence of resistance. By using the target cell-limited model that has been extended by the effect of monoclonal antibodies which inhibit the *de novo* infection rate ( $k$ ), the model predicted the clearance of infected cells and the prevention of new infection (Mailly et al., 2015). Thus, the inhibition of cellular co-factors that mediate viral entry might be a promising strategy to prevent and eradicate HCV.

## INFLUENZA VIRUS

The seasonal influenza is an acute infection of the respiratory tract caused by influenza virus of types A, B, and C. Annually, on average 3–5 million people worldwide are infected. The disease is often associated with severe symptoms and leads to 250,000–500,000 deaths per year. Two classes of antiviral drugs are available against influenza: neuraminidase inhibitors and M2 proton channel blockers. However, the most effective strategy against a seasonal influenza infection is the prevention by a vaccination, which has been proven to be safe and effective for more than 60 years (World Health Organization, 2017c).

## Viral Dynamics and Immune Response

The course of infection with IAV is characterized by an exponential growth of viral load, reaching its maximum 2 days post infection (Figure 5). Within the following days, the viral load declines until the virus becomes undetectable within 6–8 days post infection (Wright et al., 2013). Baccam et al. (2006) modified the target cell-limited model, taking the rapid dynamics of IAV into account. Their model neglects the regeneration and death of target cells (Baccam et al., 2006). With the assumption that progeny virus is undetectable within the first 6–8 h (Sedmak and Grossberg, 1973), an eclipse phase was incorporated into the model that characterized the time delay from cell infection to virus production. In order to model the eclipse phase, the authors introduced two different infected cell populations: not yet virus producing infected cells that are in the eclipse phase ( $I_1$ ) and actively virus producing infected cells ( $I_2$ , Equation 5). With data of patients experimentally infected with IAV, mathematical models with and without the eclipse phase have been analyzed. The authors could show that both models fit the patient data equally well, whereas the eclipse phase model estimated biologically more reasonable parameters with a half-life of free virion of 3.2 h. Furthermore, after a 6 h delay, the



infected cells are producing virus for about 5 h, leading to an average lifetime of about 11 h for infected cells. Additionally, the authors calculated the basic reproductive ratio  $R_0 \sim 22$  indicating a rapid viral spread ( $R_0 \gg 1$ ) where 1 cell infects  $\sim 22$  other epithelial cells in the upper respiratory tract, suggesting that an early initiation of treatment is crucial. Interestingly, in 50% of the patients a second peak in viral load has been observed. By extending the target cell-limited model by the effect of IFN (Equation 5), the second peak might be explained by a decreasing antiviral effect of IFN (Baccam et al., 2006).

During IAV infection, IFN is detectable 24 h post infection reaching a maximum after 72–96 h (Roberts et al., 1979). IFN plays a major role in the inhibition of viral infection and establishing an antiviral state (Samuel, 2001). In turn, the IAV protein NS1 has been identified as an IFN antagonist that circumvent the IFN-mediated antiviral response and correlates with pathogenicity (Garcia-Sastre et al., 1998). Saenz et al. (2010) extended the target cell-limited model by the regulation of the IIR. Herein, IFN is released by infected cells which induce an antiviral state by turning target cells into refractory cells. Model predictions demonstrated the major role of IFN in controlling early infection by protecting target cells (Saenz et al., 2010).

To capture the interaction of IAV with the IIR and AIR, Pawelek et al. (2012) included an antiviral state by refractory cells, as well as an IFN-induced infected cell killing into the target cell-limited model. The authors have shown that the early viral infection might be controlled by target cell depletion. The rapid viral post-peak decline could be explained by the enhanced infected cell killing mediated by cytokines, natural killer cells, or other cells activated by IFN. Moreover, the authors were able to mimic the bimodal pattern with a rebound of plasma viral load observed in 50% of the patients (Baccam et al., 2006). They assume that this second peak is due to a loss of the antiviral effect of IFN leading to a recovery of target cells (Pawelek et al., 2012). By comparing the dynamics of four different IAV strains in a mouse model, Manchanda et al. (2014) have

shown a strain-specific rebound in viremia leading to a second peak. Furthermore, model predictions explained the rebound by persistent inflammation that correlated with disease severity (Manchanda et al., 2014).

The AIR is mainly mediated by CTLs and antibodies which appear at day 5 after primary infection and at day 3 after reinfection in a faster memory cell-mediated secondary response (Tamura and Kurata, 2004). Handel et al. (2010) extended the target cell-limited model by simple defense mechanisms of immune mediators, e.g., inflammatory cytokines, as well as antibodies or CTLs (Equation 6). It has been shown that the models with either antibody (killing of free virions) or the CTL-mediated immune response (killing of infected cells) fit the data equally well. A distinction of the underlying mechanisms of the AIR was not possible with the available data (Handel et al., 2010). Miao et al. (2010) combined CTL and antibodies, IgG and IgM, within a mathematical model and confirmed the necessity of CTL and IgM in infection clearance, leading to average half-lives for infected cells of  $\sim 0.5$  days and for free virions of  $\sim 1.8$  min. In the absence of an AIR (days 0–5), the half-lives for infected cells have been estimated with  $\sim 1.2$  days and for free virions  $\sim 4$  h. Furthermore, the model predicted the contribution of CTLs in killing infected cells while mainly IgM cleared the viral load. Due to a low contribution of IgG in primary infection clearance, the authors suggested a role of IgG together with CD4<sup>+</sup> T cells in generating a memory and therefore a second immune response (Miao et al., 2010).

### Risk Factor Age

The recommended prevention of an influenza infection is a vaccination that reduces severity, complications, and deaths especially in elderly. However, due to a lower antibody response in elderly (age >65 years) the vaccine efficacy is only 17–53% compared with 70–90% in young adults (Goodwin et al., 2006). Hernandez-Vargas et al. (2014) studied the impact of age on the immune response to the course of IAV infection

and have shown a limited stimulation of the adaptive immune cells that led to a reduced viral growth with a 1.5 lower  $R_0$  in immune naïve aged mice. Additionally, a delayed (1–2 days) infection clearance correlated with a delayed increase of CD8+ T cells in aged mice, indicating a key role of CD8+ T cells in infection clearance. Therefore, the 10-fold lower viral burden might trigger the immune response insufficiently, explaining the striking difference between infection control and viral titers in elderly and young mice (Hernandez-Vargas et al., 2014). However, these experimental results and modeling predictions are valid for immune naïve aged mice. To study the efficacy of vaccination in elderly, the validation of these results in humans would be appropriate, but is obviously more complicated.

Modeling the effect of CD8+ T cell populations to recurrent IAV infections, Zarnitsyna et al. (2016) have shown that an increase in CD8+ T cell levels led to a decreased viral load and a shorter recovery time. The model of Cao et al. (2016) confirmed the relationship of a faster recovery with an increased level of effector CD8+ T cells. Thus, the induction of CD8+ T cells might be a promising vaccination strategy instead of boosting the antibody response that might lead to antigenic mutations and constantly evolving new influenza strains (Cao et al., 2016; Zarnitsyna et al., 2016).

## Antiviral Drugs

The effect of Amantadine, an antiviral agent acting as an M2 ion channel blocker, has been included into the eclipse model (Baccam et al., 2006) by affecting the infection rate ( $k$ ) of target cells by virions. The authors show that the maximum drug efficacy for Amantadine is only 74%, this can be explained by a possible rapid development of drug resistance. For the characterization of the viral dynamics under Adamantane treatment (e.g., Amantadine), it is therefore important to take the emergence of drug-resistance into account (Beauchemin et al., 2008).

Canini et al. (2014) investigated the effect of Oseltamivir (a neuraminidase inhibitor) using a model combining antiviral treatment regimen, IIR, and AIR, as well as a scoring system for symptoms, and the emergence of drug resistance as a random event. The authors show that the prophylactic use (pre-symptomatic phase) of Oseltamivir in low doses may cause a 27% higher emergence of drug resistance during the incubation period, due to an insufficient AIR, e.g., by natural killer cells. The initiation and duration of treatment, drug doses, as well as treatment frequency have been identified as crucial factors for the emergence of drug resistance (Canini et al., 2014). Kamal et al. (2015) studied the time course of influenza infection with and without Oseltamivir that had an effect on the virion production rate by inhibiting the release of newly produced virions (viral shedding). They have shown that a sooner initiation of Oseltamivir treatment correlates with a decreased viral secretion duration. By investigating the effect of a combined treatment, they found that the effect of Oseltamivir together with an antiviral drug affecting viral clearance had significant better effects reducing viral load, regardless of the onset of therapy (Kamal et al., 2015).

Heldt et al. (2013) developed an age-based multi-scale model combining the viral life cycle with cell-to-cell transmission with the aim to investigate the effect of DAAs. The authors found the most promising antiviral strategy by interfering with viral transcription, replication, protein synthesis, nuclear export, and assembly/secretion, while inhibiting early steps in replication—virus entry—caused only a delayed virus production. They additionally showed that some drugs could in fact increase the virus production, indicating how important a detailed understanding of the dynamic events in the virus life cycle is (Heldt et al., 2013). Schelker et al. (2016) investigated early events in the viral life cycle within a 3D diffusion modeling approach that identified the time point of endocytosis and the distance of diffusion to the nucleus as a bottleneck, supporting cytosolic degradation as limiting factors for efficient virus replication (Schelker et al., 2016).

## OTHER VIRUSES

### Ebola Virus

From 2013 on, EBOV of the type Zaire has caused the largest outbreak to date in West Africa with reported 29,000 disease cases and 11,000 deaths. An untreated acute Ebola infection causes severe illness with a fatality rate of on average 50% (World Health Organization, 2017a). EBOV is a negative-stranded RNA virus that replicates in immune cells, with the ability to persist in immune-privileged sites such as the central nervous system and may thus lead to viral relapse (Jacobs et al., 2016). No specific treatment is currently available, but recently a clinical trial with a newly developed vaccine (rVSV-ZEBOV) has shown to be highly protective against the Ebola disease (Henao-Restrepo et al., 2017).

To capture the Ebola infection dynamics, Nguyen et al. (2015) used the target cell-limited model and compared EBOV to pandemic IAV. EBOV infection time is significantly slower than IAV infection time (9.5 h vs. 30–80 min) (Holder et al., 2011; Pinilla et al., 2012; Nguyen et al., 2015). Furthermore, the viral replication rate has been estimated as  $\sim 63$  ffu/mL day<sup>-1</sup> cell<sup>-1</sup>, EBOV is hence highly efficient with a virion half-life of  $\sim 23$  h ( $c = 1.05$  day<sup>-1</sup>) (Nguyen et al., 2015). Unfortunately, these results are uncertain due to parameter identifiability problems. Nonetheless, the target cell-limited model confirmed the viral growth seen in experimental data, starting at day 3 post infection with a complete target cell depletion at day 6. Madelain et al. (2015) extended the target cell-limited model by an eclipse phase (non-/virus-producing infected cells) and found a half-life for virus-producing infected cells of 6.4 h and a basic reproductive ratio of  $R_0 \sim 9$ . The authors furthermore studied the antiviral effect in mice treated with Favipiravir, an antiviral drug that blocks the RNA-dependent RNA polymerase in a broad spectrum of RNA viruses (Furuta et al., 2013). By inhibiting the virus production rate  $p$ , they found a sharp decrease in viral load that was associated with an increasing drug efficacy of 95, 98.5, and 99.6% at days 2, 3, and 6 after the onset of treatment. Since Favipiravir achieves its maximal efficacy after 3 days, an early treatment initiation is suggested (Madelain et al., 2015). With patient data of survivors and fatalities from the Uganda Ebola disease outbreak in 2000/2001, Martyushev et al. (2016)

studied the relationship between virus replication and disease severity. For this purpose, they extended the target cell-limited model by two target cell populations: potential target cells ( $T_2$ ), that are recruited via proinflammatory cytokines (e.g., recruited macrophages, hepatocytes, splenocytes, and endotheliocytes), which become susceptible target cells ( $T_1$ ), that are the primary target for viral replication (e.g., macrophages and dendritic cells). Ebola disease severity is described by a 2 log(10) higher plasma viral load, that is correlated with an extensive recruitment of potential target cells and a 2.2-fold higher basic reproductive ratio;  $R_0 \sim 6$  for fatal cases and  $R_0 \sim 2.8$  for nonfatal cases. Hence, the higher viral load in fatal cases and a massive infection/hypersecretion of cytokines by active virus-producing replication cells is associated with the potential severity of the Ebola disease (Wauquier et al., 2010; Martyushev et al., 2016). Additionally, antiviral intervention of (i) an antibody-based therapy that affects the *de novo* infection ( $k$ ), (ii) a siRNA-based treatment that blocks viral production ( $p$ ), and (iii) a nucleoside analog-based therapy (e.g., Favipiravir) have been evaluated in mono- and combination therapy. The combination of nucleoside analog-based therapy and siRNA-based turned out to be most efficient if initiated 4 days post symptom onset, while the antibody-based therapy seemed insufficient (Martyushev et al., 2016). The authors then demonstrated that a critical inhibition rate of 80.5% in fatal cases and 58.5% in nonfatal cases is needed to prevent fatal outcomes of the Ebola virus disease.

## Dengue Virus

The DENV is a positive-stranded RNA virus, infecting annually 390 million people worldwide. DENV is spread mainly by the mosquitos *Aedes aegypti* and *Aedes albopictus*, which also transmit Chikungunya Virus, Yellow Fever Virus, and ZIKV. There are four serotypes of DENV, causing flu-like illness occasionally associated with severe complications like hemorrhagic fever. A cleared dengue infection provides a serotype-specific lifelong immunization, while secondary infections with another serotype can result in severe dengue disease. Currently, there is no antiviral treatment available, but a recently developed dengue vaccine (CYD-TDV; Villar et al., 2015) is suggested for endemic regions (World Health Organization, 2016a).

To explain inter-individual differences in DENV infection dynamics, Clapham et al. (2014) extended the target cell-limited model by a simple AIR. Moreover, differences between primary and secondary infection could be explained by the variations in the immune response. For a secondary infection, the immune response-related parameters have shown higher values, e.g., the immune cell proliferation rate and the virus clearance rate. Interestingly, the infectivity rate constant ( $k$ ) has also reached higher values in a secondary infection compared to a primary infection, supporting the hypothesis of antibody-dependent enhancement where antibodies mediate virus entry and thus increase the viral infectivity in a secondary infection (Clapham et al., 2014). In a subsequent study, Clapham et al. (2016) investigated the antibody dynamics within a target cell-limited model predicting the role of IgM and IgG in the course of a dengue infection. They showed that a primary infection was

mainly cleared by IgM while a secondary infection was cleared by IgG and IgM. These results refer to the key role of IgM in DENV infection clearance. Furthermore, best fitting results have been found by assuming that antibodies directly neutralize free virus compared to a clearance of infected cells, e.g., via antibody-dependent cell cytotoxicity. However, model predictions have shown a short life-span of infected cells with 0.3 days referring to additional immune-mediated clearance mechanisms (Clapham et al., 2016).

Ben-Shachar and Koelle (2014) developed a series of within-host dengue models integrating key players of the IIR and AIR in order to investigate the viral dynamics and development of severe dengue disease. They extended the target cell-limited model only by the IIR and were able to reproduce the viral dynamics in primary infection. Furthermore, they showed that higher rate constants for infectivity ( $k$ ; evidence for antibody-dependent enhancement) and infected cell death ( $\delta$ ; evidence for T cell response with increasing severity) were necessary to mimic the viral dynamics of a secondary infection (Ben-Shachar and Koelle, 2014). Recently, Ben-Shachar et al. (2016) refined these results by investigating serotype-specific differences. The higher infectivity rate constants ( $k$ ) estimated for DENV-2 and DENV-3 compared to DENV-1 in their model were consistent with varying replication efficacy of different dengue serotypes (Ben-Shachar et al., 2016).

With a population-based delay model coupled to the IIR, Schmid et al. (2015) studied the attenuated viral spread of a DENV mutant that is proposed as a vaccine candidate. In their work, they show that the DENV mutant has a faster IFN activation and production which establishes an antiviral state in infected cells and leads to an 8-fold decreased viral production and spread compared to the wildtype DENV. Furthermore, their model shows a stronger impact of the autocrine IFN in comparison to the paracrine effect on reducing viral spread (Schmid et al., 2015).

## Zika Virus

ZIKV is a plus-stranded RNA virus that is mainly carried and transmitted by *Aedes* mosquitos, but sexual transmission has as well been reported (Foy et al., 2011; Musso et al., 2015; D'Ortenzio et al., 2016). Human infections with ZIKV usually cause only mild disease with similar symptoms as seen in DENV infections. However, during the recent outbreak in Brazil with estimated 440,000–1,300,000 Zika cases (Heukelbach et al., 2016), ZIKV has been associated with neurologic complications such as Guillain-Barré syndrome and fetal microcephaly (World Health Organization, 2017d).

Recently, Best et al. (2017) developed a series of models with and without incorporation of the immune response and fitted those to plasma viral load data of ZIKV-infected nonhuman primates. Within that model series, the target cell-limited model only extended by an eclipse phase that distinguishes between non-actively and actively virus-producing infected cells was the best-suited model to reproduce the data. Furthermore, the incorporation of key players of the IIR or AIR, e.g., by IFN or natural killer cells, respectively, did not improve the model fitting and thus has been neglected. The simple eclipse phase

model estimated an eclipse phase of  $\sim 4$  h (already observed via modeling in Osuna et al., 2016) and a basic reproductive ratio of  $R_0 \sim 10.7$ . The degradation rate of productively infected cells was estimated with  $\delta = 4.5 \text{ day}^{-1}$ , corresponding to a lifetime of  $\sim 5$  h. The authors furthermore included the effect of antiviral therapy by inhibition of the viral production rate. With the broad spectrum RNA polymerase inhibitor Favipiravir, the time to undetectable plasma viremia could be reduced by 2 days if the initiation of therapy starts at the time point of infection ( $t = 0$  days post infection). The therapy initiation at day 2 post infection led to the same result compared to no drug treatment, leading to undetectable plasma viral load after 5 days post infection (Best et al., 2017). By integrating the immune response via IFN and neutralizing antibodies into the eclipse phase model, Aid et al. (2017) found a positive effect of both in controlling the viral infection in the periphery. The overall best fit was achieved by initiating IFN response at day 1.5 while the activity of neutralizing antibodies started at day 6 (Aid et al., 2017).

## CONCLUSION

For more than 20 years, the population-based target cell-limited model has been used to describe the dynamics of a variety of viruses. The interdisciplinary research combining experimental measurements and mathematical modeling improved our understanding of virus-host interactions and helped to quantify key parameters of the viral life cycle. Simple mathematical models allowed the investigation of the circumstances that lead to viral eradication or the development of chronic infections with an equilibrium of virus production and immune-mediated clearance. Studying antiviral drug treatments with the target cell-limited model enabled the identification of drug efficacy and modes of action. Moreover, simple extensions of the model led to insights into the different patterns of viral decline during drug treatment and the evaluation of different treatment regimens. By taking the immune system into account, mathematical modeling helped to identify the key players for viral clearance.

A comprehensive and quantitative, dynamic understanding of virus-host interactions is vital for advances in antiviral therapy,

and can be achieved by modeling the entire viral life cycle from virus entry to particle production. This would support not only the prediction of more precise modes of action of DAAs, it would also help to identify and evaluate new treatment opportunities or the potential of broad-spectrum antiviral drugs. Drugs that interact directly with viral proteins have shown enormous potential, but may lead to the emergence of virus strain mutations, multi-drug resistance, and treatment failure. Therefore, future research might focus more on resistance free antiviral drugs, e.g., by targeting host factors or by the prevention of viral diseases with vaccination. To support knowledge-based design of such drugs and vaccines, a more comprehensive view of the immune response to viral infections is necessary. Regarding the complex interplay of the first line of defense by the IIR and the establishment of an immune response memory by the AIR, questions arise how the virus hides and circumvents the immune response or why some patients are able to clear an infection that would develop to chronic infection in the majority of patients.

Furthermore, modeling techniques may consider not only the time-dependent dynamics but focus as well more on the spatial scale. By combining time and space scales, agent-based models may help to characterize viral spread in tissue, within organs or in the whole human body. Additionally, the complex interplay between the virus and the immune system may be studied by agent-based models with relatively simple rules (Bauer et al., 2009; Graw and Perelson, 2015; Kumberger et al., 2016). Mathematical modeling addressed important questions concerning the virus-host interactions and may contribute to answering open questions.

## AUTHOR CONTRIBUTIONS

All authors listed have made a substantial, direct and intellectual contribution to the work, and approved it for publication.

## FUNDING

LK received funding from the BMBF through the ERASysAPP project SysVirDrug (031A602A).

## REFERENCES

- Afdhal, N., Reddy, K. R., Nelson, D. R., Lawitz, E., Gordon, S. C., Schiffl, E., et al. (2014a). Ledipasvir and sofosbuvir for previously treated HCV genotype 1 infection. *N. Engl. J. Med.* 370, 1483–1493. doi: 10.1056/NEJMoa1316366
- Afdhal, N., Zeuzem, S., Kwo, P., Chojkier, M., Gitlin, N., Puoti, M., et al. (2014b). Ledipasvir and sofosbuvir for untreated HCV genotype 1 infection. *N. Engl. J. Med.* 370, 1889–1898. doi: 10.1056/NEJMoa1402454
- Aid, M., Abbink, P., Larocca, R. A., Boyd, M., Nityanandam, R., Nanayakkara, O., et al. (2017). Zika virus persistence in the central nervous system and lymph nodes of rhesus monkeys. *Cell* 169, 610–620.e14. doi: 10.1016/j.cell.2017.04.008
- Alizon, S., and Magnus, C. (2012). Modelling the course of an HIV infection: insights from ecology and evolution. *Viruses* 4, 1984–2013. doi: 10.3390/v4101984
- Andrade, A., Guedj, J., Rosenkranz, S. L., Lu, D., Mellors, J., Kuritzkes, D. R., et al. (2015). Early HIV RNA decay during raltegravir-containing regimens exhibits two distinct subphases (1a and 1b). *AIDS* 29, 2419–2426. doi: 10.1097/QAD.0000000000000843
- Archin, N. M., Liberty, A. L., Kashuba, A. D., Choudhary, S. K., Kuruc, J. D., Crooks, A. M., et al. (2012). Administration of vorinostat disrupts HIV-1 latency in patients on antiretroviral therapy. *Nature* 487, 482–485. doi: 10.1038/nature11286
- Asselah, T., Boyer, N., Saadoun, D., Martinot-Peignoux, M., and Marcellin, P. (2016). Direct-acting antivirals for the treatment of hepatitis C virus infection: optimizing current IFN-free treatment and future perspectives. *Liver Int.* 36, 47–57. doi: 10.1111/liv.13027
- Baccam, P., Beauchemin, C., Macken, C. A., Hayden, F. G., and Perelson, A. S. (2006). Kinetics of influenza A virus infection in humans. *J. Virol.* 80, 7590–7599. doi: 10.1128/JVI.01623-05
- Ball, C. L., Gilchrist, M. A., and Coombs, D. (2007). Modeling within-host evolution of HIV: mutation, competition and strain replacement. *Bull. Math. Biol.* 69, 2361–2385. doi: 10.1007/s11538-007-9223-z

- Bartenschlager, R., Penin, F., Lohmann, V., and André, P. (2011). Assembly of infectious hepatitis C virus particles. *Trends Microbiol.* 19, 95–103. doi: 10.1016/j.tim.2010.11.005
- Barton, K. M., Burch, B. D., Soriano-Sarabia, N., and Margolis, D. M. (2013). Prospects for treatment of latent HIV. *Clin. Pharmacol. Ther.* 93, 46–56. doi: 10.1038/clpt.2012.202
- Bauer, A. L., Beauchemin, C. A., and Perelson, A. S. (2009). Agent-based modeling of host-pathogen systems: the successes and challenges. *Inf. Sci.* 179, 1379–1389. doi: 10.1016/j.ins.2008.11.012
- Beauchemin, C. A., and Handel, A. (2011). A review of mathematical models of influenza A infections within a host or cell culture: lessons learned and challenges ahead. *BMC Public Health* 11:S7. doi: 10.1186/1471-2458-11-S1-S7
- Beauchemin, C. A. A., McSharry, J. J., Drusano, G. L., Nguyen, J. T., Went, G. T., Ribeiro, R. M., et al. (2008). Modeling amantadine treatment of influenza A virus *in vitro*. *J. Theor. Biol.* 254, 439–451. doi: 10.1016/j.jtbi.2008.05.031
- Ben-Shachar, R., and Koelle, K. (2014). Minimal within-host dengue models highlight the specific roles of the immune response in primary and secondary dengue infections. *J. R. Soc. Interface* 12:20140886. doi: 10.1098/rsif.2014.0886
- Ben-Shachar, R., Schmidler, S., and Koelle, K. (2016). Drivers of inter-individual variation in dengue viral load dynamics. *PLoS Comput. Biol.* 12:e1005194. doi: 10.1371/journal.pcbi.1005194
- Benzine, T., Brandt, R., Lovell, W. C., Yamane, D., Neddermann, P., De Francesco, R., et al. (2017). NS5A inhibitors unmask differences in functional replicase complex half-life between different hepatitis C virus strains. *PLoS Pathog.* 13:e1006343. doi: 10.1371/journal.ppat.1006343
- Best, K., Guedj, J., Madelain, V., de Lamballerie, X., Lim, S. Y., Osuna, C. E., et al. (2017). Zika plasma viral dynamics in nonhuman primates provides insights into early infection and antiviral strategies. *Proc. Natl. Acad. Sci. U.S.A.* 114, 8847–8852. doi: 10.1073/pnas.1704011114
- Binder, M., Sulaimanov, N., Clausnitzer, D., Schulze, M., Hüber, C. M., Lenz, S. M., et al. (2013). Replication vesicles are load- and choke-points in the hepatitis C virus lifecycle. *PLoS Pathog.* 9:e1003561. doi: 10.1371/journal.ppat.1003561
- Boerma, T., Mathers, C., AbouZahr, C., Somnath, C., Hogan, D., and Stevens, G. (2015). *WHO Health in 2015: From MDGs to SDGs*. World Health Organization Available online at: <http://www.who.int/gho/publications/mdgs-sdgs/en/>
- Boianelli, A., Nguyen, V. K., Ebensen, T., Schulze, K., Wilk, E., Sharma, N., et al. (2015). Modeling influenza virus infection: a roadmap for influenza research. *Viruses* 7, 5274–5304. doi: 10.3390/v7102875
- Bonhoeffer, S., May, R. M., Shaw, G. M., and Nowak, M. A. (1997). Virus dynamics and drug therapy. *Proc. Natl. Acad. Sci. U.S.A.* 94, 6971–6976. doi: 10.1073/pnas.94.13.6971
- Braciale, T. J., Hahn, Y. S., and Burton, D. R. (2013). “Adaptive immune response to viral infections,” in *Fields Virology*, eds B. N. Fields, D. M. Knipe, and P. M. Howley (Philadelphia, PA: Wolters Kluwer Health; Lippincott Williams & Wilkins), 214–285.
- Buchholtz, F., and Schneider, F. W. (1987). Computer simulation of T3 / T7 phage infection using lag times. *Biophys. Chem.* 26, 171–179. doi: 10.1016/0301-4622(87)80020-0
- Canini, L., Conway, J. M., Perelson, A. S., and Carrat, F. (2014). Impact of different oseltamivir regimens on treating influenza A virus infection and resistance emergence: insights from a modelling study. *PLoS Comput. Biol.* 10:1003568. doi: 10.1371/journal.pcbi.1003568
- Canini, L., and Perelson, A. S. (2014). Viral kinetic modeling: state of the art. *J. Pharmacokinet. Pharmacodyn.* 41, 431–443. doi: 10.1007/s10928-014-9363-3
- Cao, P., Wang, Z., Yan, A. W., McVernon, J., Xu, J., Heffernan, J. M., et al. (2016). On the role of CD8+ T cells in determining recovery time from influenza virus infection. *Front. Immunol.* 7:611. doi: 10.3389/fimmu.2016.00611
- Cardozo, E. F., Andrade, A., Mellors, J. W., Kuritzkes, D. R., Perelson, A. S., and Ribeiro, R. M. (2017). Treatment with integrase inhibitor suggests a new interpretation of HIV RNA decay curves that reveals a subset of cells with slow integration. *PLoS Pathog.* 13:e1006478. doi: 10.1371/journal.ppat.1006478
- Chomont, N., El-Far, M., Ancuta, P., Trautmann, L., Procopio, F. A., Yassine-Diab, B., et al. (2009). HIV reservoir size and persistence are driven by T cell survival and homeostatic proliferation. *Nat. Med.* 15, 893–900. doi: 10.1038/nm.1972
- Ciupé, S. M., and Heffernan, J. M. (2017). In-host modeling. *Infect. Dis. Model.* 2, 188–202. doi: 10.1016/j.idm.2017.04.002
- Clapham, H. E., Quyen, T. H., Kien, D. T., Dorigatti, I., Simmons, C. P., Ferguson, N. M., et al. (2016). Modelling virus and antibody dynamics during dengue virus infection suggests a role for antibody in virus clearance. *PLoS Comput. Biol.* 12:e1004951. doi: 10.1371/journal.pcbi.1004951
- Clapham, H. E., Tricou, V., Van Vinh Chau, N., Simmons, C. P., and Ferguson, N. M. (2014). Within-host viral dynamics of dengue serotype 1 infection. *J. R. Soc. Interface* 11, 504–507. doi: 10.1098/rsif.2014.0094
- Clausnitzer, D., Harnisch, J., and Kaderali, L. (2015). Multi-scale model for hepatitis C viral load kinetics under treatment with direct acting antivirals. *Virus Res.* 218, 96–101. doi: 10.1016/j.virusres.2015.09.011
- Conway, J. M., and Perelson, A. S. (2015). Post-treatment control of HIV infection. *Proc. Natl. Acad. Sci. U.S.A.* 6, 4–9. doi: 10.1073/pnas.1419162112
- D’Ortenzio, E., Matheron, S., Yazdanpanah, Y., de Lamballerie, X., Hubert, B., Piorowski, G., et al. (2016). Evidence of sexual transmission of Zika virus. *N. Engl. J. Med.* 374, 2195–2198. doi: 10.1056/NEJMc1604449
- Dahari, H., Canini, L., Graw, F., Uprichard, S. L., Araujo, E. S. A., Penaranda, G., et al. (2016). HCV kinetic and modeling analyses indicate similar time to cure among sofosbuvir combination regimens with daclatasvir, simeprevir or ledipasvir. *J. Hepatol.* 64, 1232–1239. doi: 10.1016/j.jhep.2016.02.022
- Dahari, H., Lo, A., Ribeiro, R. M., and Perelson, A. S. (2007a). Modeling hepatitis C virus dynamics: Liver regeneration and critical drug efficacy. *J. Theor. Biol.* 247, 371–381. doi: 10.1016/j.jtbi.2007.03.006
- Dahari, H., Major, M., Zhang, X., Mihalik, K., Rice, C. M., Perelson, A. S., et al. (2005). Mathematical modeling of primary hepatitis C infection: noncytolytic clearance and early blockage of virion production. *Gastroenterology* 128, 1056–1066. doi: 10.1053/j.gastro.2005.01.049
- Dahari, H., Ribeiro, R. M., and Perelson, A. S. (2007b). Triphasic decline of hepatitis C virus RNA during antiviral therapy. *Hepatology* 46, 16–21. doi: 10.1002/hep.21657
- Dahari, H., Ribeiro, R. M., Rice, C. M., and Perelson, A. S. (2007c). Mathematical modeling of subgenomic hepatitis C virus replication in Huh-7 cells. *J. Virol.* 81, 750–760. doi: 10.1128/JVI.01304-06
- Dee, K. U., and Shuler, M. L. (1997). A mathematical model of the trafficking of acid-dependent enveloped viruses: application to the binding, uptake, and nuclear accumulation of baculovirus. *Biotechnol. Bioeng.* 54, 468–490. doi: 10.1002/(SICI)1097-0290(19970605)54:5<468::AID-BIT7>&gt;3.0.CO;2-C
- Dee, K. U., Hammer, D. A., and Shuler, M. L. (1995). A model of the binding, entry, uncoating, and RNA synthesis of Semliki Forest virus in baby hamster kidney (BHK-21) cells. *Biotechnol. Bioeng.* 46, 485–496. doi: 10.1002/bit.260460513
- Eigen, M., Biebricher, C. K., Gebinoga, M., and Gardiner, W. C. (1991). The hypercycle. Coupling of RNA and protein biosynthesis in the infection cycle of an RNA bacteriophage. *Biochemistry* 30, 11005–11018. doi: 10.1021/bi00110a001
- Endy, D., Kong, D., and Yin, J. (1997). Intracellular kinetics of a growing virus: a genetically structured simulation for bacteriophage T7. *Biotechnol. Bioeng.* 55, 375–389. doi: 10.1002/(SICI)1097-0290(19970720)55:2<375::AID-BIT15>&gt;3.0.CO;2-G
- Fauci, A. S., Pantaleo, G., Stanley, S., and Weissman, D. (1996). Immunopathogenic mechanisms of HIV infection. *Ann. Intern. Med.* 124, 654–663. doi: 10.7326/0003-4819-124-7-199604010-00006
- Foy, B. D., Kobylinski, K. C., Chilson Foy, J. L., Blitvich, B. J., Travassos da Rosa, A., Haddow, A. D., et al. (2011). Probable non-vector-borne transmission of Zika virus, Colorado, USA. *Emerg. Infect. Dis.* 17, 880–882. doi: 10.3201/eid1705.101939
- Fried, M. W., Shiffman, M. L., Reddy, K. R., Smith, C., Marinos, G., Gonçalves, F. L., et al. (2002). Peginterferon Alfa-2a plus ribavirin for chronic hepatitis C virus infection. *N. Engl. J. Med.* 347, 975–982. doi: 10.1056/NEJMoa020047
- Furuta, Y., Gowen, B. B., Takahashi, K., Shiraki, K., Smee, D. F., and Barnard, D. L. (2013). Favipiravir (T-705), a novel viral RNA polymerase inhibitor. *Antiviral Res.* 100, 446–454. doi: 10.1016/j.antiviral.2013.09.015
- Gallay, P. A., and Lin, K. (2013). Profile of alisporivir and its potential in the treatment of hepatitis C. *Drug Des. Devel. Ther.* 7, 105–115. doi: 10.2147/DDDT.S30946
- Gao, M., Nettles, R. E., Belema, M., Snyder, L. B., Nguyen, V. N., Fridell, R. A., et al. (2010). Chemical genetics strategy identifies an HCV NS5A inhibitor with a potent clinical effect. *Nature* 465, 96–100. doi: 10.1038/nature08960

- Garcia-Sastre, A., Egorov, A., Matassov, D., Brandt, S., Levy, D. E., Durbin, J. E., et al. (1998). Influenza A virus lacking the NS1 gene replicates in interferon-deficient systems. *Virology* 252, 324–330. doi: 10.1006/viro.1998.9508
- Goodwin, K., Viboud, C., and Simonsen, L. (2006). Antibody response to influenza vaccination in the elderly: a quantitative review. *Vaccine* 24, 1159–1169. doi: 10.1016/j.vaccine.2005.08.105
- Goujard, C., Girault, I., Rouzioux, C., Lécuroux, C., Deveau, C., Chaix, M. L., et al. (2012). HIV-1 control after transient antiretroviral treatment initiated in primary infection: role of patient characteristics and effect of therapy. *Antivir. Ther.* 17, 1001–1009. doi: 10.3851/IMP2273
- Graw, F., and Perelson, A. S. (2015). Modeling viral spread. *Annu. Rev. Virol.* 3, 1–18. doi: 10.1146/annurev-virology-110615-042249
- Gray, G. E., Laher, F., Lazarus, E., Ensoli, B., and Corey, L. (2016). Approaches to preventative and therapeutic HIV vaccines. *Curr. Opin. Virol.* 17, 104–109. doi: 10.1016/j.coviro.2016.02.010
- Guedj, J., Dahari, H., Rong, L., Sansone, N. D., Nettles, R. E., Cotler, S. J., et al. (2013). Modeling shows that the NS5A inhibitor daclatasvir has two modes of action and yields a shorter estimate of the hepatitis C virus half-life. *Proc. Natl. Acad. Sci. U.S.A.* 110, 3991–3996. doi: 10.1073/pnas.1203110110
- Guedj, J., Dahari, H., Shudo, E., Smith, P., and Perelson, A. S. (2012). Hepatitis C viral kinetics with the nucleoside polymerase inhibitor mericitabine (RG7128). *Hepatology* 55, 1030–1037. doi: 10.1002/hep.24788
- Guedj, J., Pang, P. S., Denning, J., Rodriguez-Torres, M., Lawitz, E., Symonds, W., et al. (2014). Analysis of the hepatitis C viral kinetics during administration of two nucleotide analogues: sofosbuvir (GS-7977) and GS-0938. *Antivir. Ther.* 19, 211–220. doi: 10.3851/IMP2733
- Guedj, J., and Perelson, A. S. (2011). Second-phase hepatitis C virus RNA decline during telaprevir-based therapy increases with drug effectiveness: implications for treatment duration. *Hepatology* 53, 1801–1808. doi: 10.1002/hep.24272
- Guedj, J., Rong, L., Dahari, H., and Perelson, A. S. (2010). A perspective on modelling hepatitis C virus infection. *J. Viral Hepat.* 17, 825–833. doi: 10.1111/j.1365-2893.2010.01348.x
- Handel, A., Longini, I. M., and Antia, R. (2010). Towards a quantitative understanding of the within-host dynamics of influenza A infections. *J. R. Soc. Interface* 7, 35–47. doi: 10.1098/rsif.2009.0067
- Heim, M. H. (2013). 25 years of interferon-based treatment of chronic hepatitis C: an epoch coming to an end. *Nat. Rev. Immunol.* 13, 535–542. doi: 10.1038/nri3463
- Heldt, F. S., Frensing, T., Pflugmacher, A., Gröpler, R., Peschel, B., and Reichl, U. (2013). Multiscale modeling of influenza A virus infection supports the development of direct-acting antivirals. *PLoS Comput. Biol.* 9:e1003372. doi: 10.1371/journal.pcbi.1003372
- Henao-Restrepo, A. M., Camacho, A., Longini, I. M., Watson, C. H., Edmunds, W. J., Egger, M., et al. (2017). Efficacy and effectiveness of an rVSV-vectored vaccine in preventing Ebola virus disease: final results from the Guinea ring vaccination, open-label, cluster-randomised trial (Ebola Ça Suffit!). *Lancet* 389, 505–518. doi: 10.1016/S0140-6736(16)32621-6
- Herrmann, E., Lee, J. H., Marinov, G., Modi, M., and Zeuzem, S. (2003). Effect of ribavirin on hepatitis C viral kinetics in patients treated with pegylated interferon. *Hepatology* 37, 1351–1358. doi: 10.1053/jhep.2003.50218
- Hernandez-Vargas, E. A., Wilk, E., Canini, L., Toapanta, F. R., Binder, S. C., Uvarovskii, A., et al. (2014). Effects of aging on influenza virus infection dynamics. *J. Virol.* 88, 4123–4131. doi: 10.1128/JVI.03644-13
- Heukelbach, J., Alencar, C. H., Kelvin, A. A., de Oliveira, W. K., and Pamplona de Góes Cavalcanti, L. (2016). Zika virus outbreak in Brazil. *J. Infect. Dev. Ctries.* 10, 116–120. doi: 10.3855/jidc.8217
- Ho, D. D. (1996). Viral counts count in HIV infection. *Science* 272, 1124–1125. doi: 10.1126/science.272.5265.1124
- Ho, D. D., Neumann, A. U., Perelson, A. S., Chen, W., Leonard, J. M., and Markowitz, M. (1995). Rapid turnover of plasma virions and CD4 lymphocytes in HIV-1 infection. *Nature* 373, 123–126. doi: 10.1038/373123a0
- Holder, B. P., Simon, P., Liao, L. E., Abed, Y., Bouhy, X., Beauchemin, C. A., et al. (2011). Assessing the *in vitro* fitness of an oseltamivir-resistant seasonal A/H1N1 influenza strain using a mathematical model. *PLoS ONE* 6:e14767. doi: 10.1371/journal.pone.0014767
- Holford, N. H., and Sheiner, L. B. (1982). Kinetics of pharmacologic response. *Pharmacol. Ther.* 16, 143–166. doi: 10.1016/0163-7258(82)90051-1
- Hoofnagle, J. H. (2002). Course and outcome of hepatitis C. *Hepatology* 36(5 Suppl. 1), S21–S29. doi: 10.1053/jhep.2002.36227
- Hopkins, S., DiMassimo, B., Rusnak, P., Heuman, D., Lalezari, J., Sluder, A., et al. (2012). The cyclophilin inhibitor SCY-635 suppresses viral replication and induces endogenous interferons in patients with chronic HCV genotype 1 infection. *J. Hepatol.* 57, 47–54. doi: 10.1016/j.jhep.2012.02.024
- Iwasaki, A., and Medzhitov, R. (2013). “Innate Responses to Viral Infections,” in *Fields Virology*, eds B. N. Fields, D. M. Knipe, and P. M. Howley (Philadelphia, PA: Wolters Kluwer Health; Lippincott Williams & Wilkins), 189–213.
- Jacobs, M., Rodger, A., Bell, D. J., Bhagani, S., Cromptley, I., Filipe, A., et al. (2016). Late Ebola virus relapse causing meningoencephalitis: a case report. *Lancet* 388, 498–503. doi: 10.1016/S0140-6736(16)30386-5
- Jacobson, I. M., McHutchison, J. G., Dusheiko, G., Di Bisceglie, A. M., Reddy, K. R., Bzowej, N. H., et al. (2011). Telaprevir for previously untreated chronic hepatitis C virus infection. *N. Engl. J. Med.* 364, 2405–2416. doi: 10.1056/NEJMoa1012912
- Kamal, M. A., Gieschke, R., Lemuel-Diot, A., Beauchemin, C. A., Smith, P. F., and Rayner, C. R. (2015). A Drug-disease model describing the effect of oseltamivir neuraminidase inhibition on influenza virus progression. *Antimicrob. Agents Chemother.* 59, 5388–5395. doi: 10.1128/AAC.00069-15
- Karn, J., and Stoltzfus, C. M. (2012). Transcriptional and posttranscriptional regulation of HIV-1 gene expression. *Cold Spring Harb. Perspect. Med.* 2:a006916. doi: 10.1101/cshperspect.a006916
- Ke, R., Lewin, S. R., Elliott, J. H., and Perelson, A. S. (2015). Modeling the effects of vorinostat *in vivo* reveals both transient and delayed HIV transcriptional activation and minimal killing of latently infected cells. *PLoS Pathog.* 11:e1005237. doi: 10.1371/journal.ppat.1005237
- Kieffer, T. L., Sarrazin, C., Miller, J. S., Welker, M. W., Forestier, N., Reesink, H. W., et al. (2007). Telaprevir and pegylated interferon- $\alpha$ -2a inhibit wild-type and resistant genotype 1 hepatitis C virus replication in patients. *Hepatology* 46, 631–639. doi: 10.1002/hep.21781
- Kim, H., and Perelson, A. S. (2006). Viral and latent reservoir persistence in HIV-1-infected patients on therapy. *PLoS Comput. Biol.* 2:e20135. doi: 10.1371/journal.pcbi.0020135
- Kim, S., Thiessen, P. A., Bolton, E. E., Chen, J., Fu, G., Gindulyte, A., et al. (2016). PubChem substance and compound databases. *Nucleic Acids Res.* 44, D1202–D1213. doi: 10.1093/nar/gkv951
- Kowdley, K. V., Gordon, S. C., Reddy, K. R., Rossaro, L., Bernstein, D. E., Lawitz, E., et al. (2014). Ledipasvir and sofosbuvir for 8 or 12 weeks for chronic HCV without cirrhosis. *N. Engl. J. Med.* 370, 1879–1888. doi: 10.1056/NEJMoa1402355
- Kumberger, P., Frey, F., Schwarz, U. S., and Graw, F. (2016). Multiscale modeling of virus replication and spread. *FEBS Lett.* 590, 1972–1986. doi: 10.1002/1873-3468.12095
- Lawitz, E., Godofsky, E., Rouzier, R., Marbury, T., Nguyen, T., Ke, J., et al. (2011). Safety, pharmacokinetics, and antiviral activity of the cyclophilin inhibitor NIM811 alone or in combination with pegylated interferon in HCV-infected patients receiving 14 days of therapy. *Antiviral Res.* 89, 238–245. doi: 10.1016/j.antiviral.2011.01.003
- Little, S. J., Holte, S., Routy, J. P., Daar, E. S., Markowitz, M., Collier, A. C., et al. (2002). Antiretroviral-drug resistance among patients recently infected with HIV. *N. Engl. J. Med.* 347, 385–394. doi: 10.1056/NEJMoa013552
- Liu, Z., Yang, F., Robotham, J. M., and Tang, H. (2009). Critical role of cyclophilin A and its prolyl-peptidyl isomerase activity in the structure and function of the hepatitis C virus replication complex. *J. Virol.* 83, 6554–6565. doi: 10.1128/JVI.02550-08
- Maartens, G., Celum, C., and Lewin, S. R. (2014). HIV infection: epidemiology, pathogenesis, treatment, and prevention. *Lancet* 384, 258–271. doi: 10.1016/S0140-6736(14)60164-1
- Mackey, T. K., Liang, B. A., Cuomo, R., Hafen, R., Brouwer, K. C., and Lee, D. E. (2014). Emerging and reemerging neglected tropical diseases: a review of key characteristics, risk factors, and the policy and innovation environment. *Clin. Microbiol. Rev.* 27, 949–979. doi: 10.1128/CMR.00045-14
- Madelain, V., Oestereich, L., Graw, F., Nguyen, T. H., de Lamballerie, X., Mentré, F., et al. (2015). Ebola virus dynamics in mice treated with favipiravir. *Antiviral Res.* 123, 70–77. doi: 10.1016/j.antiviral.2015.08.015
- Maily, L., Xiao, F., Lupberger, J., Wilson, G. K., Aubert, P., Duong, F. H. T., et al. (2015). Clearance of persistent hepatitis C virus infection in humanized mice

- using a claudin-1-targeting monoclonal antibody. *Nat. Biotechnol.* 33, 549–554. doi: 10.1038/nbt.3179
- Major, M. E., Dahari, H., Mihalik, K., Puig, M., Rice, C. M., Neumann, A. U., et al. (2004). Hepatitis C virus kinetics and host responses associated with disease and outcome of infection in chimpanzees. *Hepatology* 39, 1709–1720. doi: 10.1002/hep.20239
- Manchanda, H., Seidel, N., Krumbholz, A., Sauerbrei, A., Schmidtke, M., and Guthke, R. (2014). Within-host influenza dynamics: a small-scale mathematical modeling approach. *Biosystems* 118, 51–59. doi: 10.1016/j.biosystems.2014.02.004
- Manns, M. P., McHutchison, J. G., Gordon, S. C., Rustgi, V. K., Shiffman, M., Reindollar, R., et al. (2001). Peginterferon alfa-2b plus ribavirin compared with interferon- $\alpha$ -2b plus ribavirin for initial treatment of chronic hepatitis C: a randomised trial. *Lancet* 358, 958–965. doi: 10.1016/S0140-6736(01)06102-5
- Markowitz, M., Louie, M., Hurley, A., Sun, E., Di Mascio, M., Perelson, A. S., et al. (2003). A novel antiviral intervention results in more accurate assessment of human immunodeficiency virus type 1 replication dynamics and T-cell decay *in vivo*. *J. Virol.* 77, 5037–5038. doi: 10.1128/JVI.77.8.5037-5038.2003
- Martyushev, A., Nakaoka, S., Sato, K., Noda, T., and Iwami, S. (2016). Modelling Ebola virus dynamics: implications for therapy. *Antiviral Res.* 135, 62–73. doi: 10.1016/j.antiviral.2016.10.004
- Miao, H., Hollenbaugh, J. A., Zand, M. S., Holden-Wiltse, J., Mosmann, T. R., Perelson, A. S., et al. (2010). Quantifying the early immune response and adaptive immune response kinetics in mice infected with influenza A virus. *J. Virol.* 84, 6687–6698. doi: 10.1128/JVI.00266-10
- Munier, M. L., and Kelleher, A. D. (2007). Acutely dysregulated, chronically disabled by the enemy within: T-cell responses to HIV-1 infection. *Immunol. Cell Biol.* 85, 6–15. doi: 10.1038/sj.icb.7100015
- Musso, D., Roche, C., Robin, E., Nhan, T., Teissier, A., and Cao-Lormeau, V. M. (2015). Potential sexual transmission of Zika virus. *Emerg. Infect. Dis.* 21, 359–361. doi: 10.3201/eid2102.141363
- Nelson, P. W., Gilchrist, M. A., Coombs, D., Hyman, J. M., and Perelson, A. S. (2004). Age-structured model of HIV infection that allows for variations in the production rate of viral particles and the death rate of productively infected cells. *Math. Biosci. Eng.* 1, 267–288. doi: 10.3934/mbe.2004.1.267
- Neumann, A. U. (1998). Hepatitis C viral dynamics *in vivo* and the antiviral efficacy of interferon- $\alpha$  therapy. *Science* 282, 103–107. doi: 10.1126/science.282.5386.103
- Nguyen, V. K., Binder, S. C., Boianelli, A., Meyer-Hermann, M., and Hernandez-Vargas, E. A. (2015). Ebola virus infection modeling and identifiability problems. *Front. Microbiol.* 6:257. doi: 10.3389/fmicb.2015.00257
- Nowak, M. A., and Bangham, C. R. (1996). Population dynamics of immune responses to persistent viruses. *Science* 272, 74–79.
- Nowak, M. A., Bonhoeffer, S., Hill, A. M., Boehme, R., Thomas, H. C., and McDade, H. (1996). Viral dynamics in hepatitis B virus infection. *Proc. Natl. Acad. Sci. U.S.A.* 93, 4398–4402. doi: 10.1073/pnas.93.9.4398
- Nowak, M. A., and May, R. (2001). *Virus Dynamics: Mathematical Principles of Immunology and Virology*. Oxford University Press.
- O’Connell, K. A., Bailey, J. R., and Blankson, J. N. (2009). Elucidating the elite: mechanisms of control in HIV-1 infection. *Trends Pharmacol. Sci.* 30, 631–637. doi: 10.1016/j.tips.2009.09.005
- Osuna, C. E., Lim, S. Y., Deleage, C., Griffin, B. D., Stein, D., Schroeder, L. T., et al. (2016). Zika viral dynamics and shedding in rhesus and cynomolgus macaques. *Nat. Med.* 22, 1448–1455. doi: 10.1038/nm.4206
- Palmer, S., Maldarelli, F., Wiegand, A., Bernstein, B., Hanna, G. J., Brun, S. C., et al. (2008). Low-level viremia persists for at least 7 years in patients on suppressive antiretroviral therapy. *Proc. Natl. Acad. Sci. U.S.A.* 105, 3879–3884. doi: 10.1073/pnas.0800050105
- Pawelek, K. A., Huynh, G. T., Quinlivan, M., Cullinane, A., Rong, L., and Perelson, A. S. (2012). Modeling within-host dynamics of influenza virus infection including immune responses. *PLoS Comput. Biol.* 8:e1002588. doi: 10.1371/journal.pcbi.1002588
- Pawlotsky, J. M. (2016). Hepatitis C Virus resistance to direct-acting antiviral drugs in interferon-free regimens. *Gastroenterology* 151, 70–86. doi: 10.1053/j.gastro.2016.04.003
- Perelson, A. S. (2002). Modelling viral and immune system dynamics. *Nat. Rev. Immunol.* 2, 28–36. doi: 10.1038/nri700
- Perelson, A. S., Essunger, P., Cao, Y., Vesanen, M., Hurley, A., Saksela, K., et al. (1997). Decay characteristics of HIV-1-infected compartments during combination therapy. *Nature* 387, 188–191. doi: 10.1038/387188a0
- Perelson, A. S., and Guedj, J. (2015). Modelling hepatitis C therapy-predicting effects of treatment. *Nat. Rev. Gastroenterol. Hepatol.* 12, 437–445. doi: 10.1038/nrgastro.2015.97
- Perelson, A. S., Kirschner, D. E., and De Boer, R. (1993). Dynamics of HIV infection of CD4+ T cells. *Math. Biosci.* 114, 81–125. doi: 10.1016/0025-5564(93)90043-A
- Perelson, A. S., Neumann, A. U., Markowitz, M., Leonard, J. M., and Ho, D. D. (1996). HIV-1 dynamics *in vivo*: virion clearance rate, infected cell life-span, and viral generation time. *Science* 271, 1582–1586. doi: 10.1126/science.271.5255.1582
- Perelson, A. S., and Ribeiro, R. M. (2013). Modeling the within-host dynamics of HIV infection. *BMC Biol.* 11:96. doi: 10.1186/1741-7007-11-96
- Persaud, D., Luzuriaga, K., Ziemniak, C., Muresan, P., Greenough, T., Fenton, T., et al. (2011). Effect of therapeutic HIV recombinant poxvirus vaccines on the size of the resting CD4+ T-cell latent HIV reservoir. *AIDS* 25, 2227–2234. doi: 10.1097/QAD.0b013e32834cdaba
- Pinilla, L. T., Holder, B. P., Abed, Y., Boivin, G., and Beauchemin, C. A. (2012). The H275Y neuraminidase mutation of the pandemic A/H1N1 influenza virus lengthens the eclipse phase and reduces viral output of infected cells, potentially compromising fitness in ferrets. *J. Virol.* 86, 10651–10660. doi: 10.1128/JVI.07244-11
- Poveda, E., Wyles, D. L., Mena, A., Pedreira, J. D., Castro-Iglesias, A., and Cachay, E. (2014). Update on hepatitis C virus resistance to direct-acting antiviral agents. *Antiviral Res.* 108, 181–191. doi: 10.1016/j.antiviral.2014.05.015
- Quintela, B. M., Conway, J. M., Hyman, J. M., Reis, R. F., dos Santos, R. W., Lobosco, M., et al. (2017). “An Age-based multiscale mathematical model of the hepatitis C virus life-cycle during infection and therapy: including translation and replication,” in *VII Latin American Congress on Biomedical Engineering CLAIB 2016*, eds I. Torres, J. Bustamante, and D. Sierra (Singapore: Springer), 508–511.
- Ramratnam, B., Bonhoeffer, S., Binley, J., Hurley, A., Zhang, L., Mittler, J. E., et al. (1999). Rapid production and clearance of HIV-1 and hepatitis C virus assessed by large volume plasma apheresis. *Lancet* 354, 1782–1785. doi: 10.1016/S0140-6736(99)02035-8
- Reddy, B., and Yin, J. (1999). Quantitative intracellular kinetics of HIV type 1. *AIDS Res. Hum. Retroviruses* 15, 273–283. doi: 10.1089/088922299311457
- Ribeiro, R. M., and Bonhoeffer, S. (2000). Production of resistant HIV mutants during antiretroviral therapy. *Proc. Natl. Acad. Sci. U.S.A.* 97, 7681–7686. doi: 10.1073/pnas.97.14.7681
- Ribeiro, R. M., Qin, L., Chavez, L. L., Li, D., Self, S. G., and Perelson, A. S. (2010). Estimation of the initial viral growth rate and basic reproductive number during acute HIV-1 infection. *J. Virol.* 84, 6096–6102. doi: 10.1128/JVI.00127-10
- Roberts, N. J., Douglas, R. G., Simons, R. M., and Diamond, M. E. (1979). Virus-induced interferon production by human macrophages. *J. Immunol.* 123, 365–369.
- Rong, L., Feng, Z., and Perelson, A. S. (2007a). Emergence of HIV-1 drug resistance during antiretroviral treatment. *Bull. Math. Biol.* 69, 2027–2060. doi: 10.1007/s11538-007-9203-3
- Rong, L., Gilchrist, M. A., Feng, Z., and Perelson, A. S. (2007b). Modeling within-host HIV-1 dynamics and the evolution of drug resistance: trade-offs between viral enzyme function and drug susceptibility. *J. Theor. Biol.* 247, 804–818. doi: 10.1016/j.jtbi.2007.04.014
- Rong, L., Guedj, J., Dahari, H., Coffield, D. J., Levi, M., Smith, P., et al. (2013). Analysis of hepatitis C virus decline during treatment with the protease inhibitor danoprevir using a multiscale model. *PLoS Comput. Biol.* 9:e1002959. doi: 10.1371/journal.pcbi.1002959
- Rong, L., and Perelson, A. S. (2009). Modeling HIV persistence, the latent reservoir, and viral blips. *J. Theor. Biol.* 260, 308–331. doi: 10.1016/j.jtbi.2009.06.011
- Ronsard, L., Ganguli, N., Singh, V. K., Mohankumar, K., Rai, T., Sridharan, S., et al. (2017a). Impact of genetic variations in HIV-1 tat on LTR-mediated transcription via TAR RNA interaction. *Front. Microbiol.* 8:706. doi: 10.3389/fmicb.2017.00706



- Ronsard, L., Lata, S., Singh, J., Ramachandran, V. G., Das, S., and Banerjee, A. C. (2014). Molecular and genetic characterization of natural HIV-1 tat exon-1 variants from North India and their functional implications. *PLoS ONE* 9:e85452. doi: 10.1371/journal.pone.0085452
- Ronsard, L., Rai, T., Rai, D., Ramachandran, V. G., and Banerjee, A. C. (2017b). *In silico* analyses of subtype specific HIV-1 Tat-TAR RNA interaction reveals the structural determinants for viral activity. *Front. Microbiol.* 8:1467. doi: 10.3389/fmicb.2017.01467
- Saenz, R. A., Quinlivan, M., Elton, D., Macrae, S., Blunden, A. S., Mumford, J. A., et al. (2010). Dynamics of influenza virus infection and pathology. *J. Virol.* 84, 3974–3983. doi: 10.1128/JVI.02078-09
- Sáez-Cirión, A., Bacchus, C., Hocqueloux, L., Avettand-Fenoel, V., Girault, I., Lecuroux, C., et al. (2013). Post-treatment HIV-1 controllers with a long-term virological remission after the interruption of early initiated antiretroviral therapy ANRS VISCONTI Study. *PLoS Pathog.* 9:e1003211. doi: 10.1371/journal.ppat.1003211
- Salgado, M., Rabi, S. A., O'Connell, K. A., Buckheit, R. W., Bailey, J. R., Chaudhry, A. A., et al. (2011). Prolonged control of replication-competent dual-tropic human immunodeficiency virus-1 following cessation of highly active antiretroviral therapy. *Retrovirology* 8:97. doi: 10.1186/1742-4690-8-97
- Samuel, C. E. (2001). Antiviral actions of interferons. *Clin. Microbiol. Rev.* 14, 778–809. doi: 10.1128/CMR.14.4.778-809.2001
- Scheel, T. K., and Rice, C. M. (2013). Understanding the hepatitis C virus life cycle paves the way for highly effective therapies. *Nat. Med.* 19, 837–849. doi: 10.1038/nm.3248
- Schelker, M., Mair, C. M., Jolmes, F., Welke, R. W., Klipp, E., Herrmann, A., et al. (2016). Viral RNA degradation and diffusion act as a bottleneck for the influenza A virus infection efficiency. *PLoS Comput. Biol.* 12:e1005075. doi: 10.1371/journal.pcbi.1005075
- Schmid, B., Rinas, M., Ruggieri, A., Acosta, E. G., Bartenschlager, M., Reuter, A., et al. (2015). Live cell analysis and mathematical modeling identify determinants of attenuation of dengue virus 2'-O-methylation mutant. *PLoS Pathog.* 11:e1005345. doi: 10.1371/journal.ppat.1005345
- Sedmak, J. J., and Grossberg, S. E. (1973). Interferon bioassay: reduction in yield of myxovirus neuraminidases. *J. Gen. Virol.* 21, 1–7. doi: 10.1099/0022-1317-21-1-1
- Shepard, D. S., Undurraga, E. A., Halasa, Y. A., and Stanaway, J. D. (2016). The global economic burden of dengue: a systematic analysis. *Lancet Infect. Dis.* 16, 935–941. doi: 10.1016/S1473-3099(16)00146-8
- Simon, V., and Ho, D. D. (2003). HIV-1 dynamics *in vivo*: implications for therapy. *Nat. Rev. Microbiol.* 1, 181–190. doi: 10.1038/nrmicro772
- Stafford, M. A., Corey, L., Cao, Y., Daar, E. S., Ho, D. D., and Perelson, A. S. (2000). Modeling plasma virus concentration during primary HIV infection. *J. Theor. Biol.* 203, 285–301. doi: 10.1006/jtbi.2000.1076
- Steigbigel, R. T., Cooper, D. A., Kumar, P. N., Eron, J. E., Schechter, M., Markowitz, M., et al. (2008). Raltegravir with Optimized background therapy for resistant HIV-1 infection. *N. Engl. J. Med.* 359, 339–354. doi: 10.1056/NEJMoa0708975
- Tamura, S., and Kurata, T. (2004). Defense mechanisms against influenza virus infection in the respiratory tract mucosa. *Jpn. J. Infect. Dis.* 57, 236–247.
- Thimme, R., Oldach, D., Chang, K. M., Steiger, C., Ray, S. C., and Chisari, F., V (2001). Determinants of viral clearance and persistence during acute hepatitis C virus infection. *J. Exp. Med.* 194, 1395–1406. doi: 10.1084/jem.194.10.1395
- United Nations (2017). *A Socio-economic Impact Assessment of the Zika Virus in Latin America and the Caribbean*. Available online at: <http://www.undp.org/content/undp/en/home/librarypage/hiv-aids/a-socio-economic-impact-assessment-of-the-zika-virus-in-latin-am.html>
- Villar, L., Dayan, G. H., Arredondo-García, J. L., Rivera, D. M., Cunha, R., Deseda, C., et al. (2015). Efficacy of a tetravalent dengue vaccine in children in Latin America. *N. Engl. J. Med.* 372, 113–123. doi: 10.1056/NEJMoa1411037
- Watahi, K., Ishii, N., Hijikata, M., Inoue, D., Murata, T., Miyanari, Y., et al. (2005). Cyclophilin B is a functional regulator of hepatitis C virus RNA polymerase. *Mol. Cell* 19, 111–122. doi: 10.1016/j.molcel.2005.05.014
- Wauquier, N., Becquart, P., Padilla, C., Baize, S., and Leroy, E. M. (2010). Human fatal zaire ebola virus infection is associated with an aberrant innate immunity and with massive lymphocyte apoptosis. *PLoS Negl. Trop. Dis.* 4:e837. doi: 10.1371/journal.pntd.0000837
- Wei, X., Ghosh, S. K., Taylor, M. E., Johnson, V. A., Emini, E. A., Deutsch, P., et al. (1995). Viral dynamics in human immunodeficiency virus type 1 infection. *Nature* 373, 117–122. doi: 10.1038/373117a0
- Wodarz, D., and Lloyd, A. L. (2004). Immune responses and the emergence of drug-resistant virus strains *in vivo*. *Proc. Biol. Sci.* 271, 1101–1109. doi: 10.1098/rspb.2003.2664
- Wodarz, D., and Nowak, M. A. (2002). Mathematical models of HIV pathogenesis and treatment. *BioEssays* 24, 1178–1187. doi: 10.1002/bies.10196
- World Health Organization (2016a). *Dengue and Severe Dengue*. World Health Organization.
- World Health Organization (2016b). *Guidelines for the Screening, Care and Treatment of Persons with Chronic Hepatitis C Infection*. WHO.
- World Health Organization (2017a). *Ebola Virus Disease*. World Health Organization. Available online at: <http://www.who.int/mediacentre/factsheets/fs103/en/>
- World Health Organization (2017b). *HIV/AIDS*. WHO. Available online at: <http://www.who.int/mediacentre/factsheets/fs360/en/>
- World Health Organization (2017c). *Influenza (Seasonal)*. World Health Organisation Available online at: <http://www.who.int/mediacentre/factsheets/fs211/en/>
- World Health Organization (2017d). *Zika Virus*. World Health Organization. Available online at: <http://www.who.int/mediacentre/factsheets/zika/en/>
- Wright, P. F., Neumann, G., and Kawaoka, Y. (2013). “Orthomyxoviruses,” in *Fields Virology*, eds B. N. Fields, D. M. Knipe, and P. M. Howley (Philadelphia, PA: Wolters Kluwer Health/Lippincott Williams & Wilkins), 1186–1123.
- Xiao, Y., Miao, H., Tang, S., and Wu, H. (2013). Modeling antiretroviral drug responses for HIV-1 infected patients using differential equation models. *Adv. Drug Deliv. Rev.* 65, 940–953. doi: 10.1016/j.addr.2013.04.005
- Zarnitsyna, V. I., Handel, A., McMaster, S. R., Hayward, S. L., Kohlmeier, J. E., and Antia, R. (2016). Mathematical model reveals the role of memory CD8 T cell populations in recall responses to influenza. *Front. Immunol.* 7:165. doi: 10.3389/fimmu.2016.00165
- Zeisel, M. B., Lupberger, J., Fofana, I., and Baumert, T. F. (2013). Host-targeting agents for prevention and treatment of chronic hepatitis C-Perspectives and challenges. *J. Hepatol.* 58, 375–384. doi: 10.1016/j.jhep.2012.09.022

**Conflict of Interest Statement:** The authors declare that the research was conducted in the absence of any commercial or financial relationships that could be construed as a potential conflict of interest.

Copyright © 2018 Zitzmann and Kaderali. This is an open-access article distributed under the terms of the Creative Commons Attribution License (CC BY). The use, distribution or reproduction in other forums is permitted, provided the original author(s) and the copyright owner(s) are credited and that the original publication in this journal is cited, in accordance with accepted academic practice. No use, distribution or reproduction is permitted which does not comply with these terms.

**Article I: Mathematical modeling of plus-strand RNA virus replication to identify a broad-spectrum antiviral treatment strategy.**

**Carolin Zitzmann\***, Christopher Dächert, Bianca Schmid, Hilde van Tongeren-van der Schaar, Alessia Ruggieri, Martijn van Hemert, Alan S. Perelson, Frank van Kuppeveld, Ralf Bartenschlager, Marco Binder, Lars Kaderali\* (2023) *Mathematical modeling of plus-strand RNA virus replication to identify a broad-spectrum antiviral treatment strategy.* PLoS computational biology 19(4): e1010423.

I contributed to conceptualization, data curation, model development and methodology, formal analysis, investigation, software, validation, visualization, and writing—original draft, review & editing.

\* Corresponding author

The supplementary material is published and can be found online.

## RESEARCH ARTICLE

## Mathematical modeling of plus-strand RNA virus replication to identify broad-spectrum antiviral treatment strategies

Carolin Zitzmann<sup>1,2\*</sup>, Christopher Dächert<sup>3#a</sup>, Bianca Schmid<sup>4</sup>, Hilde van der Schaar<sup>5#b</sup>, Martijn van Hemert<sup>6</sup>, Alan S. Perelson<sup>7</sup>, Frank J. M. van Kuppeveld<sup>5</sup>, Ralf Bartenschlager<sup>5,7,8</sup>, Marco Binder<sup>3</sup>, Lars Kaderali<sup>1\*</sup>

**1** Institute of Bioinformatics, University Medicine Greifswald, Greifswald, Germany, **2** Theoretical Biology and Biophysics, Los Alamos National Laboratory, Los Alamos, New Mexico, United States of America, **3** Research Group "Dynamics of Early Viral Infection and the Innate Antiviral Response", Division Virus-Associated Carcinogenesis (F170), German Cancer Research Center (DKFZ), Heidelberg, Germany, **4** Dept of Infectious Diseases, Molecular Virology, Heidelberg University, Heidelberg, Germany, **5** Division of infectious Diseases and Immunology, Virology Section, Dept of Biomolecular Health Sciences, Utrecht University, Utrecht, The Netherlands, **6** Department of Medical Microbiology, Leiden University Medical Center, Leiden, The Netherlands, **7** Division Virus-Associated Carcinogenesis (F170), German Cancer Research Center (DKFZ), Heidelberg, Germany, **8** German Center for Infection Research (DZIF), Heidelberg partner site, Heidelberg, Germany

<sup>#a</sup> Current address: Max von Pettenkofer Institute, Ludwig-Maximilians-University München, Germany

<sup>#b</sup> Current address: VectorY Therapeutics, Amsterdam, The Netherlands

\* [czitzmann@lanl.gov](mailto:czitzmann@lanl.gov) (CZ); [lars.kaderali@uni-greifswald.de](mailto:lars.kaderali@uni-greifswald.de) (LK)



## OPEN ACCESS

**Citation:** Zitzmann C, Dächert C, Schmid B, van der Schaar H, van Hemert M, Perelson AS, et al. (2023) Mathematical modeling of plus-strand RNA virus replication to identify broad-spectrum antiviral treatment strategies. *PLoS Comput Biol* 19(4): e1010423. <https://doi.org/10.1371/journal.pcbi.1010423>

**Editor:** Peter M. Kasson, University of Virginia, UNITED STATES

**Received:** July 22, 2022

**Accepted:** March 9, 2023

**Published:** April 4, 2023

**Peer Review History:** PLOS recognizes the benefits of transparency in the peer review process; therefore, we enable the publication of all of the content of peer review and author responses alongside final, published articles. The editorial history of this article is available here: <https://doi.org/10.1371/journal.pcbi.1010423>

**Copyright:** This is an open access article, free of all copyright, and may be freely reproduced, distributed, transmitted, modified, built upon, or otherwise used by anyone for any lawful purpose. The work is made available under the [Creative Commons CC0](https://creativecommons.org/licenses/by/4.0/) public domain dedication.

**Data Availability Statement:** Data are provided as supplementary material. Code and models underlying the manuscript are available via GitHub

## Abstract

Plus-strand RNA viruses are the largest group of viruses. Many are human pathogens that inflict a socio-economic burden. Interestingly, plus-strand RNA viruses share remarkable similarities in their replication. A hallmark of plus-strand RNA viruses is the remodeling of intracellular membranes to establish replication organelles (so-called “replication factories”), which provide a protected environment for the replicase complex, consisting of the viral genome and proteins necessary for viral RNA synthesis. In the current study, we investigate pan-viral similarities and virus-specific differences in the life cycle of this highly relevant group of viruses. We first measured the kinetics of viral RNA, viral protein, and infectious virus particle production of hepatitis C virus (HCV), dengue virus (DENV), and coxsackievirus B3 (CVB3) in the immuno-compromised Huh7 cell line and thus without perturbations by an intrinsic immune response. Based on these measurements, we developed a detailed mathematical model of the replication of HCV, DENV, and CVB3 and showed that only small virus-specific changes in the model were necessary to describe the *in vitro* dynamics of the different viruses. Our model correctly predicted virus-specific mechanisms such as host cell translation shut off and different kinetics of replication organelles. Further, our model suggests that the ability to suppress or shut down host cell mRNA translation may be a key factor for *in vitro* replication efficiency, which may determine acute self-limited or chronic infection. We further analyzed potential broad-spectrum antiviral treatment options *in silico* and found that targeting viral RNA translation, such as polyprotein cleavage and viral RNA synthesis, may be the most promising drug targets for all plus-strand RNA viruses. Moreover, we found that targeting only the formation of replicase complexes did not stop the

at [https://github.com/Carolin1901/Plus\\_Strand\\_RNA\\_Virus\\_Replication](https://github.com/Carolin1901/Plus_Strand_RNA_Virus_Replication).

**Funding:** This work received funding from the BMBF through the ERASysAPP project SysVirDrug (grant 031A602A). LK received funding from the DFG (grant number KA 2989/13-1). CD was supported by a stipend of the DKFZ International PhD Program. Portions of this work were done under the auspices of the U.S. Department of Energy under contract 89233218CNA000001 and supported by NIH grants R01-AI078881 and R01-AI116868 to ASP. The funders had no role in study design, data collection and analysis, decision to publish, or preparation of the manuscript.

**Competing interests:** The authors have declared that no competing interests exist.

*in vitro* viral replication early in infection, while inhibiting intracellular trafficking processes may even lead to amplified viral growth.

### Author summary

Plus-strand RNA viruses comprise a large group of related and medically relevant viruses. The current global pandemic of COVID-19 caused by the SARS-coronavirus-2 as well as the constant spread of diseases such as dengue and chikungunya fever show the necessity of a comprehensive and precise analysis of plus-strand RNA virus infections. Plus-strand RNA viruses share similarities in their life cycle. To understand their within-host replication strategies, we developed a mathematical model that studies pan-viral similarities and virus-specific differences of three plus-strand RNA viruses, namely hepatitis C, dengue, and coxsackievirus. By fitting our model to *in vitro* data, we found that only small virus-specific variations in the model were required to describe the dynamics of all three viruses. Furthermore, our model predicted that ribosomes involved in viral RNA translation seem to be a key player in plus-strand RNA replication efficiency, which may determine acute or chronic infection outcomes. Furthermore, our *in-silico* drug treatment analysis suggested that targeting viral proteases involved in polyprotein cleavage, in combination with viral RNA replication may represent promising drug targets with broad-spectrum antiviral activity.

### Introduction

Plus-strand RNA viruses are the largest group of human pathogens that cause re-emerging epidemics, as seen with dengue, chikungunya, and Zika virus, as well as global pandemics of acute and chronic infectious diseases such as hepatitis C and the common cold. The current global SARS-coronavirus-2 (SARS-CoV-2) pandemic shows how our lives can become affected by a rapidly spreading plus-strand RNA virus. As of May 2022, more than 500 million cases of SARS-CoV-2 infections have been reported, with over 6 million confirmed deaths [1,2]. While a global pandemic of the current scale clearly causes exceptional socio-economic burdens [3], various other plus-strand RNA viruses also cause significant burdens. For example, in 2013, symptomatic dengue cases in 141 countries caused socio-economic costs of US\$ 8.9 billion [4], while the costs of the latest Zika outbreak have been estimated to be US\$ 7–18 billion in Latin America and the Caribbean from 2015 to 2017 [5]. Furthermore, between 2014 and 2018, the USA spent around US\$ 60 billion on hepatitis C medication, with around US\$ 80,000 per patient [6,7].

Treatment options are limited for the majority of plus-strand RNA viruses. While vaccines and vaccine candidates are available for a few viruses, approved direct-acting antiviral drugs are only available against hepatitis C and SARS-CoV-2 [8,9]. Given the high disease burden and socio-economic cost caused by infections with plus-strand RNA viruses, there is an urgent need for broadly acting antiviral drugs. For their development, it is important to study the life cycles and host restriction and dependency factors in detail, not only at the level of each virus individually but also across a group of related viruses, to gain pan-viral insights. The current study investigated the life cycle of plus-strand RNA viruses. The ultimate goal was to reveal commonly effective antiviral strategies and potential therapeutic target processes in the viral life cycle. To do so, we chose three representatives of plus-strand RNA viruses, hepatitis C, dengue, and coxsackievirus B3 (compare Table 1).

**Table 1. Feature comparison of plus-strand RNA viruses.** DMV: double-membrane vesicles, ER: endoplasmic reticulum, NS: non-structural, S: structural.

	HCV	DENV	CVB3
<b>Virus characteristics</b>			
<b>Family</b>	Flaviviridae [20]	Flaviviridae [20]	Picornaviridae [20]
<b>Genus</b>	Hepacivirus [20]	Flavivirus [20]	Enterovirus [20]
<b>Transmission</b>	Human-to-human [20]	Mosquito-to-human [32]	Human-to-human [15]
<b>Tropism</b>	Hepatocytes [33]	Dendritic cells, monocytes, macrophages [32]	Brain/neuron, cardiac tissue, hepatocytes [15,34,35]
<b>Genome size</b>	9.6 kb [33]	10.7 kb [32]	7.5 kb [15]
<b>Number of genes/encoded proteins</b>	10 (3 S and 7 NS proteins) [33]	10 (3 S and 7 NS proteins) [32]	11 (4 S and 7 NS proteins) [15]
<b>Replication organelle (RO)</b>	DMV derived from ER [20]	Invaginated vesicles derived from ER [20]	DMV derived from Golgi and ER [20]
<b>Enveloped</b>	Yes [20]	Yes [20]	No [20]
<b>Host shut-off of RNA translation</b>	No [24]	Partially [23]	Yes [22]
<b>Disease characteristics</b>			
<b>Infection outcome</b>	Acute and chronic [36]	Acute [37]	Primary acute (ability of virus persistence) [15,38]
<b>Basic reproductive number (<math>R_0</math>)</b>	1–3 (strain dependent) [39]	5 [40]	2.5 to 5.5 (range for different enteroviruses [41,42])
<b>Incubation period</b>	2 weeks to 6 months [36]	4 to 10 days [37]	5 days [38]
<b>Exponential growth rate</b>	Measured in human blood: 2.2 per day (doubling time 7.6 hours) [43]	Primary infection measured in human blood: 4.0 per day (doubling time 4.2 hours) [approximated from [44]]	Measured in mouse blood: 4.5 per day (doubling time 3.7 hours) [approximated from [38]]
	Measured in chimpanzees: 1 <sup>st</sup> phase: 1.4 per day (doubling time 12 hours) [45] 2 <sup>nd</sup> phase: 0.1 per day (doubling time 7.5 days) [45]	Secondary infection measured in human blood: 4.6 per day (doubling time 3.6 hours) [approximated from [44]]	Measured in mouse heart: 14.5 per day (doubling time 1.1 hours) [approximated from [38]]
<b>Time to reach peak</b>	Measured in human blood: 21 days [43]	Measured in human blood: 7 days [44]	Measured in mouse blood and heart: 3 days [38]
<b>Peak viral load</b>	Measured in human and chimpanzee blood: $10^6$ to $10^7$ RNA per mL [43,45,46]	Measured in human blood: $10^9$ to $10^{10}$ RNA per mL [44]	In mouse blood: $10^6$ RNA per mL [38]
	Measured in human liver: $10^8$ RNA per g [43]		In mouse heart: $10^{11}$ to $10^{12}$ RNA per g [38]
<b>RNA clearance</b>	Individuals with spontaneous clearance: 4.3 per day (RNA half-life 4 hours) [approximated from [47]]	Primary infection measured in human blood: 2.8 per day (RNA half-life 6 hours) [approximated from [44]]	Measured in mouse blood: 0.7 per day (RNA half-life 24 hours) [approximated from [38]]
	Otherwise: persistent RNA [47]	Secondary infection measured in human blood: 4.0 per day (RNA half-life 4.2 hours) [approximated from [44]]	Measured in mouse heart: 1 <sup>st</sup> phase: 1.2 per day (RNA half-life 13.4 hours) [approximated from [38]] 2 <sup>nd</sup> phase: 0.05 per day (RNA half-life 14 days) [approximated from [38]]
<b>Infection duration</b>	Months to Years [36]	2 to 3 weeks [44]	2 weeks [48]

<https://doi.org/10.1371/journal.pcbi.1010423.t001>

The enveloped blood-borne hepatitis C virus (HCV) is a *Hepacivirus* of the family *Flaviviridae* that causes acute and chronic hepatitis C. An acute infection is typically mild, but once chronic and untreated, may cause life-threatening conditions, including liver cirrhosis and hepatocellular carcinoma. Approximately 70 million people worldwide live with chronic

hepatitis C, with 400,000 related deaths annually [10]. Notably, hepatitis C can be cured in more than 95% of cases with direct-acting antivirals that inhibit viral replication [10].

The re-emerging dengue virus (DENV) is a *Flavivirus* and belongs, similarly to HCV, to the family *Flaviviridae*. Annually, DENV infects 390 million people worldwide, with around 96 million becoming symptomatic. Unlike HCV, DENV is vector-borne and is spread mainly by the mosquitoes of the *Aedes* species. Infection with DENV causes flu-like illness, occasionally with severe complications primarily associated with heterotypic secondary infections (e.g., hemorrhagic fever and shock syndrome) [11]. The clinical manifestation of a DENV infection is closely related to infections with the mosquito-borne chikungunya and Zika virus, leading to frequent misdiagnosis [12].

Coxsackieviruses are members of the genus *Enterovirus* of the family *Picornaviridae*. This genus includes important human pathogens such as poliovirus, enterovirus-A71 (EV-A71), EV-D68, coxsackievirus, and rhinovirus. Enteroviruses cause 10 to 15 million infections every year and therefore belong to the most prevalent pathogens [13]. Enteroviruses cause various diseases, including hand-foot-and-mouth disease, encephalitis, meningitis, and paralysis [14]. Coxsackie B viruses are also known to infect cardiac tissue, leading to viral myocarditis, which can develop into congestive heart failure [15]. In this study, we focus on coxsackievirus B3 (CVB3).

Despite their broad range of clinical manifestations, transmission routes, and tropism (Table 1), plus-strand RNA viruses share remarkable similarities in their replication strategy. By definition, the genome of plus-strand RNA viruses has the polarity of cellular mRNAs. Therefore, after delivery into cells, the genome is translated, giving rise to a polyprotein that must subsequently be cleaved into viral proteins. These proteins induce host cell membrane rearrangements forming replication organelles (ROs). Either within those ROs or on its outer membrane facing the cytosol, viral RNAs are amplified by the viral replicase complex comprising, amongst others, the RNA-dependent RNA polymerase (RdRp). These ROs are thought to hide viral RNAs from the host immune response, thus protecting them from degradation. In addition, the membranous compartment allows the coordinated coupling of the different steps of the viral replication cycle, i.e., RNA translation, RNA replication, and virion assembly [16–19].

However, there are striking differences in the viral life cycles of the three studied viruses. For example, the morphology of the ROs in which the replication takes place differs considerably. While HCV forms double-membrane vesicles (DMV), DENV induces invaginations of host cellular membranes [20]. CVB3 infection first results in single-membrane tubular structures that subsequently transform into DMVs and multilamellar vesicles [21]. Additionally, HCV and DENV, as representatives of *Flaviviridae*, remodel membranes of the rough endoplasmic reticulum (rER), however, the *Picornaviridae* CVB3 uses the ER and Golgi apparatus for its RO formation [20]. Another interesting feature of CVB3 is its ability to trigger a so-called host translational shut-off, leading to increased viral over host RNA translation [22]. Repressed host RNA translation has also been reported for DENV [23]. However, a host shut-off has not been reported for HCV, which instead shows a parallel translation of viral and host cell RNAs, consistent with the predominantly chronic infection caused by this virus [24].

To identify an efficient, broadly active treatment strategy against viral infectious diseases, a comprehensive knowledge of viruses, as well as their exploitive interaction with the host, is of major importance. Mathematical modeling has proven to be a powerful tool to study viral pathogenesis, transmission, and disease progression and has increased our knowledge about therapeutic intervention and vaccination as well as the involvement of the immune system for viruses such as the human immunodeficiency virus (HIV), HCV, influenza A virus, DENV, Zika virus, and SARS-CoV-2 [25–31]. One of the major strengths of mathematical models is their ability to describe and analyze viral replication in a quantitative, dynamic (time-resolved)

framework and to characterize the influence individual parameters have on the ensuing dynamics. These models thus permit much more profound insights into viral replication and antiviral strategies than static, often more qualitative snapshots of host-pathogen interactions.

In the current study, we reproduced the dynamics of the initial post-infection phase of the life cycle of three representative plus-strand RNA viruses, namely HCV, DENV, and CVB3, with one common mathematical model. Using the model, we identified pan-viral similarities and virus-specific differences in the life cycle of plus-strand RNA viruses that are represented by a unique set of model parameters. The inter-viral differences among the plus-strand RNA viruses under investigation have been further analyzed to study how these differences might be related to clinical disease manifestation, particularly with regard to chronic versus acute infections. Our model suggests that the number of ribosomes available for viral RNA translation may be crucial for either acute or chronic infection outcomes. Furthermore, we studied broad-spectrum antiviral treatment options and found that inhibiting viral proteases involved in polyprotein cleavage and RNA synthesis are promising drug targets.

## Methods

### Kinetic experiments and infectivity titers

**HCV infections.**  $2 \times 10^5$  Lunet-CD81<sub>high</sub> [49] cells per 6-well were seeded in 2 mL 16 hours prior to infection. To ensure simultaneous infection of all cells, cells were kept at 4°C for 30 min before medium aspiration and inoculation with pre-cooled PEG-precipitated HCV<sub>cc</sub> (Jc1) [50] at an MOI of 1 at 4°C for one hour (1 mL per 6-well). The inoculum was removed and cells were covered with 1 ml per well pre-warmed (37°C) medium and incubated for one hour at 37°C. Medium was aspirated and cells were treated with an acid wash protocol to remove extracellular vesicles and unbound virus particles: cells were washed with an acidic solution (0.14 M NaCl, 50 mM Glycine/HCl, pH 3.0, 670  $\mu$ L per 6-well) for three minutes at 37°C before neutralization with neutralization buffer (0.14 M NaCl, 0.5 M HEPES, pH 7.5, 320  $\mu$ L per 6-well) and one wash with pre-warmed medium. After that, fresh medium was added. After indicated time-points, total cellular RNA was extracted by phenol-chloroform extraction. Infected cells were washed prior to lysis according to the acid wash protocol described above. After three washing steps with cold 1x PBS, cells were lysed in GITC buffer (700  $\mu$ L per 6 well) and RNA was extracted as described [51]. A strand-specific RT-qPCR protocol was used to quantify numbers of (+)- and (-)-strand RNA per cell [52]. TCID<sub>50</sub> of supernatants was measured and calculated as described previously [50] and converted to PFU/mL.

**CVB3 infections.** CVB3 wild-type (wt) and CVB3-Rluc, which carries *Renilla luciferase* upstream of the P1 region, were generated as described previously [53]. Subconfluent monolayers of HuH7 cells, provided by Prof. R. Bartenschlager, were infected with CVB3 wt or CVB3-Rluc at an MOI of 1 for 45 minutes. After removal of the viral inoculum, cells were washed once with PBS and fresh medium (DMEM supplemented with 10% FBS and penicillin and streptomycin) was added. Every hour up to 9 hours post-infection, cells were collected and subjected to various assays. Each assay was performed on three biological replicates. Cells were either frozen together with the medium, after which progeny virus titers were determined by endpoint titration by the method of Reed and Muench and converted to PFU/mL. Another set of cells were lysed in buffer to determine the luciferase activity as a measure of viral protein translation as described previously [53]. Lastly, cells frozen after aspiration of the medium were used for total RNA isolation and quantification of the amount of viral RNA copies per cell with quantitative PCR as described previously [54].

**DENV infections.** DENV kinetic measurements of intracellular plus-strand RNA and luciferase activity, as well as extracellular infectious virus titers, have been taken from [55]

(raw data provided by the authors). In brief,  $2 \times 10^5$  Huh7 cells were infected with DENV reporter virus expressing Renilla luciferase [56] at an MOI of 10. RNA extraction, qRT-PCR, and Renilla luciferase activity were analyzed from cell lysates. RNA was normalized to the 2 h value. Infectivity titers (TCID<sub>50</sub>/mL) were measured from viral supernatant by limited dilution assays and converted to PFU/mL; supernatants were subsequently supplemented [55].

### Plus-strand RNA virus replication model

We developed a mechanistic model using ordinary differential equations (ODEs) and mass action kinetics to analyze pan-viral similarities and virus-specific differences within the plus-strand RNA virus life cycle. Our published models on two plus-strand RNA viruses, HCV and DENV, served as a basis for the pan-viral plus-strand RNA virus replication model [19,55,57]. However, in our previous published models, we studied host dependency factors responsible for cell line permissiveness and restriction factors such as the innate immune response. Therefore, those models were modified to reflect merely the plus-strand RNA life cycle from virus entry to release of all viruses considered here.

The resulting model of plus-strand RNA virus replication is composed of four main processes: Entry of plus-strand RNA virus via receptor-mediated endocytosis and release of the viral genome (Fig 1 steps ① and ②), its subsequent translation into viral proteins (Fig 1 steps ③ to ⑤), viral RNA replication within the replication organelle (Fig 1 steps ⑥ to ⑨), and further replication (Fig 1 step ⑩) or RNA export out of the replication organelle (Fig 1 step ⑪) or virus packaging and release from the cell with subsequent reinfection of the same cell or infection of naïve cells (Fig 1 steps ⑫ and ⑬).

The virus infection process (Eqs 1 and 2), i.e., receptor-mediated virus entry, fusion, and release of the viral genome into the cytoplasm, as well as reinfection of the same cell or further infection of naïve cells (Eq 14) are represented by extracellular virus  $V$ , virus within endosomes  $V_E$ , and newly produced virus released from infected cells  $V_R$  and are given by the equations

$$\frac{dV}{dt} = -k_e^i V + k_{re}^i V_R - \mu_V^i V \quad (1)$$

and

$$\frac{dV_E}{dt} = k_e^i V - k_f^i V_E - \mu_{V_E}^i V_E. \quad (2)$$

Extracellular virus  $V$  enters a single cell via receptor-mediated endocytosis with rate constant  $k_e^i$  or degrades with constant rate  $\mu_V^i$ . Note that virus-specific parameters are marked with superscripted  $i$  with  $i \in \{HCV, DENV, CVB3\}$ . The virus within endosomes  $V_E$  either degrades with rate constant  $\mu_{V_E}^i$  or undergoes conformational changes of its nucleocapsid resulting in the release of the viral genome  $R_p$  with rate constant  $k_f^i$ . Note that extracellular virus is also replenished by the release of virus from the cell at rate  $k_{re}$ .

Viral RNA translation and replication (Eqs 3 to 13) are modeled based on our published HCV and DENV models [19,55]. In brief, our model describes the translation-associated processes in the cytoplasm (Eqs 3 to 8) starting with free viral RNA  $R_p$  in the cytoplasm, an intermediate translation initiation complex  $TC$ , as well as the translated polyprotein  $P_p$  which is cleaved into structural and non-structural viral proteins,  $P_S$  and  $P_N$ , respectively. Note that a firefly luciferase gene has been integrated into the viral genomes. The luciferase activity  $L$  was measured from cell lysates as a marker for translation activity (see Methods) reflecting protein concentration and has been introduced into the model. Translation and polyprotein processing are modeled with the following ODEs, where  $Ribo_{tot}^i$  and  $RC_{MAX}$  are the total number of



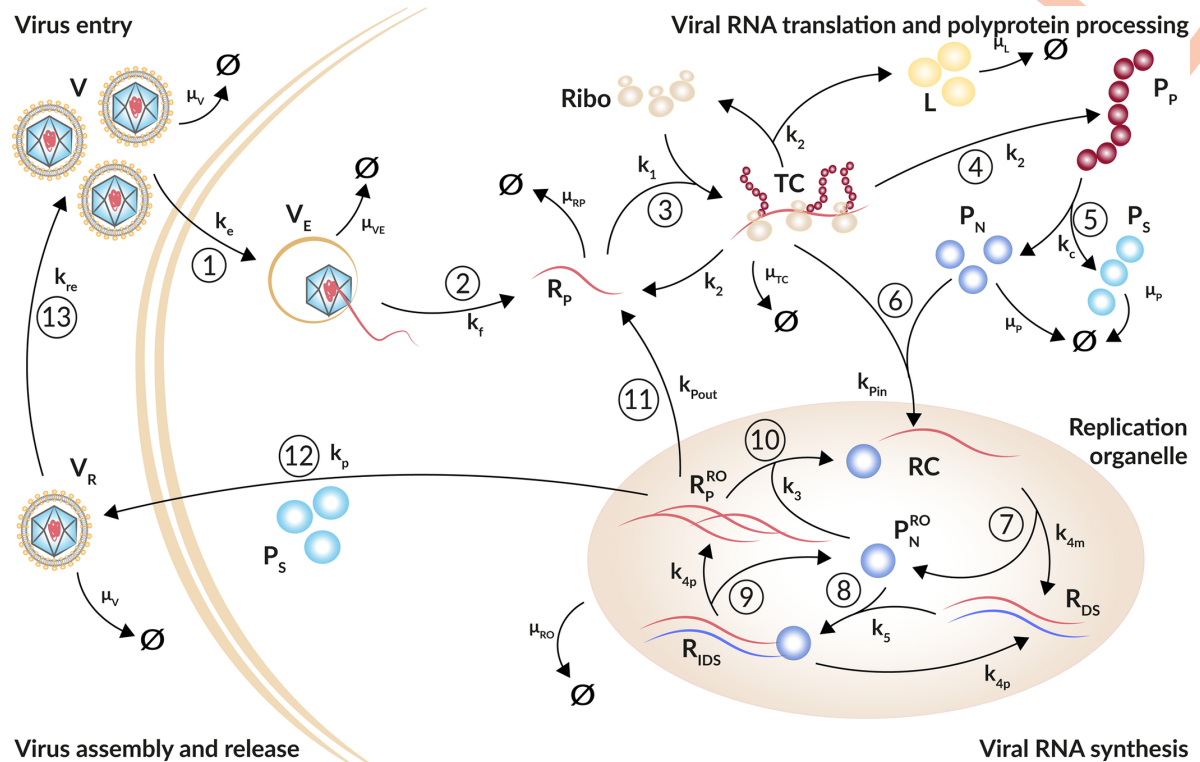


**Fig 1. Schematic illustration of the plus-strand RNA life cycle.** ① Virus ( $V$ ) enters the cell via receptor-mediated endocytosis ( $k_e$ ). ② The viral genome ( $R_p$ ) is released ( $k_f$ ). Virus within the endosome ( $V_E$ ) degrades with rate constant  $\mu_{VE}$ . ③ Ribosomes ( $Ribo$ ) bind at the viral genome and form ( $k_1$ ) a translation initiation complex ( $TC$ ) that degrades with rate constant  $\mu_{TC}$ . ④ The viral genome ( $R_p$ ) is translated ( $k_2$ ) into a polyprotein ( $P_p$ ) that ⑤ is subsequently cleaved ( $k_c$ ) into structural and non-structural viral proteins,  $P_S$  and  $P_N$ , respectively. To measure translation activity, luciferase ( $L$ ) is integrated into the viral genome and produced with RNA translation. Viral proteins degrade with rate constant  $\mu_P$ ; luciferase degrades with rate constant  $\mu_L$ . ⑥ Non-structural proteins and freshly translated viral RNA form ( $k_{pin}$ ) replicase complexes ( $RC$ ) that are associated with replication organelles (ROs) and ⑦ serve as a template for the minus-strand synthesis ( $k_{4m}$ ) leading to double-stranded RNA ( $R_{DS}$ ). ⑧ Viral non-structural proteins, such as the RdRp, within the replication organelle ( $P_N^{RO}$ ) bind to double-stranded RNA, forming ( $k_5$ ) a minus-strand replication intermediate complex ( $R_{IDS}$ ) that ⑨ initiates the plus-strand RNA synthesis ( $k_{4p}$ ) giving rise to multiple copies of viral plus-strand RNA ( $R_p^{RO}$ ). All species within the replication organelle degrade with the same rate constant  $\mu_{RO}$ . ⑩ The viral genome can remain within the replication organelle, where it undergoes multiple rounds of genome replication ( $k_3$ ), ⑪ it can be exported ( $k_{pout}$ ) out of the replication organelle into the cytoplasm starting with the translation cycle again, or ⑫ the plus-strand RNA genome ( $R_p^{RO}$ ) is packaged together with structural proteins ( $P_S$ ) into virions ( $V_R$ ) that are released from the cell ( $k_p$ ) and ⑬ may re-infect the same cell or infect naïve cells ( $k_{re}$ ). Extracellular infectious viral species ( $V$  and  $V_R$ ) degrade with rate constant  $\mu_V$ .

<https://doi.org/10.1371/journal.pcbi.1010423.g001>

ribosomes and maximal number of replicase complexes in a cell (see below for details), respectively:

$$\frac{dR_p}{dt} = k_f^i V_E - k_1 R_p (Ribo_{tot}^i - TC) + k_2^i TC + k_{pout}^i R_p^{RO} - \mu_{RP}^i R_p, \quad (3)$$

$$\frac{dTC}{dt} = k_1 R_p (Ribo_{tot}^i - TC) - k_2^i TC - k_{pin}^i \left(1 - \frac{RC}{RC_{MAX}}\right) P_N TC - \mu_{TC}^i TC, \quad (4)$$

$$\frac{dP_P}{dt} = k_2^i TC - k_c P_P, \quad (5)$$

$$\frac{dL}{dt} = k_2^i TC - \mu_L L, \quad (6)$$

$$\frac{dP_S}{dt} = k_c P_P - \mu_P^i P_S - N_{P_S}^i v_P, \quad (7)$$

$$\frac{dP_N}{dt} = k_c P_P - k_{pin}^i \left(1 - \frac{RC}{RC_{MAX}}\right) P_N TC - \mu_P^i P_N. \quad (8)$$

With rate constant  $k_1$ , free host ribosomes form a translation complex  $TC$  with the viral plus-strand RNA genome  $R_P$ . The total number of ribosomes ( $Ribo_{tot}^i$ ) available for viral RNA translation was assumed constant, and  $Ribo = Ribo_{tot}^i - TC$  gives the number of free ribosomes. Note that  $Ribo_{tot}^i$  is only a fraction of the total cellular ribosome number. Translation of the viral plus-strand RNA genome generates the viral polyprotein  $P_P$  and luciferase  $L$  with rate constant  $k_2^i$ . The viral polyprotein  $P_P$  is subsequently cleaved with rate constant  $k_c$  into structural and non-structural viral proteins,  $P_S$  and  $P_N$ , respectively. The translation complex  $TC$  decays with rate constant  $\mu_{TC}^i$ , while luciferase and viral proteins degrade with rate constants  $\mu_L$  and  $\mu_P^i$ , respectively. Note that for simplicity, we assume structural and non-structural proteins degrade with the same rate constant, which has been summarized as one virus-specific viral protein degradation rate  $\mu_P^i$ .

The subsequent processes of viral RNA synthesis in the replication organelle (RO) are modeled by Eqs 9 to 13, representing the replicase complex  $RC$ , double-stranded RNA  $R_{DS}$ , a double-stranded RNA intermediate complex  $R_{IDS}$ , newly synthesized viral plus-strand RNA in the RO  $R_P^{RO}$ , and non-structural proteins within the RO  $P_N^{RO}$ , as follows:

$$\frac{dRC}{dt} = k_{pin}^i \left(1 - \frac{RC}{RC_{MAX}}\right) P_N TC - k_{4m}^i RC + k_3 R_P^{RO} P_N^{RO} - \mu_{RO} RC, \quad (9)$$

$$\frac{dR_{DS}}{dt} = k_{4m}^i RC - k_5 R_{DS} P_N^{RO} + k_{4p}^i R_{IDS} - \mu_{RO} R_{DS}, \quad (10)$$

$$\frac{dR_{IDS}}{dt} = k_5 R_{DS} P_N^{RO} - k_{4p}^i R_{IDS} - \mu_{RO} R_{IDS}, \quad (11)$$

$$\frac{dP_N^{RO}}{dt} = k_{4m}^i RC - k_3 R_P^{RO} P_N^{RO} - k_5 R_{DS} P_N^{RO} + k_{4p}^i R_{IDS} - \mu_{RO} P_N^{RO}, \quad (12)$$

$$\frac{dR_P^{RO}}{dt} = k_{4p}^i R_{IDS} - k_3 R_P^{RO} P_N^{RO} - k_{pout}^i R_P^{RO} - v_P - \mu_{RO} R_P^{RO}. \quad (13)$$

Viral non-structural proteins recruit the viral RNA after translation to the replicase complex [58]. Hence, for viral RNA synthesis, we require translated viral RNA, i.e., the translation complex  $TC$  instead of free cytosolic viral RNA  $R_P$ , to interact with the non-structural proteins. Thus, the translation complex  $TC$  and a subset of non-structural proteins  $P_N$  are imported into the RO, leading to the formation of a replicase complex  $RC$  with rate constant  $k_{pin}^i$ . Following successful replicase complex formation, ribosomes dissociate from the complex as is accounted for in Eq (4). We furthermore assume that there is a limitation in the number of replicase

complexes formed within a cell. To do so, we extend  $k_{pin}^i$  by  $\left(1 - \frac{RC}{RC_{MAX}}\right)$  with the carrying capacity for replicase complexes  $RC_{MAX}$  [57,59].

Within the RO, minus-strand RNA synthesis occurs from the replicase complex with rate constant  $k_{4m}^i$ , leading to the formation of double-stranded RNA  $R_{DS}$ , which along with the non-structural proteins, are released from the RC,  $P_N^{RO}$ . Subsequently, the double-stranded RNA binds again to  $P_N^{RO}$  with rate constant  $k_5$  to form a double-stranded intermediate replicase complex  $R_{IDS}$ , initiating plus-strand RNA synthesis with rate constant  $k_{4p}^i$ . For simplicity, we assume that minus and plus-strand RNA synthesis occur with the same rate constant  $k_{4m}^i = k_{4p}^i$ . The newly synthesized plus-strand RNA genomes  $R_p^{RO}$  either remain within the RO to make additional replicase complexes with rate constant  $k_3$ , are exported out of the RO into the cytoplasm for further RNA translation with export rate  $k_{pout}^i$ , or are packaged together with structural proteins into virions  $V_R$  and are subsequently released from the cell. Assembly and release of virus particles is represented by a Michaelis-Menten type function  $v_p$  described below (Eq 15, compare [55,60]). The RNA and protein species within the RO ( $RC$ ,  $R_{DS}$ ,  $R_{IDS}$ ,  $R_p^{RO}$ ,  $P_N^{RO}$ ) are assumed to degrade with the same decay rate  $\mu_{RO}$  and represent the decay of the entire replication organelle.

The released virus  $V_R$  may re-infect the same cell or infect new cells with rate constant  $k_{re}$ , or degrade with rate constant  $\mu_V^i$ , resulting in the equation

$$\frac{dV_R}{dt} = v_p - k_{re} V_R - \mu_V^i V_R. \quad (14)$$

Assembly of newly synthesized viral plus-strand RNA genome  $R_p^{RO}$  and viral structural proteins  $P_S$  into viral particles and their subsequent release from the host cell are described using a Michaelis-Menten type function, with rate

$$v_p = k_p R_p^{RO} \frac{P_S}{K_D^i N_{P_S}^i + P_S}, \quad (15)$$

where  $k_p$  is the virion assembly and release rate, and  $k_p R_p^{RO}$  is the maximum release rate limited by viral resources. Let  $N_{P_S}^i$  be the number of structural proteins in a virus of type  $i$ , then to produce virus at rate  $v_p$  will require a large number of proteins  $K_D^i N_{P_S}^i$ , where  $K_D^i$  is a scaling constant and  $K_D^i N_{P_S}^i$  is the number that corresponds to the half-maximal release rate [see [55,60,61] for more details].

### Pan-viral and virus-specific model parameters

To complete the plus-strand RNA virus model, we need to specify model parameters. To prevent overfitting and parameter uncertainty, we fixed many parameter values to either experimentally determined values or values estimated in other modeling studies. In some cases, we could calculate velocities directly, such as for viral RNA translation and synthesis, which could thus be fixed as described in S1 Text. An overview of all parameter values is given in Table 2.

### Parameter estimation, model selection, and model analysis

Our model has 61 parameters; 30 of them were fixed, while 31 were estimated by fitting the model to the experimental data. As the fixed parameter values were experimentally measured, calculated, or taken from literature, we had information about which were virus-specific (S1 Text and Table 2). To determine which of the remaining model parameters are conserved across the different viruses considered (pan-viral) and which parameters are virus-specific, we

**Table 2. Parameter values and 95% confidence intervals in ().** Note that parameter values marked with \* were fixed due to previous assumptions and calculations. Furthermore, confidence intervals marked with + hit the set estimation boundary; † calculated from the data; ‡ experimentally measured for Zika virus; § experimentally measured for poliovirus.

Parameter	Description	HCV	DENV	CVB3	Unit
$k_e^i$	Virus entry rate	10 (1.9, $10^+$ )	0.31 (0.28, 0.34)	1.3 (0.9, 1.7)	1/h
$k_f^i$	RNA release rate	10 (1.7, $10^+$ )	0.008 (0.006, 0.01)	0.016 (0.006, 0.04)	1/h
$k_1$	Formation rate of the translation complex	1000 (840, $1000^+$ )			mL/molecule /h
$k_2^i$	Virus RNA translation rate	180 [65]	100 [55]	300 ‡ [66]	1/h
$k_c$	Polyprotein cleavage rate	2.24 (1.18, 7.4)			1/h
$k_3$	Formation of additional replicase complexes within the replication organelle	42 (5.5, 525)			mL/molecule /h
$k_{Am}^i = k_{Ap}^i$	Minus- and plus-strand RNA synthesis rate	1.1 [65]	1.0 [55]	50 ‡ [66]	1/h
$k_{pin}^i$	Formation rate of the replicase complex	4.4 (2.4, 7.5)	0.45 (0.29, 0.74)	1.4 (0.52, 4.09)	mL/molecule /h
$k_5$	Formation rate of the replication intermediate complex	6018 (1549, 68401)			mL/molecule /h
$k_{Pout}^i$	Export rate of viral RNA out of the replication organelle	33 (0.8, 1477)	53 (16, 432)	0.23 (0.16, 0.43)	1/h
$k_p$	Assembly and release rate	158 (47, $1000^+$ )			mL/molecule /h
$k_{re}$	Reinfection rate	0.01 (0.01†, 0.038)			1/h
$\mu_{RP}^i$	Degradation rate of cytosolic viral RNA	0.26 [65]	0.23 [67]	0.15 ‡ [68]	1/h
$\mu_{TC}^i$	Degradation rate of the translation complex	0.13 †	0.115 †	0.075 †	1/h
$\mu_{RO}^i$	Degradation rate of viral RNA and protein within the replication organelle	0.0842 [19]			1/h
$\mu_P^i$	Degradation rate of viral protein	0.08 [19]	0.46 [67]	0.43 [69]	1/h
$\mu_L^i$	Degradation rate of luciferase	0.35 [19]			1/h
$\mu_V^i$	Degradation rate of extracellular infectious virus	0.1 [57]	0.13 [70]	0.08 [71,72]	1/h
$\mu_{VE}^i$	Degradation rate of intracellular virus within the endosome	0.23 † [73]			1/h
$V_0^i$	Initial virus concentration	0.2 (0.16, 0.25)	1 (0.8, 1.3)	1 (0.4, 2.2)	molecules/mL
$Ribo_{tot}^i$	Total ribosome concentration	0.005 (0.004, 0.007)	0.48 (0.41, 0.55)	6.7 (5.0, 9.1)	molecules
$RC_{MAX}$	Maximum number of replicase complexes	0.46 (0.34, 0.64)			molecules/mL
$K_D^i$	Scaling constant for virus	0.04 †	1.8 †	40 †	virions
$N_{Ps}^i$	Number of structural proteins needed to produce 1 virion	180 [65,74]	180 [55,74]	60 [15]	molecules/virion
$f_{RP}^i$	Scale factor for plus-strand RNA	394 (274, 524)	0.76 (0.58, 1.0)	550 (245,1366)	
$f_{RM}^i$	Scale factor for minus-strand RNA	1377 (945, 1872)	-	-	
$f_L^i$	Scale factor for luciferase	-	0.41 (0.33, 0.5)	0.08 (0.06, 0.1)	

<https://doi.org/10.1371/journal.pcbi.1010423.t002>

performed several rounds of model evaluation using the Akaike information criterion (AIC) and model identifiability analysis (profile likelihood estimation). See S2 Text for a description of the model selection process.

We simultaneously fit the plus-strand RNA virus replication model to the virus-specific data sets for HCV, DENV, and CVB3. To fit the mathematical model to the experimental data, we calculated the total plus-strand RNA  $R_p^{tot} = (V_E + R_p + TC + RC + R_{DS} + R_{IDS} + R_p^{RO})$ , total minus-strand RNA  $R_M^{tot} = (R_{DS} + R_{IDS})$ , luciferase  $L$ , and total infectious virus  $V^{tot} = (V + V_R)$ . Note that our model accounts for infectious virus since infectious titers were measured for all three viruses. Further note that for the infectious virus measurements for HCV,  $V^{tot} = V_R$ , since measuring infectious virus started 20 h pi. We introduced three scale factors  $f_L$ ,  $f_{RM}$ , and  $f_{RP}$  to re-scale experimental measurements acquired in relative measurements (plus-strand

RNA for DENV), molecules per cell (plus- and minus-strand RNA measurements for HCV and plus-strand RNA for CVB3), and relative light unit (luciferase for DENV and CVB3).

We implemented the model in MATLAB (The MathWorks) 2016 using the Data2Dynamics toolbox [62]. We assessed model identifiability using the profile likelihood estimation method implemented in Data2Dynamics [62,63]. In Data2Dynamics, a parameter is identifiable if its 95% confidence interval is finite [62,63]. Note that an estimated model parameter may hit a predefined upper or lower parameter boundary which hampers the calculation of the 95% confidence interval. In such cases, a one-sided 95% confidence interval has been calculated starting from the estimated model parameter and thus with its upper or lower boundary marked with + in Table 2. Details about the model fitting and model selection process are in S2 Text.

We performed a global sensitivity analysis in MATLAB using the extended Fourier Amplitude Sensitivity Test (eFAST) [64]. We calculated sensitivities with regard to the total plus-strand RNA ( $R_p^{tot}$ ) concentrations throughout the course of infection. We studied hypothetical drug interventions by including the effects of direct-acting antivirals (DAA) into the model. For this purpose, we simulated putative drugs targeting (1) viral entry and internalization  $k_e$ , (2) release of the viral RNA genome  $k_f$ , (3) formation of the translation initiation complex  $k_1$ , (4) viral RNA translation  $k_2$ , (5) polyprotein cleavage  $k_c$ , (6) replicase complex formation  $k_{pm}$ , (7) minus- and plus-RNA synthesis  $k_{4m}$  and  $k_{4p}$ , as well as (8) virus particle production and release ( $v_p$ ). To introduce drug effects into the model, we assumed a drug efficacy parameter  $0 \leq \varepsilon \leq 1$ , and multiplied the parameters above by  $(1-\varepsilon)$  to simulate drug treatment. Similar to our previously published DENV model, we calculated the average virus particle concentration released from the cell upon drug administration ( $\varepsilon \neq 0$ ) until 5 days post-drug administration, i.e., a drug treatment observation window of 120 h. The average virus particle concentration with treatment ( $\varepsilon \neq 0$ ) has been normalized to the average virus concentration without drug treatment ( $\varepsilon = 0$ ). Note that we studied two different time points of drug administration: at the very beginning of the infection, 0 h pi, and when the system is in steady state, 100 h pi.

## Results

As shown on the left in Fig 2, the model replicates the experimental data for all three viruses. Virus-specific characteristics are revealed by comparing the dynamics of the three viruses and their plus-strand RNA genomes. CVB3 is a fast-replicating virus with a life cycle duration of about 8 hours (depending on the cell type), after which the infected cells begin to die. Similarly, DENV is cytopathic but seems to be slower replicating and thus has a longer life cycle than CVB3, with DENV starting to produce virus about 16 h pi [56]. In contrast, HCV is non-cytopathic with a consequently longer life cycle. In our experimental measurements, the CVB3 viral load peaked at the end of its life cycle with 193 PFU/mL/cell. The HCV viral load peaked at 0.06 PFU/mL/cell around 44 h pi, while the DENV viral load reached its maximum with approximately 8 PFU/mL/cell around 10 hours earlier at 30 to 34 h pi (Fig 2A, 2B, and 2C). We calculated the corresponding average virus concentration per measurement time point for HCV, DENV, and CVB3 per cell as 0.04 PFU/mL/cell, 1.8 PFU/mL/cell, and 40 PFU/mL/cell, respectively. Thus, the average infectious HCV viral load was only 4% of the average DENV viral load and only 0.3% of the average CVB3 viral load. Similarly, CVB3 reached a peak of almost 500,000 plus-strand RNA copies per cell at 8 h pi, while HCV produced only 10,000 copies per cell at 70 h pi, i.e., 98% less than CVB3. Note that both, CVB3 infectious virus and plus-strand RNA, increased several 1000-fold in time.

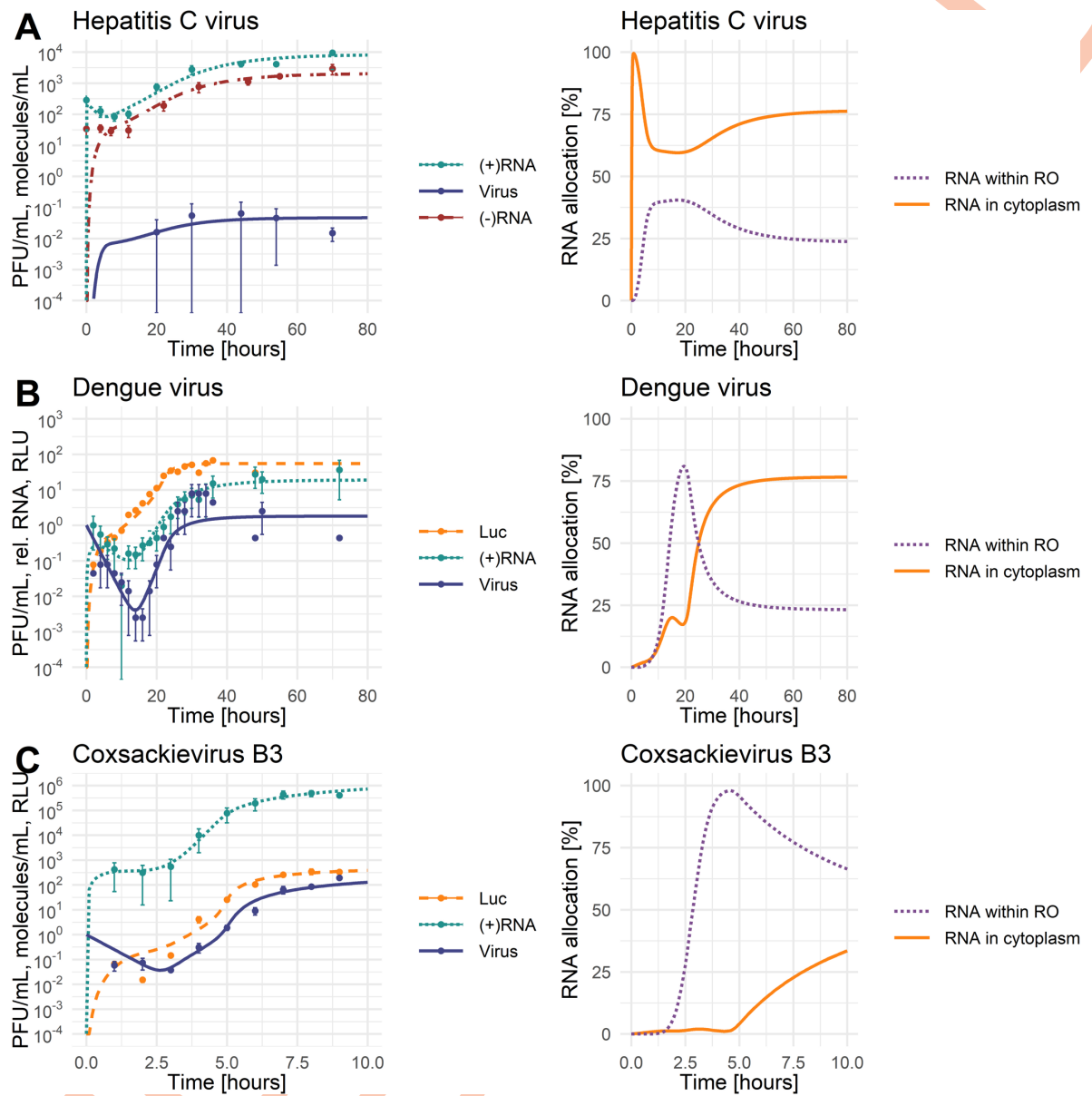


**Fig 2.** Best fit of the model to the data with standard deviation (left panel) and model prediction of plus-strand RNA allocation between the cytoplasm and replication organelle (RO) (right panel). For parameter values, see Table 2. [LEFT: green: (+)RNA =  $R_p^{tot} = (V_E + R_p + TC + RC + R_{DS} + R_{IDS} + R_p^{RO})$ , red: (-)RNA =  $R_M^{tot} = (R_{DS} + R_{IDS})$ , blue: A) Virus =  $V^{tot} = V_R$ , B) and C) Virus =  $V^{tot} = (V + V_R)$ , yellow: Luc = L; RIGHT: yellow: RNA in cytoplasm =  $(R_p + TC)/R_p^{tot}$ , purple: RNA within replication organelle (RO) =  $(RC + R_{DS} + R_{IDS} + R_p^{RO})/R_p^{tot}$ ; Infectious virus was measured in PFU/mL, (+) and (-)RNA were measured in molecules/mL or relative RNA concentration, luciferase was measured in relative light unit (RLU)].

<https://doi.org/10.1371/journal.pcbi.1010423.g002>

### Model selection and uncertainty

The intracellular model structure has been taken from our previously published HCV model [19], upon which we built with our recently published DENV model [55]. However, a striking difference from our previous HCV and DENV models is the absence of host factors involved in replicase complex formation and virus assembly and release. We have previously shown that host factors are recruited by the virus and seem beneficial for host cell permissiveness and virus replication efficiency [19,55]. Instead, here we describe intra-viral replication differences with virus-specific parameter sets based on model evaluation by AIC and profile likelihood estimation (see [Methods](#), [S1](#) and [S2](#) Texts).

Considering the maximal number of replicase complexes ( $RC_{MAX}$ ) improved the basic model AIC from 3025 to 1982 and thus served as a starting point for the virus-specific model selection process (see [S2 Text](#)). After several rounds of model selection by comparing AICs and taking model identifiability into account, we added five virus-specific processes into our basic model (from a total of 13 considered processes): (1) the total number of ribosomes  $Ribo_{tot}^i$  available for viral RNA translation, (2) virus entry  $k_e^i$ , (3) viral genome release  $k_f^i$ , (4) formation of the replicase complex  $k_{rim}^i$ , and (5) export of viral RNA from the RO into the cytoplasm  $k_{pout}^i$ . Note that based on literature data and previous assumptions, we fixed some virus-specific and pan-viral processes and degradation rates (see [S1 Text](#) and [Table 2](#)). The best-fit model showed high similarity to the virus-specific experimental measurements and a high degree of model identifiability (see [Fig 2](#) for best fit, [Fig 3](#) for the parameter profiles based on the profile likelihood estimation, and [Table 2](#) for parameter values with 95% confidence intervals).

### RNA allocation

As predicted by our model, the allocation of plus-strand RNA in the cytoplasm and within the RO shows interesting virus-specific differences ([Fig 2](#) right panel). Compared to the total amount of viral RNA, HCV has most of the RNA allocated to the cytoplasm and is thus available for viral RNA translation at any given time. In DENV, our model predicted that the allocation strategy changes throughout the viral life cycle, with most plus-strand RNA within the RO initially. At around 25 h pi, viral RNAs are equally distributed between the two compartments, while at the end of the DENV life cycle, the majority of viral RNA is in the cytoplasm. Interestingly, in steady state, the predicted allocation of both HCV and DENV is the same, with 25% of RNA allocated to the RO and 75% to the cytoplasm. In contrast, the predicted viral RNA allocation is the opposite for CVB3. CVB3 has the majority of RNA available within the RO, contributing to the 2- to 3-log higher viral load.

### Virus-specificity

For a successful virus infection, the first hurdles to overcome are virus entry and the release of the viral genome into the cytoplasm. The rate constants for virus entry  $k_e^i$  and vRNA release  $k_f^i$  had the highest estimated values for HCV. However, both values were practically non-identifiable, suggesting a limitation in the amount of data. Hence, we could only estimate the lower boundary of the 95% confidence intervals, which suggests  $k_e^{HCV} \geq 1.9 \text{ h}^{-1}$  and  $k_f^{HCV} \geq 1.7 \text{ h}^{-1}$ . CVB3 seems slightly better adapted to the cell line with a 4-times higher entry rate and 2-times higher vRNA release rates than DENV. According to our model selection process, the degradation rate of the internalized virus within endosomes  $\mu_{VE}$  was pan-viral, suggesting neither an advantage nor disadvantage for the studied viruses.

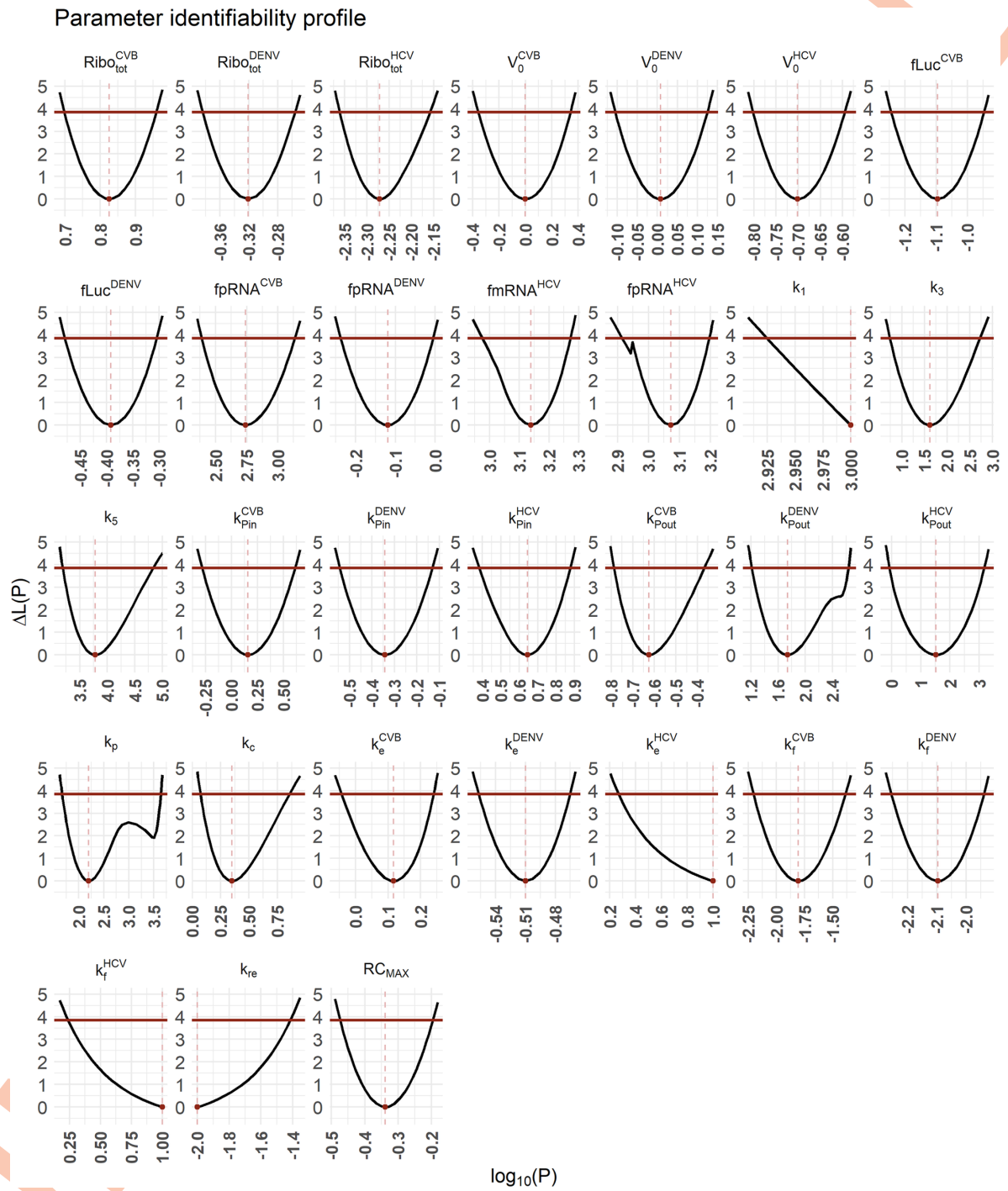


**Fig 3. Uncertainty analysis of the best-fit model.** For parameter values and 95% confidence intervals, see Table 2. The best fit is shown in Fig 2.

<https://doi.org/10.1371/journal.pcbi.1010423.g003>



The following processes in the viral life cycle are vRNA translation and polyprotein processing with parameters  $k_1$  for the formation of the translation initiation complex,  $k_2^i$  vRNA translation, and  $k_c$  polyprotein cleavage. Models including virus-specific  $k_1$  or  $k_c$  either did not improve the quality of the model fit (no AIC improvement) or were non-identifiable when tested as virus-specific and thus have been selected as pan-viral (see [S2 Text](#)). However, the viral RNA translation rate  $k_2^i$  was calculated based on genome size and ribosome density and set as virus-specific (see [S1 Text](#)). In the vRNA translation and polyprotein processing step, our model selected the total number of ribosomes  $Ribo_{tot}^i$  as the only virus-specific parameter. Since the ribosome number has been selected in the first round of model selection (see [S2 Text](#)), it emphasizes the importance of this host factor, with CVB3 showing the highest estimated ribosome number available for RNA translation. In contrast, HCV and DENV use only 0.07% and 7% of the ribosomes CVB3 uses, respectively. Interestingly, increasing the number of ribosomes in the HCV life cycle to those of CVB3 (from  $Ribo_{tot}^{HCV} = 0.005$  to  $Ribo_{tot}^{HCV} = 6.7$  molecules per mL) increases the infectious virus load by three orders of magnitude ([Fig 4A](#)). In the same way, decreasing the number of ribosomes in the CVB3 life cycle to those of HCV (from  $Ribo_{tot}^{CVB3} = 6.7$  to  $Ribo_{tot}^{CVB3} = 0.005$  molecules per mL) decreases the CVB3 virus load by three orders of magnitude ([Fig 4B](#)). In contrast, when increasing the viral RNA synthesis rates of HCV to those of CVB3 (from  $k_{4m}^{HCV} = k_{4p}^{HCV} = 1.1$  to  $k_{4m}^{HCV} = k_{4p}^{HCV} = 50 h^{-1}$ ), the viral load did not increase. However, decreasing the viral RNA synthesis rates of CVB3 to those of HCV (from  $k_{4m}^{CVB3} = k_{4p}^{CVB3} = 50$  to  $k_{4m}^{CVB3} = k_{4p}^{CVB3} = 1.1 h^{-1}$ ) decreased the viral load by one order of magnitude. This suggests an important role of ribosomes as key players in the production of structural and non-structural proteins necessary for efficient vRNA replication and virus production.

The subsequent processes of the vRNA replication depend on successful viral protein production. Viral non-structural proteins are crucial for forming the replicase complex and its formation rate  $k_{pin}^i$ , which has been selected as virus-specific. Here, HCV seems to be more efficient and better adapted to the Huh7 cell line, showing a 10- and 4-times faster formation rate compared to DENV and CVB3, respectively. Furthermore, our estimated replicase complex formation rates suggest that the formation of double-membrane vesicles may be more efficient (HCV and CVB3) compared to the formation of invaginations (DENV). However, the maximum number of replicase complexes  $RC_{MAX}$  and the degradation of species within the RO ( $\mu_{RO}$ ) were not selected as virus-specific, especially since the viral RNA synthesis rates were initially set as virus-specific ([Table 2](#)). Interestingly, even though being a pan-viral model parameter, not all viruses reached the maximal number of replicase complexes  $RC_{MAX}$  (the carrying capacity). The dynamics of replicase complexes show a clear separation between DENV and CVB3 versus HCV ([Fig 5A and 5B](#)). CVB3 reached the estimated carrying capacity of around 5 h pi, while DENV reached 98% of the possible carrying capacity of around 25 h pi. Strikingly, the replicase complex formation for HCV reached its maximum at a 74% lower level of the pan viral carrying capacity, even though our model estimated the fastest RC formation rate for HCV.

The export of viral RNA from the RO to the site of RNA translation  $k_{pout}^i$  has also been selected as virus-specific, where HCV and DENV seem more efficient than CVB3, which showed an almost 190 times slower trafficking process.

Following the production of viral proteins and RNA genomes, the single components assemble into virions and are released from the cell. Here, the virus assembly and release rate  $k_p$  and the reinfection rate  $k_r$  have been selected as pan-viral. Note that the scaling constant  $K_D^i$  and the number of structural proteins necessary per virion  $N_{ps}^i$ , were calculated from the data or taken from the literature, respectively, and thus set as virus-specific ([Table 2](#)).

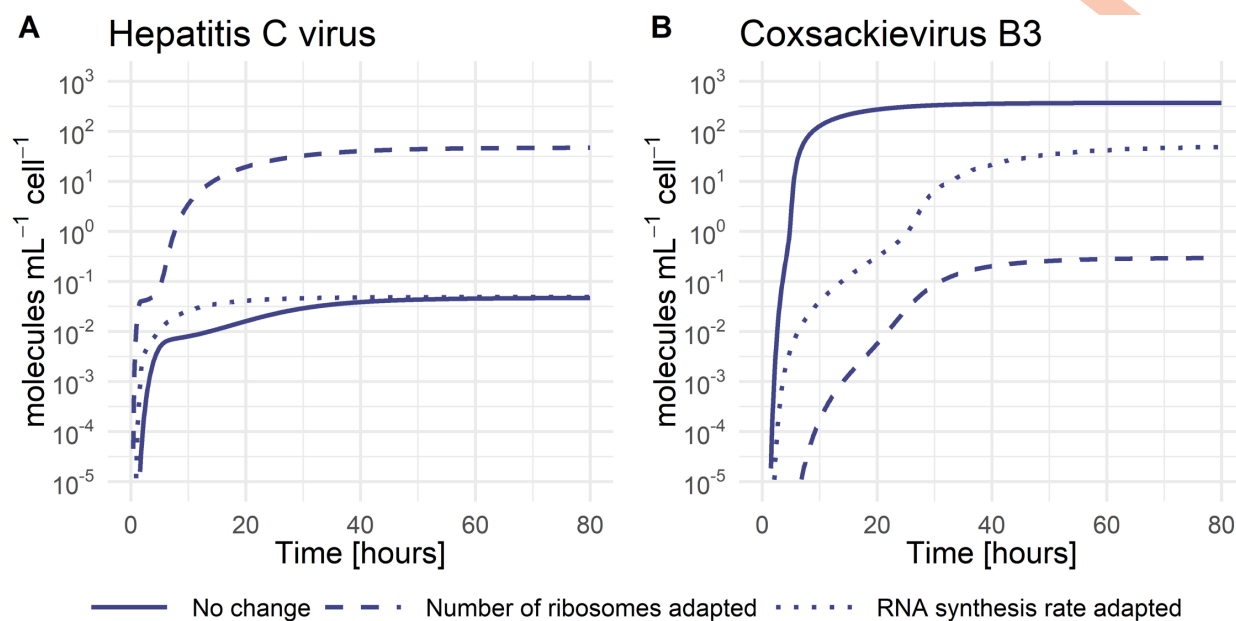


**Fig 4. Infectious virus concentration with parameter adjustments.** A) HCV concentration with estimated parameters (solid), the number of ribosomes taken from CVB3 (dashed), and the RNA synthesis rate taken from CVB3 (dotted). B) CVB3 concentration with estimated parameters (solid), the number of ribosomes taken from HCV (dashed), and the RNA synthesis rate taken from HCV (dotted).

<https://doi.org/10.1371/journal.pcbi.1010423.g004>

### Sensitivity analysis and drug intervention

Having a detailed model of the intracellular replication of plus-strand RNA viruses, we next addressed the question of which processes shared across all viruses showed the highest sensitivity index to potential drug interventions (Fig 6). Our sensitivity analysis suggests that model parameters associated with vRNA translation ( $k_2^i$ ) and synthesis within the RO ( $k_{4m}^i$  and  $k_{4p}^i$ ) are highly sensitive for all viruses. Furthermore, all viruses were sensitive to the formation of replicase complexes  $k_{pin}^i$  and its maximum number  $RC_{MAX}$ .

Interestingly, DENV and CVB3 showed a time-dependent sensitivity pattern over the course of infection, beginning with viral entry ( $k_e^i$ ) being sensitive, followed by the release of the viral genome ( $k_f^i$ ). However, both model parameters were not sensitive to HCV, possibly due to practical non-identifiability (see above). Moreover, vRNA translation and replication seem to start around 5 or 20 h pi in CVB3 and DENV, respectively, suggesting viral entry as a rate-limiting process.

There are also some interesting differences between the three viruses. While the formation of the translation initiation complex ( $k_1$ ) showed a higher sensitivity in HCV, vRNA translation ( $k_2^i$ ) was more sensitive for CVB3 and DENV. Furthermore, for HCV, the number of ribosomes available for HCV RNA translation was one of the most sensitive parameters while having negligible sensitivity for CVB3 and DENV. This may reflect the strength of the internal ribosome entry site, IRES, (CVB3) or the 5' UTR/Cap (for DENV), where a strong IRES may require fewer ribosomes for robust recruitment to initiate vRNA translation. However, for CVB3, viral RNA export  $k_{pout}^i$  is among the most sensitive processes, while being not sensitive for HCV and DENV. Interestingly, the degradation of virus in endosomes ( $\mu_{vE}$ ) showed the highest sensitivity among the degradation rates for DENV early in infection (around 10 to 25

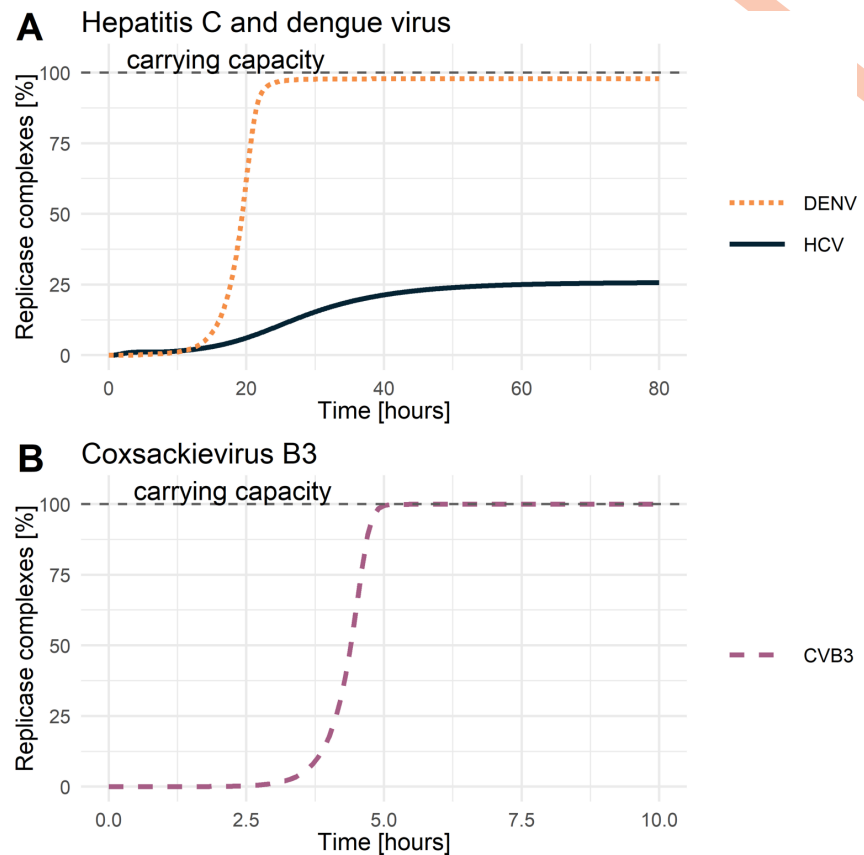


**Fig 5. Replicase complexes over time.** Dynamics of replicase complexes for A) hepatitis C and dengue virus, B) coxsackievirus B3. The dashed grey line represents the carrying capacity or the maximum number of formed replicase complexes.

<https://doi.org/10.1371/journal.pcbi.1010423.g005>

h pi). In contrast, the degradation of cytosolic vRNA ( $\mu_{RP}$ ) seems highly sensitive towards the end of infection for both DENV and CVB3.

As a next step, we aimed to analyze if any processes can be targeted, leading to a 99% reduction in extracellular virus upon inhibition. We, therefore, studied the effects of inhibiting core processes of the viral life cycle (Fig 7). We then simulated *in silico* the administration of a hypothetical drug at two different time points using our mathematical model: at the beginning of the infection (0 h pi) or in steady state (100 h pi). The drug administration at the beginning of infection (0 h pi) will give insights into infection prevention. The drug administration in a steady state (100 h pi) has the advantage of studying the system in the equilibrium of vRNA replication/virus production and vRNA degradation/virus clearance and, thus, how to treat an established infection. Therefore, we can ignore a potential bias of the drug effect when the vRNA translation and replication machinery must be established or host cellular and viral resources are exhausted, leading to inefficient viral RNA replication and, ultimately, virus production. Even though DENV and CVB3 are viruses that cause acute infections, cleared after a couple of weeks, studying both viruses in a steady state is important to gain insights about a possible drug effect during maintained virus production.

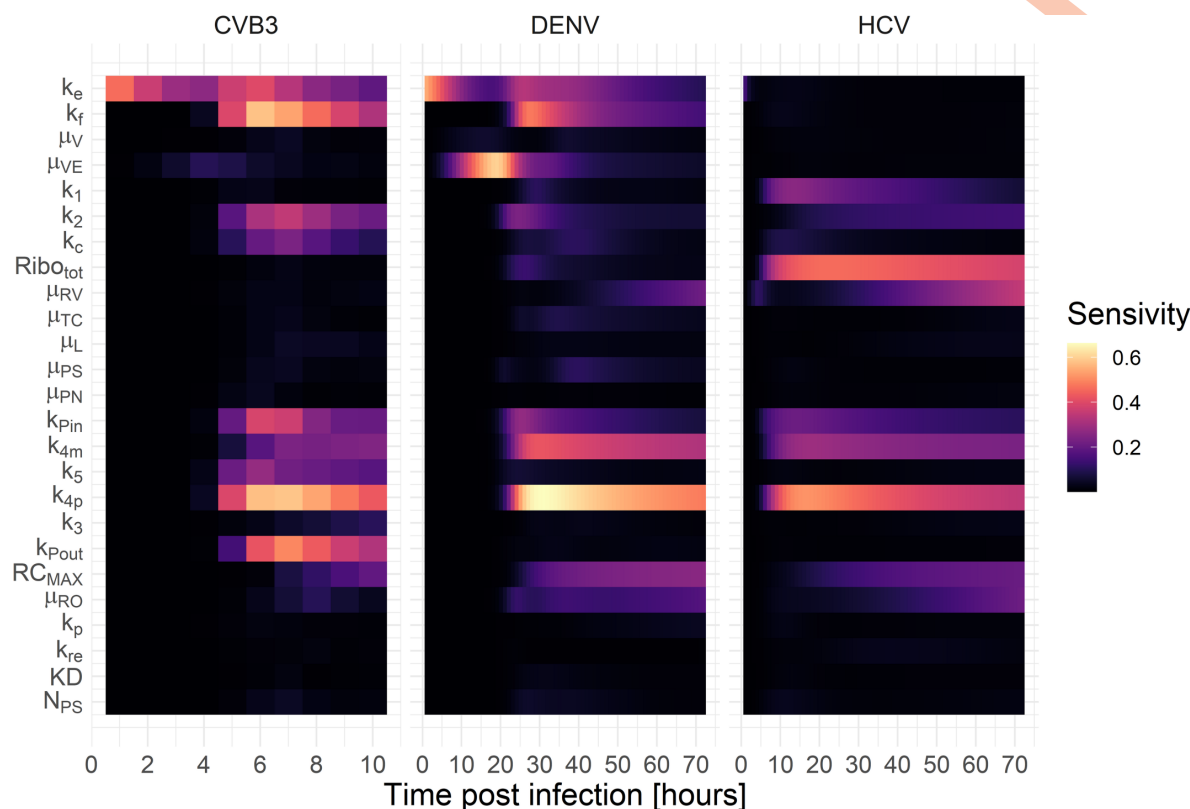


**Fig 6. Global sensitivity profile for the model species plus-strand RNA throughout infection (CVB3 = 10 hours, HCV = DENV = 72 hours).**

<https://doi.org/10.1371/journal.pcbi.1010423.g006>

For all viruses and drug administration time points, we determined the critical drug efficacy,  $\varepsilon$ , where the viral life cycle is successfully inhibited and the *in-silico* infection is cleared. Note that we define a virus infection as cleared if the extracellular virus is reduced by more than 99%. By testing both drug administration time points, we found that at the beginning of infection (0 h pi), inhibiting any process led to eradicating the virus (Fig 7). Since the viral replication machinery is not established, viral entry and vRNA release may be possible drug targets. However, an almost 100% inhibition ( $\varepsilon \sim 1$ ) was necessary to block the infection process (S1 Table). Obviously, *in-silico* drugs targeting virus entry and vRNA release at a time point after an established viral infection cannot reduce the viral load. However, for both drug administration time points, targeting vRNA translation and vRNA synthesis showed the most potent effect and, thus, are the most promising drug targets (S1 Table). Interestingly, targeting the formation of the replicase complexes could not clear (or even reduce) CVB3 infection with a drug administration given in steady state (S1 Table). Moreover, in the case of DENV, targeting vRNA export from the RO into the cytoplasm in steady state led to a 6% increase in virus with incomplete inhibition. Only a 100% inhibition and thus a drug efficacy of 1 could clear the virus by 99%.

Since most DAAs are highly efficient in combination, we determined the critical drug efficacy of individual drugs inhibiting either translation complex formation, vRNA translation, or polyprotein cleavage used in combination with drugs that inhibit vRNA synthesis or formation

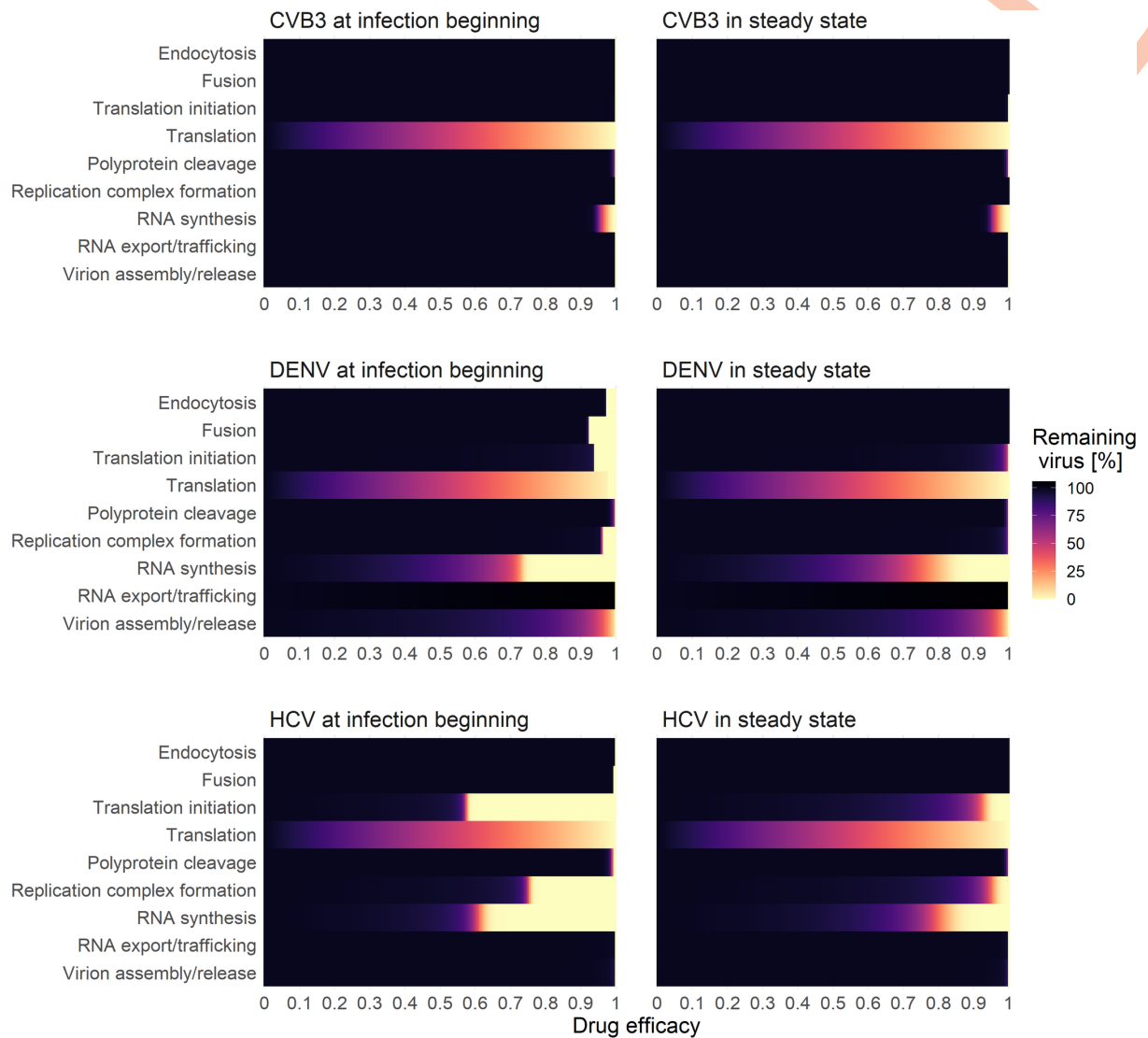


**Fig 7.** Effects of drug interventions applied to two different time points: at infection beginning (left) and in steady state (right). A successful drug treatment leads to more than 99% viral eradication (light yellow), while an ineffective drug treatment leads to 100% remaining virus (black).

<https://doi.org/10.1371/journal.pcbi.1010423.g007>

of the replicase complex in steady state (Figs 8, 9, S1, and S2 and S1 Table). Here, we identified the “sweet spot” for efficient viral eradication (by more than 99%). Our model predicted that HCV and DENV showed a comparable pattern of viral clearance to a combination of two drugs. In contrast, for the clearance of CVB3, higher drug efficacies were necessary to clear the infection. Inhibiting vRNA synthesis and either vRNA translation or polyprotein cleavage by more than 90% was an efficient combination for HCV and DENV (Figs 8B, 8C, and S2A and S1 Table). However, to clear the infection in all viruses, vRNA synthesis and either translation or polyprotein cleavage must be inhibited by more than 99% or 98%, respectively (Fig 9B and 9C).

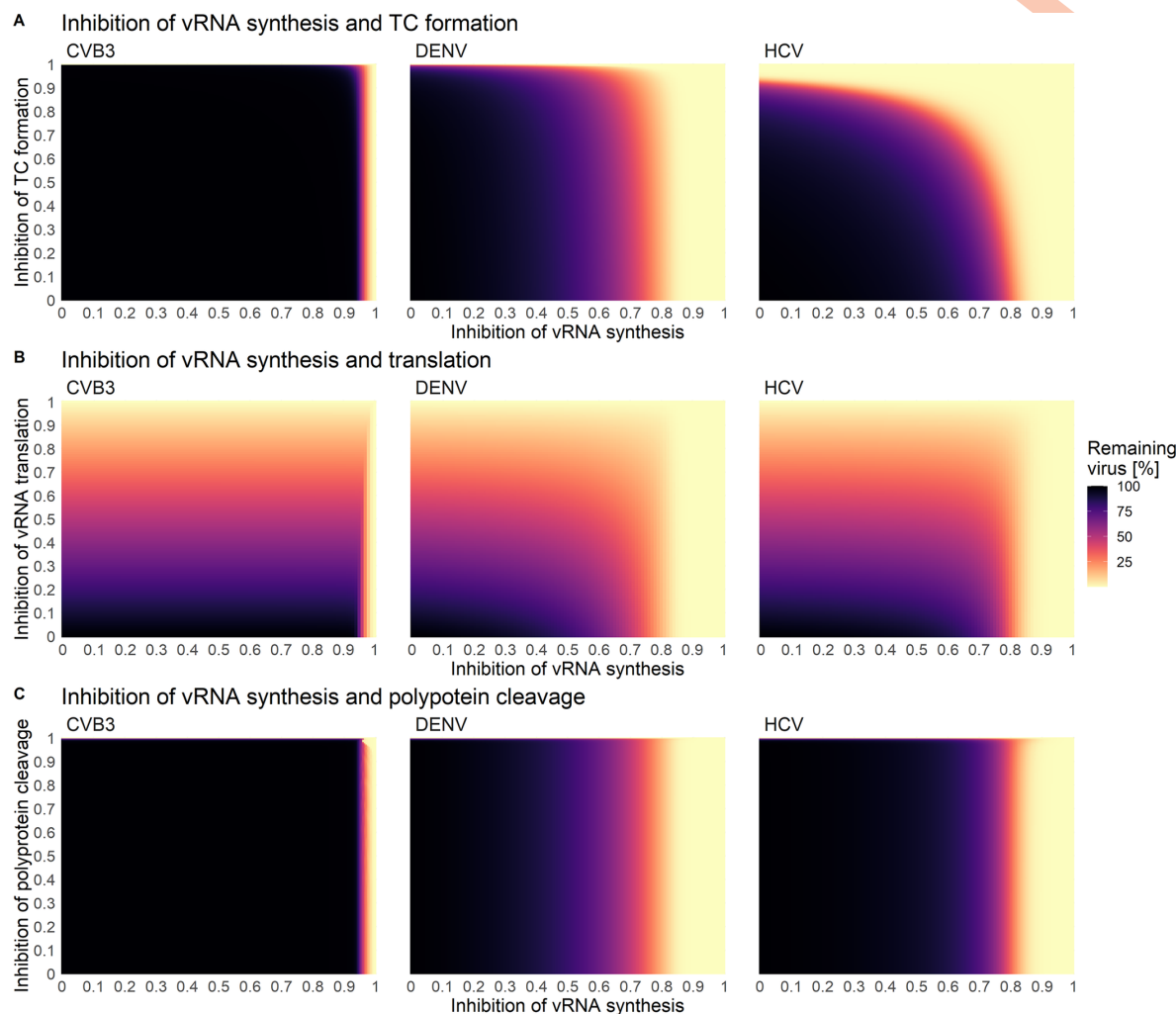


**Fig 8.** Combined drug effect on **A)** vRNA synthesis and formation of translation complex (TC), **B)** vRNA synthesis and translation, and **C)** viral RNA synthesis and polyprotein cleavage. Initiation of treatment was in steady state (100 h pi). A successful drug treatment leads to more than 99% viral eradication (light yellow), while an ineffective drug treatment leads to 100% remaining virus (black).

<https://doi.org/10.1371/journal.pcbi.1010423.g008>

Interestingly, inhibiting vRNA synthesis and translation complex formation by more than 76% showed the overall lowest critical drug efficacy to clear the infection in HCV. Nevertheless, for CVB3, the vRNA synthesis and translation complex inhibition need to be higher than 99.3% to clear the infection with an almost 10 hours time-delayed viral clearance (Figs 8A and 9A and S1 Table). Overall, we found the lowest pan-viral critical drug efficacy was for the combined inhibition of vRNA synthesis and polyprotein cleavage with a required 98% effectiveness for each drug (Figs 8C and 9C and S1 Table). Note that we also tested *in silico* the combination therapy of inhibiting translation complex formation, vRNA translation, and polyprotein cleavage together with replicase complex formation. However, higher critical drug efficacy constants were needed to clear the infection (S1 and S2 Figs and S1 Table).

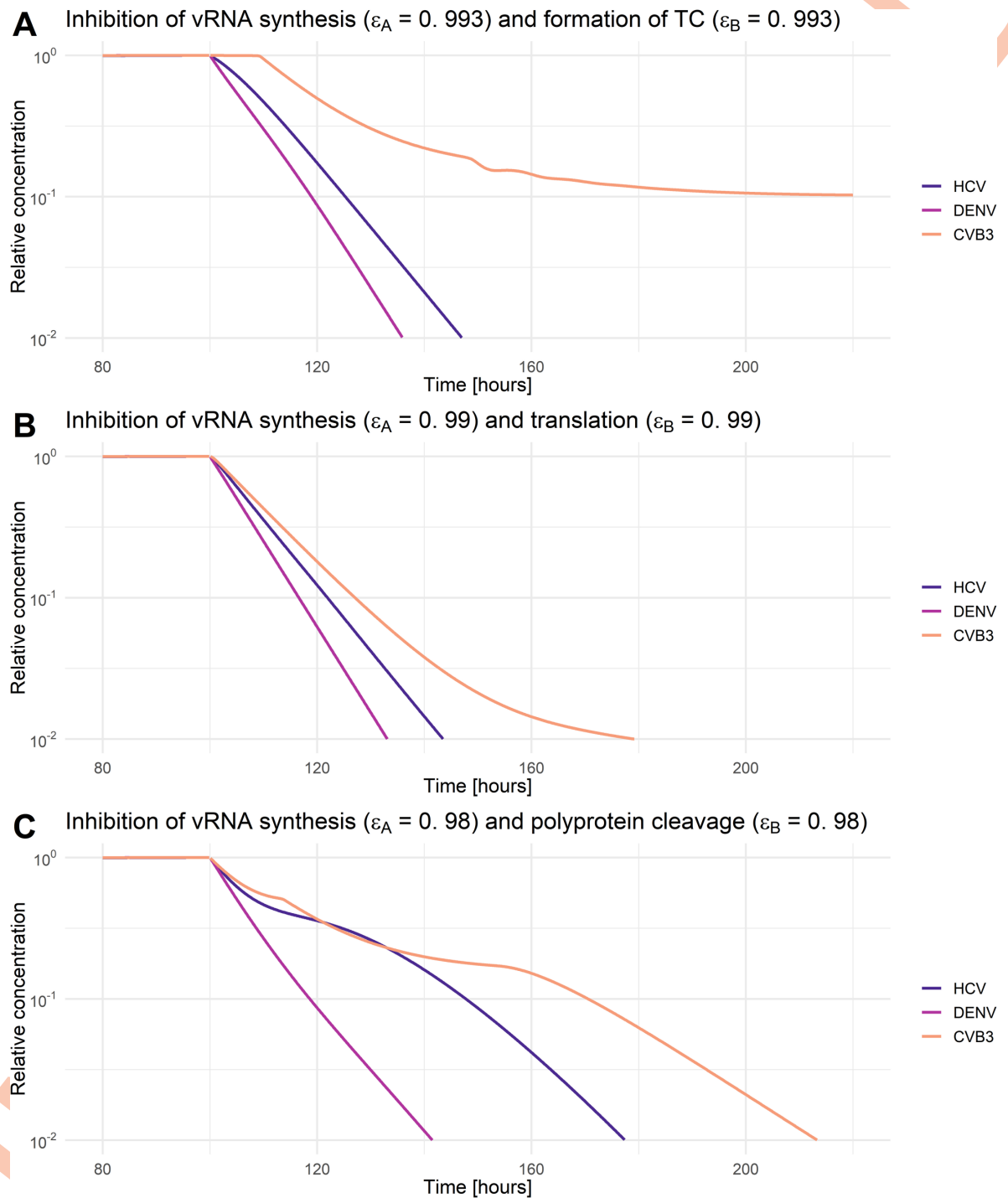


**Fig 9. Relative virus decay under combination therapy that clears HCV, DENV, and CVB3 infections.** A combined drug effect on A) vRNA synthesis and formation of translation complex (TC), B) vRNA synthesis and translation, and C) viral RNA synthesis and polyprotein cleavage. Initiation of treatment was in

steady state (100 h pi). The drug efficacy constant ( $\varepsilon_A$  and  $\varepsilon_B$ ) were chosen as minimal efficacies to clear all three viruses. For comparability, virus-specific concentrations in steady state have been normalized to their virus-specific pre-treatment steady-state concentration. A successful drug treatment leads to more than 99% viral eradication (light yellow), while an ineffective drug treatment leads to 100% remaining virus (black).

<https://doi.org/10.1371/journal.pcbi.1010423.g009>

## Discussion

Mathematical modeling of viral dynamics has a long history and has been applied to various viral infectious diseases [25]. Population-based models considering susceptible and infected cell populations, especially studying virus-host interactions and treatment opportunities for HIV, HCV, and influenza, represent the most prominent mathematical models in the field [25,75–78]. However, mathematical models considering intracellular viral replication mechanisms in detail are still limited and are usually developed for one specific virus such as HCV [19,57,59,79,80], DENV [55], CVB3 [81], HIV [82], or influenza A virus [60,61,83–88]. Furthermore, those virus-specific models are usually developed to study a particular aspect of the viral life cycle, such as cell-line-specific HCV RNA replication efficiency [19] or the life cycles of DENV or CVB3 in the presence of the immune response [55,81]. Recently, Chhajer et al. (2021) studied the viral life cycles of the plus-strand RNA viruses HCV, Japanese encephalitis virus, and poliovirus with a simplified mathematical model. The authors mainly focused on the slow and delayed kinetics of the intracellular formation of replication organelles, which may predict infection outcomes [89].

To our best knowledge, we present here the first mathematical model that simultaneously studies the complexity of intracellular viral replication kinetics for three different representatives of plus-strand RNA viruses, namely HCV, DENV, and CVB3, measured in the same cell line—Huh7. Hepatocyte-derived cells, such as Huh7, support the viral replication of many viruses, such as DENV [90–92], chikungunya [93], Zika [94–96], poliovirus [97], SARS-CoV-2 [98], and other respiratory viruses [99]. The Huh7 cell line can study the viral replication without perturbations of the host cellular immune response due to its defective RIG-I signaling [100]. As we have previously shown that different cell lines lead to different replication kinetics due to a cell-line specific gene expression [19,50,55], our aim was a standardized experimental design, where using the same cell line for all viruses may have the advantage of a mostly shared gene expression and, thus, host factor equality.

The basis for our present study were our previously published intracellular models for HCV [19,57] and DENV [55], which we generalized and adapted to reflect the intracellular replication mechanisms of plus-strand RNA viruses more broadly, as well as the underlying experimental conditions. We compare viral replication mechanisms, pan-viral similarities and virus-specific differences, which may help to understand acute or chronic infection outcomes that may be an initial step toward developing broad-spectrum antiviral treatment strategies.

Our best-fitting model showed high similarity with the virus-specific data and a high degree of parameter identifiability. However, it showed one shortcoming in capturing the dynamics of the experimental measurements of virus in DENV: the viral peak and subsequent drop of the extracellular DENV concentration around 32 h pi. However, our previously published DENV model showed that the dynamics of extracellular infectious virus was dependent on host factors that were packaged into the virions [55]. Since we did not include host factors in the current model, except for ribosomes, we aimed to describe the average extracellular virus dynamics for the first 25 h pi. In the final model, we estimated 31 parameters, of which 27 were identifiable. The 95% confidence intervals of four parameter values hit the upper or lower boundary of estimation, where changing the parameter boundaries by up to 1000-fold did not improve the model fit or improved identifiability.



The non-identifiable rate constant of the naïve cell infection  $k_{re}$  may be explained by the fact that reinfection in our culture system may not occur for each virus. However, the process remained in the final model because of different MOI infection experiments, where a lower MOI (MOI of 1, as in the case of CVB3 and HCV) may account for multiple rounds of infection. The formation rate of the translation initiation complex  $k_1$  seems to be a non-identifiable process in the model structure, as it was also non-identifiable in our previous DENV model [55]. Further, virus entry and vRNA genome release,  $k_e$  and  $k_f$ , were practically non-identifiable for HCV. An explanation for both processes being non-identifiable may be insufficient experimental measurements for HCV to uniquely estimate both rate constants, e.g., the lack of intracellular protein concentration measurements for HCV. However, since both parameters were identifiable for CVB3 and DENV and both processes were selected as virus-specific,  $k_e^{HCV}$  and  $k_f^{HCV}$ , they remained in the final model as virus-specific. For a detailed comparison of the plus-strand RNA model with our previously published HCV and DENV models, see [S3 Text](#).

### Virus-specific differences and pan-viral similarities

Studying similarities and differences in the viral RNA translation and replication strategies of different viruses is experimentally challenging. Our mathematical model may shed light on this topic by studying 25 processes, from cell infection to releasing newly packaged infectious virions. Five processes within the viral life cycle were determined to be virus-specific: (i) virus entry, (ii) release of vRNA genome, (iii) the number of ribosomes available for vRNA translation, (iv) formation of replicase complexes, and (v) trafficking of newly produced viral genomes from the RO into the cytoplasm.

**Virus internalization and genome release.** The three viruses we studied each have different internalization processes mediated by differences in attachment/entry versus uncoating receptors [101]. HCV replicates *in vivo* in hepatocytes and, consequently, showed the most efficient internalization and genome release processes in our studied hepatocyte-derived Huh7 cells. *In vitro*, HCV replicates most efficiently in Huh7 cells and its closely related sub-clones, while the infection of other cell lines has been challenging [102]. However, both DENV and CVB3 have a broad tropism. DENV infects monocytes, macrophages, and dendritic cells, while CVB3 infects the brain, cardiac tissue, and hepatocytes [15,35,103–105]. Thus, the faster internalization and genome release of CVB3 compared to DENV, and thus its ability to replicate very well in Huh7 cells, is not surprising due to its broader cellular tropism. Nevertheless, DENV RNA has been isolated from various organs and tissues, including the liver (see [106] and references within). However, whether DENV replicates in hepatocytes is under debate [107–109].

**Viral RNA translation.** Among the plus-strand RNA viruses we studied, CVB3 represents the fastest replicating virus with a life cycle of around 8 to 10 hours. Newly synthesized CVB3 RNA is detectable at two h pi in the Golgi apparatus, the site of ROs and thus vRNA synthesis. Levels of viral RNA increase rapidly and peak four h pi [110]. One key feature of successful CVB3 RNA replication is its ability to shut off host mRNA translation, carried out by the virus by degrading eukaryotic initiation factor eIF4G important for the cellular cap-dependent translation complex formation. The result is not only the rapid availability of non-structural proteins required for replicase complex formation [111] but also a lower level of components of the cell's intrinsic immune response. Interestingly, we found the highest total ribosome availability for CVB3, in agreement with its ability to shut off the translation of the host's mRNA while keeping vRNA translation high due to a very efficient IRES. According to our calculated viral RNA translation rate constants, translation is 2 to 3 times faster than HCV and DENV, respectively. It has been shown that the polysome size—the number of ribosomes

bound to a single CVB3 RNA molecule, which translate the viral genome at the same time—is around 30 ribosomes per polysome but changes throughout the CVB3 life cycle; 40 ribosomes per polysome at the beginning of the CVB3 life cycle and 20 ribosomes later in infection [66,112]. Furthermore, Boersma et al. (2020) found that CVB3 translation rates were independent of the host translation shutdown. However, the authors speculated that a host translation shutdown might boost the CVB3 translation at the end of its life cycle, where host cell resources may be limited [113]. Conversely, for DENV, it has been shown that the DENV RNA template is only sparsely loaded with ribosomes and showed a low translation efficiency [114]. Nevertheless, Roth et al. (2017) found that the host's mRNA translation decreases during DENV infection, suggesting that DENV also can repress the host mRNA translation, although not as efficiently as CVB3 [23]. A partial host cell RNA translation shut-off and, consequently, a higher number of ribosomes available for DENV RNA translation is predicted by our model, with DENV having the second-highest predicted ribosome concentration. Interestingly, even though DENV can partially shut down the host's mRNA translation, this suppression seems less efficient compared to the complete CVB3 host shut-off.

**Formation of the replicase complex.** Our model suggests a faster formation of double-membrane vesicles than invaginations, i.e., HCV and CVB3 showed faster replicase complex formation compared to DENV. Compared to DENV and CVB3, HCV showed a 10- and 4-times faster rate of replicase complex formation, respectively. A possible reason may be cell tropism, with hepatocellular-derived Huh7 cells being the cell line of choice for studying HCV. Interestingly, the host mRNA translation shut-off of CVB3 was not associated with a faster supply of non-structural proteins (RdRp) and, thus, faster replicase complex formation. However, host cell translation shut-off may be associated with higher availability and more efficient utilization of viral resources for the formation of replicase complexes, as suggested by our model. CVB3 reached the maximal number of replicase complexes after around 5 h pi, while HCV used 76% less of the possible cell's carrying capacity. However, cell tropism and, thus, a specific set of host factors involved in the process of replication organelle and replicase complex formation may be the crucial factors in this process, as we have shown previously for HCV and DENV [19,55].

**Viral RNA export from the RO into the cytoplasm.** A striking difference between *Flaviviridae* (HCV and DENV) and *Picornaviridae* (CVB3) concerns the parameter values and model sensitivity against changes of the trafficking of newly synthesized vRNA from the RO to the site of translation. For CVB3, our model suggests intra-compartment trafficking is two orders of magnitude slower than HCV and DENV, with a highly significant sensitivity of this parameter against changes. A possible explanation may lie in the involvement of different compartments or cell organelles in vRNA translation and replication. All viruses need proximity to the rough endoplasmic reticulum and its ribosomes for successful vRNA translation; however, they use different cytoplasmic membranes and, thus, different sites for forming their ROs and thus for vRNA synthesis. *Flaviviridae* remodel the rough endoplasmic reticulum, using membrane vesicles or invagination as the site for vRNA translation and synthesis without being exposed to the (possibly damaging) cytoplasmic environment. Melia et al. (2019) found that CVB3 uses the rough endoplasmic reticulum first and the Golgi later in infection, suggesting a high degree of flexibility and adaptation of CVB3 to its environment. To what extent viral replication occurs on either membrane is unknown. However, other studies suggest that Golgi-derived membranes are the primary origin of viral replication [110,115,116]. During CVB3 infection, the Golgi collapsed and was not detectable anymore, suggesting that ROs were Golgi-derived [117]. Regarding efficient viral protein production for virion packaging, CVB3 is not enveloped. It may only need a fraction of the structural proteins that DENV and HCV need for assembly (see [S1 Text](#) for details), implying that CVB3 developed strategies

to overcome longer trafficking distances. However, another explanation may be a possible regulation and competition of vRNA translation and virion packaging. Early in infection, vRNA may be used for translation, while later in infection, vRNA may be packaged into virions and thus not available for vRNA translation.

### Hypothetical mechanisms behind acute and chronic infections

The plus-strand RNA viruses studied here share the major steps in their life cycle and replication strategy, but despite these similarities, they show very different clinical manifestations. While HCV has a relatively mild symptomatic phase, it can establish a chronic infection with low-level viral replication over decades that goes mostly undetected by the host's immune response. In contrast, DENV causes a vigorous acute self-limited infection that can become life-threatening. Similarly, CVB3 usually causes an acute infection with flu-like symptoms but can become chronic. The underlying mechanisms for the development of chronic infections are unclear. Our plus-strand RNA virus replication model might help to reveal the differences in the viral dynamics leading to different clinical manifestations.

DENV/Zika virus and CVB3 produce a higher ratio of plus- to minus-strand RNA (20:1) compared to HCV, with a plus- to minus-strand RNA ratio of 3:1 (measured in our data) up to 10:1 (reported in the literature [113,118–124]), which may be HCV-strain or cell line-specific. One may speculate that a higher viral RNA synthesis rate may be responsible for the higher plus- to minus-strand RNA ratio in viruses causing acute infections. However, our calculated vRNA synthesis rates were comparable for HCV and DENV but 50 times lower compared to the CVB3 RNA synthesis rate, possibly due to faster vRNA copying or faster *de novo* initiation of vRNA synthesis. In HCV, studies found an RNA synthesis rate of 150 to 180 nt/min [125,126]. However, the rate of RNA synthesis in DENV is, to our knowledge, unknown. Nevertheless, Tan et al. (1996) found low in vitro polymerase activity for DENV NS5, which is in line with the polymerase activities for West Nile and Kunjin viruses, suggesting that this is a conserved feature of flavivirus polymerases [127] and possibly *Flaviviridae* including HCV.

As for CVB3, it has been shown that the closely related poliovirus synthesizes a single RNA template in 45 to 100 sec [66]. Additionally, it is estimated that between 3 and 10 RdRps are bound to one single PV RNA genome. However, our plus-strand RNA model did not consider the RdRp density bound to one single viral RNA template due to a lack of data for HCV and DENV. According to our model predictions, critical processes for a faster viral life cycle may be a combination of (1) faster viral RNA translation and synthesis rates and/or faster vRNA synthesis initiation, (2) host cell translation shut-off and thus higher ribosome availability for viral RNA translation and at the same time lower ribosome availability for antiviral protein production, (3) and shorter RNA half-lives for intracellular viral RNA (more important in cell lines with intrinsic immune responses or *in vivo*). Interestingly, the potential role of these key processes is in line with the global sensitivity analysis results: All CVB3 replication process rates within the RO show highly significant sensitivities, suggesting that CVB3 strongly depends on an efficient replicative cycle within the RO. Additionally, global sensitivities of vRNA degradation rates in the cytoplasm or within the RO seem rather negligible.

Our model predicted that an optimal usage of viral resources to form replicase complexes within a cell was only realized by DENV and CVB3. Strikingly, HCV only reached 26% of the cell's replicase complex carrying capacity. A possible reason may be a limitation in viral resources to form replicase complexes such as viral RNA or non-structural proteins. Both may be again related to the lower availability of ribosomes for viral protein production in HCV. In contrast, DENV and CVB3 have the advantage of a partial or complete host cell translation shut-off, respectively. However, virus-specific ribosome availability and translation activity

may be related to different translation mechanisms. While HCV and CVB3 have IRESes, i.e., the RNA translation is cap-independent, DENV's translation mechanism is cap-dependent. Furthermore, different IRES types have variations in their structural elements and recruit host factors as regulatory elements, which affects the translation initiation complex and viral RNA translation. Therefore, a higher ribosome availability for vRNA translation may be associated with different translation mechanisms, such as secondary structures and host factors assisting in ribosome binding [128–131]. Furthermore, a higher number of ribosomes available for vRNA translation may be directly associated with a higher production of viral proteins. However, the more ribosomes available for cellular mRNA translation and thus the production of proteins of the immune response, the higher the intracellular degradation of viral components may be, resulting in a limitation in viral resources. Ribosome availability and its control may thus be crucial for viral replication efficiency.

To analyze this aspect further, we asked whether we could make virus production in HCV more efficient or CVB3 less efficient. Increasing the *in-silico* ribosome availability in HCV to that of CVB3 increased the viral load by three orders of magnitude. In contrast, a 50-fold increase in the HCV RNA synthesis rate had no effect on the viral load in steady state due to a limited availability of the viral RNA polymerase in the replication organelle [19]. In contrast, using only 0.07% of ribosomes for CVB3 RNA translation, thus setting the ribosome level to the number of ribosomes used in HCV, decreased the CVB3 viral load by three orders of magnitude. Interestingly, the coronaviruses' non-structural proteins, including those of SARS-CoV-2, target multiple processes in the cellular mRNA translation, causing a host cell translation shut off similar to CVB3 and DENV [132,133]. Therefore, a repression or complete shut-off of the host mRNA translation machinery may be a key feature of acute viral infections.

Comparing *in vivo* viral dynamics with those of *in vitro* experiments is challenging. Nevertheless, we found a comparable pattern of viral dynamics: reported *in vivo* and in our *in vitro* experiments. *In vivo*, HCV showed an exponential growth rate of 2.2 per day [134], while DENV and CVB3 grow twice as fast with a rate of 4.3 and 4.5 per day in human and murine blood, respectively (approximated from [38,44]). However, in murine cardiac tissue, the *in vivo* CVB3 exponential growth rate increases to approximately 14.5 per day [38]. Furthermore, the different exponential growth rates are associated with variations in the peak viral load. At its peak, HCV produces  $10^8$  RNA copies per g liver tissue [43], DENV produces 1 to 2 orders of magnitude more virus ( $10^9$  to  $10^{10}$  RNA copies per mL blood) [44], and CVB3 produces 3 to 4 orders of magnitude more virus ( $10^{11}$  to  $10^{12}$  RNA copies per g cardiac tissue) compared to HCV [38]. We found a similar pattern in our data, with HCV producing the least amount of virus at its peak ( $\sim 1$  PFU/mL/cell), followed by DENV ( $\sim 10$  PFU/mL/cell) and CVB3 ( $\sim 200$  PFU/mL/cell). Considering the RNA synthesis rates, CVB3 replicates 50- times faster than HCV and DENV.

### Broad-spectrum antivirals?

DAAs are highly specific drugs usually designed to inhibit the function of one specific viral protein. Developing broad-spectrum antiviral drugs is challenging. Nevertheless, we were interested in the possibility of a pan-viral drug treatment option. We, therefore, studied the core processes in the life cycles of our three representatives of plus-strand RNA viruses and administered *in-silico* drugs in mono or combination therapy to identify single drug targets or combinations of drug targets that yield an efficient inhibition of all three viruses.

**Direct-acting antivirals against HCV.** Several DAAs have been developed and approved for HCV and can cure chronic hepatitis C in most patients [135]. DAAs are developed to target one specific protein such as HCV NS3/4A (e.g., first-generation telaprevir or boceprevir and second-/third generation glecaprevir, voxilaprevir and grazoprevir), HCV NS5A (e.g.,

daclatasvir, velpatasvir, ledipasvir), and HCV NS5B (e.g., sofosbuvir and dasabuvir) [136]. Therefore, the DAAs' modes of action and efficacies may be used here to validate the results of our *in-silico* drug intervention study. While DAAs block HCV NS3/4A and intervene with the polyprotein cleavage, HCV NS5A and HCV NS5B inhibitors target the RO formation and vRNA synthesis, respectively [9,59,137]. Our sensitivity and *in-silico* drug analysis suggested high sensitivities for processes associated with HCV RNA replication, which led to an efficient viral reduction by more than 99% with a more than 90% inhibition of the vRNA synthesis rate. Furthermore, our *in-silico* drug analysis predicted that complete HCV NS3/4A inhibition (more than 99.5% polyprotein cleavage inhibition) was necessary to clear the viral load. Combined with inhibiting vRNA synthesis, a combinatory inhibition of more than 90% led to HCV clearance, where viral clearance was mainly driven by inhibiting vRNA synthesis. Our results are in line with current HCV treatment recommendations that focus on a regimen based on a combination of targeting vRNA synthesis alone by inhibiting HCV NS5A and/or NS5B or in combination with HCV NS3/4A with the inhibition of NS5A as the backbone of an efficient HCV treatment regimen, e.g., the combinations of elbasvir (NS5A inhibitor) and grazoprevir (NS3/4A inhibitor), glecaprevir (NS3/4A inhibitor) and pibrentasvir (NS5A inhibitor) or sofosbuvir (NS5B inhibitor) plus velpatasvir (NS5A inhibitor) [138]. Interestingly, the combinatory inhibition of vRNA synthesis and polyprotein cleavage showed pan-viral clearance with the lowest critical efficacies of 0.98, i.e., a 98% inhibition of both processes.

**Broad-spectrum antivirals and host-directed therapy.** The cure of a chronic hepatitis C infection represents a success story for DAAs. However, a subset of HCV patients report treatment failure, severe side effects that impede treatment success, or drug resistance [139]. No successful treatment has been approved for DENV, the most prevalent mosquito-borne viral disease. Furthermore, the vaccine is only recommended for seropositive individuals due to its increased risk of severe disease in seronegative individuals [140]. Moreover, for enteroviruses, such as myocarditis causing CVB3, no antiviral treatment exists to date. Several DAAs targeting CVB3 have been tested in clinical trials but are often associated with the emergence of resistance and, thus, are not recommended [141,142].

Targeting cellular components crucial for successful and efficient viral replication (so-called host dependency factors) may offer a potential treatment option with a high resistance barrier. Additionally, plus-strand RNA viruses still represent a major health concern infecting millions of people worldwide, including the viruses in this current study—HCV, DENV, and CVB3 – and other plus-strand RNA viruses such as chikungunya, Zika, West Nile, Yellow fever, hepatitis A virus as well as the current global pandemic causing SARS-CoV-2. Even though identifying pan-serotype antiviral agents is challenging, a DENV inhibitor has been identified, which has shown high efficacy and pan-serotype activity against all known DENV genotypes and serotypes [143]. Our model may serve as a basis for the development of further virus-specific models as well as pan-viral broad-spectrum antiviral treatment strategies.

Our sensitivity and drug analysis showed that inhibiting translation complex formation, vRNA translation or polyprotein cleavage, and vRNA synthesis represent the most promising pan-viral drug targets. As in the case of HCV, targeting vRNA replication and polyprotein cleavage has been highly successful, however, directly targeting the HCV RNA translation (e.g., the HCV IRES RNA structure) or its complex formation is mainly experimental. Another treatment strategy may be targeting host factors hijacked by the virus and involved in almost every process of the viral life cycle [144]. A limited number of available ribosomes may be a key feature limiting efficient virus production due to suppressed host mRNA translation or complete host cell translation shut-off. However, targeting and thus inhibiting the biological function of ribosomes will be challenging and not beneficial for the host. Nevertheless, two proteins were found to interact with vRNA translation: RACK1 and RPS25. Both proteins may

be hijacked by DENV and promote DENV-mediated cap-independent RNA translation [145]. Additionally, in HCV RACK1 has been shown to inhibit IRES-mediated viral RNA translation and viral replication; in the latter case RACK1 binds to HCV NS5A, which induces the formation of ROs [146,147]. Similar to HCV, CVB3 RNA translation is mediated through an IRES and, thus, RACK1 may be a potential drug target. Furthermore, studying interactions of SARS-CoV-2 proteins with host mRNA identified RACK1 as a binding partner and thus may represent a pan-viral host dependency factor [148].

Interestingly, the very early processes in the viral life cycle, virus entry as well as fusion and release of the vRNA genome, showed significant sensitivities in DENV and CVB3 but were rather negligible in HCV. Further, the release of the viral RNA genome from endosomes showed a higher significant sensitivity compared to viral entry and internalization. Interestingly, cyclophilin A is a host factor involved in the enterovirus A71 (family *Picornaviridae*) fusion/uncoating process and, thus, vRNA release [149,150]. Furthermore, cyclophilin A inhibitors block or successfully decrease viral replication in several plus-strand RNA viruses such as HCV, DENV, West Nile, yellow fever, enteroviral A71, and coronavirus [142,151]. Considering that it is involved in both processes that showed the highest sensitivities, cyclophilin A may represent a promising pan-viral target [142].

The formation of the replicase complexes represented another sensitive pan-viral process. Replicase complexes are associated with membranes of the ROs either within or outside the RO facing the cytosol [152]. Several studies have shown the significance of host factors in RO formation being associated with cell permissiveness and vRNA replication efficiency [17,101,133,144]. For example, Tabata et al. (2021) have shown that the RO biogenesis in HCV and SARS-CoV-2 critically depends on the lipid phosphatidic acid synthesis since inhibiting associated pathways led to an impaired HCV and SARS-CoV-2 RNA replication [153]. However, even though successful in clearing HCV and DENV, in an established infection of a fast-replicating virus such as CVB3, the formation of replicase complexes may not represent an efficient drug target. In steady state, CVB3 replicase complexes are already formed, and the virus cannot be cleared even with a 100% inhibition given for 5 days. Similar results have been found by targeting host factors involved in the formation of replicase complexes of other picornaviruses. Two tested compounds targeting RO formation could not block viral replication, suggesting that viral replication continues if ROs are already formed [154]. Furthermore, targeting host factors involved in RO formation showed lethal cytotoxicity, as in the case of PI4KIII $\beta$  and HCV [155]. Interestingly, inhibiting the host factor PI4KB showed that CVB3 RO formation was delayed and CVB3 RNA replication occurred at the Golgi apparatus [116].

Interestingly, incomplete inhibition of some processes may promote viral growth. Our model predicted that targeting viral export from the RO into the cytoplasm in the DENV life cycle led to a 6% increase in virus. Therefore, low-efficacy drugs may lead to the opposite of the desired outcome. Thus, host-directed therapy may have an enormous potential on the one hand but may result in substantial side effects on the other hand. Identifying host factors with pan-viral activity without lethal toxicity represents a challenge for future research.

### Limitations and outlook

In the current study, we developed the first mathematical model for the intracellular replication of a group of related plus-strand RNA viruses. Even though our model allowed a high degree of parameter identifiability, fit the *in vitro* kinetic data, and is consistent with the current biological knowledge of our studied viruses, there are some weaknesses to consider.

First, our model focuses on a single cell and does not include viral spread. Especially in acute infections with rapidly replicating viruses, viral transmission within organs may be

highly relevant to consider. However, since our model was developed for a single-step growth curve, we neglected viral spread and focused mainly on intracellular replication processes. Virus-specific mechanisms of viral spread from infected to susceptible cells may be interesting to study in the future.

Second, our experiments were performed in the immuno-compromised Huh7 cell line, and we did not consider an intrinsic immune response here. In the future, considering an intrinsic immune response may be an important addition.

Third, even though plus-strand RNA viruses share remarkable similarities in their replication strategy, our model does not consider viruses with more than one open reading frame and ribosomal frameshift. The difference between viruses with one and more open reading frames is the presence of sub-genomic RNA, as in the case of coronaviruses. However, the life cycle of coronaviruses, and in particular SARS-CoV-2, differs from our model by producing non-structural proteins first, followed by viral RNA and sub-genomic RNA synthesis [156]. The sub-genomic RNA is later translated into structural proteins. However, since the core processes of viral non-structural protein production (necessary for vRNA synthesis) and vRNA synthesis are common, we do not think that the presence of sub-genomic RNA would considerably impact our presented results. Adaptation of the model to coronaviruses is an ongoing topic being followed up on in our group.

Fourth, *in vitro* experiments are not a reliable system for an *in vivo* application. Especially our drug treatment study needs experimental validation. However, our model and *in silico* drug analysis showed a high degree of similarity with the knowledge and efficacy of DAAs available for HCV.

Fifth, our model has been developed for a one-step growth experiment and, consequently, a single cycle of virus growth. Thus, our model predictions are short-term and do not study long-term effects.

In summary, in the present study, we measured the *in vitro* kinetics of three representatives of plus-strand RNA viruses: HCV, DENV, and CVB3. We developed a mathematical model of the intracellular plus-strand RNA virus life cycle based on these experimental measurements. In order to study pan-viral similarities and virus-specific differences, the model was fit simultaneously to the *in vitro* measurements, where the best-fit model was selected based on the AIC and model parameter identifiability. According to our model, the viral life cycles of our three plus-strand RNA representatives differ mainly in processes of viral entry and genome release, the availability of ribosomes involved in viral RNA translation, the formation of the replicase complex, and the viral trafficking of newly produced viral RNA. Furthermore, our model predicted that the availability of ribosomes involved in viral RNA translation and, thus, the degree of the host cell translation shut-off may play a key role in acute infection outcome. Interestingly, our modeling predicted that increasing the number of ribosomes available for HCV RNA translation remarkably enhanced the HCV RNA replication efficiency and increased the HCV viral load by three orders of magnitude, a feature we could not achieve by increasing the HCV RNA synthesis rate. Furthermore, our *in-silico* drug analysis found that targeting processes associated with vRNA translation, especially polyprotein cleavage and viral RNA replication, substantially decreased viral load and may represent promising drug targets with broad-spectrum antiviral activity.

## Supporting information

**S1 Text. Pan-viral and virus specific model parameters.**  
(DOCX)

**S2 Text. Model selection process.**

(DOCX)

**S3 Text. Comparison of the plus-strand RNA virus replication model with our previous models.**

(DOCX)

**S1 Data. Experimental data and data underlying manuscript figures.**

(XLSX)

**S1 Table. Critical drug efficacy constants in mono and combination therapy and an in-silico drug administration in steady state (100 h pi).** For simplicity, we assume that both drugs have the same efficacy in combination therapy. The lowest critical drug efficacies to clear the virus-specific infection is highlighted in red (TC = translation complex, RC = replicase complex)

(DOCX)

**S1 Fig.** Combined drug effect on **A**) replicase complex (RC) formation and formation of translation complex (TC), **B**) replicase complex (RC) formation and polyprotein cleavage, and **C**) replicase complex (RC) formation and vRNA translation and drug administration in steady state (100 h pi). A successful drug treatment leads to more than 99% viral eradication (light yellow), while an ineffective drug treatment leads to 100% remaining virus (black).

(TIFF)

**S2 Fig. Relative virus decay under combination therapy that clears HCV, DENV, and CVB3 infections.** A combined drug effect on **A**) formation of replicase complex (RC) and formation of translation complex (TC), **B**) formation of replicase complex (RC) and translation, and **C**) formation of replicase complex (RC) and polyprotein cleavage. Initiation of treatment was in steady state (100 h pi). The drug efficacy constant ( $\epsilon_A$  and  $\epsilon_B$ ) were chosen as minimal efficacies to clear all three viruses. For comparability, virus-specific concentrations in steady state have been normalized to their virus-specific pre-treatment steady-state concentration. A successful drug treatment leads to more than 99% viral eradication (light yellow), while an ineffective drug treatment leads to 100% remaining virus (black) (see [S1 Data](#)).

(TIFF)

**Author Contributions**

**Conceptualization:** Carolin Zitzmann, Marco Binder, Lars Kaderali.

**Data curation:** Carolin Zitzmann, Christopher Dächert, Bianca Schmid, Hilde van der Schaar, Marco Binder.

**Formal analysis:** Carolin Zitzmann, Lars Kaderali.

**Funding acquisition:** Martijn van Hemert, Frank J. M. van Kuppeveld, Ralf Bartenschlager, Marco Binder, Lars Kaderali.

**Investigation:** Carolin Zitzmann, Christopher Dächert, Bianca Schmid, Hilde van der Schaar, Martijn van Hemert.

**Methodology:** Carolin Zitzmann, Marco Binder, Lars Kaderali.

**Project administration:** Marco Binder, Lars Kaderali.

**Resources:** Martijn van Hemert, Alan S. Perelson, Frank J. M. van Kuppeveld, Ralf Bartenschlager, Marco Binder, Lars Kaderali.



**Software:** Carolin Zitzmann.

**Supervision:** Martijn van Hemert, Alan S. Perelson, Frank J. M. van Kuppeveld, Ralf Bartenschlager, Marco Binder, Lars Kaderali.

**Validation:** Carolin Zitzmann.

**Visualization:** Carolin Zitzmann.

**Writing – original draft:** Carolin Zitzmann, Frank J. M. van Kuppeveld.

**Writing – review & editing:** Christopher Dächert, Martijn van Hemert, Alan S. Perelson, Ralf Bartenschlager, Marco Binder, Lars Kaderali.

## References

1. Ciotti M, Angeletti S, Minieri M, Giovannetti M, Benvenuto D, Pascarella S, et al. COVID-19 outbreak: An overview. *Chemotherapy*. 2020; 64: 215–223. <https://doi.org/10.1159/000507423> PMID: 32259829
2. World Health Organization. WHO coronavirus (COVID-19) dashboard with vaccination data. In: WHO [Internet]. 2021 [cited 7 Mar 2022] pp. 1–5. Available from: <https://covid19.who.int/>.
3. Cutler DM, Summers LH. The COVID-19 pandemic and the \$16 trillion virus. *JAMA—Journal of the American Medical Association*. American Medical Association; 2020. pp. 1495–1496. <https://doi.org/10.1001/jama.2020.19759> PMID: 33044484
4. Shepard DS, Undurraga EA, Halasa YA, Stanaway JD. The global economic burden of dengue: a systematic analysis. *Lancet Infect Dis*. 2016; 16: 935–941. [https://doi.org/10.1016/S1473-3099\(16\)00146-8](https://doi.org/10.1016/S1473-3099(16)00146-8) PMID: 27091092
5. United Nations. A socio-economic impact assessment of the Zika virus in Latin America and the Caribbean. 2017.
6. Barber MJ, Gotham D, Khwairakpam G, Hill A. Price of a hepatitis C cure: Cost of production and current prices for direct-acting antivirals in 50 countries. *J Virus Erad*. 2020; 6: 100001. <https://doi.org/10.1016/j.jve.2020.06.001> PMID: 33251019
7. Shakeri A, Srimurugathan N, Suda KJ, Gomes T, Tadrous M. Spending on hepatitis C antivirals in the United States and Canada, 2014 to 2018. *Value in Health*. 2020; 23: 1137–1141. <https://doi.org/10.1016/j.jval.2020.03.021> PMID: 32940230
8. FDA. Coronavirus (COVID-19) update: FDA authorizes first oral antiviral for treatment of COVID-19. In: Food and Drug Administration [Internet]. 2021 p. 1. Available from: <https://www.fda.gov/news-events/press-announcements/coronavirus-covid-19-update-fda-authorizes-first-oral-antiviral-treatment-covid-19>.
9. Hayes CN, Imamura M, Tanaka J, Chayama K. Road to elimination of HCV: Clinical challenges in HCV management. *Liver International*. John Wiley & Sons, Ltd; 2022. <https://doi.org/10.1111/liv.15150> PMID: 34967486
10. World Health Organization. Hepatitis C. 2019. Available from: <https://www.who.int/news-room/fact-sheets/detail/hepatitis-c>.
11. World Health Organization. Dengue and severe dengue. 2016. <https://doi.org/10.1111/1469-0691.12442>
12. Colpitts GC, El-Saghire H, Pochet N, Schuster C, Baumert TF. High-throughput approaches to unravel hepatitis C virus-host interactions. *Virus Res*. 2016; 218: 18–24. <https://doi.org/10.1016/j.virusres.2015.09.013> PMID: 26410623
13. Genoni A, Canducci F, Rossi A, Broccolo F, Chumakov K, Bono G, et al. Revealing enterovirus infection in chronic human disorders: An integrated diagnostic approach. *Sci Rep*. 2017; 7: 5013. <https://doi.org/10.1038/s41598-017-04993-y> PMID: 28694527
14. Baggen J, Thibaut HJ, Strating JRPM, Van Kuppeveld FJM. The life cycle of non-polio enteroviruses and how to target it. *Nature Reviews Microbiology*. Nat Rev Microbiol; 2018. pp. 368–381. <https://doi.org/10.1038/s41579-018-0005-4> PMID: 29626210
15. Garmaroudi FS, Marchant D, Hendry R, Luo H, Yang D, Ye X, et al. Coxsackievirus B3 replication and pathogenesis. 2015; 10: 629–652. <https://doi.org/10.2217/fmb.15.5> PMID: 25865198

16. Romero-Brey I, Merz A, Chiramel A, Lee JY, Chlanda P, Haselman U, et al. Three-dimensional architecture and biogenesis of membrane structures associated with hepatitis C virus replication. Luo GG, editor. *PLoS Pathog.* 2012; 8: e1003056. <https://doi.org/10.1371/journal.ppat.1003056> PMID: 23236278
17. Belov GA, van Kuppeveld FJ. (+)RNA viruses rewire cellular pathways to build replication organelles. *Curr Opin Virol.* 2012; 2: 740–747. <https://doi.org/10.1016/j.coviro.2012.09.006> PMID: 23036609
18. Miller S, Krijnse-Locker J. Modification of intracellular membrane structures for virus replication. *Nat Rev Microbiol.* 2008; 6: 363–374. <https://doi.org/10.1038/nrmicro1890> PMID: 18414501
19. Binder M, Sulaimanov N, Clausnitzer D, Schulze M, Hüber CM, Lenz SM, et al. Replication vesicles are load- and choke-points in the hepatitis C virus lifecycle. *PLoS Pathog.* 2013; 9: e1003561. <https://doi.org/10.1371/journal.ppat.1003561> PMID: 23990783
20. Paul D, Bartenschlager R. Architecture and biogenesis of plus-strand RNA virus replication factories. *World J Virol.* 2013; 2: 32–48. <https://doi.org/10.5501/wjv.v2.i2.32> PMID: 24175228
21. Limpens RWAL, van der Schaar HM, Kumar D, Koster AJ, Snijder EJ, van Kuppeveld FJM, et al. The transformation of enterovirus replication structures: A three-dimensional study of single- and double-membrane compartments. *mBio.* 2011; 2. <https://doi.org/10.1128/mBio.00166-11> PMID: 21972238
22. Gale M, Tan SL, Katze MG. Translational control of viral gene expression in eukaryotes. *Microbiol Mol Biol Rev.* 2000; 64: 239–80. <https://doi.org/10.1128/MMBR.64.2.239-280.2000> PMID: 10839817
23. Roth H, Magg V, Uch F, Mutz P, Klein P, Haneke K, et al. Flavivirus infection uncouples translation suppression from cellular stress responses. *mBio.* 2017; 8. <https://doi.org/10.1128/mBio.02150-16> PMID: 28074025
24. Huang J-Y, Su W-C, Jeng K-S, Chang T-H, Lai MMC. Attenuation of 40S ribosomal subunit abundance differentially affects host and HCV translation and suppresses HCV replication. *PLoS Pathog.* 2012; 8: e1002766. <https://doi.org/10.1371/journal.ppat.1002766> PMID: 22792060
25. Zitzmann C, Kaderali L. Mathematical analysis of viral replication dynamics and antiviral treatment strategies: From basic models to age-based multi-scale modeling. *Front Microbiol.* *Frontiers*; 2018. p. 1546. <https://doi.org/10.3389/fmicb.2018.01546> PMID: 30050523
26. Perelson AS, Ke R. Mechanistic modelling of SARS-CoV-2 and other infectious diseases and the effects of therapeutics. *Clin Pharmacol Ther.* 2021. <https://doi.org/10.1002/cpt.2160> PMID: 33410134
27. Layden TJ, Layden JE, Ribeiro RM, Perelson AS. Mathematical modeling of viral kinetics: A tool to understand and optimize therapy. *Clin Liver Dis.* 2003; 7: 163–178. [https://doi.org/10.1016/s1089-3261\(02\)00063-6](https://doi.org/10.1016/s1089-3261(02)00063-6) PMID: 12691465
28. Perelson AS, Ribeiro RM. Hepatitis B virus kinetics and mathematical modeling. *Semin Liver Dis.* 2004; 24: 11–16. <https://doi.org/10.1055/s-2004-828673> PMID: 15192796
29. Smith AM, Perelson AS. Influenza A virus infection kinetics: Quantitative data and models. *Wiley Interdiscip Rev Syst Biol Med.* 2011; 3: 429–445. <https://doi.org/10.1002/wsbm.129> PMID: 21197654
30. Bonhoeffer S, Coffin JM, Nowak MA. Human immunodeficiency virus drug therapy and virus load. *J Virol.* 1997; 71: 3275–3278.
31. Perelson AS, Ribeiro RM. Modeling the within-host dynamics of HIV infection. *BMC Biol.* 2013; 11: 96. <https://doi.org/10.1186/1741-7007-11-96> PMID: 24020860
32. Tuiskunen Bäck A, Lundkvist Å. Dengue viruses—an overview. *Infect Ecol Epidemiol.* 2013; 3: 19839. <https://doi.org/10.3402/iee.v3i0.19839> PMID: 24003364
33. Moradpour D, Penin F, Rice CM. Replication of hepatitis C virus. *Journal of General Virology.* 2007; 5: 453–463. <https://doi.org/10.1038/nrmicro1645> PMID: 17487147
34. Chen BS, Lee HC, Lee KM, Gong YN, Shih SR. Enterovirus and encephalitis. *Frontiers in Microbiology.* *Frontiers Media S.A.*; 2020. p. 261. <https://doi.org/10.3389/fmicb.2020.00261> PMID: 32153545
35. Koestner W, Spanier J, Klause T, Tegtmeyer P-K, Becker J, Herder V, et al. Interferon-beta expression and type I interferon receptor signaling of hepatocytes prevent hepatic necrosis and virus dissemination in Coxsackievirus B3-infected mice. Lemon SM, editor. *PLoS Pathog.* 2018; 14: e1007235. <https://doi.org/10.1371/journal.ppat.1007235> PMID: 30075026
36. WHO. Hepatitis C. 2019 [cited 20 Aug 2019]. Available from: <https://www.who.int/news-room/fact-sheets/detail/hepatitis-c>.
37. E Cogan J. Dengue and severe dengue. In: World Health Organization [Internet]. 2018. Available from: <https://www.who.int/news-room/fact-sheets/detail/dengue-and-severe-dengue>.
38. Reetoo KN, Osman SA, Illavia SJ, Cameron-Wilson CL, Banatvala JE, Muir P. Quantitative analysis of viral RNA kinetics in coxsackievirus B3-induced murine myocarditis: Biphasic pattern of clearance following acute infection, with persistence of residual viral RNA throughout and beyond the inflammatory

- phase of disease. *Journal of General Virology*. 2000; 81: 2755–2762. <https://doi.org/10.1099/0022-1317-81-11-2755> PMID: 11038389
39. Pybus OG, Charleston MA, Gupta S, Rambaut A, Holmes EC, Harvey PH. The epidemic behavior of the hepatitis C virus. *Science* (1979). 2001; 292: 2323–2325. <https://doi.org/10.1126/science.1058321> PMID: 11423661
  40. Liu Y, Lillepold K, Semenza JC, Tozan Y, Quam MBM, Rocklöv J. Reviewing estimates of the basic reproduction number for dengue, Zika and chikungunya across global climate zones. *Environmental Research*. Academic Press Inc.; 2020. p. 109114. <https://doi.org/10.1016/j.envres.2020.109114> PMID: 31927301
  41. Lim CTK, Jiang L, Ma S, James L, Ang LW. Basic reproduction number of coxsackievirus type A6 and A16 and enterovirus 71: Estimates from outbreaks of hand, foot and mouth disease in Singapore, a tropical city-state. *Epidemiol Infect*. 2016; 144: 1028–1034. <https://doi.org/10.1017/S0950268815002137> PMID: 26374168
  42. Ma E, Fung C, Yip SHL, Wong C, Chuang SK, Tsang T. Estimation of the basic reproduction number of enterovirus 71 and coxsackievirus A16 in hand, foot, and mouth disease outbreaks. *Pediatric Infectious Disease Journal*. 2011; 30: 675–679. <https://doi.org/10.1097/INF.0b013e3182116e95> PMID: 21326133
  43. Martinelli A de LC, Brown D, Morris A, Dhillon A, Dayley P, Dusheiko G. Quantitation of HCV RNA in liver of patients with chronic hepatitis C. *Am J Gastroenterol*. 2000; 37: 203–207. <https://doi.org/10.1590/s0004-2803200000400003> PMID: 11469223
  44. Ben-Shachar R, Koelle K. Transmission-clearance trade-offs indicate that dengue virulence evolution depends on epidemiological context. *Nat Commun*. 2018; 9: 2355. <https://doi.org/10.1038/s41467-018-04595-w> PMID: 29907741
  45. Major ME, Dahari H, Mihalik K, Puig M, Rice CM, Neumann AU, et al. Hepatitis C virus kinetics and host responses associated with disease and outcome of infection in chimpanzees. *Hepatology*. 2004; 39: 1709–1720. <https://doi.org/10.1002/hep.20239> PMID: 15185313
  46. Nainan O V., Alter MJ, Kruszon-Moran D, Gao FX, Xia G, McQuillan G, et al. Hepatitis C virus genotypes and viral concentrations in participants of a general population survey in the United States. *Gastroenterology*. 2006; 131: 478–484. <https://doi.org/10.1053/j.gastro.2006.06.007> PMID: 16890602
  47. Hajarizadeh B, Grady B, Page K, Kim AY, McGovern BH, Cox AL, et al. Patterns of hepatitis C Virus RNA levels during acute infection: The InC3 study. Blackard J, editor. *PLoS One*. 2015; 10: e0122232. <https://doi.org/10.1371/journal.pone.0122232> PMID: 25837807
  48. Cherry JD, Krogstad P. Enterovirus and parechovirus infections. *Infectious diseases of the fetus and newborn infant*. W.B. Saunders; 2011. pp. 756–799. <https://doi.org/10.1016/B978-1-4160-6400-8.00024-9>
  49. Koutsoudakis G, Herrmann E, Kallis S, Bartenschlager R, Pietschmann T. The level of CD81 cell surface expression is a key determinant for productive entry of hepatitis C virus into host cells. *J Virol*. 2007; 81: 588–598. <https://doi.org/10.1128/JVI.01534-06> PMID: 17079281
  50. Dächert C, Gladilin E, Binder M. Gene expression profiling of different HuH7 variants reveals novel hepatitis C virus host factors. *Viruses*. 2019; 12. <https://doi.org/10.3390/v12010036> PMID: 31905685
  51. P C, N S. Single-step method of RNA isolation by acid guanidinium thiocyanate-phenol-chloroform extraction. *Anal Biochem*. 1987; 162: 156–159. <https://doi.org/10.1006/abio.1987.9999> PMID: 2440339
  52. Grünvogel O, Colasanti O, Lee JY, Klöss V, Belouzard S, Reustle A, et al. Secretion of hepatitis C virus replication intermediates reduces activation of toll-like receptor 3 in hepatocytes. *Gastroenterology*. 2018; 154: 2237–2251.e16. <https://doi.org/10.1053/j.gastro.2018.03.020> PMID: 29535029
  53. Lanke KHW, van der Schaar HM, Belov GA, Feng Q, Duijsings D, Jackson CL, et al. GBF1, a guanine nucleotide exchange factor for Arf, is crucial for coxsackievirus B3 RNA replication. *J Virol*. 2009; 83: 11940–9. <https://doi.org/10.1128/JVI.01244-09> PMID: 19740986
  54. Feng Q, Hato S V., Langereis MA, Zoll J, Virgen-Slane R, Peisley A, et al. MDA5 detects the double-stranded RNA replicative form in picornavirus-infected cells. *Cell Rep*. 2012; 2: 1187–1196. <https://doi.org/10.1016/j.celrep.2012.10.005> PMID: 23142662
  55. Zitzmann C, Schmid B, Ruggieri A, Perelson AS, Binder M, Bartenschlager R, et al. A coupled mathematical model of the intracellular replication of dengue virus and the host cell immune response to infection. *Front Microbiol*. 2020; 11: 725. <https://doi.org/10.3389/fmicb.2020.00725> PMID: 32411105
  56. Schmid B, Rinas M, Ruggieri A, Acosta EG, Bartenschlager M, Reuter A, et al. Live cell analysis and mathematical modeling identify determinants of attenuation of dengue virus 2-O-methylation mutant. *PLoS Pathog*. 2015; 11: e1005345. <https://doi.org/10.1371/journal.ppat.1005345> PMID: 26720415

57. Zitzmann C, Kaderali L, Perelson AS. Mathematical modeling of hepatitis C RNA replication, exosome secretion and virus release. *PLoS Comput Biol.* 2020; 16: e1008421. <https://doi.org/10.1371/journal.pcbi.1008421> PMID: 33151933
58. Kazakov T, Yang F, Ramanathan HN, Kohlway A, Diamond MS, Lindenbach BD. Hepatitis C virus RNA replication depends on specific cis- and trans-acting activities of viral nonstructural proteins. *PLoS Pathog.* 2015; 11: e1004817. <https://doi.org/10.1371/journal.ppat.1004817> PMID: 25875808
59. Benzine T, Brandt R, Lovell WC, Yamane D, Neddermann P, De Francesco R, et al. NS5A inhibitors unmask differences in functional replicase complex half-life between different hepatitis C virus strains. Randall G, editor. *PLoS Pathog.* 2017; 13: e1006343. <https://doi.org/10.1371/journal.ppat.1006343> PMID: 28594932
60. Heldt FS, Frensing T, Reichl U. Modeling the intracellular dynamics of influenza virus replication to understand the control of viral RNA synthesis. *J Virol.* 2012; 86: 7806–17. <https://doi.org/10.1128/JVI.00080-12> PMID: 22593159
61. Laske T, Heldt FS, Hoffmann H, Frensing T, Reichl U. Modeling the intracellular replication of influenza A virus in the presence of defective interfering RNAs. *Virus Res.* 2016; 213: 90–99. <https://doi.org/10.1016/j.virusres.2015.11.016> PMID: 26592173
62. Raue A, Steiert B, Schelker M, Kreutz C, Maiwald T, Hass H, et al. Data2Dynamics: a modeling environment tailored to parameter estimation in dynamical systems. *Bioinformatics.* 2015; 31: 3558–3560. <https://doi.org/10.1093/bioinformatics/btv405> PMID: 26142188
63. Raue A, Kreutz C, Maiwald T, Bachmann J, Schilling M, Klingmüller U, et al. Structural and practical identifiability analysis of partially observed dynamical models by exploiting the profile likelihood. *Bioinformatics.* 2009; 25: 1923–1929. <https://doi.org/10.1093/bioinformatics/btp358> PMID: 19505944
64. Marino S, Hogue IB, Ray CJ, Kirschner DE. A methodology for performing global uncertainty and sensitivity analysis in systems biology. *J Theor Biol.* 2008; 254: 178–96. <https://doi.org/10.1016/j.jtbi.2008.04.011> PMID: 18572196
65. Aunins TR, Marsh KA, Subramanya G, Uprichard SL, Perelson AS, Chatterjee A. Intracellular hepatitis C modeling predicts infection dynamics and viral protein mechanisms. *J Virol.* 2018; 92: JVI.02098–17. <https://doi.org/10.1128/JVI.02098-17> PMID: 29563295
66. Regoes RR, Crotty S, Antia R, Tanaka MM. Optimal replication of poliovirus within cells. *Am Nat.* 2005; 165: 364–73. <https://doi.org/10.1086/428295> PMID: 15729666
67. Byk LA, Iglesias NG, De Maio FA, Gebhard LG, Rossi M, Gamarnik A V. Dengue virus genome uncoating requires ubiquitination. *mBio.* 2016; 7: e00804–16. <https://doi.org/10.1128/mBio.00804-16> PMID: 27353759
68. Simoes EA, Sarnow P. An RNA hairpin at the extreme 5' end of the poliovirus RNA genome modulates viral translation in human cells. *J Virol.* 1991; 65: 913–921. <https://doi.org/10.1128/JVI.65.2.913-921.1991> PMID: 1846205
69. Gohara DW, Arnold JJ, Cameron CE. Poliovirus RNA-dependent RNA polymerase (3Dpol): Kinetic, thermodynamic, and structural analysis of ribonucleotide selection. *Biochemistry.* 2004; 43: 5149–5158. <https://doi.org/10.1021/bi035429s> PMID: 15122880
70. Goo L, Dowd KA, Smith ARY, Pelc RS, Demaso CR, Pierson TC. Zika virus is not uniquely stable at physiological temperatures compared to other flaviviruses. *mBio.* 2016; 7. <https://doi.org/10.1128/mBio.01396-16> PMID: 27601578
71. Carson SD, Hafenstein S, Lee H. MOPS and coxsackievirus B3 stability. *Virology.* 2017; 501: 183–187. <https://doi.org/10.1016/j.virol.2016.12.002> PMID: 27940223
72. Carson SD, Chapman NM, Hafenstein S, Tracy S. Variations of coxsackievirus B3 capsid primary structure, ligands, and stability Are selected for in a coxsackievirus and adenovirus receptor-limited environment. *J Virol.* 2011; 85: 3306–3314. <https://doi.org/10.1128/JVI.01827-10> PMID: 21270163
73. Persaud M, Martinez-Lopez A, Buffone C, Porcelli SA, Diaz-Griffero F. Infection by Zika viruses requires the transmembrane protein AXL, endocytosis and low pH. *Virology.* 2018; 518: 301–312. <https://doi.org/10.1016/j.virol.2018.03.009> PMID: 29574335
74. Chatel-Chaix L, Bartschlagler R. Dengue virus- and hepatitis C virus-induced replication. *J Virol.* 2014; 88: 5907–5911.
75. Perelson AS, Neumann AU, Markowitz M, Leonard JM, Ho DD. HIV-1 dynamics in vivo: virion clearance rate, infected cell life-span, and viral generation time. *Science* (1979). 1996; 271: 1582–1586. <https://doi.org/10.1126/science.271.5255.1582> PMID: 8599114
76. Neumann AU, Lam NP, Dahari H, Gretch DR, Wiley TE, Layden TJ, et al. Hepatitis C viral dynamics in vivo and the antiviral efficacy of interferon- $\alpha$  therapy. *Science* (1979). 1998; 282: 103–107. <https://doi.org/10.1126/science.282.5386.103> PMID: 9756471

77. Perelson AS, Essunger P, Cao Y, Vesanen M, Hurley A, Saksela K, et al. Decay characteristics of HIV-1-infected compartments during combination therapy. *Nature*. 1997; 387: 188–191. <https://doi.org/10.1038/387188a0> PMID: 9144290
78. Baccam P, Beauchemin C, Macken CA, Hayden FG, Perelson AS. Kinetics of influenza A virus infection in humans. *J Virol*. 2006; 80: 7590–9. <https://doi.org/10.1128/JVI.01623-05> PMID: 16840338
79. Dahari H, Ribeiro RM, Rice CM, Perelson AS. Mathematical modeling of subgenomic hepatitis C virus replication in Huh-7 cells. *J Virol*. 2007; 81: 750–60. <https://doi.org/10.1128/JVI.01304-06> PMID: 17035310
80. Quintela B de M, Conway JM, Hyman JM, Guedj J, dos Santos RW, Lobosco M, et al. A new age-structured multiscale model of the hepatitis C virus life-cycle during infection and therapy with direct-acting antiviral agents. *Front Microbiol*. 2018; 9: 601. <https://doi.org/10.3389/fmicb.2018.00601> PMID: 29670586
81. Lopacinski AB, Sweatt AJ, Smolko CM, Gray-Gaillard E, Borgman CA, Shah M, et al. Modeling the complete kinetics of coxsackievirus B3 reveals human determinants of host-cell feedback. *Cell Syst*. 2021; 12: 304. <https://doi.org/10.1016/j.cels.2021.02.004> PMID: 33740397
82. Reddy B, Yin J. Quantitative intracellular kinetics of HIV type 1. *AIDS Res Hum Retroviruses*. 1999; 15: 273–283. <https://doi.org/10.1089/088922299311457> PMID: 10052758
83. Heldt FS, Frensing T, Pflugmacher A, Gröpler R, Peschel B, Reichl U. Multiscale modeling of influenza A virus infection supports the development of direct-acting antivirals. Koelle K, editor. *PLoS Comput Biol*. 2013; 9: e1003372. <https://doi.org/10.1371/journal.pcbi.1003372> PMID: 24278009
84. Reichl U, Sidorenko Y. Dynamics of virus-host cell interaction. *Bioinformatics-From Genomes to Therapies*. Weinheim, Germany: Wiley-VCH Verlag GmbH; 2008. pp. 861–898. <https://doi.org/10.1002/9783527619368.ch23>
85. Frensing T, Heldt FS, Pflugmacher A, Behrendt I, Jordan I, Flockerzi D, et al. Continuous influenza virus production in cell culture shows a periodic accumulation of defective interfering particles. Pöhlmann S, editor. *PLoS One*. 2013; 8: e72288. <https://doi.org/10.1371/journal.pone.0072288> PMID: 24039749
86. Heldt FS, Kupke SY, Dori S, Reichl U, Frensing T. Single-cell analysis and stochastic modelling unveil large cell-to-cell variability in influenza A virus infection. *Nat Commun*. 2015; 6: 8938. <https://doi.org/10.1038/ncomms9938> PMID: 26586423
87. Sidorenko Y, Voigt A, Schulze-Horsel J, Reichl U, Kienle A. Stochastic population balance modeling of influenza virus replication in vaccine production processes. II. Detailed description of the replication mechanism. *Chem Eng Sci*. 2008. <https://doi.org/10.1016/j.ces.2007.12.034>
88. Sidorenko Y, Reichl U. Structured model of influenza virus replication in MDCK cells. *Biotechnol Bioeng*. 2004; 88: 1–14. <https://doi.org/10.1002/bit.20096> PMID: 15384040
89. Chhajer H, Rizvi VA, Roy R. Life cycle process dependencies of positive-sense RNA viruses suggest strategies for inhibiting productive cellular infection. *J R Soc Interface*. 2021; 18. <https://doi.org/10.1098/rsif.2021.0401> PMID: 34753308
90. Lin Y-L, Liu C-C, Lei H-Y, Yeh T-M, Lin Y-S, Chen RM-Y, et al. Infection of five human liver cell lines by dengue-2 virus. *J Med Virol*. 2000; 60: 425–431. [https://doi.org/10.1002/\(sici\)1096-9071\(200004\)60:4<425::aid-jmv10>3.0.co;2-a](https://doi.org/10.1002/(sici)1096-9071(200004)60:4<425::aid-jmv10>3.0.co;2-a) PMID: 10686026
91. Gutiérrez-Barbosa H, Castañeda NY, Castellanos JE. Differential replicative fitness of the four dengue virus serotypes circulating in Colombia in human liver Huh7 cells. *The Brazilian Journal of Infectious Diseases*. 2020; 24: 13. <https://doi.org/10.1016/j.bjid.2019.11.003> PMID: 31843340
92. Alcalá AC, Maravillas JL, Meza D, Ramirez OT, Ludert JE, Palomares LA. Dengue Virus NS1 Uses Scavenger Receptor B1 as a Cell Receptor in Cultured Cells. *J Virol*. 2022; 96. <https://doi.org/10.1128/JVI.01664-21> PMID: 34986002
93. Roberts GC, Zothner C, Remenyi R, Merits A, Stonehouse NJ, Harris M. Evaluation of a range of mammalian and mosquito cell lines for use in Chikungunya virus research. *Sci Rep*. 2017; 7: 14641. <https://doi.org/10.1038/s41598-017-15269-w> PMID: 29116243
94. Tricot T, Helsen N, Kaptein SJF, Neyts J, Verfaillie CM. Human stem cell-derived hepatocyte-like cells support Zika virus replication and provide a relevant model to assess the efficacy of potential antivirals. *PLoS One*. 2018; 13: e0209097. <https://doi.org/10.1371/journal.pone.0209097> PMID: 30566505
95. Sherman KE, Rouster SD, Kong LX, Aliota MT, Blackard JT, Dean GE. Zika virus replication and cytopathic effects in liver cells. *PLoS One*. 2019; 14. <https://doi.org/10.1371/journal.pone.0214016> PMID: 30893357
96. Cortese M, Goellner S, Acosta EG, Neufeldt CJ, Oleksiuk O, Lampe M, et al. Ultrastructural characterization of Zika virus replication factories. *Cell Rep*. 2017; 18: 2113–2123. <https://doi.org/10.1016/j.celrep.2017.02.014> PMID: 28249158

97. Álvarez E, Castelló A, Carrasco L, Izquierdo JM. Poliovirus 2A protease triggers a selective nucleocytoplasmic redistribution of splicing factors to regulate alternative pre-mRNA splicing. *PLoS One*. 2013; 8: e73723. <https://doi.org/10.1371/journal.pone.0073723> PMID: 24066065
98. Chu H, Chan JF-W, Yuen TT-T, Shuai H, Yuan S, Wang Y, et al. Comparative tropism, replication kinetics, and cell damage profiling of SARS-CoV-2 and SARS-CoV with implications for clinical manifestations, transmissibility, and laboratory studies of COVID-19: an observational study. *Lancet Microbe*. 2020; 1: e14–e23. [https://doi.org/10.1016/S2666-5247\(20\)30004-5](https://doi.org/10.1016/S2666-5247(20)30004-5) PMID: 32835326
99. Freymuth F, Vabret A, Rozenberg F, Dina J, Petitjean J, Gouarin S, et al. Replication of respiratory viruses, particularly influenza virus, rhinovirus, and coronavirus in HuH7 hepatocarcinoma cell line. *J Med Virol*. 2005; 77: 295. <https://doi.org/10.1002/jmv.20449> PMID: 16121382
100. Sumpter R, Loo Y-M, Foy E, Li K, Yoneyama M, Fujita T, et al. Regulating intracellular antiviral defense and permissiveness to hepatitis C virus RNA replication through a cellular RNA helicase, RIG-I. *J Virol*. 2005; 79: 2689–2699. <https://doi.org/10.1128/JVI.79.5.2689-2699.2005> PMID: 15708988
101. Baggen J, Thibaut HJ, Strating JRPM, Van Kuppeveld FJM. The life cycle of non-polio enteroviruses and how to target it. *Nature Reviews Microbiology*. Nature Publishing Group; 2018. pp. 368–381. <https://doi.org/10.1038/s41579-018-0005-4> PMID: 29626210
102. Lohmann V, Bartenschlager R. On the history of hepatitis C virus cell culture systems. *J Med Chem*. 2014; 57: 1627–1642. <https://doi.org/10.1021/jm401401n> PMID: 24164647
103. Fischl W, Bartenschlager R. Exploitation of cellular pathways by Dengue virus. *Current Opinion in Microbiology*. 2011. pp. 470–475. <https://doi.org/10.1016/j.mib.2011.07.012> PMID: 21798792
104. Clyde K, Kyle JL, Harris E. Recent advances in deciphering viral and host determinants of dengue virus replication and pathogenesis. *J Virol*. 2006; 80: 11418–11431. <https://doi.org/10.1128/JVI.01257-06> PMID: 16928749
105. Anderson R. Manipulation of cell surface macromolecules by flaviviruses. *Adv Virus Res*. 2003; 59: 229–274. [https://doi.org/10.1016/s0065-3527\(03\)59007-8](https://doi.org/10.1016/s0065-3527(03)59007-8) PMID: 14696331
106. Martina BEE, Koraka P, Osterhaus ADME. Dengue virus pathogenesis: an integrated view. *Clin Microbiol Rev*. 2009; 22: 564–581. <https://doi.org/10.1128/CMR.00035-09> PMID: 19822889
107. Paes MV, Lenzi HL, Nogueira ACM, Nuovo GJ, Pinhão ÂT, Mota EM, et al. Hepatic damage associated with dengue-2 virus replication in liver cells of BALB/c mice. *Laboratory Investigation*. 2009; 89: 1140–1151. <https://doi.org/10.1038/labinvest.2009.83> PMID: 19721415
108. Win MM, Charngkaew K, Punyadee N, Aye KS, Win N, Chaisri U, et al. Ultrastructural features of human liver specimens from patients who died of dengue hemorrhagic fever. *Trop Med Infect Dis*. 2019; 4. <https://doi.org/10.3390/tropicalmed4020063> PMID: 31013708
109. Póvoa TF, Alves AMB, Oliveira CAB, Nuovo GJ, Chagas VLA, Paes M v. The pathology of severe dengue in multiple organs of human fatal cases: histopathology, ultrastructure and virus replication. *PLoS One*. 2014; 9: e83386. <https://doi.org/10.1371/journal.pone.0083386> PMID: 24736395
110. Hsu NY, Illynska O, Belov G, Santiana M, Chen YH, Takvorian PM, et al. Viral reorganization of the secretory pathway generates distinct organelles for RNA replication. *Cell*. 2010; 141: 799–811. <https://doi.org/10.1016/j.cell.2010.03.050> PMID: 20510927
111. Bushell M, Sarnow P. Hijacking the translation apparatus by RNA viruses. *Journal of Cell Biology*. The Rockefeller University Press; 2002. pp. 395–399. <https://doi.org/10.1083/jcb.200205044> PMID: 12163463
112. Summers DF, Maizel J V., Darnell JE. The decrease in size and synthetic activity of poliovirus polyosomes late in the infectious cycle. *Virology*. 1967; 31: 427–435. [https://doi.org/10.1016/0042-6822\(67\)90222-x](https://doi.org/10.1016/0042-6822(67)90222-x) PMID: 4290171
113. Boersma S, Rabouw HH, Bruurs LJM, Pavlovič T, van Vliet ALW, Beumer J, et al. Translation and replication dynamics of single RNA viruses. *Cell*. 2020; 183: 1930–1945.e23. <https://doi.org/10.1016/j.cell.2020.10.019> PMID: 33188777
114. Reid DW, Campos RK, Child JR, Zheng T, Chan KWK, Bradrick SS, et al. Dengue virus selectively annexes endoplasmic reticulum-associated translation machinery as a strategy for co-opting host cell protein synthesis. *J Virol*. 2018; 92: 1766–1783. <https://doi.org/10.1128/JVI.01766-17> PMID: 29321322
115. Melia CE, Peddie CJ, de Jong AWM, Snijder EJ, Collinson LM, Koster AJ, et al. Origins of enterovirus replication organelles established by whole-cell electron microscopy. *mBio*. 2019; 10. <https://doi.org/10.1128/mBio.00951-19> PMID: 31186324
116. Melia CE, van der Schaar HM, Lyoo H, Limpens RWAL, Feng Q, Wahedi M, et al. Escaping host factor PI4KB inhibition: Enterovirus genomic RNA replication in the absence of replication organelles. *Cell Rep*. 2017; 21: 587–599. <https://doi.org/10.1016/j.celrep.2017.09.068> PMID: 29045829

117. Li X, Wang M, Cheng A, Wen X, Ou X, Mao S, et al. Enterovirus replication organelles and inhibitors of their formation. *Frontiers in Microbiology*. Frontiers Media S.A.; 2020. p. 1817. <https://doi.org/10.3389/fmicb.2020.01817> PMID: 32973693
118. Iglesias NG, Gamarnik A V. RNA biology dynamic RNA structures in the dengue virus genome. 2011. <https://doi.org/10.4161/rna.8.2.14992>
119. Villordo SM, Alvarez DE, Gamarnik A V. A balance between circular and linear forms of the dengue virus genome is crucial for viral replication. *RNA*. 2010; 16: 2325–2335. <https://doi.org/10.1261/rna.2120410> PMID: 20980673
120. Bolten R, Egger D, Gosert R, Schaub G, Landmann L, Bienz K. Intracellular localization of poliovirus plus- and minus-Strand RNA visualized by strand-specific fluorescent in situ hybridization. *J Virol*. 1998; 72: 8578–8585. <https://doi.org/10.1128/JVI.72.11.8578-8585.1998> PMID: 9765396
121. Guo J-T, Bichko V V., Seeger C. Effect of alpha interferon on the hepatitis C virus replicon. *J Virol*. 2001; 75: 8516–8523. <https://doi.org/10.1128/jvi.75.18.8516-8523.2001> PMID: 11507197
122. Quinkert D, Bartenschlager R, Lohmann V. Quantitative analysis of the hepatitis C virus replication complex. *J Virol*. 2005; 79: 13594–13605. <https://doi.org/10.1128/JVI.79.21.13594-13605.2005> PMID: 16227280
123. Iwasaki A, Medzhitov R. Innate responses to viral infections. 6th ed. In: Fields BN, Knipe DM, Howley PM, editors. *Fields Virology: Sixth Edition*. 6th ed. Wolters Kluwer Health/Lippincott Williams & Wilkins; 2013. pp. 189–213.
124. Lohmann V, Körner F, Koch JO, Herian U, Theilmann L, Bartenschlager R. Replication of subgenomic hepatitis C virus RNAs in a hepatoma cell line. *Science* (1979). 1999; 285: 110–113. <https://doi.org/10.1126/science.285.5424.110> PMID: 10390360
125. Oh J-W, Ito T, Lai MMC. A recombinant hepatitis C virus RNA-dependent RNA polymerase capable of copying the full-length viral RNA. *J Virol*. 1999; 73: 7694–7702. <https://doi.org/10.1128/JVI.73.9.7694-7702.1999> PMID: 10438859
126. Ma H, Leveque V, De Witte A, Li W, Hendricks T, Clausen SM, et al. Inhibition of native hepatitis C virus replicase by nucleotide and non-nucleoside inhibitors. *Virology*. 2005; 332: 8–15. <https://doi.org/10.1016/j.virol.2004.11.024> PMID: 15661135
127. Tan BH, Fu J, Sugrue RJ, Yap EH, Chan YC, Tan YH. Recombinant dengue type 1 virus NS5 protein expressed in *Escherichia coli* exhibits RNA-dependent RNA polymerase activity. *Virology*. 1996; 216: 317–325. <https://doi.org/10.1006/viro.1996.0067> PMID: 8607261
128. Yang Y, Wang Z. IRES-mediated cap-independent translation, a path leading to hidden proteome. *J Mol Cell Biol*. 2019; 11: 911–919. <https://doi.org/10.1093/jmcb/mjz091> PMID: 31504667
129. Lee KM, Chen CJ, Shih SR. Regulation mechanisms of viral IRES-driven translation. *Trends in Microbiology*. Elsevier; 2017. pp. 546–561. <https://doi.org/10.1016/j.tim.2017.01.010> PMID: 28242053
130. Pelletier J, Sonenberg N. The organizing principles of eukaryotic ribosome recruitment. *Annual Review of Biochemistry*. 2019. pp. 307–335. <https://doi.org/10.1146/annurev-biochem-013118-111042> PMID: 31220979
131. Fernández-García L, Angulo J, Ramos H, Barrera A, Pino K, Vera-Otarola J, et al. The internal ribosome entry site of dengue virus mRNA is Active when cap-dependent translation initiation is inhibited. *J Virol*. 2021; 95. <https://doi.org/10.1128/jvi.01998-20> PMID: 33298544
132. Finkel Y, Gluck A, Nachshon A, Winkler R, Fisher T, Rozman B, et al. SARS-CoV-2 uses a multi-pronged strategy to impede host protein synthesis. *Nature*. 2021; 594: 240–245. <https://doi.org/10.1038/s41586-021-03610-3> PMID: 33979833
133. de Wilde AH, Snijder EJ, Kikkert M, van Hemert MJ. Host factors in coronavirus replication. *Current Topics in Microbiology and Immunology*. Springer Verlag; 2018. pp. 1–42. [https://doi.org/10.1007/82\\_2017\\_25](https://doi.org/10.1007/82_2017_25) PMID: 28643204
134. Ribeiro RM, Li H, Wang S, Stoddard MB, Learn GH, Korber BT, et al. Quantifying the diversification of hepatitis C virus (HCV) during primary infection: Estimates of the in vivo mutation rate. *PLoS Pathog*. 2012; 8. <https://doi.org/10.1371/journal.ppat.1002881> PMID: 22927817
135. Li DK, Chung RT. Overview of direct-acting antiviral drugs and drug resistance of hepatitis C virus. *Methods in Molecular Biology*. Humana Press Inc.; 2019. pp. 3–32. [https://doi.org/10.1007/978-1-4939-8976-8\\_1](https://doi.org/10.1007/978-1-4939-8976-8_1) PMID: 30593615
136. Perales C, Quer J, Gregori J, Esteban JI, Domingo E. Resistance of hepatitis C virus to inhibitors: Complexity and clinical implications. *Viruses*. MDPI AG; 2015. pp. 5746–5766. <https://doi.org/10.3390/v7112902> PMID: 26561827
137. McGivern DR, Masaki T, Williford S, Ingravallo P, Feng Z, Lahser F, et al. Kinetic analyses reveal potent and early blockade of hepatitis C virus assembly by NS5A inhibitors. *Gastroenterology*. 2014; 147. <https://doi.org/10.1053/j.gastro.2014.04.021> PMID: 24768676

138. Bhattacharjee C, Singh M, Das D, Chaudhuri S, Mukhopadhyay A. Current therapeutics against HCV. *Virusdisease*. 2021; 32: 228. <https://doi.org/10.1007/s13337-021-00697-0> PMID: 34307769
139. Alazard-Dany N, Denolly S, Boson B, Cosset FL. Overview of hcv life cycle with a special focus on current and possible future antiviral targets. *Viruses*. MDPI AG; 2019. p. 30. <https://doi.org/10.3390/v11010030> PMID: 30621318
140. Obi JO, Gutiérrez-Barbosa H, Chua J v., Deredge DJ. Current trends and limitations in dengue antiviral research. *Trop Med Infect Dis*. 2021; 6: 180. <https://doi.org/10.3390/tropicalmed6040180> PMID: 34698303
141. Abzug MJ, Michaels MG, Wald E, Jacobs RF, Romero JR, Sánchez PJ, et al. Editor's choice: a randomized, double-blind, placebo-controlled trial of pleconaril for the treatment of neonates with enterovirus sepsis. *J Pediatric Infect Dis Soc*. 2016; 5: 53. <https://doi.org/10.1093/JPIDS/PIV015>
142. Bauer L, Lyoo H, van der Schaar HM, Strating JR, van Kuppeveld FJ. Direct-acting antivirals and host-targeting strategies to combat enterovirus infections. *Curr Opin Virol*. 2017; 24: 1–8. <https://doi.org/10.1016/j.coviro.2017.03.009> PMID: 28411509
143. Kaptein SJF, Goethals O, Kiemel D, Marchand A, Kesteleyn B, Bonfanti JF, et al. A pan-serotype dengue virus inhibitor targeting the NS3–NS4B interaction. *Nature* 2021 598:7881. 2021; 598: 504–509. <https://doi.org/10.1038/s41586-021-03990-6> PMID: 34616043
144. Nagy PD, Pogany J. The dependence of viral RNA replication on co-opted host factors. *Nat Rev Microbiol*. 2012; 10: 137–149. <https://doi.org/10.1038/nrmicro2692> PMID: 22183253
145. Hafirassou ML, Meertens L, Umaña-Díaz C, Labeau A, Dejarnac O, Bonnet-Madin L, et al. A global interactome map of the dengue virus NS1 identifies virus restriction and dependency host factors. *Cell Rep*. 2017; 21: 3900–3913. <https://doi.org/10.1016/j.celrep.2017.11.094> PMID: 29281836
146. Lee JS, Tabata K, Twu WI, Rahman MS, Kim HS, Yu JB, et al. RACK1 mediates rewiring of intracellular networks induced by hepatitis C virus infection. *PLoS Pathog*. 2019; 15: e1008021. <https://doi.org/10.1371/journal.ppat.1008021> PMID: 31525236
147. Majzoub K, Hafirassou ML, Meignin C, Goto A, Marzi S, Fedorova A, et al. RACK1 controls IRES-mediated translation of viruses. *Cell*. 2014; 159: 1086–1095. <https://doi.org/10.1016/j.cell.2014.10.041> PMID: 25416947
148. Adams DR, Ron D, Kiely PA. RACK1, A multifaceted scaffolding protein: Structure and function. *Cell Communication and Signaling*. 2011; 9: 22. <https://doi.org/10.1186/1478-811X-9-22> PMID: 21978545
149. Kobayashi K, Koike S. Cellular receptors for enterovirus A71. *Journal of Biomedical Science* 2020 27:1. 2020; 27: 1–12. <https://doi.org/10.1186/s12929-020-0615-9> PMID: 31924205
150. Qing J, Wang Y, Sun Y, Huang J, Yan W, Wang J, et al. Cyclophilin A associates with enterovirus-71 virus capsid and plays an essential role in viral infection as an uncoating regulator. *PLoS Pathog*. 2014; 10: e1004422. <https://doi.org/10.1371/journal.ppat.1004422> PMID: 25275585
151. Dawar FU, Tu J, Khattak MNK, Mei J, Lin L. Cyclophilin a: A key factor in virus replication and potential target for anti-viral therapy. *Curr Issues Mol Biol*. 2017; 21: 1–20. <https://doi.org/10.21775/cimb.021.001> PMID: 27033630
152. Paul D, Hoppe S, Saher G, Krijnse-Locker J, Bartenschlager R. Morphological and biochemical characterization of the membranous hepatitis C virus replication compartment. *J Virol*. 2013; 87: 10612–27. <https://doi.org/10.1128/JVI.01370-13> PMID: 23885072
153. Tabata K, Prasad V, Paul D, Lee JY, Pham MT, Twu WI, et al. Convergent use of phosphatidic acid for hepatitis C virus and SARS-CoV-2 replication organelle formation. *Nature Communications* 2021 12:1. 2021; 12: 1–15. <https://doi.org/10.1038/s41467-021-27511-1> PMID: 34907161
154. Ford Siltz LA, Viktorova EG, Zhang B, Kouivaskaia D, Dragunsky E, Chumakov K, et al. New small-molecule inhibitors effectively blocking picornavirus replication. *J Virol*. 2014; 88: 11091–11107. <https://doi.org/10.1128/JVI.01877-14> PMID: 25008939
155. LaMarche MJ, Borawski J, Bose A, Capacci-Daniel C, Colvin R, Dennehy M, et al. Anti-hepatitis C virus activity and toxicity of type III phosphatidylinositol-4-kinase beta inhibitors. *Antimicrob Agents Chemother*. 2012; 56: 5149–5156. <https://doi.org/10.1128/AAC.00946-12> PMID: 22825118
156. V'kovski P, Kratzel A, Steiner S, Stalder H, Thiel V. Coronavirus biology and replication: implications for SARS-CoV-2. *Nature Reviews Microbiology*. Nature Publishing Group; 2021. pp. 155–170. <https://doi.org/10.1038/s41579-020-00468-6> PMID: 33116300



## **Article II: A coupled mathematical model of the intracellular replication of dengue virus and the host cell immune response to infection.**

**Carolin Zitzmann**, Bianca Schmid, Alessia Ruggieri, Alan S Perelson, Marco Binder, Ralf Bartenschlager, Lars Kaderali\* (2020) *A coupled mathematical model of the intracellular replication of dengue virus and the host cell immune response to infection*. *Frontiers in microbiology* 11:725.

I contributed to data curation, model development, formal analysis, investigation, software, validation, visualization, and writing–original draft, review & editing.

\* Corresponding author

The supplementary material is published and can be found online.



# A Coupled Mathematical Model of the Intracellular Replication of Dengue Virus and the Host Cell Immune Response to Infection

Carolin Zitzmann<sup>1,2</sup>, Bianca Schmid<sup>3†</sup>, Alessia Ruggieri<sup>3</sup>, Alan S. Perelson<sup>2</sup>, Marco Binder<sup>4</sup>, Ralf Bartenschlager<sup>3</sup> and Lars Kaderali<sup>1\*</sup>

## OPEN ACCESS

### Edited by:

Erna Geessien Kroon,  
Federal University of Minas  
Gerais, Brazil

### Reviewed by:

Renata Retkute,  
University of Cambridge,  
United Kingdom  
Udo Reichl,  
Max-Planck-Gesellschaft  
(MPG), Germany

### \*Correspondence:

Lars Kaderali  
lars.kaderali@uni-greifswald.de

### † Present address:

Bianca Schmid,  
CSL Behring GmbH,  
Hattersheim, Germany

### Specialty section:

This article was submitted to  
Virology,  
a section of the journal  
Frontiers in Microbiology

**Received:** 21 July 2019

**Accepted:** 27 March 2020

**Published:** 29 April 2020

### Citation:

Zitzmann C, Schmid B, Ruggieri A,  
Perelson AS, Binder M,  
Bartenschlager R and Kaderali L  
(2020) A Coupled Mathematical  
Model of the Intracellular Replication  
of Dengue Virus and the Host Cell  
Immune Response to Infection.  
*Front. Microbiol.* 11:725.  
doi: 10.3389/fmicb.2020.00725

<sup>1</sup> Center for Functional Genomics of Microbes, Institute of Bioinformatics, University Medicine Greifswald, Greifswald, Germany, <sup>2</sup> Theoretical Biology and Biophysics, Los Alamos National Laboratory, Los Alamos, NM, United States, <sup>3</sup> Department of Infectious Diseases, Molecular Virology, Heidelberg University, Heidelberg, Germany, <sup>4</sup> Research Group "Dynamics of Early Viral Infection and the Innate Antiviral Response", Division Virus-Associated Carcinogenesis (F170), German Cancer Research Center (DKFZ), Heidelberg, Germany

Dengue virus (DV) is a positive-strand RNA virus of the *Flavivirus* genus. It is one of the most prevalent mosquito-borne viruses, infecting globally 390 million individuals per year. The clinical spectrum of DV infection ranges from an asymptomatic course to severe complications such as dengue hemorrhagic fever (DHF) and dengue shock syndrome (DSS), the latter because of severe plasma leakage. Given that the outcome of infection is likely determined by the kinetics of viral replication and the antiviral host cell immune response (HIR) it is of importance to understand the interaction between these two parameters. In this study, we use mathematical modeling to characterize and understand the complex interplay between intracellular DV replication and the host cells' defense mechanisms. We first measured viral RNA, viral protein, and virus particle production in Huh7 cells, which exhibit a notoriously weak intrinsic antiviral response. Based on these measurements, we developed a detailed intracellular DV replication model. We then measured replication in IFN competent A549 cells and used this data to couple the replication model with a model describing IFN activation and production of IFN stimulated genes (ISGs), as well as their interplay with DV replication. By comparing the cell line specific DV replication, we found that host factors involved in replication complex formation and virus particle production are crucial for replication efficiency. Regarding possible modes of action of the HIR, our model fits suggest that the HIR mainly affects DV RNA translation initiation, cytosolic DV RNA degradation, and naive cell infection. We further analyzed the potential of direct acting antiviral drugs targeting different processes of the DV lifecycle *in silico* and found that targeting RNA synthesis and virus assembly and release are the most promising anti-DV drug targets.

**Keywords:** dengue virus, mathematical model, innate immune response, virus replication, computational simulation

## INTRODUCTION

Dengue virus (DV) is the most prevalent vector-borne virus in the world, with an estimated global number of 390 million new infections annually, thereof 90 million with clinical manifestations, including severe dengue disease (Bhatt et al., 2013). DV poses a huge burden on human populations and health systems in affected countries, and significantly impacts the economy in tropical countries, including the southern United States (WHO, 2012). Fueled by climate change and globalization and accelerated further by viral evolution, the expansion of DV is expected to increase further (Murray et al., 2013). DV is transmitted mainly by female *Aedes* mosquitos, and with the spread of its vector, DV is spreading as well (Campbell et al., 2015). In consequence, the global incidence of DV infection has already risen 30-fold during the past 50 years. Infection with DV causes flu-like symptoms but is occasionally associated with severe complications. The fatality rate of dengue infection is between 1 and 5%, and below 1% with proper symptomatic treatment (Ranjit and Kisson, 2011). There is no antiviral therapy available against DV, and the recently approved vaccine has limited efficacy and depends on baseline serostatus of the vaccine recipient (World Health Organization, 2016).

DV infects dendritic cells (DC), B cells, T cells, monocytes, macrophages, but also the liver. DV is an enveloped, positive-sense (+)RNA virus of the *Flaviviridae* family within the genus *Flavivirus*, consisting of four distinct serotypes (DV1/2/3/4). Its approximately 10.7 kb genome encodes the three structural proteins capsid (C), precursor membrane (prM), and envelope (E) protein and seven non-structural proteins (NS1, NS2A, NS2B, NS3, NS4A, NS4B, and NS5). Upon entry into the host cell, the viral RNA genome is translated at the rough endoplasmic reticulum (rER) giving rise to a polyprotein, ~3,400 amino acids in length, which is co- and post-translationally cleaved by viral and host proteases into the structural and non-structural proteins (Neufeldt et al., 2018). DV induces membrane alterations at the rER, forming membrane invaginations. The viral RNA genome is amplified in these replication compartments (RC), starting with minus-strand synthesis to obtain a double-stranded RNA (dsRNA) intermediate which then serves as template for further plus-strand synthesis. The newly synthesized viral (+)RNA genomes leave the RC and are then either packaged into virions, which after maturation are released from the infected cell, or are again used for the next round of viral RNA translation (Bartenschlager and Miller, 2008; Rodenhuis-Zybert et al., 2010; Tuiskunen Bäck and Lundkvist, 2013; Screaton et al., 2015).

**Abbreviations:** AIC, Aikake's information criterion; (+)RNA, Positive-sense RNA; DAA, Direct acting antiviral; DC, Dendritic cell; DF, Dengue fever; DHF, Dengue haemorrhagic fever; dsRNA, Double-stranded RNA; DSS, Dengue shock syndrome; DV, Dengue virus; rER, Rough Endoplasmic reticulum; HIR, Host cell immune response; HCV, Hepatitis C virus; HF, Host factor; hpi, hours post infection; IFN, Interferon; IIR, Innate immune response; ISG, Interferon stimulated gene; JAK, Janus kinase; MDA-5, Melanoma differentiation associated gene-5; MOI, Multiplicity of infection; NS, Non-structural protein; ODE, Ordinary differential equations; PRR, Pattern recognition receptor; RC, Replication compartment; RIG-I, Retinoic acid inducible gene-I; RLR, RIG-I like receptors; STAT, Signal transducer and activator of transcription factor; TLR, Toll-like receptors; WHO, World health organization.

The host cell's defense against DV is mediated via pattern recognition receptors (PRRs), in case of DV mainly via the endosomal Toll-like receptors (TLR3/TLR7/TLR8) and the cytosolic RNA helicases *retinoic acid inducible gene 1* (RIG-I) and *melanoma differentiation associated gene 5* (MDA-5) (Muñoz-Jordán and Fredericksen, 2010; Morrison et al., 2012). TLR3 recognizes dsRNA, while TLR7 and TLR8 recognize viral single-stranded RNA (Xagorari and Chlichlia, 2008). All three TLRs activate signaling cascades that lead to the production of interferon  $\alpha/\beta$  (IFN  $\alpha/\beta$ ) and inflammatory cytokines. RIG-I/MDA-5 signals via *mitochondrial antiviral signaling protein* (MAVS) and *tumor necrosis factor receptor-associated factor 3* (TRAF3), activating *tank-binding kinase 1* (TBK1) and ultimately phosphorylating *interferon regulatory factor 3* (IRF3) and activating *nuclear factor kappa B* (NF- $\kappa$ B). The subsequent type I ( $\alpha/\beta$ ) and type III ( $\lambda$ ) IFN production induces the activation of hundreds of IFN stimulated genes (ISGs), bringing the cells into an antiviral state and resulting in an inhibition of DV (Nasirudeen et al., 2011; Tuiskunen Bäck and Lundkvist, 2013; Dalrymple et al., 2015).

DV, however, is not defenseless, and has evolved a number of mechanisms antagonizing the antiviral response of the cell both at the level of activation of the host cell immune response (HIR) and the induced effector phase. For instance, 2'-O-methylation of the DV RNA genome, mediated by NS5, was shown to slow down the activation kinetics of the IFN response (Schmid et al., 2015). In addition, the DV NS2B-3 protease cleaves the stimulator of interferon genes (STING), thus reducing type I IFN production (Diamond and Pierson, 2015). In fact, several groups have shown that the suppression of the early IFN induction by DV is critical for successful virus infection and replication (Shrestha et al., 2004; Perry et al., 2009). Moreover, Schmid et al. (2015) have shown that the ability of IFN to control DV spread might be stochastic and "leaky." While secreted IFN protects surrounding naïve cells from infection, this protection is incomplete with cells infected with DV prior to activation of the IFN response (Schmid et al., 2015). DV replication occurs inside membrane vesicles corresponding to invaginations into the rER lumen, likely shielding viral dsRNA intermediates from recognition by the HIR (Welsch et al., 2009). At the level of the effector phase, DV NS5, which contains the enzymatic activity for capping and amplification of the viral RNA genome, was shown to bind to and induce the degradation of the signal transducer and activator of transcription factor (STAT) 2 via a proteasome-dependent mechanism (reviewed in Neufeldt et al., 2018), thus blocking ISG induction downstream of the IFN receptor. Therefore, the interplay between DV and the innate immune response (IIR) is complex, and its exact magnitude and dynamics likely impact and possibly determine clinical outcome of the infection.

Mathematical modeling is a valuable tool to study complex dynamical systems and has been employed to analyze infection dynamics for a number of different viruses (Zitzmann and Kaderali, 2018). Most previous work on modeling viral infection has built on the basic model introduced by Nowak and Bangham (1996) and Nowak et al. (1996), focusing on the dynamics of susceptible cells, infected cells, and virus at the cell population level. Especially, the within-host dynamics of human immunodeficiency virus (HIV) and hepatitis C virus

(HCV) have been studied in detail with simple models on the cell population scale with regard to the antiviral immune response and treatment opportunities (Ho et al., 1995; Wei et al., 1995; Perelson et al., 1996, 1997; Bonhoeffer et al., 1997; Neumann, 1998; Stafford et al., 2000; Perelson, 2002; Rong and Perelson, 2009; Perelson and Ribeiro, 2013; Perelson and Guedj, 2015). In the case of DV modeling, these so-called target cell-limited models have been linked to the adaptive immune response via modeling of antibodies and T cell responses (Clapham et al., 2014; Ben-Shachar et al., 2016), and the IIR by IFN (Ben-Shachar and Koelle, 2014; Schmid et al., 2015). Several authors have furthermore developed intracellular replication models for related viruses (Dahari et al., 2007; Heldt et al., 2012, 2013; Binder et al., 2013; Guedj et al., 2013; Clausnitzer et al., 2015; Laske et al., 2016; Benzine et al., 2017; Aunins et al., 2018), but to our knowledge there is no mathematical model describing the intracellular steps of DV replication to date. In this manuscript, we focus on the highly dynamic initial phase post cell infection and developed a detailed differential equations model capable of quantitatively describing the intracellular infection dynamics. We measured viral replication in two different cell lines, Huh7 cells (with very little HIR) and A549 cells (with high HIR competence). By integrating the main steps of the HIR into the model, we were able to describe the infection kinetics in both cell types. Our investigation focuses on the cell line-specific impact of host factors, which determine RNA synthesis efficiency, and the involvement of the HIR. Using our mathematical model, we identified possible antiviral modes of action of the HIR on the DV lifecycle and the viral countermeasures suppressing DV recognition and activation of the HIR. We further identified the most sensitive processes in the DV lifecycle, which might constitute promising antiviral drug targets, and we evaluated possible antiviral intervention strategies *in silico*.

## MATERIALS AND METHODS

### Measuring DV Replication in Huh7 and A549 Cells

#### Cell Lines

A549 and Huh7 cells were cultivated at 37°C, 5% CO<sub>2</sub> in DMEMcpl (2 mmol/L L-glutamine, non-essential amino acids, 100 U/ml penicillin, 100 µg/ml streptomycin and 10% fetal calf serum).

#### Kinetics Experiments (120830 and 120921)

$2 \times 10^5$  A549 and Huh7 cells were seeded 1 day prior infection. Cells were infected with DV reporter virus expressing Renilla Luciferase (Schmid et al., 2015) at a MOI of 10. After 1 h, the inoculum was removed and cells washed thrice with sterile PBS prior addition of DMEMcpl. Cells were incubated at 37°C for the indicated time points.

#### Infectivity Titers

Supernatants were harvested and filtered through a 0.45 µm-pore size membrane. Supernatants were supplemented with 15 mM HEPES and stored at -80°C. Infectivity titers of virus supernatants were determined by limiting dilution assay using Huh7.5 cells as described elsewhere (Lindenbach et al., 2005).

### Interferon Lambda ELISA

Supernatants of infected cells were supplemented with 1% (v/v) Triton X-100 to inactivate DENV infectious particles and subsequently stored at -80°C until further use. Interferon lambda protein release was determined by VeriKine-DIYTM Human Interferon Lambda/IL-28B/29/28A ELISA (PBL Interferon Source, USA) with an assay range of 62.5 to 4,000 pg/ml. ELISA procedure was conducted according to the manufacturer's protocol using high binding 96 well ELISA microplates (Greiner Bio-One, Frickenhausen, Germany). The optical density of each well was determined immediately using a microplate reader set to 450 nm.

### RT-qPCR

Cells were lysed for RNA extraction and subsequent qRT-PCR analysis by adding 350 µl RA1 lysis buffer (Macherey-Nagel, Düren, Germany) supplemented with 1% β-mercapto-ethanol and stored at -80°C. Total RNA was extracted using the NucleoSpin RNA II Kit (Macherey-Nagel) as recommended by the manufacturer. RT-qPCR was described elsewhere (Schmid et al., 2015). The following primers were used: DENV2 (forward 5'-GCC CTT CTG TTC ACA CCA TT-3'; reverse 5'-CCA CAT TTG GGC GTA AGA CT-3'); IFIT1 (forward 5'-GAA GCA GGC AAT CAC AGA AA-3'; reverse 5'-TGA AAC CGA CCA TAG TGG AA-3'). GAPDH mRNA (primer forward 5'-GAA GGT GAA GGT CGG AGT C-3'; reverse 5'-GAA GAT GGT GAT GGG ATT TC-3') was used for normalization of input RNA.

### Luciferase Assay

Cells were lysed in 100 µl Luciferase lysis buffer (1% Triton X-100, 25 mM glycyl-glycine, 15 mM MgSO<sub>4</sub>, 4 mM EGTA, and 1 mM DTT, pH 7.8) and stored at -80°C. For detection of Renilla luciferase activity, 20 µl lysate was mixed with 100 µl assay buffer (25 mM glycyl-glycine, 15 mM MgSO<sub>4</sub>, 4 mM EGTA, and 15 mM potassium phosphate pH 7.8) containing 1.4 µM coelenterazine (P.J.K.). All measurements were done in duplicate by using a tube luminometer (Berthold, Pforzheim, Germany). Replication efficiency was determined by normalization to the 2 h values reflecting infection efficiency.

### Mathematical Model

We developed a mechanistic mathematical model using ordinary differential equations (ODEs) and mass action kinetics to analyze the interplay between DV and the HIR. We have previously published a detailed intracellular replication model for HCV (Binder et al., 2013). Both DV and HCV are closely related (+)RNA viruses of the same family, and their intracellular replication proceeds in similar steps. We therefore used the mathematical model of HCV replication as the basis for the model structure of the current DV model. This model was then extended to the full virus lifecycle by adding infection and assembly of new virus particles to the model. We then adapted the model to DV where necessary (see details below), refitted model parameters on the Huh7/DV infection data and complemented the replication model by an HIR sub-model that comprises the key components of the IIR. **Figure 1** gives an overview of the DV

replication sub-model and **Figure 2** shows the HIR sub-model; we describe each of the main model components in the following.

### DV Replication

Our DV replication sub-model (**Figure 1**) is composed of four main processes in the DV lifecycle: (1) Binding of DV particles to the cell surface and viral entry via endocytosis. (2) Uncoating and release of the viral RNA genome into the cytoplasm, followed by translation into a polyprotein that is subsequently cleaved into the structural and non-structural viral proteins. (3) The non-structural viral proteins initiate the formation of a RC, in which the viral RNA replication takes place via a dsRNA intermediate. (4) The newly synthesized (+)RNA can then be used as a template for further RNA replication, for protein production at the ribosomes, or it is used together with the

structural proteins to assemble new virus particles, which are then released from the cell. The cycle thereafter starts over again with further infection of naïve cells.

We model the infection process by the following three ODEs, where  $V$  describes extracellular virus,  $V_A$  is virus that has attached to the host cell but is still at the cell surface, and  $V_E$  is virus that has been endocytosed:

$$\frac{dV}{dt} = k_{re} V_{INF} - k_a V - \mu_V V - wV \quad (1)$$

$$\frac{dV_A}{dt} = k_a V - k_e V_A \quad (2)$$

$$\frac{dV_E}{dt} = k_e V_A - k_f V_E - \mu_{V_E} V_E \quad (3)$$

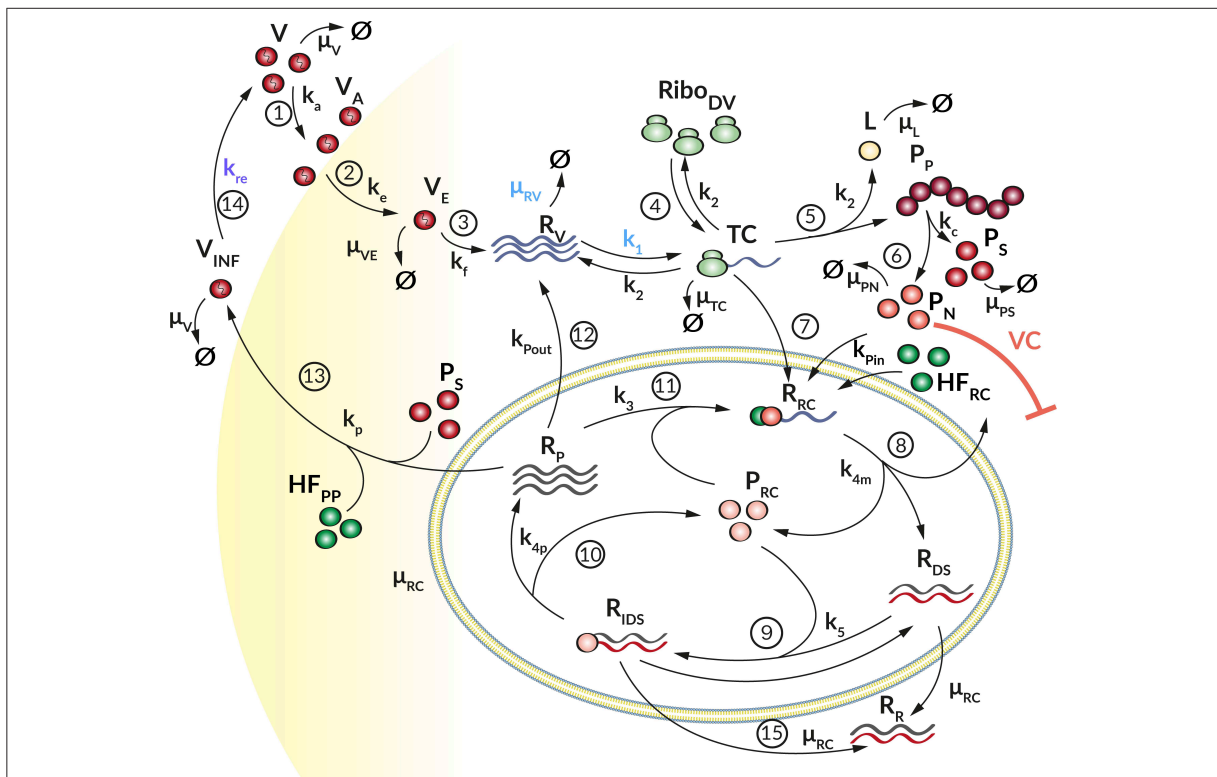
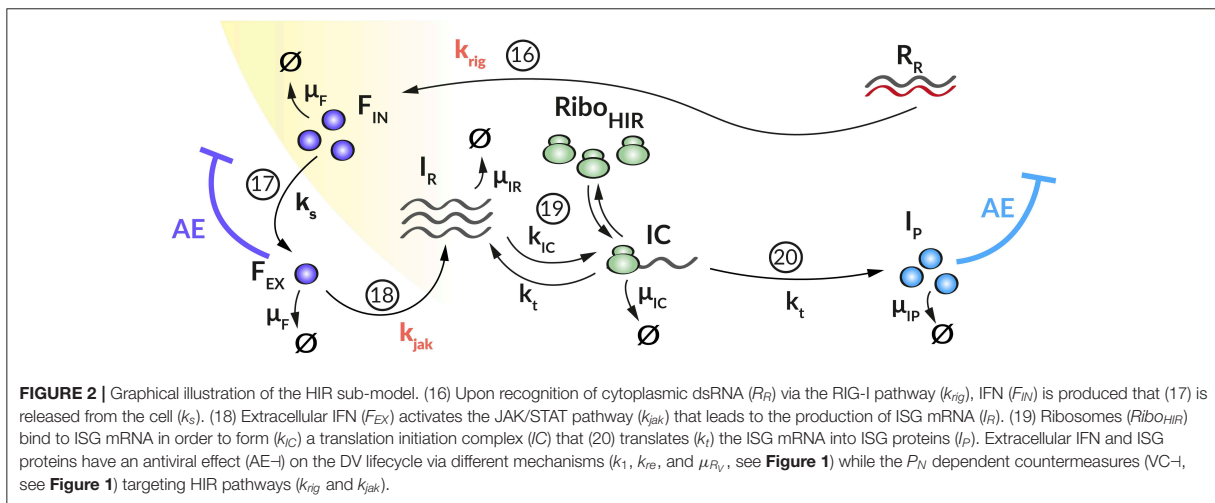


**FIGURE 1 |** Graphical illustration of the DV replication model. (1) The Virus ( $V$ ) attaches to a permissive cell ( $k_a$ ) and (2) enters via receptor-mediated endocytosis ( $k_e$ ). (3) The virus in the endosome ( $V_E$ ) is degraded with rate ( $\mu_{V_E}$ ). The viral and endosomal membrane fuse ( $k_f$ ) and release the viral RNA genome ( $R_V$ ), which is degraded with rate  $\mu_{R_V}$ . (4) Ribosomes ( $Ribo_{DV}$ ) bind ( $k_1$ ) at the viral RNA genome, forming a translation complex ( $TC$ ), which in turn is degraded with rate  $\mu_{TC}$ . (5) The viral genome is translated ( $k_2$ ) into a long polyprotein ( $P_P$ ) and (6) subsequently cleaved ( $k_c$ ) into structural ( $P_S$ ) and non-structural proteins ( $P_N$ ), which degrade with rate  $\mu_{P_S}$  and  $\mu_{P_N}$ , respectively. During the translation, luciferase ( $L$ ) is produced as a marker for translation activity and is degraded with rate  $\mu_L$ . (7) The  $TC$  together with non-structural proteins and host factors ( $HF$ ) initiating the formation ( $k_{pin}$ ) of a replication complex ( $R_{RC}$ ). (8) The antisense synthesis ( $k_{4m}$ ) leads to production of double-stranded RNA (dsRNA) that (9) binds to non-structural proteins in the Replication Compartment  $RC$  ( $P_{RC}$ ) forming ( $k_5$ ) a minus-strand RNA intermediate complex ( $R_{IDS}$ ).  $R_{IDS}$  in turn (10) initiates plus-strand RNA synthesis ( $k_{4p}$ ). (11) The newly synthesized plus-strand RNA ( $R_P$ ) can be exported out of the  $RC$  into the cellular cytoplasm ( $k_{pout}$ ), (12) undergoes another round of replication ( $k_3$ ) or (13) is packed into virus particles and released ( $k_r$ ) from the host cell (14), where it can infect naïve cells ( $k_{re}$ ) for a further round of replication. Species in the  $RC$  degrade with constant rate  $\mu_{RC}$ , (15) except the dsRNA species which get transported out the  $RC$  with rate constant  $\mu_{RC}$  resulting in an accumulation of dsRNA in the cytoplasm ( $R_R$ ). Extracellular IFN and ISG proteins have an antiviral effect (AE-) see **Figure 2** on the DV lifecycle via different mechanisms ( $k_1$ ,  $k_{re}$ , and  $\mu_{R_V}$ ) while the  $P_N$  dependent countermeasures (VC-) targeting HIR pathways ( $k_{rig}$  and  $k_{jak}$ , see **Figure 2**).



Equation (1) and (2) describe how extracellular virus ( $V$ ) binds at the cell surface of a permissive host cell with rate constant  $k_a$  and degrades with rate constant  $\mu_V$  (Equation 1). To keep the model simple, we assume that attachment is non-reversible. According to the experimental set-up, the cells were washed to remove unbound virus from the initial infection. This is considered in the model through the term  $wV$ , where  $w$  is modeled as

$$w = \omega_s \frac{1}{\sqrt{2\pi\omega_d^2}} e^{-\frac{(t-\omega_t)^2}{2\omega_d^2}}, \quad (4)$$

with washing time point  $\omega_t$ , washing duration  $\omega_d$ , and washing strength  $\omega_s$  (for more details, see **Supplementary Material**). The term  $k_{re}V_{INF}$  in Equation (1) describes newly released infectious virus particles from previous rounds of virus replication, which can infect naïve cells. Equations (2) and (3) describe cell entry: Attached virus ( $V_A$ ) enters the cell with rate constant  $k_e$  via receptor-mediated endocytosis. Subsequently, virus in the endosome ( $V_E$ ) undergoes conformational changes of the nucleocapsid, leading to fusion of the viral and endosomal membranes with rate constant  $k_f$  (Equation 3). Endocytosed virus  $V_E$  decays with rate constant  $\mu_{V_E}$ .

The steps associated with RNA translation are described by the following ODEs, which are based on our previously published HCV replication model (Binder et al., 2013). Here,  $R_V$  describes viral (+)RNA in the cytoplasm,  $TC$  corresponds to active translation complexes,  $P_P$  describes viral polyprotein, and  $P_S$  and  $P_N$  are representatives for the structural and non-structural viral proteins, respectively. In our experimental data,  $P_P$  is measured via a bicystronic luciferase reporter system, the species  $L$  is therefore required for model fitting purposes and gives luciferase protein concentration, which degrades with rate constant  $\mu_L$ . The following ODEs describe the temporal

evolution of these species:

$$\frac{dR_V}{dt} = k_f V_E - k_1 R_V (Ribo_{DV_{tot}} - TC) + k_2 TC + k_{P_{out}} R_P - \mu_{R_V} R_V \quad (5)$$

$$\frac{dTC}{dt} = k_1 R_V (Ribo_{DV_{tot}} - TC) - k_2 TC - k_{P_{in}} P_N TC (HF_{RC_0} - R_{RC}) - \mu_{TC} TC \quad (6)$$

$$\frac{dP_P}{dt} = k_2 TC - k_c P_P \quad (7)$$

$$\frac{dL}{dt} = k_2 TC - \mu_L L \quad (8)$$

$$\frac{dP_S}{dt} = k_c P_P - \mu_{P_S} P_S - N_{P_S} \nu_P \quad (9)$$

$$\frac{dP_N}{dt} = k_c P_P - k_{P_{in}} P_N TC (HF_{RC_0} - R_{RC}) - \mu_{P_N} P_N \quad (10)$$

After cell entry, the viral RNA genome  $R_V$  is released into the cytoplasm and is subsequently translated giving rise to viral protein or is degraded with rate constant  $\mu_{R_V}$  (Equation 5). Free ribosomes ( $Ribo_{DV}$ ) reversibly bind to the viral RNA genome ( $R_V$ ) to form a translation initiation complex ( $TC$ , Equation 6) with rate constant  $k_1$ . We assume that the total number of ribosomes,  $Ribo_{DV_{tot}}$ , is constant, hence free ribosomes available for translation are given by  $Ribo_{DV}(t) = Ribo_{DV_0} - TC$  and it is not necessary to introduce a separate equation for the ribosomes.  $HF_{RC_0}$  represents one or more unspecified host cell factor(s) that are required for formation of the RC and is assumed constant (see **Table S1**). Upon translation of the viral genome into a polyprotein ( $P_P$ , Equation 7) with rate constant  $k_2$ , the translation initiation complex ( $TC$ ) dissociates into free viral RNA ( $R_V$ ) and ribosomes ( $Ribo_{DV}$ ). Furthermore, during  $TC$  degradation with rate constant  $\mu_{TC}$ , ribosomes dissociate from the complex:  $Ribo_{DV} + R_V \rightarrow TC \rightarrow Ribo_{DV} + R_V + P_P + L$ . We measure polyprotein production using a luciferase reporter system, and hence include luciferase ( $L$ , Equation 8)

into the mathematical model.  $L$  is produced with rate constant  $k_2$  and is degraded with rate constant  $\mu_L$ . The polyprotein ( $P_P$ ) is cleaved into structural ( $P_S$ ) and non-structural proteins ( $P_N$ ) with rate constant  $k_c$ , which degrade with rate constants  $\mu_{P_S}$  and  $\mu_{P_N}$ , respectively. We note here further that later in the virus lifecycle, the structural proteins ( $P_S$ , Equation 9) are packed together with newly synthesized (+)RNA ( $R_P$ ) into virions, thus the corresponding term involving  $v_p$  in equation (9), which is detailed in equation (17) below. Furthermore, the non-structural proteins ( $P_N$ ), e.g., the RNA-dependent-RNA polymerase, are required for viral RNA synthesis (compare Equation 11).

Equations (11) to (16) describe the viral RNA replication inside the replication vesicles. The species  $R_{RC}$  describes a replication intermediate complex for minus strand RNA synthesis inside the RC, whereas  $R_{IDS}$  is the corresponding intermediate complex for (+)RNA production.  $R_{DS}$  and  $R_P$  describe dsRNA and single (+)RNA in the RC.  $P_{RC}$  corresponds to the viral RNA polymerase in the RC that is required for RNA replication. Replication is thus modeled by the following equations:

$$\frac{dR_{RC}}{dt} = k_{pin}P_NTC(HF_{RC_0} - R_{RC}) - k_{4m}R_{RC} + k_3R_P P_{RC}(HF_{RC_0} - R_{RC}) - \mu_{RC}R_{RC} \quad (11)$$

$$\frac{dR_{DS}}{dt} = k_{4m}R_{RC} - k_5R_{DS}P_{RC} + k_{4p}R_{IDS} - \mu_{RC}R_{DS} \quad (12)$$

$$\frac{dR_{IDS}}{dt} = k_5R_{DS}P_{RC} - k_{4p}R_{IDS} - \mu_{RC}R_{IDS} \quad (13)$$

$$\frac{dR_R}{dt} = \mu_{RC}(R_{DS} + R_{IDS}) - \mu_{R_V}R_R \quad (14a)$$

$$\frac{dP_{RC}}{dt} = k_{4m}R_{RC} - k_3R_P P_{RC}(HF_{RC_0} - R_{RC}) - k_5R_{DS}P_{RC} + k_{4p}R_{IDS} - \mu_{RC}P_{RC} \quad (15)$$

$$\frac{dR_P}{dt} = k_{4p}R_{IDS} - k_3R_P P_{RC}(HF_{RC_0} - R_{RC}) - k_{pout}R_P - v_p - \mu_{RC}R_P \quad (16)$$

By analogy to HCV, we assume here that the initiation of RNA replication occurs from freshly translated viral RNA, hence Equations (6) and (11) model RNA import into the RC from  $TC$  (instead of  $R_V$ ) with rate constant  $k_{pin}$ . At the same time, non-structural proteins ( $P_N$ ), required for RNA synthesis, and an unspecified host factor  $HF_{RC}$ , required for the formation of the RC, are imported into the RC. These assumptions directly match those made in our published HCV replication model (Binder et al., 2013). As the total amount of host factor  $HF_{RC}$  is assumed constant during the time scales considered in the model, a separate equation for  $HF_{RC}$  is not necessary. We furthermore note that, while numerous replication vesicles can be observed during DV replication in every single cell (Welsch et al., 2009), we assume in the model that the sum of all replication vesicles is regarded as a single, large replication compartment, compare (Dahari et al., 2007).

After formation of the replication initiation complex  $R_{RC}$ , minus-strand RNA synthesis is initiated with rate constant

$k_{4m}$ , leading to the production of dsRNA ( $R_{DS}$ , Equation 12) and liberation of viral proteins which remain in the RC ( $P_{RC}$ , Equation 15). For the synthesis of (+)RNA ( $R_P$ , Equation 16), dsRNA ( $R_{DS}$ ) binds again to  $P_{RC}$  with constant rate  $k_5$  in order to form a minus-strand RNA intermediate complex ( $R_{IDS}$ , Equation 13). The minus-strand RNA intermediate complex ( $R_{IDS}$ ) serves as a template for (+)RNA synthesis with constant rate  $k_{4p}$  and subsequently dissociates into dsRNA ( $R_{DS}$ ) and viral protein ( $P_{RC}$ ). The newly synthesized (+)RNA ( $R_P$ ) can then either be transported out of the RC into the cytoplasm with rate constant  $k_{pout}$ , it can be used for a further round of replication with rate constant  $k_3$ , or it is used to assemble new virions, which are then released from the cell ( $v_p$ ). We assume that all species in the RC are protected from active degradation, and decay together with the membrane vesicles with a common rate constant  $\mu_{RC}$ .

Since the RCs might represent a protective environment for DV replication by shielding DV RNA from the host's immune response recognition (Scutigliani and Kikkert, 2017), we introduced a cytosolic dsRNA species ( $R_R$ , Equation 14a). Therefore, for the dsRNA species within the RC,  $R_{DS}$  and  $R_{IDS}$ ,  $\mu_{RC}$  represents a transfer rate into the cytoplasm and leads to the accumulation of cytosolic dsRNA that is detectable by the innate immune sensor (Chazal et al., 2018), while the RNA species within the RC remain protected. In order to account for a slow transfer rate without introducing another model parameter, we use the RNA degradation rate inside the replication compartment,  $\mu_{RC}$ , for this purpose. Similar to the single stranded RNA species within the cytoplasm, the cytosolic dsRNA degrades with rate  $\mu_{R_V}$ .

Finally, Equations (17) to (19) model the assembly and release of new virus particles. To produce one infectious virion, the newly synthesized (+)RNA ( $R_P$ ) assembles together with structural proteins: 180 C proteins, 180 E, and 180 prM/M proteins (Kuhn et al., 2002). Moreover, it has been shown that non-structural proteins support DV particle production as well, e.g., DV NS1 (Scaturro et al., 2015). However, we observed during model fitting that non-structural proteins were not rate limiting for virus assembly and therefore we neglected  $P_N$  in the assembly process, while we focused on structural proteins and host factors required or participating in virus assembly and release (for more information see **Supplementary Material**).

We model DV assembly and release ( $v_p$ ) using a Michaelis-Menten type equation, as

$$v_p = k_p R_P \prod_j \frac{P_j}{K_D \cdot N_{P_j} + P_j}, \quad (17)$$

with  $j \in \{P_S, HF_{PP}\}$ ,  $N_{P_j}$  the number of each protein  $P_j$ , and cell line-specific virion release rate constant  $k_p$ , compare (Heldt et al., 2012). We require here that sufficient proteins per virion need to be available in order to reach the half-maximal virion release rate  $K_D$ . Furthermore, we introduced a second host factor  $HF_{PP}$  for particle production, with a cell line-specific basal production rate  $k_{HF_{PP}}$ :

$$\frac{dHF_{PP}}{dt} = k_{HF_{PP}} - N_{HF_{PP}} v_p. \quad (18)$$

The infectious virions ( $V_{INF}$ ) are released from the cell and are then able to infect naïve cells with a reinfection rate constant  $k_{re}$  (Equation 19); they furthermore are assumed to degrade with rate constant  $\mu_V$ , thus

$$\frac{dV_{INF}}{dt} = v_p - k_{re}V_{INF} - \mu_VV_{INF}. \quad (19)$$

### Host Cell Immune Response

We coupled the replication model with a simple model containing the central steps of the cell's IIR to infection. This HIR sub-model (Figure 2) comprises four main processes: (1) The recognition of viral RNA by cellular PRRs, leading to the initiation of a signaling cascade that causes (2) the production and release of IFN. (3) Subsequently, secreted IFN triggers the transcription of mRNAs of hundreds of ISG, which are then (4) translated into ISG proteins that act upon multiple processes in the DV lifecycle. To keep the model simple, we subsume the different ISGs by a single representative species, included in the model by its mRNA ( $I_R$ ) and protein ( $I_P$ ) species.

As mentioned above and to keep the model simple, we include only dsRNA recognition via RIG-I/MDA-5 into the model. As soon as dsRNA is detectable in the cytoplasm, it activates the HIR. We therefore modified the equation for  $R_R$  (Equation 14a) as follows (changes in bold), where  $k_{rig}$  describes the rate at which the RIG-I pathway is activated and IFN is produced when cytoplasmic  $R_R$  is bound by the receptor:

$$\frac{dR_R}{dt} = \mu_{RC}(R_{DS} + R_{IDS}) - \mu_{RV}R_R - \mathbf{k_{rig}R_R}. \quad (14b)$$

The dynamics of key components of the HIR, namely intracellular IFN ( $F_{IN}$ ), secreted IFN ( $F_{EX}$ ), ISG mRNA ( $I_R$ ), and ISG protein ( $I_P$ ) are given by the following ODEs:

$$\frac{dF_{IN}}{dt} = k_{rig}R_R - k_sF_{IN} - \mu_F F_{IN}, \quad (20)$$

$$\frac{dF_{EX}}{dt} = k_sF_{IN} - k_{jak}F_{EX} - \mu_F F_{EX}, \quad (21)$$

$$\frac{dI_R}{dt} = k_{jak}F_{ex} - k_{IC}I_R(Ribo_{HIRtot} - IC) + k_tIC - \mu_{I_R}I_R, \quad (22)$$

$$\frac{dIC}{dt} = k_{IC}I_R(Ribo_{HIRtot} - IC) - k_tIC - \mu_{IC}IC, \quad (23)$$

$$\frac{dI_P}{dt} = k_tIC - \mu_{I_P}I_P. \quad (24)$$

Here, upon recognition of cytoplasmic dsRNA ( $R_R$ , Equation 14b), the cell produces IFN ( $F_{IN}$ , Equation 20) via the RIG-I/MDA-5 pathway with rate constant  $k_{rig}$ . IFN either degrades with rate constant  $\mu_F$  or is secreted from the cell ( $F_{EX}$ , Equation 21) with rate constant  $k_s$  and then degrades extracellularly with rate constant  $\mu_F$ . Extracellularly,  $F_{EX}$  binds to receptors that activate the JAK/STAT pathway, we assume this to happen with rate constant  $k_{jak}$ . Activation of the JAK/STAT pathway then triggers the production of ISG mRNAs ( $I_R$ , Equation 22), which we assume to degrade with rate constant  $\mu_{I_R}$ . Ribosomes

( $Ribo_{HIR}$ ) bind to  $I_R$  to form a translation initiation complex ( $IC$ , Equation 23) with rate constant  $k_{IC}$ , which in turn degrades with rate constant  $\mu_{IC}$ . The subsequent translation of the translation initiation complex ( $IC$ ) with rate constant  $k_t$  leads to the production of ISG proteins ( $I_P$ , Equation 24). We assume that  $I_P$  degrades with rate constant  $\mu_{I_P}$ . Similar to  $TC$ ,  $IC$  dissociates into  $Ribo_{HIR}$  and  $I_R$  ( $I_R + Ribo_{HIR} \rightarrow IC \rightarrow I_P + I_R + Ribo_{HIR}$ ). Note that in order to prevent ribosomal competition in the model, we discriminate between ribosomes used for DV RNA translation ( $Ribo_{DV}$ ) and ribosomes used for the HIR ( $Ribo_{HIR}$ ).

The ISG proteins ( $I_P$ ) affect numerous processes in the viral lifecycle. Here we focus on effects it has on the formation of the translation initiation complex ( $k_t$ ) and the degradation of viral RNA in the cytoplasm ( $\mu_{RV}$ ) (Diamond, 2014; Castillo Ramirez and Urcuqui-Inchima, 2015). We furthermore assume that the ISGs cannot reach species inside of the replication vesicles, which thus provides a protected environment for viral replication (see **Supplementary Material** for details). We include these effects into the model by decreasing the corresponding reaction rate constant  $k_t$  to

$$\widehat{k_t} = \frac{k_t}{1 + \varepsilon_{k_t}I_P}, \quad (25)$$

and increasing the degradation rate  $\mu_{RV}$  to

$$\widehat{\mu_{RV}} = \mu_{RV}(1 + \varepsilon_{\mu_{RV}}I_P). \quad (26)$$

Furthermore, we take into account that IFN released from infected cells can protect naïve cells from infection by bringing them into an antiviral state, this has been integrated into the model by decreasing the corresponding reaction rate constant  $k_{re}$  to

$$\widehat{k_{re}} = \frac{k_{re}}{1 + \varepsilon_{k_{re}}F_{EX}}. \quad (27)$$

The efficacy constants  $\varepsilon_*$  measures the efficacy of the inhibition on a range from 0 (no effect) to 1 (full inhibition).

### Viral Countermeasures

DV is not only subjected to the HIR, but viral proteins in turn also impair the host's immune response, thus constituting a negative feedback loop of mutual inhibition. Several viral proteins have been described inhibiting HIR pathway activation. For example, DV NS3, NS4A, and NS5 inhibit the RIG-I pathway activation by the methylation of the DV RNA (DV NS5) or by blocking the RIG-I/MAVS interaction (DV NS4A) (Chazal et al., 2018). Additionally, by promoting the degradation of STAT2, DV NS5 impairs activation of the JAK/STAT pathway and thus ultimately inhibits ISG production upon exposure of the cell to exogenous IFN (Ashour et al., 2009; Mazzon et al., 2009). Therefore, we incorporated the ability of DV to circumvent the HIR in two ways ( $\widehat{\varepsilon}_x$ ): (i) by reducing the reaction rate of the RIG-I pathway activation that may lead to a decreased IFN production ( $k_{rig}$ ), and (ii) by decreasing the reaction rate for the JAK/STAT pathway activation that may result in a decreased ISG expression ( $k_{jak}$ ).



Similarly, to the antiviral HIR effect, we incorporated these viral countermeasure effects into our model

$$\widehat{c}_x = \frac{c_x}{1 + \varepsilon_x P_N}, \quad (28)$$

with  $c_x \in \{k_{rig}, k_{jak}\}$  and its efficiency constant  $\varepsilon_x \in [10^{-5}, 1]$ , dependent on DV non-structural protein concentration. Hence, we replaced the rate constants  $k_{rig}$  and  $k_{jak}$  in equations (14b), (20), (21), and (22) by the terms  $\widehat{k}_{rig}$  and  $\widehat{k}_{jak}$  as defined above (see **Supplementary Material** for details).

### Parameter Estimation

We implemented the mathematical model in Matlab Release 2016b (The Mathworks). Twenty out of the total 56 model parameters were fixed based on evidence from literature, direct calculations or observations made during the optimization process, see **Tables S6, S7**. In brief, since infection experiments were carried out at a multiplicity of infection (MOI) of 10 and assuming that the fraction of infected cells follows a Poisson distribution (Flint et al., 2009; Wulff et al., 2012), we computed an initial virus concentration of  $V_0 = 10$  infectious virus particles per ml per cell. Washing of cells to remove unbound virus was performed thrice after 1 h for a duration of 6 min, we therefore set  $\omega_t = 1$  h,  $\omega_d = 0.1$  h and assume a washing strength of  $\omega_s = 100$ . Model parameters for translation and replication rates were estimated based on the DV genome length of approximately 10,700 nucleotides and DV polyprotein length of 3,400 amino acids. During the fitting process, we observed no difference whether the ribosomes bind to viral RNA ( $R_V$ ) or host cell mRNA ( $I_R$ ) and set  $k_1 = k_{IC}$ . Assuming a translation velocity of 3 to 8 AA/s per polysome and assuming 10 ribosomes bound to each 2,000 AA (Dahari et al., 2009), we obtain  $k_2 = 100$  h<sup>-1</sup>. The translation rate ( $k_t$ ) for the ISG proteins ( $I_P$ ) was calculated accordingly as  $k_t = 120$  h<sup>-1</sup>, using the IFIT1 protein as a representative ISG with a length of 478 AA (Safran et al., 2010). RNA synthesis rate constants were calculated as  $k_{4m} = k_{4p} = 1.01$  h<sup>-1</sup>, using a transcription rate of 180 nt per min (Dahari et al., 2009). Degradation rates for extracellular virus and IFN were set to  $\mu_V = 0.4$  h<sup>-1</sup> and  $\mu_F = 0.15$  h<sup>-1</sup> (Schmid et al., 2015). Note that for simplicity, we assumed that the intracellular IFN degradation equals the extracellular degradation,  $\mu_F$ . We observed a higher stability of virus within endosomes ( $\mu_{V_E}$ ) compared to extracellular virus ( $\mu_V$ ) and fixed the degradation rate of virus within endosomes to  $\mu_{V_E} = 0.5 \cdot \mu_V$ . The degradation rate for luciferase  $\mu_L = 0.35$  h<sup>-1</sup> as well as the polyprotein cleavage rate  $k_c = 1$  h<sup>-1</sup> were taken from our HCV replication model (Binder et al., 2013). The translation initial complexes  $TC$  and  $IC$  are assumed to be more stable than free cytosolic DV RNA genome ( $R_V$ ) and ISG mRNA ( $I_R$ ) due to the bound ribosomes. Therefore, the degradation rates  $\mu_{TC}$  and  $\mu_{IC}$  are assumed to be lower than the degradation rates  $\mu_{R_V}$  and  $\mu_{I_R}$ . The degradation rate for ISG proteins was fixed to  $\mu_{I_P} = 0.03$  h<sup>-1</sup>, corresponding to a half-life of  $t_{1/2} = 24$  h based on literature showing half-lives for ISG proteins in the range of 12 h and 2.3 days (Ronni et al., 1993; Martensen and Justesen, 2004; Haller et al., 2007; Bogunovic et al., 2013). The half-maximal virion release

rate ( $K_D$ ) needed for the virus assembly and release term ( $v_p$ ) was approximated based on the experimental measurements of extracellular virus particles. Here, we calculated that in Huh7 cells,  $K_D = 1.8$  virions/ml per measurement time point were produced, while in A549 cells,  $K_D = 0.7$  virions/ml per measurement time point were produced. The number of structural proteins required to produce one virion has been taken from literature with  $N_{P_S} = 180$  molecules/virion (Kuhn et al., 2002). During the fitting process, we observed a 10 times higher basal production rate for the host factor involved in assembly/release in Huh7 cells than in A549 cells. We therefore set  $k_{HF_{PP}}^{Huh7} = 10 \cdot k_{HF_{PP}}^{A549}$ . Furthermore, we observed that the initial concentration of the cell line specific host factor involved in virus assembly and release was fitted to the same value and thus set  $HF_{PP_0}^{Huh7} = HF_{PP_0}^{A549} = HF_{PP_0}$ . However, we assume that the initial host factor ( $HF_{RC_0}$ ,  $HF_{PP_0}$ ) and ribosome ( $Ribo_{DV_0}$ ,  $Ribo_{HIR_0}$ ) concentrations, as well as the number of consumed host factors in the virus assembly and release process ( $N_{HF_{PP}}$ ) are  $\geq 1$  molecules/virion. The antiviral HIR and DV countermeasure efficiency constants were estimated within  $\varepsilon_* \in [10^{-5}, 1]$ , while the remaining model parameters have been estimated within the range  $[10^{-5}, 10^3]$ . Initial specie concentrations were  $V_{A_0} = V_{E_0} = V_{INF_0} = 0$  virions/ml for virus species,  $R_{V_0} = TC_0 = R_{RC_0} = R_{DS_0} = R_{IDS_0} = R_{R_0} = R_P = P_{P_0} = P_{S_0} = P_{N_0} = L_0 = P_{RC_0} = 0$  molecules/ml for viral RNA, protein and luciferase species and  $F_{IN_0} = F_{EX_0} = I_{R_0} = IC_0 = I_{P_0} = 0$  molecules/ml for the IFN and ISG species, while the initial concentrations of host factors ( $HF_{RC_0} \neq HF_{PP_0} \neq 0$  molecules/ml) and ribosomes ( $Ribo_{DV_0} \neq Ribo_{HIR_0} \neq 0$  molecules/ml) have been estimated (for more details, see **Supplementary Material**).

To fit the model to the experimental data, we computed  $R_P^{tot} = (V_E + R_V + TC + R_{RC} + R_{DS} + R_{IDS} + R_R + R_P)$ ,  $V^{tot} = (V + V_A + V_{INF})$ , and  $I_R^{tot} = (I_R + IC)$  and introduced four scaling factors  $f_{Scale_L}$ ,  $f_{Scale_R}$ ,  $f_{Scale_F}$ , and  $f_{Scale_{I_R}}$  to rescale experimental measurements acquired in relative values (Luciferase, DV RNA, and ISG mRNA) and pg/ml (IFN). Remaining free model parameters were then estimated from the experimental data. Parameter estimation was performed using the Data2Dynamics Matlab toolbox (Raue et al., 2015), using a deterministic trust region algorithm (lsqnonlin) with Latin hyper cube multi-start, minimizing the log likelihood function (Raue et al., 2013) (for more details see **Supplementary Material**). Parameter estimation was performed simultaneously for the Huh7 and A549 cell lines, where only the DV replication sub-model was used in the Huh7 cells and the full model including the immune response sub-model in the A549 cell line. The only other parameters that were allowed to vary between the two cell lines were the initial concentrations of the host factor for the formation of the minus-strand synthesis complex ( $HF_{RC_0}$ ) as well as the basal production ( $k_{HF_{PP}}$ ) of the host factor for particle production ( $HF_{PP_0}$ ). It is likely that more processes are cell line specific, however, here we summarized all model parameters that did not show any impact on the model fit and focused mainly on cell line specific host factor availability and HIR effects. **Tables S6, S7** summarize the final, resulting model parameters used after model fitting.

## Model Analysis

### Simulation of Antiviral Intervention

We used the model to study potential antiviral strategies. For this purpose, we extended the model by effects of direct-acting antiviral drugs (DAAs). A drug efficacy parameter  $0 \leq \varepsilon \leq 1$  was introduced to simulate drug effects on viral attachment ( $k_a$ ), viral entry ( $k_e$ ), formation of the translation initiation complex ( $k_1$ ), translation ( $k_2$ ), polyprotein cleavage ( $k_c$ ), replication complex formation ( $k_{pin}$ ), minus- and (+)RNA synthesis ( $k_{Am}$  and  $k_{Ap}$ ), virus particle production and release ( $v_p$ ), and infection of naïve cells ( $k_{re}$ ), by multiplying the corresponding parameter with  $(1 - \varepsilon)$ . We then calculated the time-averaged infectious virus particle concentration released from the cell upon drug administration ( $\varepsilon > 0$ ) within a time interval of 5 days ( $\Delta t = 120$  h), normalized to the time-averaged infectious virus concentration without drug treatment ( $\varepsilon = 0$ ) as

$$\psi = \frac{\langle V_{INF}(t)_{T_{\varepsilon>0}} \rangle}{\langle V_{INF}(t)_{T_{\varepsilon=0}} \rangle}, \quad (29)$$

with

$$\langle V_{INF}(t)_T \rangle = \frac{1}{\Delta t} \int_t^{T+\Delta t} dt V_{INF}(t), \quad (30)$$

where  $T$  refers to the time point of drug administration ( $T \leq t \leq T + \Delta t$ ).

### Identifiability and Sensitivity Analysis

We assessed model identifiability using the profile likelihood method, which analyzes both structural and practical identifiability. The profile likelihood method evaluates the change in the likelihood function after modification of one individual model parameter by re-optimizing the remaining model parameters (Raue et al., 2009; Kreutz et al., 2013; Maiwald et al., 2016), thus assessing if changes in a given parameter can be compensated by modifications in other model parameters. Based on the profile likelihood, we calculated 95% confidence intervals on model parameters, which imply parameter identifiability if the confidence interval is finite (Raue et al., 2009, 2015). Local and global sensitivity analysis were carried out in Matlab using the SensSB toolbox (Rodríguez-Fernandez and Banga, 2010) and the extended Fourier Amplitude Sensitivity Test (eFAST) (Marino et al., 2008). Sensitivities with regard to polyprotein ( $P_p$ ), total (+)RNA ( $R_p^{tot}$ ) and total Virus ( $V^{tot}$ ) concentrations were calculated for the two time points  $t = 4$  hpi (early during infection) and  $t = 72$  hpi (at steady state).

## RESULTS

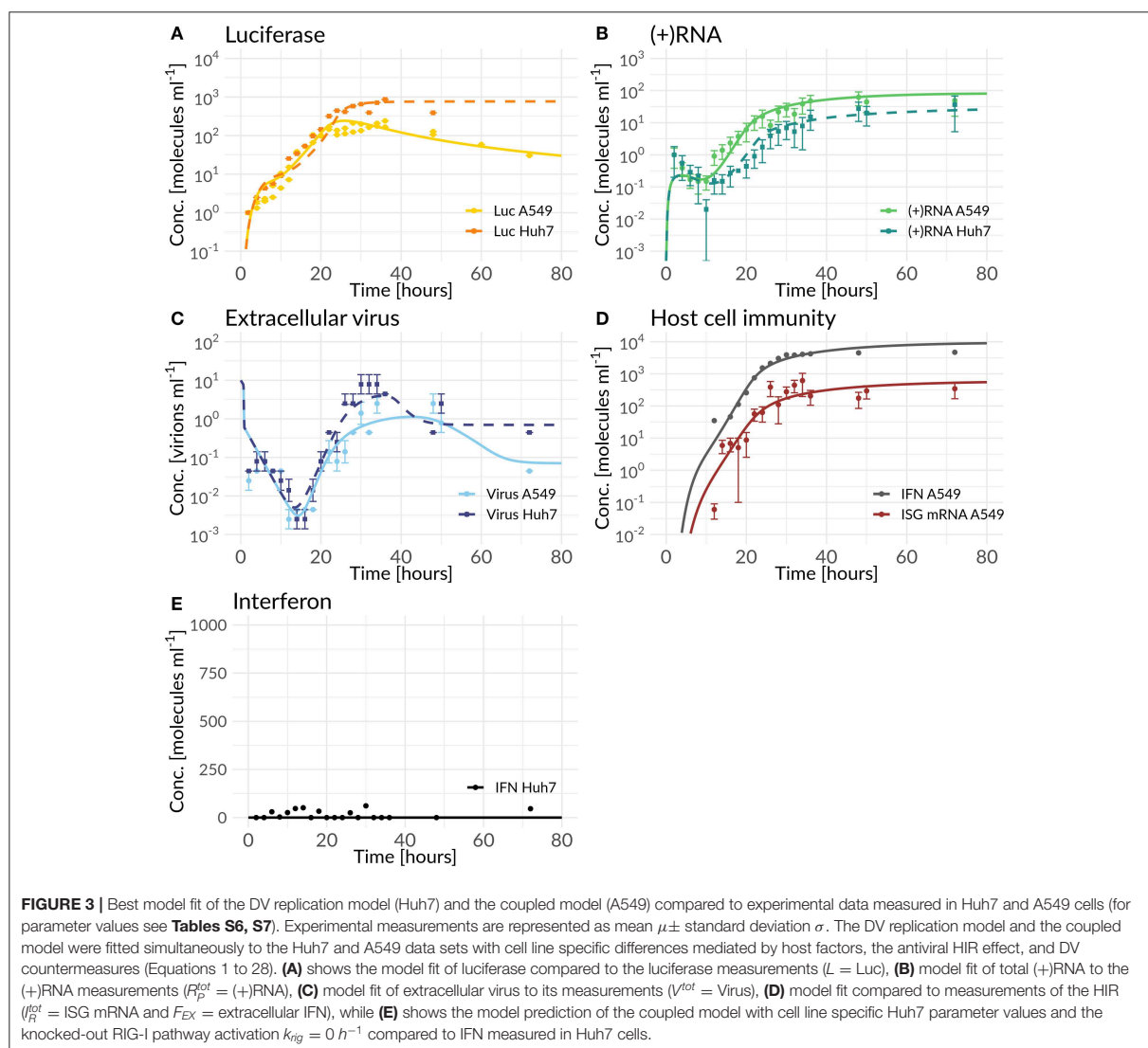
In order to *in silico* analyze the full DV lifecycle in the absence and presence of HIR mechanisms, we developed a detailed model of the intracellular DV lifecycle and coupled this model to an HIR model, taking into account the antiviral effect of an active immune response on the DV lifecycle as well as DV's ability to in return attenuate the HIR (Figures 1, 2). Model calibration was performed by estimating model parameters simultaneously on experimental data measured in two different

cell lines, Huh7 and A549 cells (for details see Materials and Methods). For this purpose, we measured viral polyprotein (luciferase readout), (+)RNA, extracellular virus, and IFN in both cell lines, while ISG mRNA was measured only in A549 cells, as the Huh7 cell do not show activation of the interferon system after DV infection. Polyprotein (luciferase) showed a 1-log<sub>10</sub> higher translation activity in Huh7 cells compared to A549 cells (Figure 3A). Similarly, Huh7 cells showed a higher extracellular infectious virus concentration compared to A549 cells (Figure 3C). However, in both cell lines, the extracellular virus concentration drops after reaching a peak (~32 hpi in Huh7 and 36 hpi in A549 cells). Nevertheless, against our expectations, DV (+)RNA measurements showed the opposite trend with a faster RNA production in A549 cells (Figure 3B). Additionally, IFN has been measured in both cell lines and showed an increase in secreted IFN in A549 cells (which is followed by ISG mRNA) and a baseline IFN level in Huh7 cells (Figures 3D,E).

Our coupled model, developed based on best biological knowledge, showed high agreement with our experimental cell-line specific measurements after fitting model parameters to the data (Figure 3). Due to the high degree of freedom of the model and in order to prevent overfitting, we analyzed structural and practical identifiability of model parameters. Results are shown in Figure S12; as can be seen in the figure, due to the high model complexity, not all model parameters are identifiable. In particular the parameters for replication within the RC ( $k_3$ ) and DV RNA export out of the RC ( $k_{pout}$ ) are non-identifiable. Both parameters concern the use of newly synthesized plus-strand RNA and reflect the allocation of such newly synthesized RNA to either further rounds of RNA replication ( $k_3$ ) or to export from the replication compartment and use for protein translation. The fact that these two parameters are non-identifiable is surprising at first, as allocation of newly synthesized RNA between these processes should significantly affect viral replication dynamics. However, this can be explained by other processes that are rate-limiting. In fact, we observed a similar behavior in our HCV replication model (Binder et al., 2013), where in high permissive cell lines the HCV RNA-dependent RNA polymerase became in fact rate limiting for RNA replication inside of the replication vesicles, and led to a similar insensitivity of the model to the parameter  $k_3$ . This is reflected in DV as well, with only limited impact of parameters  $k_3$  and  $k_{pout}$  on the replication dynamics in both cell lines.

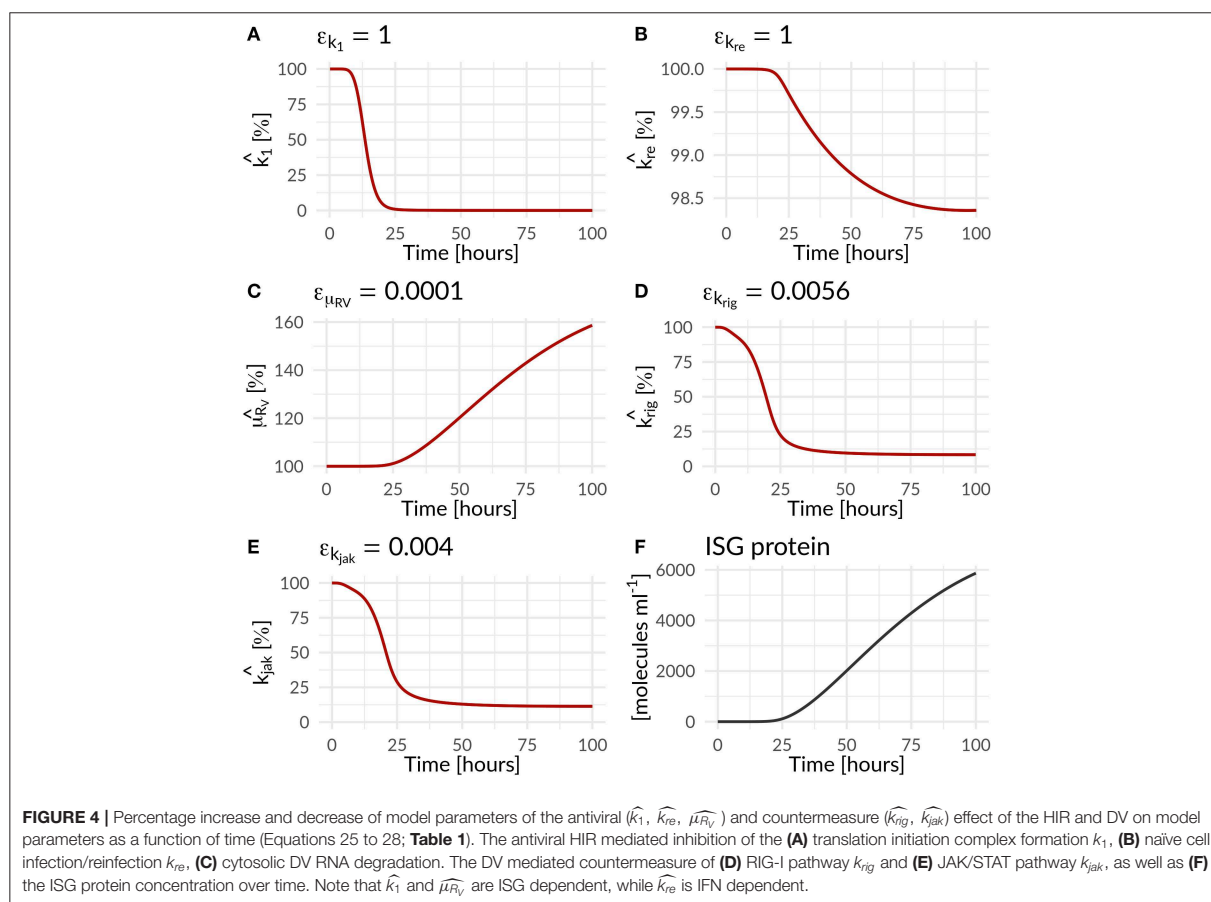
### Host Dependency and Restriction Factors

The first question we addressed was cell line specificity. In contrast to our expectations, we observed a faster onset and more efficient viral replication in the HIR-competent A549 cells. Here, our model was not able to describe the DV RNA dynamics in A549 cells that seemed unaffected by the HIR and showed a faster increase and an overall 2.7-fold higher amount of DV RNA (time-averaged concentration) compared to Huh7 cells. Viruses strongly depend on their living hosts and hijack host cell membranes, proteins, and lipids for their own replication. We thus speculated that other host processes explain this difference between the two cell lines. We tested different such potential host factors by including



corresponding cell-line specific parameters into the model, compare **Table S3**, and discriminated between these models using model selection based on Akaike's Information Criterion (AIC). In line with our previous findings with our published HCV model (Binder et al., 2013), we introduced an unspecific cell line specific host factor,  $HF_{RC}$ , that participates in the assembly of the replication complex and RC formation. In model fitting, this host factor showed a higher availability leading to a faster onset of DV replication in A549 cells compared to Huh7 cells (**Table S6**). We furthermore tested cell-line specific effects on different host factor supported processes such as virus entry, that improved the overall model fit without explaining the cell line specific DV RNA dynamics (see **Table S3**).

We additionally observed a cell line specific variation in the extracellular DV dynamics, resulting in a 2.8-fold lower extracellular virus concentration (time-averaged) in A549 cells, that could not be described by the HIR alone. Thus, we introduced another unspecific host factor,  $HF_{PP}$ , involved in virus particle production and release, with a cell line specific basal production,  $k_{HF_{PP}}$ , and a cell line specific virus assembly and release rate,  $k_p$ . During model parameter estimation, we observed a faster virus assembly and release and an around 10 times faster basal production of the host factor involved in DV assembly and release in Huh7 cells compared to A549 cells. This basal host factor production was the key parameter for the lower virus concentration in A549 cells in steady state. Furthermore, this host factor represented a limiting species for particle production



and release, since the drop in the extracellular DV concentration following the peak was associated with a drop in the host factor concentration. Interestingly, the availability of structural proteins had no effect on the drop in released virus (see **Figure S1**).

### The Antiviral HIR Effect and Viral Countermeasures

During an acute infection, the IIR represents the first line of defense against an invading pathogen. The IIR is mounted by the production of IFN and subsequent ISG translation; the ISGs in turn subsequently inhibit multiple steps in the viral lifecycle. Having developed a detailed model coupling the DV lifecycle with key players of the HIR, we studied the antiviral modes of action in detail and introduced three possible antiviral HIR effects on (i) the translation initiation ( $k_1$ ), (ii) the degradation of free cytosolic DV RNA ( $\mu_{RV}$ ), and (iii) the reinfection of naive cells ( $k_{re}$ ) into the model. Selection of these three main mechanisms was based on model selection using the least squared error with the AIC to account for model complexity. For details we refer to the **Supplementary Material**. By comparing the model fits and its AICs, we observed the best model fit and lowest AIC for a model in which the HIR inhibits the translation initiation

complex formation ( $k_1$ ), followed by a model, that increases the degradation of free cytosolic viral RNA ( $\mu_{RV}$ ). However, the model considering only the increase in the cytosolic RNA degradation ( $\mu_{RV}$ ) resulted in a very high cytosolic DV RNA degradation rate of  $\widehat{\mu}_{RV} = 987 \text{ h}^{-1}$ . The model that led to an antiviral state by inhibiting reinfection of naive cell infection led to the third best model. Since we are interested in combinatory effects, we chose all three antiviral ISG and IFN dependent effects as our working model.

In the combined HIR effect model, the inhibition of the translation initiation ( $k_1$ ) and the reinfection of susceptible cells ( $k_{re}$ ) by the HIR showed the highest efficacy constants with  $\varepsilon_{k_1} = \varepsilon_{k_{re}} = 1$  (**Table S7**). Comparing the inhibitory effect on the effective rate constants over time, the rate constant for  $k_1$  dropped by 99.983% from its initial value, while  $k_{re}$  showed a negligible 1.6% decrease (**Figure 4** and **Table 1**). The cytoplasmic RNA degradation rate was increased by 58.7%. DV has the ability to evade the HIR by decreasing or inhibiting its own recognition, correspondingly, the rate constants for RIG-I pathway activation and dsRNA recognition was reduced by 93.6%, while the JAK/STAT pathway activation was reduced by 88.6% (**Table 1**).

**TABLE 1 |** Effect of the immune response on DV replication parameters and of Dengue on parameters of the immune pathways—change in parameter values over 100 h for HIR affected processes in the DV lifecycle and HIR pathways that are targeted by DV: Translation initiation complex formation ( $k_1$ ), naïve cell infection/reinfection ( $k_{re}$ ), cytosolic RNA degradation ( $\mu_{RV}$ ), RIG-I pathway ( $k_{rig}$ ), and JAK/STAT pathway ( $k_{jak}$ ).

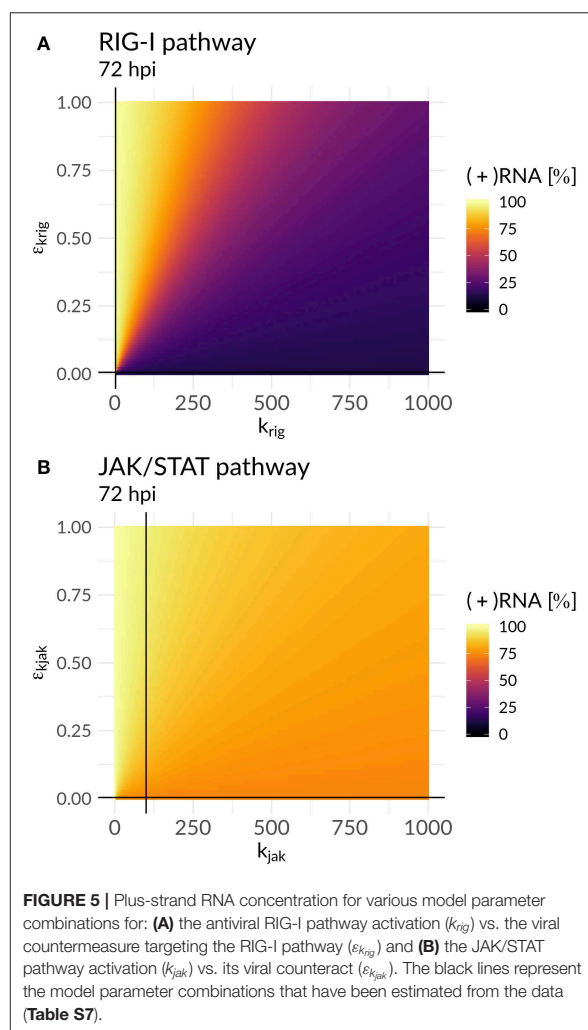
Parameter	t = 0 h	t = 100 h	Unit	Increase/Decrease in %
$k_1$	1,000	0.17	$ml\ molecules^{-1}\ h^{-1}$	-99.983%
$k_{re}$	1e-4	9.8e-5	$h^{-1}$	-1.6%
$\mu_{RV}$	2.8	4.4	$h^{-1}$	+58.7%
$k_{rig}$	2.6	0.2	$h^{-1}$	-93.6%
$k_{jak}$	100	11.4	$h^{-1}$	-88.6%

In order to further mathematically analyze the interplay of antiviral effects ( $k_{rig}$  and  $k_{jak}$ ) and the viral ability to attenuate the HIR ( $\varepsilon_{k_{rig}}$  and  $\varepsilon_{k_{jak}}$ ), we performed a bifurcation analysis at time 72 hpi. Here, we compared the (+)RNA concentration to various effect combinations: (i) the recognition of DV dsRNA ( $k_{rig}$ ) vs. DV’s ability to attenuate its own recognition ( $\varepsilon_{k_{rig}}$ ) and (ii) the activation of the JAK/STAT pathway ( $k_{jak}$ ) vs. DV countermeasures targeting the JAK/STAT pathway ( $\varepsilon_{k_{jak}}$ ) (Figure 5). In the first scenario, we observed a clear separation: with increasing  $k_{rig}$  the HIR wins and the infection is effectively cleared with only minimal residual (+)RNA, while with increasing  $\varepsilon_{k_{rig}}$  the virus wins and the infection is ongoing. In contrast, in the second scenario we found that increasing the activation of the JAK/STAT signaling pathway ( $k_{jak}$ ) did not lead to significant decreases in viral RNA levels.

### Antiviral Drug Intervention

We were further interested in using the mathematical model to identify processes with a high impact on the DV lifecycle, as those might constitute attractive targets for antiviral drug development. For this purpose, we performed a global sensitivity analysis to analyze the effect of all model parameters on viral polyprotein, total DV (+)RNA and extracellular virus concentrations at two distinct time points, 4 and 72 hpi (Figures 6, 7).

Both cell lines showed a comparable sensitivity profile for polyprotein, DV (+)RNA, and the extracellular virus and showed high sensitivities to processes associated with cell infection, polyprotein translation and processing, and DV RNA synthesis. For all the three species, early processes in the viral lifecycle were associated with highly significant sensitivities at 4 hpi, such as virus attachment ( $k_a$ ), entry ( $k_e$ ), and fusion ( $k_f$ ), as well as polyprotein translation ( $k_2$ ). Later in infection (72 hpi), ongoing polyprotein translation as well as processes within the RC dominated in their sensitivities for the three studied species. Especially polyprotein cleavage ( $k_c$ ) became the dominant process with the highest impact of all steps involved in viral protein translation. Of the processes occurring inside of the RC, the most sensitive rate constants were associated with RNA synthesis ( $k_{4m}$ ,  $k_{4p}$ ) and the host factor involved in the formation of the RC ( $HF_{RC}$ ) for both cell lines. For the extracellular virus, the number of host factors ( $N_{HFpp}$ ) involved in assembly and release showed a higher sensitivity compared



to the number of viral structural proteins ( $N_{Ps}$ ). Amongst the HIR model parameters, the RIG-I pathway activation ( $k_{rig}$ ) showed a slightly higher, significant sensitivity on the polyprotein species. Furthermore, the HIR efficacy constant decreasing the rate constant of the naïve cell infection ( $\varepsilon_{\mu_{RV}}$ ) showed the highest sensitivity of all antiviral HIR constants, albeit not reaching statistical significance.

As a next step, we were interested in the question whether the highly sensitive processes identified in the previous analysis might represent potent drug targets. We therefore performed a theoretical antiviral intervention by simulating a possible drug administration. In this simulation, we monitored the release of infectious virus for 5 days following drug administration. Several processes in the DV lifecycle were inhibited by simulated drug administration at 0 hpi, 24 hpi, and 72 hpi (Figure 8). An early drug administration at 0 hpi led to an efficient viral clearance in both cell lines, using a hypothetical drug acting on

any process in the DV lifecycle except for putative drugs targeting reinfection. With the support from the HIR, the overall drug efficacy constants necessary to eradicate the virus in A549 cells were lower. In particular drugs targeting translation initiation and the DV RNA synthesis were able to induce viral clearance even with low drug efficacy constants, and administering a drug targeting the DV RNA synthesis process showed a viral clearance with the lowest drug efficacy constant ( $\varepsilon \approx 0.5$ ) in A549 cells. For drugs targeting any one of the remaining processes, drug efficacy constants higher than  $\varepsilon \geq 0.9$  were needed to clear the viral infection. Administering a hypothetical drug at 24 and 72 hpi led to comparable viral clearance patterns, but with higher drug efficacy constants. Obviously, if a drug is administered late in the viral lifecycle and targets early processes of the viral lifecycle such as virus attachment, endocytosis and fusion as well as formation of the (membranous) replication compartment, leads to a loss of the drug effect and non-clearance of the DV infection in both cell lines. In both cell lines, the DV infection can still be cleared when blocking DV RNA synthesis and virus assembly/release with <3% DV left with the highest drug efficacy of 1 (thus completely shutting of RNA synthesis and assembly/release), an outcome which cannot be achieved by targeting any of the other processes in the DV lifecycle according to our model simulations.

## DISCUSSION

In the present study, we investigated the intracellular virus replication and HIR dynamics in two different cell lines: Huh7 cells with very low HIR-competence and highly HIR-competent A549 cells. Several cell population models have been developed to analyze DV dynamics under influence of the innate (Schmid et al., 2015) and the adaptive immune response (Ben-Shachar and Koelle, 2014; Clapham et al., 2014, 2016; Ben-Shachar et al., 2016). These models, however, do not take intracellular processes into account and thus lack molecular detail. In order to study the intracellular dynamics during the DV lifecycle, we developed the first mathematical model that reflects the initial dynamics of key components of the intracellular DV genome replication. Our detailed model is derived from previous mathematical models that have been used to describe the intracellular RNA replication of a HCV replicon system after RNA transfection (Dahari et al., 2007; Binder et al., 2013). We extended these models by including virus entry and release of infectious virus particles. Furthermore, we coupled the virus dynamics model to a model of the HIR activation and effector phases in order to study the modes of action of the HIR, and to analyze potential antiviral intervention strategies acting at the level of intracellular mechanisms.

### Host Factors

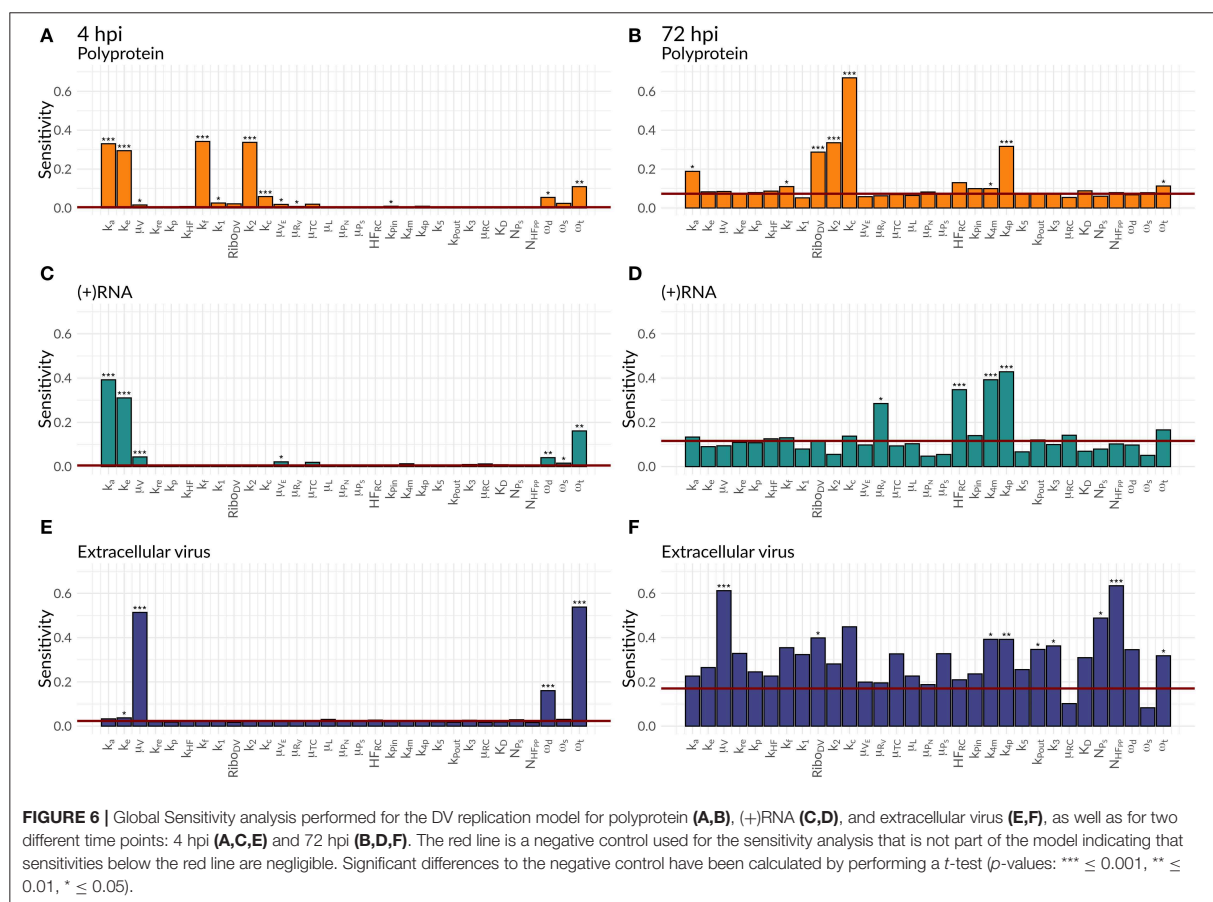
Our experimental measurements were performed in two different cell lines: Huh7 cells which show no interferon response, and A549 cells showing a strong immune reaction. However, Huh7 cells are based on hepatoma (liver) cells, whereas A549 cells are of pulmonary epithelial origin, thus they likely differ in several other aspects as well. In fact, some characteristics of our experimental data cannot be explained by the lack of an

interferon response in the Huh7 cells alone. Contrary to our expectations, we observed a faster onset and more efficient DV genome replication in the immuno-competent A549 cells. We therefore tested which other host factors may explain such cell line specific differences. We set up several different models for such host factors, fitted the corresponding models to the experimental data, and compared different models using AIC; details are given in the **Supplementary Material**. In our previous HCV study, we have shown that host factors involved in replication complex formation play a crucial role in cell permissiveness and viral replication efficiency (Binder et al., 2013). Similarly, for DV, such a host factor best explained differences in replication efficiency between the two cell lines. According to our model, the more efficient RNA replication (earlier increase and a higher steady state concentration of total (+)RNA in the A549 cell line) is directly associated with a higher concentration of this putative host factor in A549 cells, similar to our previous results considering HCV replication in different Huh7 cell clones (Binder et al., 2013).

Concerning the extracellular virus dynamics, our model was not able to explain the drop in infectious virus titers observed in the experimental data after ~40 h post infection—at different degrees in both cell lines—by a limitation in structural viral proteins. In fact, our simulation results show that structural proteins do not limit the process of particle production and release. Similar to our finding, Heldt et al. (2012) in a mathematical model of influenza A virus replication did not find a limitation in structural proteins and suggested that transport and budding processes might limit the viral production. Furthermore, the drop in virus titers that we observed in our data is qualitatively present in both cell lines, i.e., in the presence and in the absence of the HIR, it is therefore unlikely that it is due to effects of the HIR on virus assembly and release. Therefore, we integrated another unspecific host factor, *HF<sub>PP</sub>*, that is involved in virion assembly, maturation, and release into the mathematical model with a cell line-specific basal host factor production and a cell line specific virus assembly and release rate. Fitting of this extended model resulted in a higher production rate of this assembly/release host factor in Huh7 cells, explaining the higher viral steady state level in these cells. Several host factors affecting DV assembly / release are known; we recently employed siRNA screening to identify such factors and described a mechanisms involving Fibroblast Growth Factor Receptor 4 (FGFR4), a host factor supporting DV RNA replication when FGFR4 concentration is high, but leading to increased assembly and maturation of virus particles when this host factor is depleted (Cortese et al., 2019). While FGFR4 is one potential mechanism, the exact identity and mechanisms of host factors differences between A459 and Huh7 based cell lines needs more exploration in the future.

### DV and the HIR

We next employed our mathematical model to characterize the interplay between virus replication on the one hand and the HIR on the other. During DV infection, activation of the interferon system leads to the transcription of hundreds of antiviral ISG proteins at different time points, with effects on multiple steps in



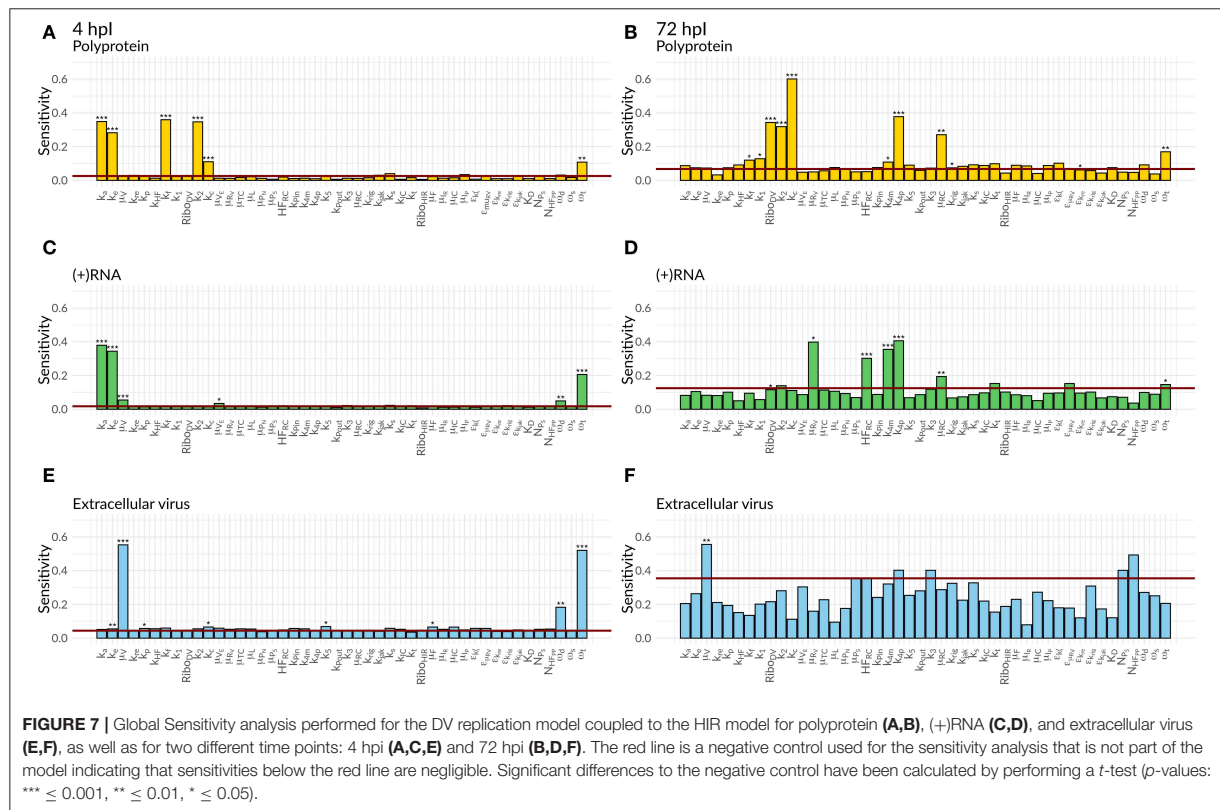
the viral lifecycle. In case of HCV, which is closely related to DV and one of the best studied (+)RNA viruses, ISG proteins have been identified to act on almost every step in the HCV replication cycle (Schoggins and Rice, 2011; Metz et al., 2013; Gokhale et al., 2014). Integrating such a multitude of mechanisms into a mathematical model is therefore a daunting task. To keep things simple, we tested different potential antiviral ISG mechanisms individually by including them into our mathematical model and retained the combination of mechanisms leading to the lowest AIC values in model comparison. As we assumed that the intracellular RC protects the newly synthesized viral RNA from detection by and effector mechanisms of the HIR, we did not include any ISG effects on species inside of the RC in our model (Welsch et al., 2009; Belov and van Kuppeveld, 2012; Romero-Brey et al., 2012; Cortese et al., 2017).

According to our single effect models, ISGs inhibiting RNA translation initiation and/or promoting the cytoplasmic RNA degradation led to best fits of the experimental data. However, this model resulted in a 98,600% increase in the degradation rate constant with  $\widehat{\mu_{RV}} = 987 h^{-1}$ , corresponding to an unrealistic RNA half-life of  $t_{1/2} \approx 2$  sec. A model including only IFN dependent inhibition of the reinfection of naïve cells (promoting

an antiviral state in susceptible cells) was not able to reproduce the experimental data.

A combination of mechanisms based on model selection criteria described above resulted in a model including ISG effects on (1) translation initiation, (2) cytosolic RNA degradation, and (3) new infection of naïve cells. In this model, DV RNA degradation was increased by 59%, resulting in a degradation rate and half-life of  $\widehat{\mu_{RV}} = 4.4 h^{-1}$  and  $t_{1/2} = 9$  min, respectively. Concerning the reinfection of naïve cells, we observed an inhibition of about 2%, which was rather negligible. Since cells were infected with a high MOI in our experiments, i.e., virtually every cell is infected, viral spread and infection of naïve cells play only a minor role in our experimental data.

While DV is subject to ISG effects, it has also developed several strategies to evade the antiviral HIR by antagonizing and inhibiting the induction of the HIR and the antiviral state induced by it. Several DV NS proteins have been described as highly potent inhibitors of IFN signaling and production. For example, DV NS4B protein has been shown to inhibit STAT1 phosphorylation (Munoz-Jordan et al., 2003), while the DV NS5 protein is well-known to degrade STAT2 and thus result in an inhibition of type I IFN signaling (Ashour et al.,



2009). According to our model simulations, during the course of infection, DV inhibits both phases of the HIR, the RLR-mediated induction of IFN by ~94%, as well as IFN signaling through the JAK/STAT signaling pathway by ~ 89%. However, in our model sensitivity analysis at 72 hpi, we found that inhibition of the JAK/STAT signaling pathway may be the more important viral defense mechanism: Increasing the efficiency of the JAK/STAT signaling pathway in a sensitivity analysis did not lead to viral eradication, but still resulted in ongoing viral replication with a constant viral RNA concentration of 73%, indicating that DV efficiently counteracts activation of this pathway. In fact, DV's ability to efficiently counteract the JAK/STAT pathway has been confirmed experimentally (Muñoz-Jordán and Fredericksen, 2010). In contrast, we found that increasing the efficiency of DV recognition by the RIG-I pathway led to viral replication at a significantly lower level of only 11% remaining DV RNA. DV's ability to target the JAK/STAT pathway and thus prevent the establishing of an antiviral cellular state mediated by IFN therefore is an efficient and important viral survival mechanism.

### Comparison to HCV

DV and HCV are both (+)RNA viruses of the family *Flaviviridae* and share key features in their lifecycles, but there are striking differences in their clinical manifestation. While a primary

dengue infection is acute and occasionally associated with severe complications (DHF, DSS) but does not lead to chronic infection, the rather asymptomatic acute hepatitis C infection may develop into lifelong chronic hepatitis C with life threatening secondary manifestations, such as liver cirrhosis or hepatocellular carcinoma without successful treatment.

Comparing the dynamics of our DV model with our previous HCV model (Binder et al., 2013), we observed that the overall dynamics of luciferase and total (+)RNA in DV is comparable with the HCV dynamics with a highly dynamic initial phase that results in steady states for all the measured species. Most estimated model parameters involved in DV replication showed higher rate constants in DV compared to HCV (Table 2). Considering that DV is causing an acute infection, the faster DV replication seems reasonable, while HCV that may develop into chronicity is in comparison rather slow in its lifecycle.

### Hypothetical Drug Therapy Against DENV

The recent Zika outbreak in Brazil showed the potential health risks of (re-)emerging viruses. Therefore, a comprehensive understanding of the virus-host interaction is necessary in order to suggest antiviral treatment strategies. According to our global sensitivity analysis and simulated antiviral interventions, the most effective drug targets in the DV lifecycle are processes associated with viral entry, translation, and DV RNA synthesis.



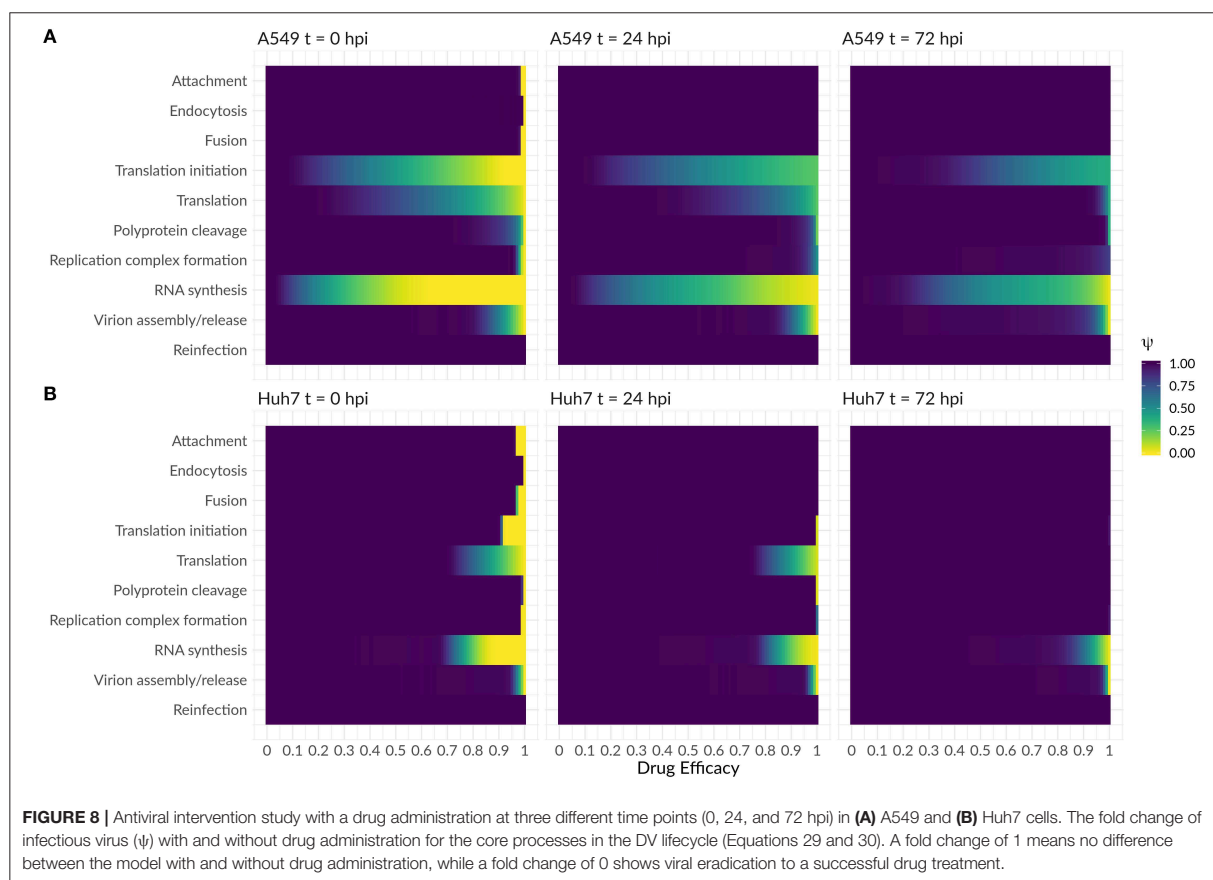


**TABLE 2** | Comparison of DV and HCV model parameters.

Description	Parameter	DV	HCV
Translation initiation complex formation	$k_1$	$1,000 \text{ ml molecules}^{-1} \text{ h}^{-1}$	$1 \text{ molecules}^{-1} \text{ h}^{-1} *$
RC formation	$k_{Pin}$	$0.012 \text{ ml}^2 \text{ molecules}^{-2} \text{ h}^{-1}$	$9.04e-6 \text{ molecules}^{-2} \text{ h}^{-1} *$
RNA export	$k_{Pout}$	$1,000 \text{ h}^{-1}$	$0.307 \text{ h}^{-1} *$
Further replication within RC	$k_3$	$510 \text{ ml molecules}^{-1} \text{ h}^{-1}$	$10^{-4} \text{ molecules}^{-1} \text{ h}^{-1} *$
Replication intermediate complex formation	$k_5$	$1,000 \text{ ml molecules}^{-1} \text{ h}^{-1}$	$10 \text{ molecules}^{-1} \text{ h}^{-1} *$
Initial host factor concentration involved in RC formation	$HF_{RC}$	$1 \text{ to } 4.5 \text{ molecules ml}^{-1}$	$4 \text{ to } 48 \text{ molecules} *$
Initial ribosome concentration	$Ribo$	$2.8 \text{ molecules ml}^{-1}$	$628 \text{ molecules} *$
Viral RNA degradation rate	$\mu_{RV}$	$2.8 \text{ h}^{-1}$	$0.363 \text{ h}^{-1}$
Viral protein degradation rate	$\mu_P$	$0.001 \text{ to } 0.0025 \text{ h}^{-1}$	$0.06 \text{ h}^{-1}$

\*Parameter values for HCV have been taken from Binder et al. (2013).

However, a drug administration earlier than 24 hpi is highly unrealistic, since dengue symptoms usually start 4 to 7 days following a mosquito bite and last for 3 to 10 days (CDC, 2014). However, targeting viral entry is suggested to prevent viral spread. Later in infection, processes associated with DV RNA synthesis and virus assembly and release still represented the most promising drug targets. The antiviral effect on post-translational and early RNA synthesis proposed by our antiviral

drug intervention study might be achievable by drugs like Bromocriptine, which has shown antiviral effects against all DV-Serotypes (Kato et al., 2016). In combination with inhibitors of the DV RNA-dependent RNA polymerase, effective antiviral treatment strategies may be possible. Since all processes in the DV lifecycle depend on host factors, a future antiviral therapy may focus on host factor-targeting with the development of pan-serotype or even pan-viral antiviral drugs. As an example,

the global sensitivity analysis of our model showed a high impact of the host factors involved in RC formation on DV RNA and assembly/release. To this end, the inclusion of further host factors in viral replication models might be an important challenge for future, *in-silico* based design of anti-DV treatment strategies.

### Limitations and Outlook

In the current study, we developed the first detailed mathematical model of the intracellular DV lifecycle, coupling viral entry, protein translation, RNA replication and assembly and release with a model of the host cell immune response to infection. It has been shown in literature that stochastic effects play an important role in the activation of the IIR and individual cells in a population respond differently (Rand et al., 2012). Schmid et al. (2015) have shown that on a single cell level the IFN response to DV is stochastic and leaky with a fraction of remaining unprotected cells, in which DV replication is ongoing, emphasizing the complex nature of the IIR and virus-host interactions (Schmid et al., 2015). However, we here studied intracellular processes following DV infection in a single, “average” cell, and thus we do not take into account inter-cell differences. Since cells were infected with a high MOI, where virtually every cell is infected, viral spread is negligible and therefore, the impact of IFN released from infected cells to render non-infected, IFN-exposed cells non-permissive to DV infection is not relevant in our experimental data. We furthermore neglected cell proliferation in our model, which would require a multi-scale model combining effects at the cell population scale with a detailed intracellular model. Overall, we model an average response of an infected cell in order to study the DV lifecycle in absence and presence of the HIR, identifying HIR modes of action and sensitive processes, which might represent suitable targets for antiviral treatment.

In order to keep the HIR sub-model tractable, we simplified the activation of the HIR and took only key players of the HIR into account. Here, we model the recognition of dsRNA that is present in the cytoplasm, assuming that the replication vesicles represent a protective environment in which no RNA recognition occurs. We thus assume that DV replication intermediates are subject of detection, either when leaked into the cytosol through the replication vesicle pore or by replication vesicle decay. However, other cytosolic DV RNA species might be

recognized as well, such as highly structured RNA regions in the single-stranded genome.

Furthermore, following the HIR activation, we subsume the different ISG proteins by a single species. This is a simplification that we make to keep the model simple. It is known that different ISGs are active at different time points (Metz et al., 2012), even after uniform IFN treatment (Schmid et al., 2015), hence, we here model an “average” effect. However, with our coupled model, we set the basis to study the DV-host interaction. Modeling the IIR in detail, possibly even coupling it to the adaptive immune response is needed in order to better understand and prevent severe dengue complications and to evaluate treatment strategies that suppress high-level viremia.

### DATA AVAILABILITY STATEMENT

The datasets generated for this study are available on request to the corresponding author.

### AUTHOR CONTRIBUTIONS

LK, MB, and RB contributed conception and design of the study. BS and AR performed experiments. CZ and LK developed the model. CZ implemented and analyzed the model and data and wrote the first draft of the manuscript. CZ, AR, MB, RB, and LK wrote sections of the manuscript. All authors contributed to manuscript revision, read, and approved the submitted version.

### FUNDING

LK, CZ, MB, and RB received funding from the German BMBF, grant numbers 031A602A, B and C (EraSysApp/SysVirDrug). LK acknowledges funding from the BMBF, grant number 031L0032 (LiSyM). Parts of this work were done under the auspices of the U.S. Department of Energy under contract 89233218CNA000001 and supported by NIH grant R01-AI078881 awarded to AP.

### SUPPLEMENTARY MATERIAL

The Supplementary Material for this article can be found online at: <https://www.frontiersin.org/articles/10.3389/fmicb.2020.00725/full#supplementary-material>

### REFERENCES

- Ashour, J., Laurent-Rolle, M., Shi, P.-Y., and Garcia-Sastre, A. (2009). NS5 of dengue virus mediates STAT2 binding and degradation. *J. Virol.* 83, 5408–5418. doi: 10.1128/JVI.02188-08
- Aunins, T. R., Marsh, K. A., Subramanya, G., Uprichard, S. L., Perelson, A. S., and Chatterjee, A. (2018). Intracellular hepatitis C modeling predicts infection dynamics and viral protein mechanisms. *J. Virol.* 92:JVI.02098-7. doi: 10.1128/JVI.02098-17
- Bartenschlager, R., and Miller, S. (2008). Molecular aspects of dengue virus replication. *Future Microbiol.* 3, 155–165. doi: 10.2217/17460913.3.2.155
- Belov, G. A., and van Kuppeveld, F. J. (2012). (+)RNA viruses rewire cellular pathways to build replication organelles. *Curr. Opin. Virol.* 2, 740–747. doi: 10.1016/j.coviro.2012.09.006
- Ben-Shachar, R., and Koelle, K. (2014). Minimal within-host dengue models highlight the specific roles of the immune response in primary and secondary dengue infections. *J. R. Soc. Interface* 12:20140886. doi: 10.1098/rsif.2014.0886
- Ben-Shachar, R., Schmidler, S., and Koelle, K. (2016). Drivers of inter-individual variation in dengue viral load dynamics. *PLoS Comput. Biol.* 12:e1005194. doi: 10.1371/journal.pcbi.1005194
- Benzine, T., Brandt, R., Lovell, W. C., Yamane, D., Neddermann, P., De Francesco, R., et al. (2017). NS5A inhibitors unmask differences in functional replicase

- complex half-life between different hepatitis C virus strains. *PLoS Pathog.* 13:e1006343. doi: 10.1371/journal.ppat.1006343
- Bhatt, S., Gething, P. W., Brady, O. J., Messina, J. P., Farlow, A. W., Moyes, C. L., et al. (2013). The global distribution and burden of dengue. *Nature* 496, 504–507. doi: 10.1038/nature12060
- Binder, M., Sulaimanov, N., Clausnitzer, D., Schulze, M., Hüber, C. M. C. M., Lenz, S. M., et al. (2013). Replication vesicles are load- and choke-points in the hepatitis C virus lifecycle. *PLoS Pathog.* 9:e1003561. doi: 10.1371/journal.ppat.1003561
- Bogunovic, D., Boisson-Dupuis, S., and Casanova, J.-L. (2013). ISG15: leading a double life as a secreted molecule. *Exp. Mol. Med.* 45:e18. doi: 10.1038/emmm.2013.36
- Bonhoeffer, S., May, R. M., Shaw, G. M., and Nowak, M. A. (1997). Virus dynamics and drug therapy. *Proc. Natl. Acad. Sci. U.S.A.* 94, 6971–6976. doi: 10.1073/pnas.94.13.6971
- Campbell, L. P., Luther, C., Moo-Llanes, D., Ramsey, J. M., Danis-Lozano, R., and Peterson, A. T. (2015). Climate change influences on global distributions of dengue and chikungunya virus vectors. *Philos. Trans. R. Soc. Lond. B. Biol. Sci.* 370:20140135. doi: 10.1098/rstb.2014.0135
- Castillo Ramirez, J. A., and Urcuqui-Inchima, S. (2015). Dengue virus control of type I IFN responses: a history of manipulation and control. *J. Interf. Cytokine Res.* 35, 421–430. doi: 10.1089/jir.2014.0129
- CDC (2014). *Epidemiology Dengue*. CDC.
- Chazal, M., Beauclair, G., Golé Ne Gracias, S., Rie Najburg, V., Simon-Lorié, E., Dé, F., et al. (2018). RIG-I recognizes the 5' region of dengue and zika virus genomes. *Cell Rep.* 24, 320–328. doi: 10.1016/j.celrep.2018.06.047
- Clapham, H. E., Quyen, T. H., Kien, D. T. H., Dorigatti, I., Simmons, C. P., Ferguson, N. M., et al. (2016). Modelling virus and antibody dynamics during dengue virus infection suggests a role for antibody in virus clearance. *PLoS Comput. Biol.* 12:e1004951. doi: 10.1371/journal.pcbi.1004951
- Clapham, H. E., Tricou, V., Van Vinh Chau, N., Simmons, C. P., and Ferguson, N. M. (2014). Within-host viral dynamics of dengue serotype 1 infection. *J. R. Soc. Interface* 11, 504–507. doi: 10.1098/rsif.2014.0094
- Clausnitzer, D., Harnisch, J., and Kaderali, L. (2015). Multi-scale model for hepatitis C viral load kinetics under treatment with direct acting antivirals. *Virus Res.* 218, 96–101. doi: 10.1016/j.virusres.2015.09.011
- Cortese, M., Goellner, S., Acosta, E. G., Chatel-Chaix, L., Ruggieri, A., and Correspondence, R. B. (2017). Ultrastructural characterization of zika virus replication factories. *Cell Rep.* 18, 2113–2123. doi: 10.1016/j.celrep.2017.02.014
- Cortese, M., Kumar, A., Matula, P., Kaderali, L., Scaturro, P., Erfle, H., et al. (2019). Reciprocal effects of fibroblast growth factor receptor signaling on dengue virus replication and virion production. *Cell Rep.* 27, 2579–2592.e6. doi: 10.1016/j.celrep.2019.04.105
- Dahari, H., Ribeiro, R. M., Rice, C. M., and Perelson, A. S. (2007). Mathematical modeling of subgenomic hepatitis C virus replication in Huh-7 cells. *J. Virol.* 81, 750–760. doi: 10.1128/JVI.01304-06
- Dahari, H., Sainz, B., Perelson, A. S., and Uprichard, S. L. (2009). Modeling subgenomic hepatitis C virus RNA kinetics during treatment with alpha interferon. *J. Virol.* 83, 6383–6390. doi: 10.1128/JVI.02612-08
- Dalrymple, N. A., Cimica, V., and Mackow, E. R. (2015). Dengue virus NS proteins inhibit RIG-I/MAVS signaling by blocking TBK1/IRF3 phosphorylation: dengue virus serotype 1 NS4A is a unique interferon-regulating virulence determinant. *MBio* 6, e00553–e00515. doi: 10.1128/mBio.00553-15
- Diamond, M. S. (2014). IFIT1: a dual sensor and effector molecule that detects non-2'-O methylated viral RNA and inhibits its translation. *Cytokine Growth Factor Rev.* 25, 543–550. doi: 10.1016/j.cytogfr.2014.05.002
- Diamond, M. S., and Pierson, T. C. (2015). Molecular insight into dengue virus pathogenesis and its implications for disease control. *Cell* 162, 488–492. doi: 10.1016/j.cell.2015.07.005
- Flint, S. J., Enquist, L. W., Racaniello, V. R., and Skalka, A. M. (2009). *Principles of Virology*, 3rd Edn. Washington, DC: ASM Press.
- Gokhale, N. S., Vazquez, C., and Horner, S. M. (2014). Hepatitis C virus. *Strategies to evade antiviral responses. Future Virol.* 9, 1061–1075. doi: 10.2217/fvl.14.89
- Guedj, J., Dahari, H., Rong, L., Sansone, N. D., Nettles, R. E., Cotler, S. J., et al. (2013). Modeling shows that the NS5A inhibitor daclatasvir has two modes of action and yields a shorter estimate of the hepatitis C virus half-life. *Proc. Natl. Acad. Sci. U.S.A.* 110, 3991–3996. doi: 10.1073/pnas.1203110110
- Haller, O., Staeheli, P., and Kochs, G. (2007). Interferon-induced Mx proteins in antiviral host defense. *Biochimie* 89, 812–818. doi: 10.1016/j.biochi.2007.04.015
- Heldt, F. S., Frensing, T., Pflugmacher, A., Gröpler, R., Peschel, B., and Reichl, U. (2013). Multiscale modeling of influenza A virus infection supports the development of direct-acting antivirals. *PLoS Comput. Biol.* 9:e1003372. doi: 10.1371/journal.pcbi.1003372
- Heldt, F. S., Frensing, T., and Reichl, U. (2012). Modeling the intracellular dynamics of influenza virus replication to understand the control of viral RNA synthesis. *J. Virol.* 86, 7806–7817. doi: 10.1128/JVI.00080-12
- Ho, D. D., Neumann, A. U., Perelson, A. S., Chen, W., Leonard, J. M., and Markowitz, M. (1995). Rapid turnover of plasma virions and CD4 lymphocytes in HIV-1 infection. *Nature* 373, 123–126. doi: 10.1038/373123a0
- Kato, F., Ishida, Y., Oishi, S., Fujii, N., Watanabe, S., Vasudevan, S. G., et al. (2016). Novel antiviral activity of bromocriptine against dengue virus replication. *Antiviral Res.* 131, 141–147. doi: 10.1016/j.antiviral.2016.04.014
- Kreutz, C., Raue, A., Kaschek, D., and Timmer, J. (2013). Profile likelihood in systems biology. *FEBS J.* 280, 2564–2571. doi: 10.1111/febs.12276
- Kuhn, R. J., Zhang, W., Rossmann, M. G., Pletnev, S. V., Corver, J., Lenches, E., et al. (2002). Structure of dengue virus: implications for flavivirus organization, maturation, and fusion. *Cell* 108, 717–725. doi: 10.1016/S0092-8674(02)00660-8
- Lindenbach BD, Evans MJ, Syder AJ, Wölk B, Tellinghuisen TL, Liu CC, et al. (2005). Complete Replication of Hepatitis C Virus in Cell Culture. *Science*. 309, 623–626. doi: 10.1126/science.1114016
- Laske, T., Heldt, F. S., Hoffmann, H., Frensing, T., and Reichl, U. (2016). Modeling the intracellular replication of influenza A virus in the presence of defective interfering RNAs. *Virus Res.* 213, 90–99. doi: 10.1016/j.virusres.2015.11.016
- Maiwald, T., Hass, H., Steiert, B., Vanlier, J., Engesser, R., Raue, A., et al. (2016). Driving the model to its limit: profile likelihood based model reduction. *PLoS ONE* 11:e0162366. doi: 10.1371/journal.pone.0162366
- Marino, S., Hogue, I. B., Ray, C. J., and Kirschner, D. E. (2008). A methodology for performing global uncertainty and sensitivity analysis in systems biology. *J. Theor. Biol.* 254, 178–196. doi: 10.1016/j.jtbi.2008.04.011
- Martensen, P. M., and Justesen, J. (2004). *Small ISGs coming forward. J. Interferon Cytokine Res.* 24, 1–19. doi: 10.1089/107999004772719864
- Mazzon, M., Jones, M., Davidson, A., Chain, B., and Jacobs, M. (2009). Dengue virus NS5 inhibits interferon- $\alpha$  signaling by blocking signal transducer and activator of transcription 2 phosphorylation. *J. Infect. Dis.* 200, 1261–1270. doi: 10.1086/605847
- Metz, P., Dazert, E., Ruggieri, A., Mazur, J., Kaderali, L., Kaul, A., et al. (2012). Identification of type I and type II interferon-induced effectors controlling hepatitis C virus replication. *Hepatology* 56, 2082–2093. doi: 10.1002/hep.25908
- Metz, P., Reuter, A., Bender, S., and Bartenschlager, R. (2013). Interferon-stimulated genes and their role in controlling hepatitis C virus. *J. Hepatol.* 59, 1331–1341. doi: 10.1016/j.jhep.2013.07.033
- Morrison, J., Aguirre, S., and Fernandez-Sesma, A. (2012). Innate immunity with dengue virus. *Viruses* 4, 397–413. doi: 10.3390/v4030397
- Muñoz-Jordán, J. L., and Fredericksen, B. L. (2010). How flaviviruses activate and suppress the interferon response. *Viruses* 2, 676–691. doi: 10.3390/v2020676
- Munoz-Jordan, J. L., Sanchez-Burgos, G. G., Laurent-Rolle, M., and Garcia-Sastre, A. (2003). Inhibition of interferon signaling by dengue virus. *Proc. Natl. Acad. Sci. U.S.A.* 100, 14333–14338. doi: 10.1073/pnas.2335168100
- Murray, N. E. A., Quam, M. B., and Wilder-Smith, A. (2013). Epidemiology of dengue: past, present and future prospects. *Clin. Epidemiol.* 5, 299–309. doi: 10.2147/CLEP.S34440
- Nasirudeen, A. M. A., Wong, H. H., Thien, P., Xu, S., Lam, K. P., and Liu, D. X. (2011). RIG-I, MDA5 and TLR3 synergistically play an important role in restriction of dengue virus infection. *PLoS Negl. Trop. Dis.* 5:e926. doi: 10.1371/journal.pntd.0000926
- Neufeldt, C. J., Cortese, M., Acosta, E. G., and Bartenschlager, R. (2018). Rewiring cellular networks by members of the flaviviridae family. *Nat. Rev. Microbiol.* 16, 125–142. doi: 10.1038/nrmicro.2017.170
- Neumann, A. U. (1998). Hepatitis C viral dynamics *in vivo* and the antiviral efficacy of interferon-alpha therapy. *Science* 282, 103–107. doi: 10.1126/science.282.5386.103

- Nowak, M. A., and Bangham, C. R. (1996). Population dynamics of immune responses to persistent viruses. *Science* 272, 74–79. doi: 10.1126/science.272.5258.74
- Nowak, M. A., Bonhoeffer, S., Hill, A. M., Boehme, R., Thomas, H. C., and McDade, H. (1996). Viral dynamics in hepatitis B virus infection. *Proc. Natl. Acad. Sci. U.S.A.* 93, 4398–4402. doi: 10.1073/pnas.93.9.4398
- Perelson, A. S. (2002). Modelling viral and immune system dynamics. *Nat. Rev. Immunol.* 2, 28–36. doi: 10.1038/nri700
- Perelson, A. S., Essunger, P., Cao, Y., Vesanen, M., Hurley, A., Saksela, K., et al. (1997). Decay characteristics of HIV-1-infected compartments during combination therapy. *Nature* 387, 188–191. doi: 10.1038/387188a0
- Perelson, A. S., and Guedj, J. (2015). Modelling hepatitis C therapy-predicting effects of treatment. *Nat. Rev. Gastroenterol. Hepatol.* 12, 437–445. doi: 10.1038/nrgastro.2015.97
- Perelson, A. S., Neumann, A. U., Markowitz, M., Leonard, J. M., and Ho, D. D. (1996). HIV-1 dynamics *in vivo*: virion clearance rate, infected cell life-span, and viral generation time. *Science* 271, 1582–1586. doi: 10.1126/science.271.5255.1582
- Perelson, A. S., and Ribeiro, R. M. (2013). Modeling the within-host dynamics of HIV infection. *BMC Biol.* 11:96. doi: 10.1186/1741-7007-11-96
- Perry, S. T., Prestwood, T. R., Lada, S. M., Benedict, C. A., and Shresta, S. (2009). Cardif-mediated signaling controls the initial innate response to dengue virus *in vivo*. *J. Virol.* 83, 8276–8281. doi: 10.1128/JVI.00365-09
- Rand, U., Rinas, M., Schwerk, J., Nöhren, G., Linnes, M., Kröger, A., et al. (2012). Multi-layered stochasticity and paracrine signal propagation shape the type-I interferon response. *Mol. Syst. Biol.* 8:584. doi: 10.1038/msb.2012.17
- Ranjit, S., and Kisson, N. (2011). Dengue hemorrhagic fever and shock syndromes. *Pediatr. Crit. Care Med.* 12, 90–100. doi: 10.1097/PCC.0b013e3181e911a7
- Raue, A., Kreutz, C., Maiwald, T., Bachmann, J., Schilling, M., Klingmüller, U., et al. (2009). Structural and practical identifiability analysis of partially observed dynamical models by exploiting the profile likelihood. *Bioinformatics* 25, 1923–1929. doi: 10.1093/bioinformatics/btp358
- Raue, A., Schilling, M., Bachmann, J., Matteson, A., Schelker, M., Schelke, M., et al. (2013). Lessons learned from quantitative dynamical modeling in systems biology. *PLoS ONE* 8:e74335. doi: 10.1371/annotation/ea0193d8-1f7f-492a-b0b7-d877629fdcee
- Raue, A., Steiert, B., Schelker, M., Kreutz, C., Maiwald, T., Hass, H., et al. (2015). Data2Dynamics: a modeling environment tailored to parameter estimation in dynamical systems. *Bioinformatics* 31, 3558–3560. doi: 10.1093/bioinformatics/btv405
- Rodenhuis-Zybert, I. A., Wilschut, J., and Smit, J. M. (2010). Dengue virus life cycle: viral and host factors modulating infectivity. *Cell. Mol. Life Sci.* 67, 2773–2786. doi: 10.1007/s00018-010-0357-z
- Rodriguez-Fernandez, M., and Banga, J. R. (2010). SensSB: a software toolbox for the development and sensitivity analysis of systems biology models. *Bioinformatics* 26, 1675–1676. doi: 10.1093/bioinformatics/btq242
- Romero-Brey, I., Merz, A., Chiramel, A., Lee, J. Y., Chlanda, P., Haselman, U., et al. (2012). Three-dimensional architecture and biogenesis of membrane structures associated with hepatitis C virus replication. *PLoS Pathog.* 8:e1003056. doi: 10.1371/journal.ppat.1003056
- Rong, L., and Perelson, A. S. (2009). Modeling HIV persistence, the latent reservoir, and viral blips. *J. Theor. Biol.* 260, 308–331. doi: 10.1016/j.jtbi.2009.06.011
- Ronni, T., Melén, K., Malygin, A., and Julkunen, I. (1993). Control of IFN- $\gamma$ -inducible MxA gene expression in human cells. *J. Immunol.* 150, 1715–1726.
- Safran, M., Dalah, I., Alexander, J., Rosen, N., Iny Stein, T., Shmoish, M., et al. (2010). GeneCards version 3: the human gene integrator. *Database* 2010:baq020. doi: 10.1093/database/baq020
- Scaturro, P., Cortese, M., Chatel-Chaix, L., Fischl, W., and Bartenschlager, R. (2015). Dengue virus non-structural protein 1 modulates infectious particle production via interaction with the structural proteins. *PLoS Pathog.* 11:e1005277. doi: 10.1371/journal.ppat.1005277
- Schmid, B., Rinas, M., Ruggieri, A., Acosta, E. G., Bartenschlager, M., Reuter, A., et al. (2015). Live cell analysis and mathematical modeling identify determinants of attenuation of dengue virus 2'-O-methylation mutant. *PLoS Pathog.* 11:e1005345. doi: 10.1371/journal.ppat.1005345
- Schoggins, J. W., and Rice, C. M. (2011). Interferon-stimulated genes and their antiviral effector functions. *Curr. Opin. Virol.* 1, 519–525. doi: 10.1016/j.coviro.2011.10.008
- Screaton, G., Mongkolsapaya, J., Yacoub, S., and Roberts, C. (2015). New insights into the immunopathology and control of dengue virus infection. *Nat. Rev. Immunol.* 15, 745–759. doi: 10.1038/nri3916
- Scutigliani, E. M., and Kikkert, M. (2017). Interaction of the innate immune system with positive-strand RNA virus replication organelles. *Cytokine Growth Factor Rev.* 37, 17–27. doi: 10.1016/j.cytogfr.2017.05.007
- Shresta, S., Kyle, J. L., Snider, H. M., Basavapatna, M., Beatty, P. R., and Harris, E. (2004). Interferon-dependent immunity is essential for resistance to primary dengue virus infection in mice, whereas T- and B-cell-dependent immunity are less critical. *J. Virol.* 78, 2701–2710. doi: 10.1128/JVI.78.6.2701-2710.2004
- Stafford, M. A., Corey, L., Cao, Y., Daar, E. S., Ho, D. D., and Perelson, A. S. (2000). Modeling plasma virus concentration during primary HIV infection. *J. Theor. Biol.* 203, 285–301. doi: 10.1006/jtbi.2000.1076
- Tuiskunen Bäck, A., and Lundkvist, Å. (2013). Dengue viruses – an overview. *Infect. Ecol. Epidemiol.* 3:19839. doi: 10.3402/iee.v3i0.19839
- Wei, X., Ghosh, S. K., Taylor, M. E., Johnson, V. A., Emin, E. A., Deutsch, P., et al. (1995). Viral dynamics in human immunodeficiency virus type 1 infection. *Nature* 373, 117–122. doi: 10.1038/373117a0
- Welsch, S., Miller, S., Romero-Brey, I., Merz, A., Bleck, C. K. E., Walther, P., et al. (2009). Composition and three-dimensional architecture of the dengue virus replication and assembly sites. *Cell Host Microbe* 5, 365–375. doi: 10.1016/j.chom.2009.03.007
- WHO (2012). *Global Strategy for Dengue Prevention and Control 2012–2020*. World Health Organization.
- World Health Organization (2016). *Dengue Vaccine: WHO Position Paper – July 2016*. *Weekly Epidemiological Record (WER)*. World Health Organization, 2016, 349–364.
- Wulff, N. H., Tzatzaris, M., and Young, P. J. (2012). Monte carlo simulation of the spearman-kaerber TCID50. *J. Clin. Bioinformatics* 2:5. doi: 10.1186/2043-9113-2-5
- Xagorari, A., and Chlichlia, K. (2008). Toll-like receptors and viruses: induction of innate antiviral immune responses. *Open Microbiol. J.* 2, 49–59. doi: 10.2174/1874285800802010049
- Zitzmann, C., and Kaderali, L. (2018). Mathematical analysis of viral replication dynamics and antiviral treatment strategies: from basic models to age-based multi-scale modeling. *Front. Microbiol.* 9:1546. doi: 10.3389/fmicb.2018.01546

**Conflict of Interest:** The authors declare that the research was conducted in the absence of any commercial or financial relationships that could be construed as a potential conflict of interest.

Copyright © 2020 Zitzmann, Schmid, Ruggieri, Perelson, Binder, Bartenschlager and Kaderali. This is an open-access article distributed under the terms of the Creative Commons Attribution License (CC BY). The use, distribution or reproduction in other forums is permitted, provided the original author(s) and the copyright owner(s) are credited and that the original publication in this journal is cited, in accordance with accepted academic practice. No use, distribution or reproduction is permitted which does not comply with these terms.

## **Article III: Modeling of hepatitis C replication, exosome secretion and virus release.**

**Carolin Zitzmann**, Lars Kaderali, Alan S Perelson\* (2020) *Modeling of hepatitis C replication, exosome secretion and virus release*. PLoS computational biology 16(11):e1008421

I contributed to data curation, model development, formal analysis, investigation, software, validation, visualization, and writing—original draft, review & editing.

\* Corresponding author

The supplementary material is published and can be found online.

## RESEARCH ARTICLE

# Mathematical modeling of hepatitis C RNA replication, exosome secretion and virus release

Carolin Zitzmann<sup>1,2</sup>, Lars Kaderali<sup>1</sup>, Alan S. Perelson<sup>2\*</sup>

**1** University Medicine Greifswald, Institute of Bioinformatics and Center for Functional Genomics of Microbes, Greifswald, Germany, **2** Theoretical Biology and Biophysics, Los Alamos National Laboratory, Los Alamos, New Mexico, United States of America

\* [asp@lanl.gov](mailto:asp@lanl.gov)



## OPEN ACCESS

**Citation:** Zitzmann C, Kaderali L, Perelson AS (2020) Mathematical modeling of hepatitis C RNA replication, exosome secretion and virus release. *PLoS Comput Biol* 16(11): e1008421. <https://doi.org/10.1371/journal.pcbi.1008421>

**Editor:** Kathryn Miller-Jensen, Yale University, UNITED STATES

**Received:** June 23, 2020

**Accepted:** October 6, 2020

**Published:** November 5, 2020

**Copyright:** This is an open access article, free of all copyright, and may be freely reproduced, distributed, transmitted, modified, built upon, or otherwise used by anyone for any lawful purpose. The work is made available under the [Creative Commons CC0](https://creativecommons.org/licenses/by/4.0/) public domain dedication.

**Data Availability Statement:** All relevant data are within the manuscript and its [Supporting Information](#) files.

**Funding:** Portions of this work were done under the auspices of the U.S. Department of Energy under contract 89233218CNA000001 and was supported by NIH grants R01-OD011095 (ASP), R01-AI028433 (ASP) and R01-AI 078881 (ASP). Parts of this work were supported by the BMBF through the ERASysAPP project SysVirDrug 031A602A (LK). The funders had no role in study

## Abstract

Hepatitis C virus (HCV) causes acute hepatitis C and can lead to life-threatening complications if it becomes chronic. The HCV genome is a single plus strand of RNA. Its intracellular replication is a spatiotemporally coordinated process of RNA translation upon cell infection, RNA synthesis within a replication compartment, and virus particle production. While HCV is mainly transmitted via mature infectious virus particles, it has also been suggested that HCV-infected cells can secrete HCV RNA carrying exosomes that can infect cells in a receptor independent manner. In order to gain insight into these two routes of transmission, we developed a series of intracellular HCV replication models that include HCV RNA secretion and/or virus assembly and release. Fitting our models to *in vitro* data, in which cells were infected with HCV, suggests that initially most secreted HCV RNA derives from intracellular cytosolic plus-strand RNA, but subsequently secreted HCV RNA derives equally from the cytoplasm and the replication compartments. Furthermore, our model fits to the data suggest that the rate of virus assembly and release is limited by host cell resources. Including the effects of direct acting antivirals in our models, we found that in spite of decreasing intracellular HCV RNA and extracellular virus concentration, low level HCV RNA secretion may continue as long as intracellular RNA is available. This may possibly explain the presence of detectable levels of plasma HCV RNA at the end of treatment even in patients that ultimately attain a sustained virologic response.

## Author summary

Approximately 70 million people are chronically infected with hepatitis C virus (HCV), which if left untreated may lead to cirrhosis and liver cancer. However, modern drug therapy is highly effective and hepatitis C is the first chronic virus infection that can be cured with short-term therapy in almost all infected individuals. The within-host transmission of HCV occurs mainly via infectious virus particles, but experimental studies suggest that there may be additional receptor-independent cell-to-cell transmission by exosomes that carry the HCV genome. In order to understand the intracellular HCV lifecycle and HCV

design, data collection and analysis, decision to publish, or preparation of the manuscript.

**Competing interests:** The authors have declared that no competing interests exist.

RNA spread, we developed a series of mathematical models that take both exosomal secretion and viral secretion into account. By fitting these models to *in vitro* data, we found that secretion of both HCV RNA as well as virus probably occurs and that the rate of virus assembly is likely limited by cellular co-factors on which the virus strongly depends for its own replication. Furthermore, our modeling predicted that the parameters governing the processes in the viral lifecycle that are targeted by direct acting antivirals are the most sensitive to perturbations, which may help explain their ability to cure this infection.

## Introduction

Hepatitis C virus (HCV) causes an acute infection that is cleared in some individuals, but which if it becomes chronic can cause liver cirrhosis and hepatocellular carcinoma. Approximately 70 million people worldwide live with chronic hepatitis C, with 400,000 related deaths annually [1]. Hepatitis C can be cured with combinations of direct acting antivirals that inhibit viral replication and which can achieve cure rates above 95% [2]. HCV is a *Hepacivirus* belonging to the family *Flaviviridae* and has a single plus-strand RNA genome. A common feature of all plus-strand RNA viruses including HCV is their ability to rearrange intracellular host membranes to generate so-called replication compartments (RCs) or “replication factories” [3]. In HCV, these RCs derived from the rough endoplasmic reticulum represent a distinct environment for efficient viral genome replication and antiviral immune response protection [4].

Intracellular HCV replication is a controlled spatiotemporal process starting with translation of the viral genome into viral non-structural (NS) and structural proteins, required for HCV genome replication and virus particle formation. The NS proteins form the replicase complex (or replication complex) that is associated with the RC and which is required for viral RNA (vRNA) synthesis. Within the RC the plus-strand RNA genome is replicated into a minus-strand RNA intermediate, which then gives rise to multiple plus-stranded HCV RNA copies. The progeny plus-strand RNA can either undergo another round of RNA synthesis within the RC or be transported out of the RC into the cytoplasm to be translated in order to produce more viral proteins, or together with structural proteins be packaged into virus particles that are secreted from the host cell [4,5].

HCV particle production occurs in association with cytoplasmic lipid droplets (cLDs) that are in close proximity to the endoplasmic reticulum and thus to the RCs. Viral structural proteins and host cellular co-factors are recruited to the cLDs and form together with the viral plus-strand RNA genome virus particles that mature and are released from the cell [3,6]. Due to their limited genome size, viruses depend strongly on cellular co-factors for their own replication. Those host factors are hijacked by the virus and are involved in almost all steps of the viral lifecycle and represent potential drug targets [7,8].

Releasing HCV as enveloped and matured infectious virus particles does not represent the only strategy for viral spread. An infected cell can also secrete vRNA containing exosomes, i.e., small extracellular vesicles [9]. Exosomes are produced from nearly all cell-types with the function of cell-to-cell communication by transferring cellular components, RNAs, and proteins [10]. HCV RNA exosomes and infectious HCV virions are comparable in size (~100 nm for HCV RNA exosomes and 35–100 nm for HCV virions) and density (~1.08 g/ml for HCV RNA exosomes and ~1.10–1.14 g/ml for HCV virions) which makes separation of the particle types difficult [11–13].

Longatti et al. [13] suggest exosomal transfer is a means of HCV transmission between hepatocytes, albeit one that may be less efficient than transmission by true viral particles.

These authors showed virion-independent transfer of replication competent HCV RNA in exosomes *in vitro* using an HCV subgenomic replicon lacking viral structural genes including that coding for envelope protein, which suggests that transfer was cell-to-cell. The transfer appeared to require cell-cell contact since coculture experiments done in Transwell plates did not lead to exosomal HCV RNA transfer. Further, concentrated exosomes were not able to directly infect target cells, suggesting that infection by free exosomes is very inefficient compared to infection by authentic viral particles [13]. In comparing the models developed below with data we assume that infectious virus titers measured as focus-forming units is due only to extracellular infectious virions and not exosomes.

In HCV-positive patients and in infected cell cultures, extracellular HCV RNA exosomes have been found in blood plasma and supernatant, respectively [12,14]. These HCV RNA genome carrying exosomes have been shown to generate a “normal” viral HCV infection in HCV-naïve cells by a receptor-independent transmission mechanism [15], although this result remains controversial. Liu et al. [16] found in HCV-positive patient plasma a 3 to 20-fold higher HCV RNA concentration in exosomes compared to exosome-free HCV particles and strongly suggested that HCV infection and transmission occurs as an exosome-associated process. Exosome-associated HCV RNA was found to be infectious and resistant to neutralizing anti-HCV antibodies [16,17]. Furthermore, HCV exosomes carry Ago2, miR-122, and HSP90 proteins that potentially enhance viral replication, as blocking Ago2 or miR-122 leads to suppression of exosomal cell-to-cell transmission [15]. Additionally, HCV exosomes carrying Ago2 and miR-122 trigger macrophage differentiation, which increase inflammation by releasing pro-inflammatory cytokines and collagen, and thereby promotes fibrosis [18,19].

Mathematical modeling of virus-host interactions has proven to be a powerful tool to study viral pathogenesis and transmission as well as antiviral treatment strategies [20–29]. Here we used a previously published intracellular HCV replication model [30] in order to study HCV RNA secretion routes. In that model by Quintela et al. [30] a viral assembly compartment was absent and HCV secretion was modeled simply as a process that leads to loss of intracellular HCV RNA but whether the loss was via exosomes or virus particle production was not specified. Further, the model assumed that HCV RNA secretion occurred from the site of HCV RNA translation, i.e. the cytoplasm, as well as the site of HCV RNA replication. Here we first examine models in which secretion is from the site of translation, the site of replication or as in the Quintela et al. model from both. We then extend this model and make it more biologically realistic by including a separate virion assembly compartment. We fit the set of models we develop to *in vitro* experiments and show that both exosomal secretion and viral production appear to play a role in HCV RNA release from infected cells. Further, the best model fits to the *in vitro* data are obtained when virus assembly/release is limited by host cell resources.

## Methods

### Intracellular HCV replication and HCV RNA secretion models (SM models)

The intracellular HCV replication model of [30] contains four different HCV RNA species: plus-strand HCV RNA used for translation ( $T$ ), plus-strand HCV RNA in the RC ( $R$ ) used for replication, minus-strand HCV RNA ( $C$ ) in the RC, which may be in the form of replication complexes, used for replication, and secreted HCV RNA ( $S$ ) (Fig 1A). Here the secretion of intracellular RNA can be due to the RNA being in either exosomes or viral particles or both. We will simply refer to this as secretion of RNA containing particles. The plus-strand RNA in the cytoplasm that can be used for translation,  $T$ , may be transferred into the RC at rate  $\sigma$ . This plus-strand RNA in the RC,  $R$ , can now be used for the synthesis of minus-strand RNA



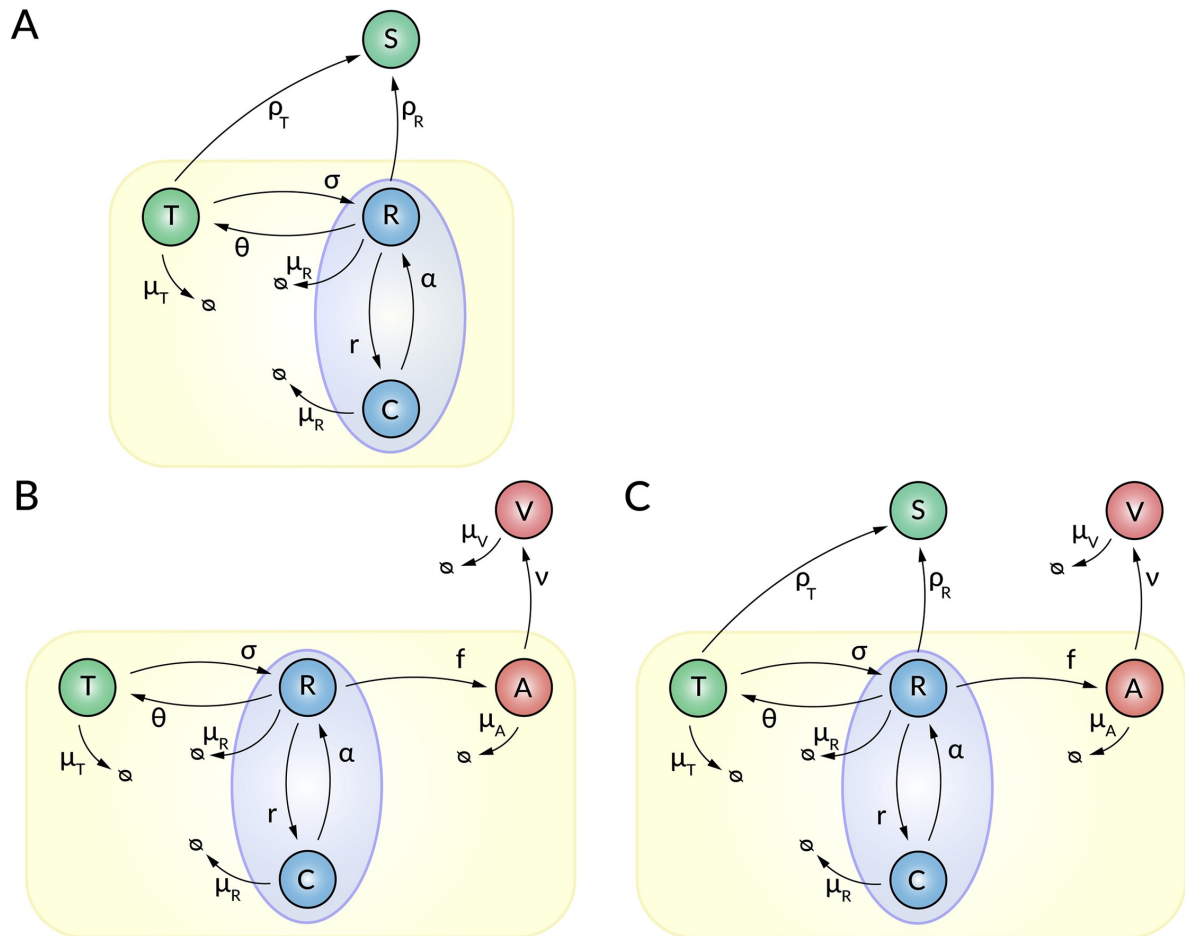


**Fig 1. Schematic illustration of the intracellular HCV replication models.** (A) The hepatitis C RNA secretion model (SM), (B) the replication model extended by virus assembly and release without considering RNA secretion (AM), and (C) the combined model (CM) accounting for secretion and virus release. Intracellular HCV replication is initiated by plus-strand RNA that is translated (T) and transferred into the replication compartment (RC) at rate  $\sigma$ . Within the RC, the plus-strand RNA (R) is used to synthesize minus-strand RNA (C) at maximum rate  $r$ , which in turn is used for plus-strand RNA synthesis at rate  $\alpha$ . Plus-strand RNA located at the site of translation (T) and/or in proximity to the RC (R) may be secreted as HCV RNA containing particles (S) at rate  $\rho_T$  and/or  $\rho_R$ , respectively. Newly synthesized plus-strand RNA (R) may be transferred to sites of viral assembly (A) at rate  $f$ . HCV particles (V) are released from the cell at rate  $v$  and degrade with rate  $\mu_V$ . Intracellular RNA in the cytoplasm (T) degrades with rate  $\mu_T$ , while RNA species (R and C) within the RC degrade with rate  $\mu_R$ .

<https://doi.org/10.1371/journal.pcbi.1008421.g001>

containing replication complexes, C, which in turn can produce more plus-strand RNA, R, at rate  $\alpha$ . As in prior models [30,31], due to limited availability of host factors, the minus-strand RNA synthesis follows a logistic growth law, with maximum rate  $r$ , which slows as the number of negative strands approaches the RCs carrying capacity  $C_{max}$ . Newly synthesized plus-strand RNA, R, is transferred back to the site of vRNA translation at rate  $\theta$  in order to produce more viral proteins. The HCV RNA species located at the site of translation degrade with rate  $\mu_T$ . As in Quintela et al. [30], we assume that the HCV RNA species within the RC (R and C) degrade with the same rate  $\mu_R$ .

Since the secretion route of HCV RNA-containing particles is unknown, we include different pathways in our model: (1) secretion of particles at the site of RNA translation that contain the HCV RNA species,  $T$ , at rate  $\rho_T(t)$  (2) the secretion of particles containing newly synthesized HCV RNA in proximity to the RCs,  $R$ , at rate  $\rho_R(t)$  and (3) both secretion routes (1) and (2). The mathematical model is described by the following ordinary differential equations (ODEs):

$$\begin{aligned}\frac{d}{dt}T &= \theta R - (\sigma + \rho_T(t) + \mu_T)T, \\ \frac{d}{dt}R &= \alpha C + \sigma T - (\theta + \rho_R(t) + \mu_R)R, \\ \frac{d}{dt}C &= r\left(1 - \frac{C}{C_{max}}\right)R - \mu_R C, \\ \frac{d}{dt}S &= \rho_T(t)T + \rho_R(t)R,\end{aligned}\tag{1}$$

with initial conditions reflective of an *in vitro* transfection experiment or high MOI infection experiment in which an average of  $T_0$  positive HCV RNAs are delivered to a cell's cytoplasm to initiate an infection, i.e.  $T(0) = T_0$ ,  $R(0) = 0$ ,  $C(0) = 0$ , and  $S(0) = 0$ . Secretion Model T ( $SM_T$ ) refers to the secretion route with  $\rho_T(t) \neq 0$  and  $\rho_R(t) = 0$ , Secretion Model R ( $SM_R$ ) accounts for the secretion route with  $\rho_T(t) = 0$  and  $\rho_R(t) \neq 0$ , while Secretion Model TR ( $SM_{TR}$ ) combines both secretion routes with  $\rho_T(t) \neq 0$  and  $\rho_R(t) \neq 0$ .

In the Quintela et al. [30] model, the secretion of RNA does not begin the instant a cell is infected, but rather it is delayed and then the secretion rate smoothly increases, i.e. ramps up, according to the following function:

$$\rho_i(t) = \begin{cases} 0, & t < \tau_\rho \\ (1 - e^{-k_\rho(t-\tau_\rho)})\rho_i, & \text{otherwise} \end{cases}\tag{2}$$

with  $\rho_i(t) \in \{\rho_T(t), \rho_R(t)\}$ . We refer to the secretion models that use this delayed ramp-up function as type 1 models and denote them  $SM_{T1}$ ,  $SM_{R1}$ , and  $SM_{TR1}$ . Additionally, we studied the  $SM_{TR1}$  model with equal maximal HCV RNA secretion rates, i.e.  $\rho_T = \rho_R$ , and secretion delays  $\tau_T = \tau_R$  ( $SM_{T1=R1}$ ), and a version with individual secretion rates, i.e.  $\rho_T \neq \rho_R$  and  $\tau_T \neq \tau_R$  ( $SM_{T1 \neq R1}$ ).

In addition to this function, we also tested secretion models  $SM_T$ ,  $SM_R$ , and  $SM_{TR}$  that use a simple step-function time delay

$$\rho_i(t) = \begin{cases} 0, & t < \tau_\rho \\ \rho_i, & \text{otherwise} \end{cases}\tag{3}$$

rather than the delay given by Eq (2) and refer to those models as type 2 models and denote them  $SM_{T2}$ ,  $SM_{R2}$ ,  $SM_{T2=R2}$ , and  $SM_{T2 \neq R2}$ , respectively.

Lastly, we explored the possibility that vRNA secretion might be limited by host cellular resources. Thus, we also studied a time delayed release function that after the delay decreases exponentially over time due to host factor limitation

$$\rho_i(t) = \begin{cases} 0, & t < \tau_\rho \\ (e^{-k_\rho(t-\tau_\rho)})\rho_i, & \text{otherwise} \end{cases}\tag{4}$$

and refer to those models using this function as type 3 models and denote them  $SM_{T3}$ ,  $SM_{R3}$ ,  $SM_{T3=R3}$ , and  $SM_{T3 \neq R3}$ , (Table 1). Other decreasing functions could also be used but in this initial exploration of the effect of host factor limitation we restrict our analysis to this simple function.

**Table 1. Secretion model variants.** Overview of the different vRNA secretion models (SM) with different secretion routes and time delay functions.

Model	Secretion Route	Time delay function
SM <sub>T1</sub>	Secretion from the site of translation (T) $\rho_T(t)$	Delay then ramp-up (Eq 2)
SM <sub>T2</sub>		Simple delay (Eq 3)
SM <sub>T3</sub>		Delayed exponential decrease (Eq 4)
SM <sub>R1</sub>	Secretion from the RC (R) $\rho_R(t)$	Delay then ramp-up (Eq 2)
SM <sub>R2</sub>		Simple delay (Eq 3)
SM <sub>R3</sub>		Delayed exponential decrease (Eq 4)
SM <sub>T1=R1</sub>	Equal secretion from sites T and R $\rho_T(t) = \rho_R(t)$ and $\tau_T = \tau_R$	Delay then ramp-up (Eq 2)
SM <sub>T2=R2</sub>		Simple delay (Eq 3)
SM <sub>T3=R3</sub>		Delayed exponential decrease (Eq 4)
SM <sub>T1≠R1</sub>	Individual secretion from sites T and R $\rho_T(t) \neq \rho_R(t)$ and $\tau_T \neq \tau_R$	Delay then ramp-up (Eq 2)
SM <sub>T2≠R2</sub>		Simple delay (Eq 3)
SM <sub>T3≠R3</sub>		Delayed exponential decrease (Eq 4)

<https://doi.org/10.1371/journal.pcbi.1008421.t001>

### Intracellular HCV replication and virus assembly/release model (AM models)

In order to study HCV RNA secretion in exosomes as distinct from that in virions, we extended the Quintela et al. model (Eq 1) by including an explicit compartment in which the assembly and release of virus occurs in a manner inspired by Benzine et al. [31]. In this model, newly synthesized plus-strand RNA within the RC, R, is transferred to sites of virus assembly that are associated with cLDs and assembled at rate  $f(t)$  into intracellular virions, A, which are released from the cell and become extracellular virions, V, at rate  $v$  (Fig 1B). Extracellular virus is lost at per capita rate  $\mu_V$ , which in an *in vitro* system is due to degradation or replacement of the culture medium. The intracellular HCV replication model extended by virus assembly and release is given by the following ODEs (extensions in bold):

$$\begin{aligned}
 \frac{d}{dt}T &= \theta R - (\sigma + \mu_T)T, \\
 \frac{d}{dt}R &= \alpha C + \sigma T - (\theta + \mu_R)R - \mathbf{f(t)R}, \\
 \frac{d}{dt}C &= r \left(1 - \frac{C}{C_{max}}\right)R - \mu_R C, \\
 \frac{d}{dt}\mathbf{A} &= \mathbf{f(t)R} - vA, \\
 \frac{d}{dt}V &= vA - \mu_V V.
 \end{aligned}
 \tag{5}$$

with  $T(0) = T_0$ ,  $R(0) = 0$ ,  $C(0) = 0$ ,  $S(0) = 0$ ,  $A(0) = 0$ , and  $V(0) = 0$ .

Virus assembly is limited by the availability of structural and non-structural proteins necessary to form the virion as well as the host cell resources involved in virus assembly. Due to these considerations we tested different models for the rate of HCV RNA transport to the assembly site and virion assembly,  $f(t)$ . First, a constant rate, i.e.,  $f(t) = f = const$ . Second, a simple time delayed virus assembly rate

$$f(t) = \begin{cases} 0, & t < \tau_f \\ f, & \text{otherwise} \end{cases}
 \tag{6}$$

Third, a time-delayed viral assembly rate similar to Eq (2), assuming that after a fixed delay the

viral assembly rate increases smoothly until reaching a maximum

$$f(t) = \begin{cases} 0, & t < \tau_f \\ (1 - e^{-k_f(t-\tau_f)})f, & \text{otherwise} \end{cases} \quad (7)$$

In analogy with Eq (2), we will call this a delayed ramp-up function.

Fourth, a time-delayed virus assembly rate that then decreases over time due to a limitation or restriction of viral or host cell resources

$$f(t) = \begin{cases} 0, & t < \tau_f \\ e^{-k_f(t-\tau_f)}f, & \text{otherwise} \end{cases} \quad (8)$$

The various choices for  $f(t)$  that we explore are listed in Table 2.

### The combined intracellular HCV replication, exosome secretion and virus release model (CM Model)

In order to develop a combined intracellular HCV model, we combined the HCV replication model with the HCV RNA secretion and viral assembly and release models (Fig 1C). This changed the ODEs of Eq (5) to the following with the added exosomal secretion terms indicated in bold:

$$\begin{aligned} \frac{d}{dt}T &= \theta R - (\sigma + \rho_T(t) + \mu_T)T, \\ \frac{d}{dt}R &= \alpha C + \sigma T - (\theta + \rho_R(t) + \mu_R)R - f(t)R, \\ \frac{d}{dt}C &= r \left(1 - \frac{C}{C_{max}}\right)R - \mu_C C, \\ \frac{d}{dt}S &= \rho_T(t)T + \rho_R(t)R, \\ \frac{d}{dt}A &= f(t)R - \nu A \\ \frac{d}{dt}V &= \nu A - \mu_V V. \end{aligned} \quad (9)$$

In summary, we study three main models: (A) the HCV RNA secretion model (SM model), (B) the HCV assembly/release model (AM model) and (C) the combination of both, i.e. a combined model (CM model). All models have several sub-models that differ in their time delay functions for HCV RNA secretion ( $\rho_i(t)$ ) and virus assembly ( $f(t)$ ).

### Fitting the models to data

In order to fit these models to data, global optimization was performed using the Data2Dynamics environment [32] for Matlab 2016b. Parameters were estimated by minimizing the

**Table 2. Assembly model variants.** Overview of the different virion assembly models (AM).

Model	Virus assembly $f(t)$
AM <sub>1</sub>	Constant
AM <sub>2</sub>	Simple delay (Eq 6)
AM <sub>3</sub>	Delay then ramp-up (Eq 7)
AM <sub>4</sub>	Delayed exponential decrease (Eq 8)

<https://doi.org/10.1371/journal.pcbi.1008421.t002>

negative of the log likelihood function with the deterministic optimization algorithm *lsqnonlin* and a *Latin hypercube sampling* procedure for generating initial parameter guesses [33]. Uncertainty analysis and the calculation of 95% confidence intervals were performed using the profile likelihood estimation (PLE) routine in Data2Dynamics [32,34].

The models were calibrated using *in vitro* data extracted from Keum et al. [35] using the tool *WebPlotDigitizer* [36]. Here, we focused on measurements of intracellular HCV plus-strand RNA, intracellular minus-strand RNA, secreted HCV RNA, intracellular cell-associated HCV infectious virus, and released infectious HCV particles [35]. In the Keum et al. experiments, Huh7.5.1 cells were infected with a high multiplicity of infection (MOI = 5) leading to a one-step growth curve where theoretically 99.3% of the cells were infected with at least one HCV particle.

The SM models were fitted to the Keum et al. [35] data shown in their Figs 1A–1C and 2A, where (+)RNA = T+R, (-)RNA = C, and secreted RNA = S. The models extended by the viral particle production (AM and CM models) have also been fitted to the cell-associated infectious (intracellular) virus and the extracellular infectious virus data, *inV* and *exV*, respectively, where  $inV = A * f_{inf}$  and  $exV = V * f_{inf}$  and  $f_{inf}$  is the fraction of virus that is infectious and assumed to be the same for intracellular and extracellular virus. Intracellular and extracellular infectious virus measurements were made from the cells and culture media collected from each cell culture well and expressed as focus forming units per well in Fig 2A of Keum et al.

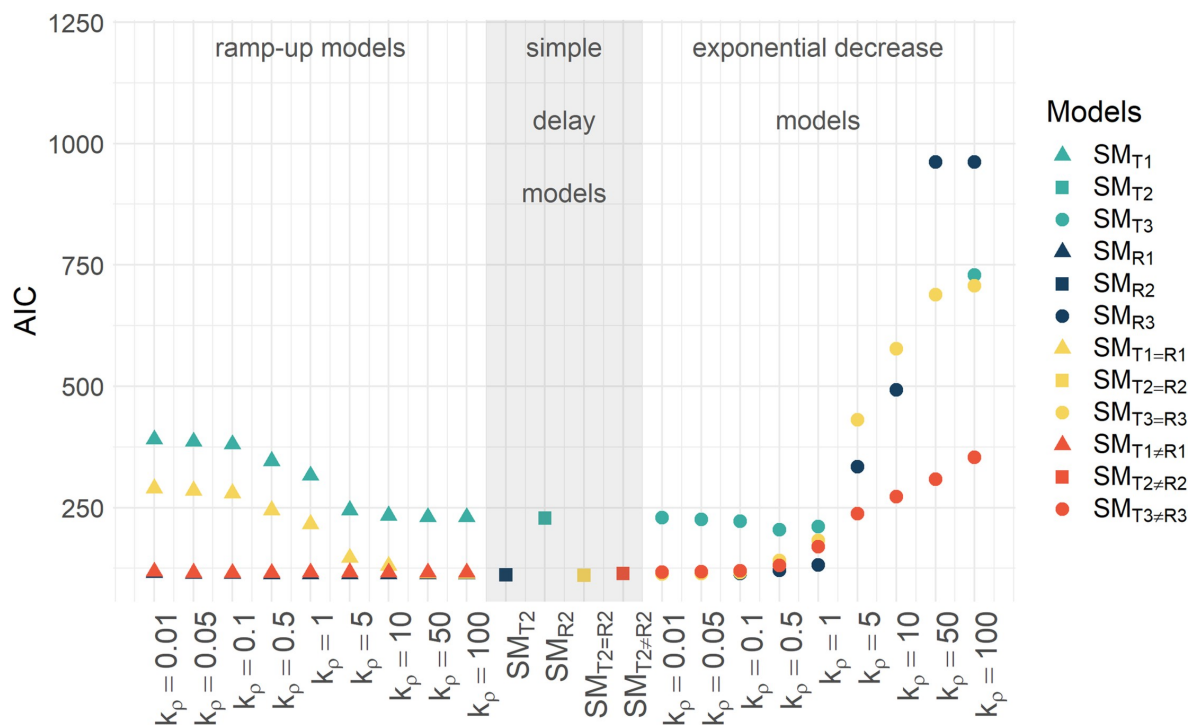


**Fig 2. AICs of the HCV RNA secretion models.** Best-fit model AICs of the HCV RNA secretion models (Eqs 1 to 4) when the parameter  $k_p$  determining the rate of ramp-up or limitation was varied (see S1 Data). [▲ = ramp-up models, ■ = simple delay models, ● = exponential decrease models; green = secretion exclusively from site of translation, blue = secretion exclusively from RC, yellow = equal secretion from site of translation and RC ( $\rho_T = \rho_R$  and  $\tau_T = \tau_R$ ), red = individual secretion from site of translation and RC ( $\rho_T \neq \rho_R$  and  $\tau_T \neq \tau_R$ )].

<https://doi.org/10.1371/journal.pcbi.1008421.g002>

[35]. We divided these measurements by the number of cells per well at each time point given in Fig 2D of Keum et al. [35] in order to change units from focus forming units (FFU) per well to infectious virus particles per cell and infectious particles released per cell. The model combining virus assembly/release and HCV RNA secretion was fitted to the entire data set where secreted  $RNA = S+V$  with  $S = T+R$ . Thus, in the combined model (CM) secreted RNA comprises HCV RNA secreted from the site of translation, from the RC, and extracellular virus, while intracellular and extracellular infectious virus are  $inV = A^*f_{inf}$  and  $exV = V^*f_{inf}$ . Model selection theory [37,38] based on comparing Akaike Information Criterion (AIC) values was used to find the preferred model.

A global parameter sensitivity analysis and the calculation of the first- and total-order sensitivity index was performed using the extended Fourier Amplitude Sensitivity Test (eFAST) package for Matlab 2016b [39]. In brief, the first-order total sensitivity index calculates the sensitivity of a given model parameter  $x_i$  on the model output. The total-order sensitivity index is the sum of the first-order sensitivity of a given parameter  $x_i$  and the summed sensitivities of the remaining model parameters  $\bar{x}_i$ . The advantage of calculating the total-order sensitivity is that information about parameter interactions are considered, which are not considered by calculating only the first-order sensitivities. Additionally, a dummy parameter has been introduced into the global sensitivity analysis that has no impact on the model output. Hence, model parameters are considered as sensitive, if their total-order sensitivity indices are larger than the total-sensitivity index of this so-called negative control that is ideally zero. For more information see [39].

## Results

### HCV RNA replication and secretion (SM) model

Quintela et al. [30] developed a simple HCV RNA replication and secretion model in which they assumed for simplicity that HCV RNA was secreted from both the cytoplasm and RC at the same rate. Further, they assumed that the secretion was delayed and then ramped-up to a maximum secretion rate as given by Eq (2). Here we revisit the assumptions about the route of secretion and the functional form used to describe the rate of secretion. We evaluated the different possible HCV RNA secretion routes and different functional forms for the rate of secretion by fitting different versions of the model to *in vitro* measurements of plus-strand RNA, minus-strand RNA, and secreted HCV RNA taken from Keum et al. [35]. In all we considered 13 possible models (Tables 1 and 3).

We found that the estimated values of the HCV RNA secretion rates  $\rho_i(t), i = R, T$ , depend strongly on the time delay associated parameters  $\tau_\rho$  and  $k_\rho$ . Both parameters led to identifiability problems where small changes in  $k_\rho$  hampered the identifiability of the remaining model parameters. Note that a model incorporating a delay followed by a ramp-up function, Eq (2), with large  $k_\rho$  becomes equivalent to a model with a simple time delay, Eq (3), as the ramp-up occurs almost instantaneously for large  $k_\rho$ . Also, if  $k_\rho$  is very small, then hardly any ramp-up occurs and hence very little RNA secretion occurs. The same two limits apply for the resource limited model, Eq (4), but with effects of large and small  $k_\rho$  reversed. For these reasons, we only studied an intermediate range of fixed  $k_\rho$  values with  $k_\rho \in [0.01, 100]d^{-1}$  (Fig 2). We found the model  $SM_{T1 \neq R1}$  with secretion from both the site of HCV RNA translation, i.e., the cytoplasm, as well as from the RC, both with compartment specific delayed ramp-up HCV RNA secretion rates was the most likely, i.e., had the lowest negative log likelihood value (-LL), and also was the preferred model, i.e., had the lowest AIC (Table 3).

The different best-fit HCV RNA secretion models for each secretion route generate a different shape for the HCV RNA secretion curve versus time, while the models accounting for the

**Table 3. Model comparison of the SM models.** Negative log likelihood (-LL), AICs, number of estimated model parameters (#P), and  $k_{p_i}$  values of the best-fit models SM<sub>T1</sub> to SM<sub>TR3</sub>, which were fitted to measurements of plus-strand RNA, minus-strand RNA, and secreted HCV RNA in Keum et al. [35]. The model with the lowest AIC is highlighted in beige and the lowest AIC for each model variant is shown in bold.

Model	Secretion route	Time delay function	#P	$k_{p_i}$	$\tau_{p_i}$	$\rho_i$	-LL	AIC
SM <sub>T1</sub>	Secretion from the site of translation ( <i>T</i> )	Delay then ramp-up (Eq 2)	11	$k_T = 100 d^{-1}$	$\tau_T = 0.2 d$	$\rho_T = 1.4 d^{-1}$	91.4	113.4
SM <sub>T2</sub>		Simple delay (Eq 3)	10	-	$\tau_T = 0.2 d$	$\rho_T = 1.4 d^{-1}$	<b>91.4</b>	<b>111.4</b>
SM <sub>T3</sub>		Delayed exponential decrease (Eq 4)	11	$k_T = 0.01 d^{-1}$	$\tau_T = 0.2 d$	$\rho_T = 1.4 d^{-1}$	91.7	113.7
SM <sub>R1</sub>	Secretion from the RC ( <i>R</i> )	Delay then ramp-up (Eq 2)	11	$k_R = 100 d^{-1}$	$\tau_R = 0.01 d$	$\rho_R = 0.05 d^{-1}$	208.6	230.6
SM <sub>R2</sub>		Simple delay (Eq 3)	10	-	$\tau_R = 0.01 d$	$\rho_R = 0.05 d^{-1}$	208.5	228.5
SM <sub>R3</sub>		Delayed exponential decrease (Eq 4)	11	$k_R = 0.5 d^{-1}$	$\tau_R = 0.01 d$	$\rho_R = 0.1 d^{-1}$	<b>182.5</b>	<b>204.5</b>
SM <sub>T1 = R1</sub>	Secretion from both sites ( <i>T</i> and <i>R</i> ) with $\rho_T = \rho_R$ and $\tau_T = \tau_R$	Delay then ramp-up (Eq 2)	11	$k_T = k_R = 100 d^{-1}$	$\tau_T = \tau_R = 0.01 d$	$\rho_T = \rho_R = 0.03 d^{-1}$	91.5	113.5
SM <sub>T2 = R2</sub>		Simple delay (Eq 3)	10	-	$\tau_T = \tau_R = 0.01 d$	$\rho_T = \rho_R = 0.03 d^{-1}$	<b>90.7</b>	<b>110.7</b>
SM <sub>T3 = R3</sub>		Delayed exponential decrease (Eq 4)	11	$k_T = k_R = 0.01 d^{-1}$	$\tau_T = \tau_R = 0.01 d$	$\rho_T = \rho_R = 0.03 d^{-1}$	91.0	113.0
SM <sub>T1≠R1</sub>	Secretion from both sites ( <i>T</i> and <i>R</i> ) with $\rho_T \neq \rho_R$ and $\tau_T \neq \tau_R$	Delay then ramp-up (Eq 2)	13	$k_T = k_R = 100 d^{-1}$	$\tau_T = 0.01 d$ $\tau_R = 0.4 d$	$\rho_T = 0.04 d^{-1}$ $\rho_R = 0.03 d^{-1}$	90.4	116.4
SM <sub>T2≠R2</sub>		Simple delay (Eq 3)	12	-	$\tau_T = 0.02 d$ $\tau_R = 0.4 d$	$\rho_T = 0.04 d^{-1}$ $\rho_R = 0.03 d^{-1}$	<b>90.4</b>	<b>114.4</b>
SM <sub>T3≠R3</sub>		Delayed exponential decrease (Eq 4)	13	$k_T = k_R = 0.01 d^{-1}$	$\tau_T = 0.2 d$ $\tau_R = 0.4 d$	$\rho_T = 0.05 d^{-1}$ $\rho_R = 0.03 d^{-1}$	90.8	116.8
SM <sub>T1≠R1</sub>	(+)RNA secretion from the RC ( <i>R</i> ) and the site of translation ( <i>T</i> ) with $\rho_T \neq \rho_R$ and $\tau_T \neq \tau_R$ and $k_T \neq k_R$	Delay then ramp-up (Eq 2)	14	$k_T = 50 d^{-1}$ $k_R = 5 d^{-1}$	$\tau_T = 0.1 d$ $\tau_R = 3 d$	$\rho_T = 0.8 d^{-1}$ $\rho_R = 0.05 d^{-1}$	<b>81.6</b>	<b>109.6</b>

<https://doi.org/10.1371/journal.pcbi.1008421.t003>

same HCV RNA secretion route generate the same shape HCV RNA release curve (S1 and S2 Figs). The models assuming HCV RNA secretion from the site of translation (SM<sub>Ti</sub>, SM<sub>Ti = Ri</sub>, SM<sub>Ti≠Ri</sub> with  $i = 1,2,3$ ) showed a very rapid initiation of HCV RNA secretion followed by a slower increase and represented the models with the lowest AIC (Fig 3A–3C, S1 and S2 Tables), while the models that only considered HCV RNA secretion from the RC (SM<sub>Ri</sub> with  $i = 1,2,3$ ) showed a smooth increase in extracellular HCV and did not fit the early secreted RNA data well (S1 and S2 Figs). Hence, models including RNA secretion at the site of translation were highly preferred compared to models in which the secretion of HCV RNA was exclusively from the RC. Moreover, the majority of HCV RNA secreted from the cell was associated with HCV RNA at the site of translation. More specifically, 57% of the secreted HCV RNA came from the site of translation and 43% from the RC when summed over the 5 day experiment. Initially, HCV RNA is secreted exclusively from the site of translation starting about 3 hours post-infection (hpi). After 3 days, HCV RNA starts being secreted from the RC and on average over the period from days 3 to 5 secretion from the site of translation and the RCs contribute equally to the HCV RNA secretion (Fig 3D).

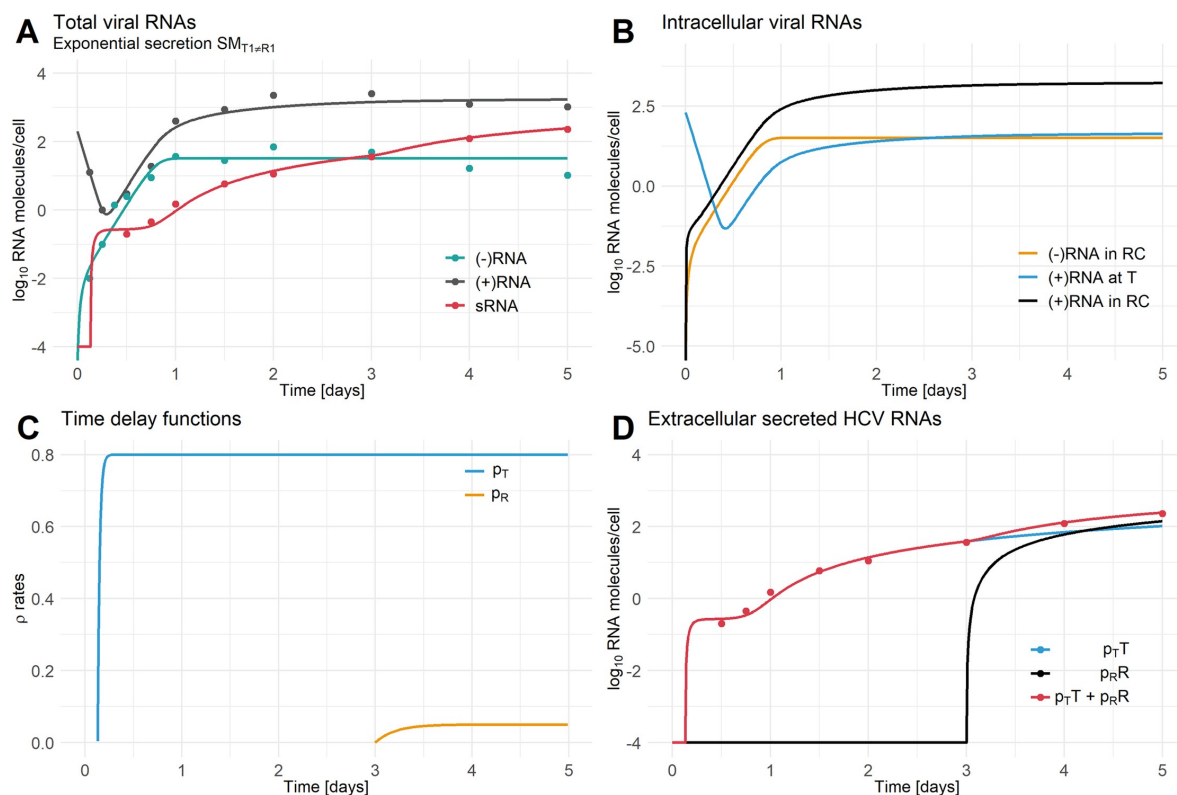


**Fig 3. Individual HCV secretion from the site of translation and the replication compartment.** A) Best-fit secretion model which includes independent HCV RNA secretion from the site of translation and the RC ( $SM_{T1 \neq R1}$ ) with  $\tau_T = 0.1$  d,  $\tau_R = 3$  d,  $\rho_T = 0.8$  d<sup>-1</sup>,  $\rho_R = 0.05$  d<sup>-1</sup>,  $k_T = 50$  d<sup>-1</sup>, and  $k_R = 5$  d<sup>-1</sup>. B) Intracellular HCV RNA species at the site of translation (T) and in the RC (R). C) Time delay functions for the HCV RNA secretion with  $\rho_T = (+)$ RNA secretion rate from site of translation and  $\rho_R = (+)$ RNA secretion rate from the RC. D) Composition of extracellular secreted HCV RNA with  $\rho_T T$  denoting the amount of extracellular secreted (+)RNA from the site of translation,  $\rho_R R$  denoting the amount of extracellular secreted (+)RNA from the RC and  $\rho_T T + \rho_R R$  denoting the sum of all extracellular secreted HCV (+)RNA species (sRNA). [(-)RNA = minus-stranded RNA, (+)RNA = plus-stranded RNA, sRNA = secreted HCV RNA (see S1 Data)]. Data has been taken from [35] Fig 1A–1C. See Table 4 for parameter information.

<https://doi.org/10.1371/journal.pcbi.1008421.g003>

Lastly, we examined the possibility that minus-strand RNA or double stranded RNA containing a minus-strand might also be secreted (S1 Text and S6 Fig) since double stranded HCV RNA has been seen in exosomes [40]. We found the best model with minus-strand secretion (lowest AIC, S7, S8 and S9 Figs) had plus-strand RNA secretion from the sites of translation and replication and minus-strand RNA secretion from the RC ( $SM_{T1 \neq R1 \neq C1}$ , S3 Table). The models including minus-strand RNA secretion showed lower AICs compared to the models excluding minus-strand RNA (S3 and S4 Tables). However, we have not pursued this model further as we have no quantitative measurements of minus-strand secretion to fit the model to and validate these results.

### HCV replication model with virion assembly and release (AM)

Quintela et al. [30] implicitly assumed that secreted HCV RNA was packaged into virions but did not explicitly model virion assembly. Benzine et al. [31] introduced a model that had an



explicit virion assembly compartment, which is truer to the biology as virion assembly is known to occur in association with cLD [41]. Inspired by the Benzine et al. model, we explicitly modeled virus particle production. To do this, we modified the HCV replication and secretion model by eliminating HCV RNA secretion and replacing it by virus assembly and release (Eq 5). Thus, this model is more akin to the standard viral dynamics model that only considers viral production as a source of extracellular HCV RNA [21,42]. In the context of this model, we examined four different functions for the rate of virus assembly [ $f(t)$ ]: (i) a constant viral assembly rate, (ii) a simple time delayed virus assembly rate (Eq 6), (iii) a delayed ramp-up virus assembly rate (Eq 7), and (iv) a delayed decrease in the viral assembly rate, which we interpret as indicating a limitation in viral or host cell resources (Eq 8). For each different function  $f(t)$ , we evaluated the HCV assembly and release models (AM models) without accounting for HCV RNA secretion via exosomes (Table 2).

The extracellular infectious virus loss rate was set to  $\mu_V = 2.77 \text{ d}^{-1}$ , which corresponds to an infectivity half-life of 6 h, a value measured at 37° C in *in vitro* experiments (S. Uprichard, personal communication). However, similar to the HCV RNA secretion model, trying to estimate the continuous time delay associated parameter,  $k_f$ , for the function describing the rate of virus assembly,  $f(t)$ , led to identifiability problems and hampered the calculation of 95% confidence intervals of the estimated model parameters. Therefore, we performed various model fits with fixed values of  $k_f \in [0.1, 10] \text{ d}^{-1}$ . From the identifiability analysis of the AM models using likelihood profiling, we found that the degradation rates of RNA within the RC,  $\mu_R$ , could not be uniquely identified. When we set a lower bound on the parameter value, fitting would generate an estimate at this bound. Trying even lower bounds did not improve this and thus we decided to set  $\mu_R = 0$  consistent with the observation that the replication compartment provides protection against nuclease mediated degradation of HCV RNA [43]. Note that we also neglected intracellular virus degradation, since we estimated a very small value for the intracellular virus decay ( $\mu_A < 0.001 \text{ d}^{-1}$ ) that was in agreement with the expectation that intracellular virus is protected from degradation within the assembly compartment. Hence, we set  $\mu_A = 0$ . The remaining model parameters were estimated by fitting each model to the measurements of plus-strand RNA, minus-strand RNA, intracellular and extracellular infectious virus from Keum et al. [35]. Note that we introduced a parameter,  $f_{inf}$ , that scales the assembled (intracellular) and released (extracellular) virus to infectious virus as infectious virus was measured in Keum et al. [35]. We found that the model incorporating a delayed limitation in the viral assembly process (Eq 8) was the best model as it had the lowest AIC (AM<sub>4</sub>) (Fig 4, Table 5).

### An HCV replication model with both virion assembly and release and exosome secretion: the combined model (CM)

As experimental evidence suggests, HCV infected cells produce virions as well as secrete HCV RNA containing exosomes [15], we combined the HCV replication model with the HCV RNA secretion and virus assembly and release model (Eq 9). Here, we built upon our previous best model fits of the HCV RNA secretion (SM) and the HCV assembly and release model (AM). Since we found the preferred model (SM) included HCV RNA secretion via  $T$  and  $R$  (SM<sub>T1≠R1</sub> with  $k_{pT} \neq k_{pR}$ ), we chose to allow both HCV RNA secretion pathways for the combined model. In order to study, whether our assumption of a limited virus assembly and release is still valid or if HCV RNA secretion via exosomes has an impact on the rate of virus assembly and release, we again tested the four possible virus assembly rate functions in this CM model with HCV RNA secretion: CM<sub>1</sub> with a const. virus assembly rate, CM<sub>2</sub> with a simple delayed virus assembly rate (Eq 6), CM<sub>3</sub> with a delayed virus assembly rate that ramps-up (Eq 7), and CM<sub>4</sub> with a delayed virus assembly rate that decreases exponentially over time (Eq 8) (Table 6).

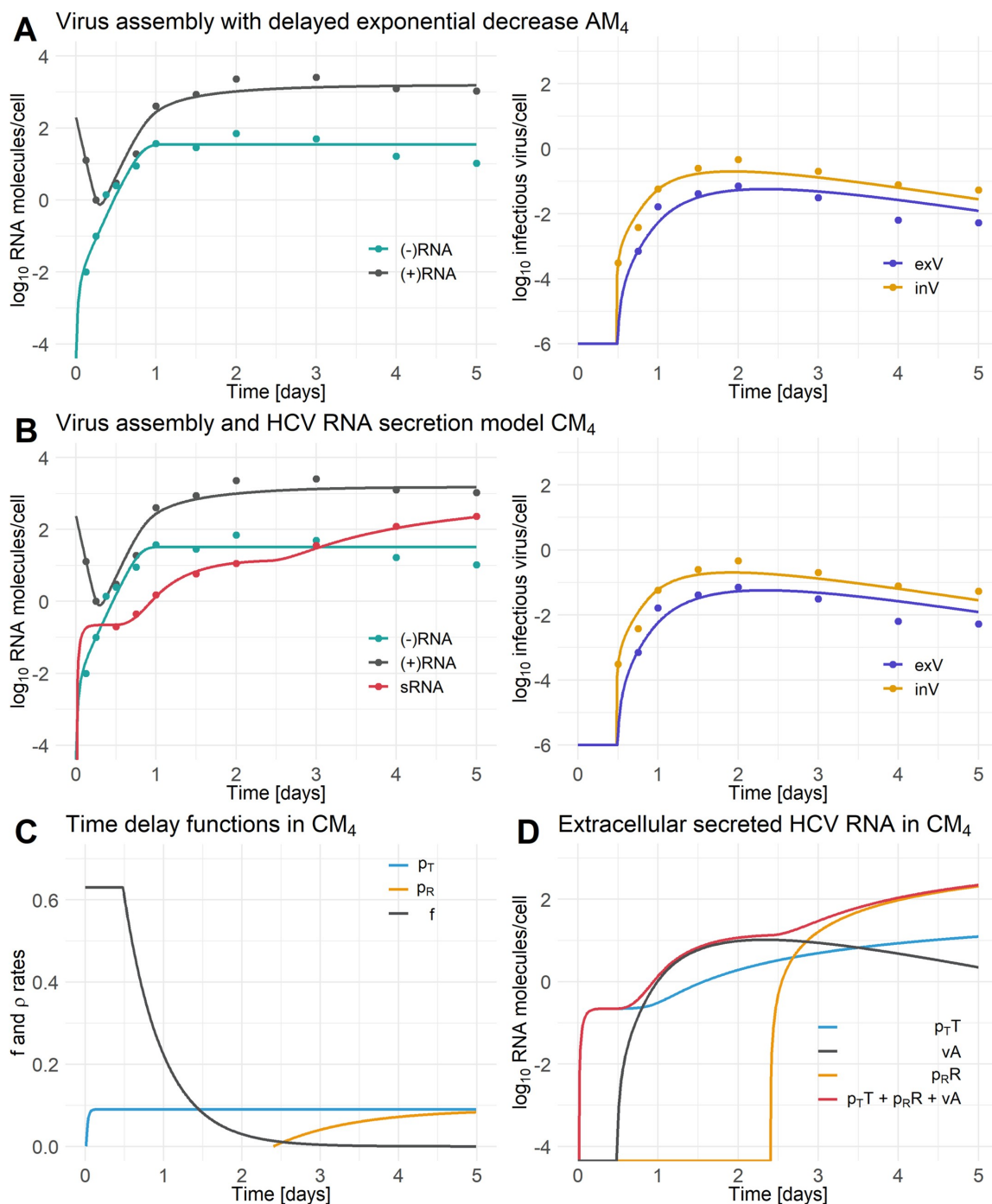


**Fig 4. Best fits of the AM<sub>4</sub> and CM<sub>4</sub> models.** A) Best-fit of the HCV assembly and release models AM<sub>4</sub> (Eqs 4 to 9). B) Best fit of the combined HCV model CM (Eq 9) with individual HCV RNA secretion ( $\rho_T \neq \rho_R$ ,  $\tau_T \neq \tau_R$ , and  $k_T \neq k_R$ ). C) Time delay functions of the combined model (CM) for virus assembly rate and HCV RNA secretion rates with  $\rho_T$  = (+)RNA secretion rate from site of translation,  $\rho_R$  = (+)RNA secretion rate from the RC and  $f$  = virus assembly rate. D) Extracellular secreted HCV RNA in the combined model (CM) with  $\rho_T T$  denoting the amount of extracellular secreted (+)RNA from the site of translation,  $\rho_R R$  denoting the amount of extracellular secreted (+)RNA from the RC,  $\rho_T T + \rho_R R$  denoting the sum of all extracellular secreted HCV (+)RNA species (sRNA), and  $\rho_T T + \rho_R R + vA$  denoting the sum of all extracellular secreted HCV (+)RNA species and virus (exV). [(−)RNA = minus-stranded RNA, (+)RNA = plus-stranded RNA, sRNA = secreted HCV RNA, exV = extracellular infectious virus, inV = intracellular infectious virus in the assembly compartment (see S1 Data)]. Data has been taken from [35] Figs 1A–1C and 2A. The data in Fig 2A of Keum et al. was given per well. We divided the measured data by the number of cells per well (Fig 2D Keum et al. [35]) to give the infectious intracellular and extracellular virus released per cell. See for parameter information Table 4.

<https://doi.org/10.1371/journal.pcbi.1008421.g004>

The combined models (CM<sub>1</sub>, CM<sub>2</sub>, CM<sub>3</sub>, and CM<sub>4</sub>) were fitted to measurements of plus-strand RNA, minus-strand RNA, secreted HCV RNA, intracellular, and extracellular infectious virus from Keum et al. [35]. Similar to the HCV assembly and release model, we fixed the loss rate for extracellular infectious virus to  $\mu_V = 2.77 d^{-1}$ , set the degradation rates  $\mu_R = \mu_A = 0$  and performed independent model fits scanning through fixed values of  $k_f \in [0.1, 10] d^{-1}$  and  $k_{\rho_i} \in [0.01, 100] d^{-1}$  and then utilized the values that gave the lowest AIC (Table 6). The remaining model parameters were estimated (Table 4).

The model that takes into account a delayed decrease in the virus assembly and release rate (CM<sub>4</sub>) was able to fit the five types of longitudinal measurements made by Keum et al. [35] and showed a substantially lower AIC than the other three CM models (Table 6). Furthermore, model CM<sub>4</sub> had a lower AIC than the model neglecting HCV RNA secretion, i.e., model AM<sub>4</sub>

**Table 4. Parameter values and 95% confidence intervals of the best-fit models SM<sub>T1≠R1</sub>, AM<sub>4</sub>, and CM<sub>4</sub>.** Note that parameter values marked with \* were fixed due to previous assumptions (time delay parameters:  $k_f, k_{\rho_T}, k_{\rho_R}$ ), fixed after sensitivity/identifiability analysis ( $\mu_R$ ) and personal communication ( $\mu_V$ ) (see Methods). The degradation rate of HCV RNA within the RC was set to  $\mu_R = 0$  as was the rate of degradation of intracellular virus  $\mu_A = 0$  (see main text). For parameter identifiability profiles see S3, S4 and S5 Figs.

Parameter	Description	SM <sub>T1≠R1</sub>	AM <sub>4</sub>	CM <sub>4</sub>	Unit
AIC		109.6	214.0	198.1	
$\rho_T$	S secretion rate	0.8 [0.4, 2.0]	-	0.09 [0.05, 0.2]	$d^{-1}$
$\rho_R$	S secretion rate	0.05 [0.01, 0.09]	-	0.09 [0.06, 0.1]	$d^{-1}$
$\tau_{\rho_T}$	S secretion delay	0.13 [0.09, 0.18]	-	0.01 [0.01, 0.05]	$d$
$\tau_{\rho_R}$	S secretion delay	3 [2.4, 3]	-	2.3 [2, 2.5]	$d$
$k_{\rho_T}$	S secretion rate parameter	50 *	-	10 *	$d^{-1}$
$k_{\rho_R}$	S secretion rate parameter	5 *	-	1 *	$d^{-1}$
$f$	V assembly rate	-	2.7 [2.2, 8.3]	0.63 [0.58, 0.7]	$d^{-1}$
$\tau_f$	V assembly delay	-	0.48 [0.46, 0.49]	0.48 [0.46, 0.49]	$d$
$k_f$	V assembly rate parameter	-	2 *	2 *	$d^{-1}$
$T_0$	Initial number of HCV RNAs	202 [66, 250]	196 [160, 262]	236 [88, 588]	molecules/cell
$C_{max}$	Maximal number of C	32.5 [27.2, 38.8]	35.1 [30.6, 40.8]	32.7 [27.6, 38.6]	molecules/cell
$\sigma$	Rate of transfer of T to the RC	0.007 [0.003, 0.02]	0.006 [0.005, 0.009]	0.006 [0.002, 0.01]	$d^{-1}$
$\theta$	Rate of transfer of R to the cytoplasm	0.6 [0.3, 1.0]	0.9 [0.6, 1.2]	0.7 [0.5, 1.0]	$d^{-1}$
$r$	C replication rate	3.5 [2.5, 5.1]	3.5 [3.1, 3.9]	3.6 [2.8, 4.6]	$d^{-1}$
$\alpha$	R replication rate	34.8 [26.5, 45.9]	38.6 [34.9, 42.5]	35.6 [27.7, 45.9]	$d^{-1}$
$v$	V release rate	-	0.86 [0.74, 0.97]	0.85 [0.76, 0.97]	
$\mu_T$	Cytoplasmic RNA degradation rate	22.3 [16.1, 25.8]	22.2 [20.2, 24.5]	23.1 [17.5, 30.0]	$d^{-1}$
$\mu_R$	R and C degradation rates	0	0	0	$d^{-1}$
$\mu_A$	A degradation rate	0	0	0	$d^{-1}$
$\mu_V$	V degradation rate	-	2.77 *	2.77 *	$d^{-1}$
$f_{inf}$	Fraction of A and V that is infectious	-	0.0014 [0.0009, 0.0018]	0.0055 [0.0048, 0.0063]	

**Table 5. Model comparison of the AM models.** Negative log likelihood (-LL), AICs and number of estimated model parameters (#P) of the assembly models (AM) without exosome secretion. AM<sub>1</sub> to AM<sub>4</sub> were each fitted to plus-strand RNA, minus-strand RNA, intracellular and extracellular virus from Keum et al. [35]. The model with the lowest AIC is highlighted in beige.

Model	$f(t)$	# P	$k_f$	$\tau_f$	-LL	AIC
AM <sub>1</sub>	Virus assembly $f(t)$ const.	12	-	-	443.1	467.1
AM <sub>2</sub>	Virus assembly $f(t)$ simple delay (Eq 6)	13	-	0.2 $d$	436.6	462.6
AM <sub>3</sub>	Virus assembly $f(t)$ delayed then ramp-up (Eq 7)	14	0.1 $d^{-1}$	0.4 $d$	317.8	345.8
AM <sub>4</sub>	Virus assembly $f(t)$ delayed exponential decrease (Eq 8)	14	2.0 $d^{-1}$	0.35 $d$	<b>186.0</b>	<b>214.0</b>

<https://doi.org/10.1371/journal.pcbi.1008421.t005>

(Table 4). However, despite allowing HCV RNA to be secreted, the model could still accurately fit the total intracellular plus-strand RNA and showed a comparable dynamic to the plus-strand RNA in model AM<sub>4</sub> that neglects HCV RNA secretion (Fig 4A and 4B). Similar to the HCV RNA secretion model (SM<sub>T1≠R1</sub>), the HCV RNA secretion process of the combined model (CM<sub>4</sub>) showed immediate HCV RNA secretion from the site of translation, while RNA secretion from the RC was 2.3 days delayed and contributes the majority of the extracellular secreted HCV RNA amount (Fig 4C and 4D). After around 10 hrs. virus starts being secreted from the cell, reaches a peak at 2 days post-infection (dpi) and falls slightly subsequently (Fig 4B, right panel).

### Sensitivity analysis

In order to gain insight into the impact of model parameters on the combined model, we performed a global sensitivity analysis for all HCV species (plus-strand RNA, minus-strand RNA, secreted RNA, intracellular and extracellular infectious virus) for two different time points, day 1 and day 3 post-infection (see S2 Text and S10 Fig). The amount of secreted HCV RNA was highly sensitive to the rate of cytoplasmic RNA degradation,  $\mu_T$ , and to the parameters describing the secretion process from the site of translation,  $\tau_{pT}$  and  $k_{pT}$ , at 1 dpi as well as the virus replication and transfer parameters,  $r, \alpha, \tau$  and  $C_{max}$  at 3 dpi. The amount of intracellular infectious virus at 3 dpi was sensitive to the secretion process parameters, while the amounts of both infectious virus species at 3 dpi were sensitive to the virus assembly and release parameters.

**Table 6. Model comparison of the CM models.** Negative log likelihood (-LL), AICs and number of estimated model parameters (#P) of the combined model (CM) with exosome secretion and virus assembly and release. CM<sub>1</sub> to CM<sub>4</sub> were each fitted to plus-strand RNA, minus-strand RNA, secreted HCV RNA, intracellular and extracellular virus from Keum et al. [35]. The model with the lowest AIC is highlighted in beige.

Model	$f(t)$	# P	$k_{p_i}$	$\tau_{p_i}$	$\rho_i$	$k_f$	$\tau_f$	$f$	-LL	AIC
CM <sub>1</sub>	Virus assembly $f(t)$ const.	18	$k_{p_T} = 50 d^{-1}$ $k_{p_R} = 1 d^{-1}$	$\tau_{p_T} = 0.3 d$ $\tau_{p_R} = 2.5 d$	$\rho_T = 1000 d^{-1}$ $\rho_R = 0.2 d^{-1}$	-	-	0.0001 $d^{-1}$	571.7	607.7
CM <sub>2</sub>	Virus assembly $f(t)$ simple delay (Eq 6)	19	$k_{p_T} = 50 d^{-1}$ $k_{p_R} = 1 d^{-1}$	$\tau_{p_T} = 0.3 d$ $\tau_{p_R} = 2.5 d$	$\rho_T = 1000 d^{-1}$ $\rho_R = 0.15 d^{-1}$	-	0.01 $d$	0.0001 $d^{-1}$	571.7	609.7
CM <sub>3</sub>	Virus assembly $f(t)$ delayed then ramp-up (Eq 7)	20	$k_{p_T} = 50 d^{-1}$ $k_{p_R} = 1 d^{-1}$	$\tau_{p_T} = 0.3 d$ $\tau_{p_R} = 2.5 d$	$\rho_T = 1000 d^{-1}$ $\rho_R = 0.19 d^{-1}$	2 $d^{-1}$	0.01 $d$	0.02 $d^{-1}$	614.6	654.6
CM <sub>4</sub>	Virus assembly $f(t)$ delayed exponential decrease (Eq 8)	20	$k_{p_T} = 10 d^{-1}$ $k_{p_R} = 1 d^{-1}$	$\tau_{p_T} = 0.01 d$ $\tau_{p_R} = 2.35 d$	$\rho_T = 0.09 d^{-1}$ $\rho_R = 0.09 d^{-1}$	2 $d^{-1}$	0.5 $d$	0.7 $d^{-1}$	<b>158.1</b>	<b>198.1</b>

<https://doi.org/10.1371/journal.pcbi.1008421.t006>

### Antiviral drug treatment

Having developed a combined model of the viral lifecycle including virion assembly and secretion, we explored its use in predicting the effects of antiviral drug treatment. To this end, we simulated the effect of giving the direct acting antiviral daclatasvir 10 dpi when plus-strand and minus-strand RNA are in steady state. Daclatasvir interacts with the HCV NS5A protein and effectively blocks both viral replication ( $\epsilon_R = 0.99$ ) and assembly ( $\epsilon_A = 0.998$ ) and a single dose can lead to a 3 log decline in viral load *in vivo* [42,44,45]. To mimic daclatasvir's *in vivo* activity, we multiplied the RNA synthesis rates,  $r$  and  $\alpha$ , by the factor  $(1-\epsilon_R)$  and the virus assembly rate,  $f$ , by the factor  $(1-\epsilon_A)$ , where the drug efficacies  $\epsilon_R = 0.99$  and  $\epsilon_A = 0.998$  were chosen based on previous estimates [42]. We found that plus-strand RNA decreased following drug administration (Fig 5A). However, due to the assumed lack of degradation of RNA species within the RC, the model exhibited no noticeable decrease of (-)RNA after drug administration Fig 5B. Intracellular and extracellular infectious virus were unaffected by the drug administration due to the late drug administration (Fig 5D and 5E). Lastly, under drug therapy secreted HCV RNA reached a constant level (Fig 5C) as the model did not include a mechanism for degradation of secreted exosomes.

### Discussion

Modeling HCV dynamics has a rich history and has been used for studying viral pathogenesis and spread, as well as the effects of antiviral treatment [20,44,46–50]. Some models have included intracellular events that occur during HCV replication and viral spread [20,30,31,51–53], but there is still a lack of detailed knowledge about these processes. The secretion of HCV RNA in the form of exosomes is currently not well understood, but experimental studies have shown that HCV RNA carrying exosomes derived from infected cells are able to infect naïve cells [15] as well as stimulate type I interferon responses from plasmacytoid dendritic cells [54]. Quintela et al. [30] introduced a mathematical model of intracellular HCV RNA replication that takes HCV RNA secretion into account. However, all plus-strand RNA species within their model can potentially be secreted and the model did not distinguish between secretion in exosomes from that in viral particles [30]. In the present study, we distinguish these two routes of secretion.

Experimentally, studying routes of secretion is challenging. Therefore, we introduced models that allowed us to compare three different hypotheses about the HCV RNA secretion routes: HCV RNA secretion from (i) the site of translation, (ii) the replication compartment, RC, and (iii) a combination of both. We also assumed that there may be a delay between viral infection and secretion of HCV RNA and examined different time delay models. By fitting these models to experimental data, we found that the preferred model included both sites of secretion with individual secretion route-specific model parameters.

In the experiments we analyzed, multiples copies of positive-strand HCV RNA entered the cell and on average about 13 copies were detected 3 hpi. Thus, it is not surprising that our secretion model suggested that HCV RNA was initially secreted from the cytoplasm, i.e., the site of translation. As HCV RNA is introduced into the cytoplasm following viral entry its secretion in exosomes as well as its degradation in the cytoplasm might be host cell defenses against viral infection. The loss of HCV RNA introduced by natural infection could be studied using a stochastic model as has been done for HIV [55]. However, in our model which is deterministic and is calibrated against an experimental system that involves the entry of multiple copies of HCV RNA extinction is not possible. Rather, from day 3 post-infection on positive-strand HCV RNA, which by that time has replicated, is mainly secreted from the RC. Before that plus-strand RNA within the RC is transported back to the cytoplasm at a per capita rate  $\theta$

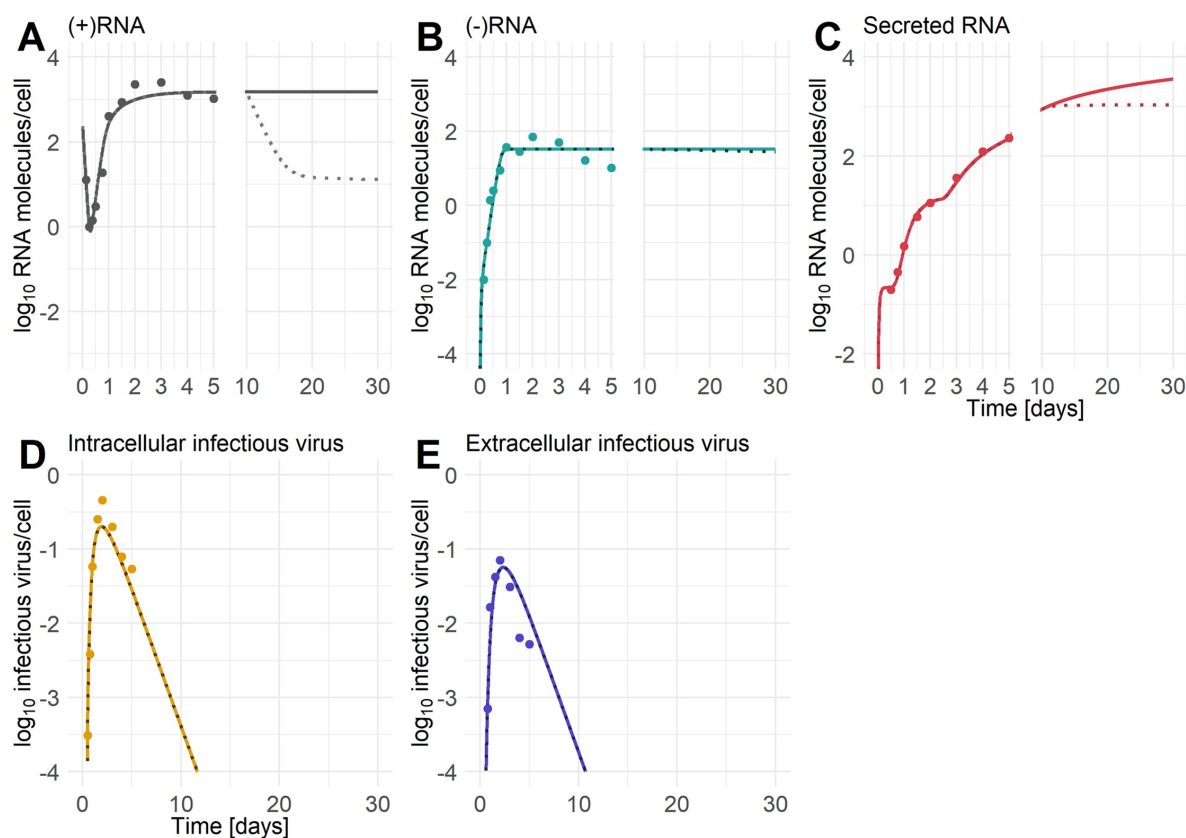


**Fig 5. Effect of antiviral drug treatment given 10 dpi in the combined model (CM<sub>4</sub>).** Here we assume the drug is the NS5A inhibitor daclatasvir and that it acts by inhibiting HCV RNA synthesis with an effectiveness  $\epsilon_R = 0.99$  and virus assembly with an effectiveness  $\epsilon_A = 0.998$ . The solid line denotes the model's prediction with no drug present, whereas the dotted line shows the model's prediction after drug treatment is started on day 10 pi (see [S1 Data](#)).

<https://doi.org/10.1371/journal.pcbi.1008421.g005>

that is more than 10 times higher than its rate of secretion from the RC (see [Table 4](#), SM parameters), suggesting early after infection this RNA is mainly used for protein synthesis in the cytoplasm.

Since experimental studies have shown that HCV-derived exosomes contain both plus-strand RNA as well as minus-strand RNA and possibly to a higher extent double stranded RNA [40], we studied the possibility that both plus- and minus-strand RNA are secreted from the cell. However, consistent with the experimental finding that the plus-strand to minus-strand HCV RNA ratio is 10:1 [56], we found that the minus-strand RNA contribution to the total secreted HCV RNA was negligible ([S1 Text](#)).

We also studied a model with HCV RNA secretion, presumably through exosomes, as well as through virus assembly and release. Fitting this model to data that included both secreted RNA and infectious virus release, we found that a function in which (after a delay) the rate of virion assembly decreased with time after infection best fit the *in vitro* data, suggesting that host or viral factors may limit the rate at which new infectious virions can be assembled. Further, the initial delay which we estimated to be about 6 hours long, would account for the early

event in the viral lifecycle including production of the viral proteins needed for virion assembly.

The processes of HCV assembly, maturation, and release are closely linked to host cell lipid droplet assembly and the very-low-density lipoprotein (VLDL) pathway, as the HCV core protein is accumulating on cLD [4,57]. However, the precise structure of the HCV virion is still unknown due to its high lipid composition and the “lack of discernable surface features” [4]. Several if not all viral proteins are involved in virion assembly which is a tightly connected process between translation/replication and virus assembly/release [57]. It has been suggested that not only HCV proteins are involved in HCV assembly, maturation, and release but that several host factors also participate in HCV particle production, e.g. apolipoprotein (apo) E [57]. ApoE has been found to be a major component of cell culture grown HCV and primary-derived HCV [58]. Keum et al. [35] found that the apoE concentration associated with HCV particles decreases throughout infection, which might lead to a change in HCV infectivity. HCV particles produced early in infection are associated with a higher amount of apoE, while later in infection the HCV associated apoE concentration decreases. Catanese et al. [58] have shown that more copies of apoE were incorporated into the virion particle than the HCV structural protein E2 suggesting that apoE plays an important role in HCV attachment [58]. Deng et al. [59] suggest that the HCV glycoprotein E2 together with syntenin might be components of exosomes derived from HCV infected cells. Syntenin, a host factor regulating the exosome biogenesis, has been found to promote HCV E2 secretion, while the production of infectious virions remained unaffected and thus appears to be a parallel process to HCV exosome release. Deng et al. further suggest that HCV exosomes might support HCV escape from neutralizing E2-specific antibodies in chronic-phase patient sera and therefore might promote HCV infection [59]. Some host factors, such as the Y-box-binding protein (YB-1), have been found to restrict the process of viral assembly and release [7]. YB-1 has been shown to be a dynamic interacting partner of HCV NS3/4A, which impairs HCV replication, but promotes HCV particle production upon knockdown [60]. Furthermore, YB-1 has been suggested as regulating an equilibrium between HCV translation/replication and virus particle production [60]. However, little is known about its regulation in the HCV lifecycle and targeting a particular host factor that restricts viral assembly/release on the one hand but promotes viral replication on the other hand might lead to an increased secretion of HCV RNA with the ability to spread the infection. However, other host factors, such as miR-122, have been found balancing HCV RNA translation and replication. miR-122 increases HCV RNA levels available for synthesis in two different ways: (i) miR-122 stabilizes HCV RNA by preventing its degradation and (ii) it reduces the HCV RNA levels available for translation by dissolving the ribosome HCV RNA complex [61].

Another possible explanation for our finding of a decrease in infectious virus assembly and release with time might be the death of cells, which would also lead to less average release per unit time. However, such increased death was not seen in Keum et al. [35] until the last measurement time point at 5 dpi where increased cytotoxicity was detected in the infected cell cultures (Keum et al. Fig 2E). In the viral dynamics literature, there is a lack of models that take the complex processes of virion assembly and release into account. One exception is a model of influenza A virus developed by Heldt et al. [62] and these authors did not find a limitation in viral proteins or any viral components that are necessary for virus packaging and suggested that transport and budding processes might limit virus release [62]. However, unlike influenza A, HCV does not bud off the plasma membrane and instead is assembled intracellularly and then secreted.

Although not discussed in the main text, we also examined the possibility that cytosolic vRNA located at the site of translation might also serve as a source of vRNA that is packaged

into virions. However, our model fits and AIC calculations showed that models where this possibility was absent were preferred. Instead, we found that models in which HCV RNA in the RC (or in close proximity to it) is used for virus assembly gave good fits to the data and were preferred based on AIC, consistent with the idea that cLDs associated with the endoplasmic reticulum membrane create an environment for HCV assembly. Overall, our analysis and observational data suggest that HCV replication and assembly are tightly linked processes within the membranous web [6,63]. Recently, by using correlative light and electron microscopy, Lee et al. [41] found that cLDs are wrapped by those endoplasmic reticulum membranes, which generate the RCs suggesting a close proximity and a short distance transport of vRNA from the site of HCV replication to assembly [41]. Due to the endoplasmic reticulum wrapped cLDs, which serve as sites of HCV assembly, the intracellular virus might be protected from decay, consistent with its degradation rate estimated by our model as being rather negligible.

It is becoming more and more evident that viruses use different transmission routes: the classic cell-free (receptor-mediated cell entry) and cell-to-cell (exosomal) transmission to infect neighboring cells [64,65]. Viral entry is a complex multi-step and highly regulated process involving viral proteins (HCV glycoproteins E1 and E2) and cellular (host) factors (e.g. CD81, claudin-1, occludin, SR-B1). *In vitro*, the viral entry process critically depends on the E1/E2-CD81 interaction as it has been shown that blocking CD81 or E1/E2 inhibits HCV infection [66–70]. In contrast, other studies [71–73], report that the presence of anti-E2 and anti-CD81 neutralizing antibodies do not block *in vitro* viral transmission completely and HCV is still transmitted to naïve target cells. This suggests not only multiple transmission routes but also the insufficiency in blocking viral entry as a therapeutic strategy [71–73]. It has been shown that anti-E2 treatment blocks HCV particle transmission but not exosomal HCV RNA transfer [15]. On the one hand, it is thought that receptor-mediated cell entry is crucial for infection initiation, since it has been shown that the presence of anti-envelope antibodies led to HCV resistance in HCV exposed patients [15]. On the other hand, exosomal cell-to-cell transfer seems to be an important feature of hepatitis C persistence and immune evasion and results in the resistance to neutralizing antibodies and complement attack [17,71,73–75]. Exosomes isolated from HCV-infected patients have been found to be enriched with CD81 and thus soluble CD81 may be of exosomal origin and represent an exosomal marker [14,76]. Increased soluble CD81 levels were significantly higher in patients with chronic hepatitis C [75].

Interestingly, our best-fit model (CM<sub>4</sub>) suggests secretion of HCV RNA from the site of translation starts almost immediately after infection, while Keum et al. [35] reported extracellular viral RNA was first detected 12 hpi. However, forcing a longer time delay, e.g. HCV RNA secretion starting at 8 hpi, increased the AIC from 198 (Table 6) to 240. An even larger increase in the AIC (281) was observed by starting HCV RNA secretion 11 hpi. One possible explanation for this discrepancy is that the amount of secreted HCV RNA per cell before 12 hpi is below the limit of detection as the amount measured at 12 hpi is only one molecule per 5 cells. Another possibility is that at these early time points with so few molecules being secreted, the secretion process is better described by a stochastic model than with our ODE model, but developing such models is outside the scope of this paper.

Taking our findings of the global sensitivity analysis into account, we found that HCV RNA synthesis and viral assembly might represent potent processes to target early and late in infection. Those processes are already targeted by direct acting antivirals such as sofosbuvir and mericitabine that inhibit the RNA-dependent RNA polymerase (HCV NS5B) and thus viral replication, as well as daclatasvir, ledipasvir, and elbasvir that inhibit the HCV NS5A protein, a phosphoprotein involved in both HCV replication and assembly [20,44]. A sustained virologic response above 95% can be achieved by blocking both, HCV replication with sofosbuvir and virus assembly and release with ledipasvir which represented the most sensitive processes in



our global sensitivity analysis [77]. The NS5A inhibitor daclatasvir might lead to an almost complete shutoff of the HCV replication and spread due to its suggested ability to inhibit the formation of RCs and its ability to prevent HCV genome transfer to sites of virus assembly [78]. However, by using our model to study the effects of inhibiting both RNA synthesis and virus assembly, we found that blocking both processes led to a decrease in intracellular and extracellular virus concentration, as has been observed *in vitro* [42]. Nevertheless, as current direct acting antivirals are not 100% effective, our model predicted that HCV RNA was still being made and secreted at a low level. Our model was not designed for the *in vivo* situation and thus did not account for degradation or clearance of HCV RNA containing exosomes after their secretion from an infected cell. Interestingly, clinical trials aiming to predict the sustained virologic response rate to combination direct acting antiviral therapy regimens in HCV-infected patients have shown that some patients still had low level HCV RNA detectable at the end of therapy despite achieving a sustained virologic response [79,80]. Some possible explanations are that the detected HCV RNA might be non-infectious or very unfit due to mutations or defective due to aberrant virus assembly or because the HCV RNA was packaged in exosomes that poorly transmitted infection, i.e. had an  $R_0 < 1$  [79].

In summary, in the present study we compared several mathematical models of intracellular HCV replication coupled to HCV RNA secretion and/or virus assembly and release. Using a model that did not distinguish between HCV RNA secretion in exosomes or viral particles, we found that initially HCV RNA from the cytoplasm served as the main source of secreted RNA, but after a delay the HCV RNA from the site of translation and the RC served equally as the sources for secreted HCV RNA. By expanding our model to explicitly include HCV assembly and release, we found that a model in which after a delay the rate of viral assembly/release decreased with the additional amount of time a cell had been infected fit the data best, suggesting that these processes might be limited by the availability of viral components and/or host factors involved in assembly and release. Alternatively, there might be host restriction factors that are induced following infection that limit virus particle production. Moreover, if the rate of HCV RNA replication and the amount of intracellular HCV RNA increase with time after infection, this might increase the secretion of HCV RNA in exosomes, which can evade host antibody responses to viral envelope proteins, such as E2, and have the ability to infect naïve cells and thus spread the infection. HCV dynamics models have focused on HCV RNA dispersion in viral particles. Our work suggests that HCV RNA spread in exosomes is also likely and further research concerning exosomal secretion, its infective potential, as well as its contribution to viral spread is needed.

### Supporting information

**S1 Fig. HCV secretion model fits.** Best fits of the HCV RNA secretion models for the three different time delay functions: ramp-up secretion (type 1 models), simple time delayed secretion (type 2 models), exponential decreasing HCV RNA secretion (type 3 models). A) Best-fit model for secretion exclusively from the site of translation. B) Best-fit model for secretion exclusively from the RC. C) Best-fit model for equal ( $\tau_T = \tau_R$  and  $\rho_T = \rho_R$ ) secretion from both sites, the site of translation and the RC. D) Best-fit model for individual ( $\tau_T \neq \tau_R$  and  $\rho_T \neq \rho_R$ ) secretion from both sites, the site of translation and the RC. [(-)RNA = minus-stranded RNA, (+)RNA = plus-stranded RNA, sRNA = secreted HCV RNA (see S1 Data)]. Data has been taken from [35] Fig 1A–1C. See S1 and S2 Tables for parameter information. (TIFF)

**S2 Fig. Best fits of the HCV RNA secretion models.** A) Best-fit model for secretion exclusively from the site of translation. B) Best-fit model for secretion exclusively from the RC. C)

Best-fit model for equal ( $\tau_T = \tau_R$  and  $\rho_T = \rho_R$ ) secretion from both sites, the site of translation and the RC (left), as well as sources of secreted HCV RNA (right). D) Best-fit model for individual ( $\tau_T \neq \tau_R$  and  $\rho_T \neq \rho_R$ ) secretion from both sites, the site of translation and the RC (left), as well as sources of secreted HCV RNA (right). [(-)RNA = minus-stranded RNA, (+) RNA = plus-stranded RNA, sRNA = secreted HCV RNA (see [S1 Data](#))]. Data has been taken from [35] [Fig 1A–1C](#). See [S1 Table](#) for parameter information.

(TIFF)

**S3 Fig. Parameter identifiability profile for the best-fit HCV secretion model.** Parameter identifiability profile for the best-fit HCV secretion model ( $SM_{T1 \neq R1}$ ) that considers independent HCV RNA secretion ( $\tau_T \neq \tau_R$ ,  $\rho_T \neq \rho_R$ ,  $k_T \neq k_R$ ). The x-axis shows the scanned parameter profile (as  $\log_{10}$  values), y-axis shows the corresponding log-likelihood values [ $\Delta L(P)$  is the difference of the log likelihood value], the red dot shows the estimated parameter value and the red line describes the statistical 95% threshold (95% confidence intervals are listed in [Table 4](#), see [S1 Data](#) for details). A parameter is identifiable if the black parameter profile line is crossing the statistical threshold (the 95% confidence interval is finite).

(TIFF)

**S4 Fig. Parameter identifiability profile for the best-fit HCV assembly model ( $AM_4$ ).** The x-axis shows the scanned parameter profile (as  $\log_{10}$  values), y-axis shows the corresponding log-likelihood values [ $\Delta L(P)$  is the difference of the log likelihood value], the red dot shows the estimated parameter value and the red line describes the statistical 95% threshold (95% confidence intervals are listed in [Table 4](#), see [S1 Data](#) for details). A parameter is identifiable if the black parameter profile line is crossing the statistical threshold (the 95% confidence interval is finite).

(TIFF)

**S5 Fig. Parameter identifiability profile for the best-fit HCV RNA secretion and virus assembly model ( $CM_4$ ).** The x-axis shows the scanned parameter profile (as  $\log_{10}$  values), y-axis shows the corresponding log-likelihood values [ $\Delta L(P)$  is the difference of the log likelihood value], the red dot shows the estimated parameter value and the red line describes the statistical 95% threshold (95% confidence intervals are listed in [Table 4](#), see [S1 Data](#) for details). A parameter is identifiable if the black parameter profile line is crossing the statistical threshold (the 95% confidence interval is finite).

(TIFF)

**S6 Fig. (+) and (-)RNA secretion model.** Schematic illustration of the intracellular HCV RNA replication extended by  $\rho_C$ , where (-)RNA from the RC serves as a source of HCV RNA secretion. For more details, see [Fig 1](#).

(TIF)

**S7 Fig. AICs of the (+) and (-)RNA secretion models.** Best-fit model AICs of the HCV (+) and (-)RNA secretion models when the parameter  $k_p$  determining the rate of ramp-up or limitation was varied. [ $\blacktriangle$  = ramp-up models,  $\blacksquare$  = simple delay models,  $\bullet$  = exponential decrease models; blue = (-)RNA secretion from the RC, green = equal (+)RNA secretion from site of translation and (-)RNA secretion from the RC ( $\tau_T = \tau_C$ ,  $\rho_T = \rho_C$ ), yellow = individual (+)RNA secretion from site of translation and (-)RNA secretion from the RC ( $\tau_T \neq \tau_C$ ,  $\rho_T \neq \rho_C$ ), red = equal (+)RNA secretion from site of translation and (+) and (-) RNA secretion from the RC ( $\tau_T = \tau_R = \tau_C$ ,  $\rho_T = \rho_R = \rho_C$ ), black = individual (+)RNA secretion from site of translation and (+) and (-)RNA secretion from the RC ( $\tau_T \neq \tau_R \neq \tau_C$ ,  $\rho_T \neq \rho_R \neq \rho_C$ ) (see [S1 Data](#))]. For the best model for each HCV RNA secretion route and corresponding time delay function see [S3](#)

Table.

(TIFF)

**S8 Fig. (+) and (-)RNA secretion model fit.** A) Best-fit model for individual HCV (+)RNA and (-)RNA secretion from site of translation and the RC ( $\tau_T \neq \tau_R \neq \tau_C$ ,  $\rho_T \neq \rho_R \neq \rho_C$ , and  $k_T \neq k_R \neq k_C$ ). B) Sources of secreted HCV RNA. C) Ratios of intracellular HCV RNA species. D) Time delay functions. [(-)RNA = minus-stranded RNA, (+)RNA = plus-stranded RNA, sRNA = secreted HCV RNA (see [S1 Data](#))]. Data has been taken from [35] [Fig 1A–1C](#). See [S4 Table](#) for parameter information.

(TIFF)

**S9 Fig. Parameter identifiability profile for the best-fit (+) and (-)HCV secretion model.**

Parameter identifiability profile for the best-fit (+) and (-)HCV secretion model ( $SM_{T1 \neq R1 \neq M1}$ ) that considers independent HCV RNA secretion ( $\tau_T \neq \tau_R \neq \tau_C$ ,  $\rho_T \neq \rho_R \neq \rho_C$ ,  $k_T \neq k_R \neq k_C$ ). The x-axis shows the scanned parameter profile (as  $\log_{10}$  values), y-axis shows the corresponding log-likelihood values [ $\Delta L(P)$  is the difference of the log likelihood value], the red dot shows the estimated parameter value and the red line describes the statistical 95% threshold (95% confidence intervals are listed in [S4 Table](#), see [S1 Data](#) for details). A parameter is identifiable if the black parameter profile line is crossing the statistical threshold (the 95% confidence interval is finite).

(TIFF)

**S10 Fig. Global sensitivity of the  $CM_4$  model parameters.**

Global sensitivity analysis performed for model  $CM_4$  showing the total-order sensitivities for all model parameters for two different time points: 1 (A, C, E) and 3 (B, D, F, G, H) days post infection (dpi). The red line represents a threshold, a so-called negative control or dummy parameter that does not appear in the mathematical model equations, where sensitivities above the line are considered as relevant while those below are negligible (see [Methods](#) section and [S1 Data](#) for details). Significant differences of the total sensitivity of a model parameter to the threshold have been calculated by performing a t-Test (p-values: \*\*\*  $\leq 0.001$ , \*\*  $\leq 0.01$ , \*  $\leq 0.05$ ) (see [S2 Text](#) for more information).

(TIFF)

**S1 Table. Parameter values of secretion models with one HCV (+)RNA secretion route.**

Parameter values of the best-fit models with a delayed ramp-up secretion (type 1 models:  $SM_{T1}$  and  $SM_{R1}$ ), simple time delayed secretion (type 2 models:  $SM_{T2}$  and  $SM_{R2}$ ), and an exponential decreasing secretion (type 3 models:  $SM_{T3}$  and  $SM_{R3}$ ).

(DOCX)

**S2 Table. Parameter values of secretion models with both HCV (+)RNA secretion route.**

Parameter values of the best-fit models with a delayed ramp-up secretion (type 1 models:  $SM_{T1 = R1}$  and  $SM_{T1 \neq R1}$ ), simple time delayed secretion (type 2 models:  $SM_{T2 = R2}$  and  $SM_{T2 \neq R2}$ ), and an exponential decreasing secretion (type 3 models:  $SM_{T3 = R3}$  and  $SM_{T3 \neq R3}$ ). Note that for models where HCV RNA is secreted from both routes (the site of translation and the RC) we discriminate between two different cases: (i) secretion specific model parameters are the same for both secretion routes, i.e.  $\tau_T = \tau_R$  and  $\rho_T = \rho_R$  ( $SM_{T_i = R_i}$  with  $i = 1, 2, 3$ ), or (ii) secretion specific model parameters are individual for both secretion routes, i.e.  $\tau_T \neq \tau_R$  and  $\rho_T \neq \rho_R$  ( $SM_{T_i \neq R_i}$  with  $i = 1, 2, 3$ ). Parameter values in [] show 95% confidence intervals, while values marked with \* were kept fixed throughout the profile likelihood estimation.

(DOCX)

**S3 Table. Model comparison of the (+) and (-)RNA secretion models.** AICs, number of estimated model parameters (#P), time delay parameters ( $k_{\rho_i}$ ,  $\tau_{\rho_i}$ ,  $\rho_i$ ) values of the best-fit models

that take into account the secretion of (-)RNA and were fitted to measurements of plus-strand RNA, minus-strand RNA, and secreted HCV RNA in Keum et al. [35]. The model with the lowest AIC is highlighted in beige and the lowest AIC for each model is shown in bold. (DOCX)

**S4 Table. Parameter values of the (+) and (-)RNA secretion model.** Parameter values of the best-fit model that consider the secretion of HCV (+)RNA and (-)RNA (S2 and S4 Figs, S3 Table) with a delayed ramp-up secretion. Note that every secretion route is individual and hence,  $k_T \neq k_R \neq k_C$ ,  $\tau_T \neq \tau_R \neq \tau_C$ , and  $\rho_T \neq \rho_R \neq \rho_C$ . Parameter values in [] show 95% confidence intervals, while values marked with \* were kept fixed throughout the profile likelihood estimation. The degradation rate of HCV RNA within the RC was set to  $\mu_R = 0$  (see main text). (DOCX)

**S1 Text. Minus-strand and plus-strand HCV RNA as secretion sources.** (DOCX)

**S2 Text. Sensitivity analysis of the best fit model (CM<sub>4</sub>).** (DOCX)

**S1 Data.** (XLSX)

## Author Contributions

**Conceptualization:** Alan S. Perelson.

**Data curation:** Carolin Zitzmann, Alan S. Perelson.

**Formal analysis:** Carolin Zitzmann, Alan S. Perelson.

**Funding acquisition:** Lars Kaderali, Alan S. Perelson.

**Investigation:** Carolin Zitzmann, Alan S. Perelson.

**Methodology:** Alan S. Perelson.

**Project administration:** Alan S. Perelson.

**Resources:** Lars Kaderali, Alan S. Perelson.

**Software:** Carolin Zitzmann, Lars Kaderali, Alan S. Perelson.

**Supervision:** Alan S. Perelson.

**Validation:** Carolin Zitzmann, Alan S. Perelson.

**Visualization:** Carolin Zitzmann.

**Writing – original draft:** Carolin Zitzmann.

**Writing – review & editing:** Carolin Zitzmann, Lars Kaderali, Alan S. Perelson.

## References

1. World Health Organization. Hepatitis C. In: WHO [Internet]. 2018. Available from: <https://www.who.int/news-room/fact-sheets/detail/hepatitis-c>.
2. World Health Organization. Guidelines for the screening, care and treatment of persons with chronic hepatitis C infection. WHO. 2016; 140. <https://doi.org/10.1186/1471-2334-13-288> PMID: 23799878
3. Paul D, Bartenschlager R. Architecture and biogenesis of plus-strand RNA virus replication factories. World J Virol. 2013; 2:32–48. <https://doi.org/10.5501/wjv.v2.i2.32> PMID: 24175228

4. Paul D, Madan V, Bartschlagler R. Hepatitis C virus RNA replication and assembly: Living on the fat of the land. *Cell Host and Microbe*. 2014. pp. 569–579. <https://doi.org/10.1016/j.chom.2014.10.008> PMID: 25525790
5. Scheel TKH, Rice CM. Understanding the hepatitis C virus life cycle paves the way for highly effective therapies. *Nat Med*. 2013; 19:837–49. <https://doi.org/10.1038/nm.3248> PMID: 23836234
6. Chatel-Chaix L, Bartschlagler R. Dengue virus- and hepatitis C virus-induced replication. *J Virol*. 2014; 88:5907–5911.
7. Zhou L-Y, Zhang L-L. Host restriction factors for hepatitis C virus. *World J Gastroenterol*. 2016; 22:1477–86. <https://doi.org/10.3748/wjg.v22.i4.1477> PMID: 26819515
8. Randall G, Panis M, Cooper JD, Tellinghuisen TL, Sukhodolets KE, Pfeffer S, et al. Cellular cofactors affecting hepatitis C virus infection and replication. *Proc Natl Acad Sci U S A*. 2007; 104:12884–9. <https://doi.org/10.1073/pnas.0704894104> PMID: 17616579
9. Raab-Traub N, Dittmer DP. Viral effects on the content and function of extracellular vesicles. *Nat Rev Microbiol*. 2017; 15:559–572. <https://doi.org/10.1038/nrmicro.2017.60> PMID: 28649136
10. Vlassov A V., Magdaleno S, Setterquist R, Conrad R. Exosomes: Current knowledge of their composition, biological functions, and diagnostic and therapeutic potentials. *Biochimica et Biophysica Acta—General Subjects*. Elsevier; 2012. pp. 940–948. <https://doi.org/10.1016/j.bbagen.2012.03.017> PMID: 22503788
11. Meckes DG, Raab-Traub N. Microvesicles and viral infection. *J Virol*. 2011; 85: 12844–12854. <https://doi.org/10.1128/JVI.05853-11> PMID: 21976651
12. Gastaminza P, Dryden KA, Boyd B, Wood MR, Law M, Yeager M, et al. Ultrastructural and biophysical characterization of hepatitis C virus particles produced in cell culture. *J Virol*. 2010; 84:10999–1009. <https://doi.org/10.1128/JVI.00526-10> PMID: 20686033
13. Longatti A, Boyd B, Chisari F V. Virion-independent transfer of replication-competent hepatitis C virus RNA between permissive cells. Ou J-HJ, editor. *J Virol*. 2014; 89:2956–2961. <https://doi.org/10.1128/JVI.02721-14> PMID: 25505060
14. Masciopinto F, Giovani C, Campagnoli S, Galli-Stampino L, Colombatto P, Brunetto M, et al. Association of hepatitis C virus envelope proteins with exosomes. *Eur J Immunol*. 2004; 34:2834–2842. <https://doi.org/10.1002/eji.200424887> PMID: 15368299
15. Bukong TN, Momen-Heravi F, Kodys K, Bala S, Szabo G. Exosomes from hepatitis C infected patients transmit HCV infection and contain replication competent viral RNA in complex with Ago2-miR122-HSP90. Luo G, editor. *PLoS Pathog*. 2014; 10:e1004424. <https://doi.org/10.1371/journal.ppat.1004424> PMID: 25275643
16. Liu Z, Zhang X, Yu Q, He JJ. Exosome-associated hepatitis C virus in cell cultures and patient plasma. *Biochem Biophys Res Commun*. 2014; 455:218–222. <https://doi.org/10.1016/j.bbrc.2014.10.146> PMID: 25449270
17. Ramakrishnaiah V, Thumann C, Fofana I, Habersetzer F, Pan Q, de Ruiter PE, et al. Exosome-mediated transmission of hepatitis C virus between human hepatoma Huh7.5 cells. *Proc Natl Acad Sci*. 2013; 110:13109–13113. <https://doi.org/10.1073/pnas.1221899110> PMID: 23878230
18. Zhang W, Jiang X, Bao J, Wang Y, Liu H, Tang L. Exosomes in pathogen infections: A bridge to deliver molecules and link functions. *Front Immunol*. *Frontiers Media SA*; 2018. p. 90. <https://doi.org/10.3389/fimmu.2018.00090> PMID: 29483904
19. Saha B, Kodys K, Adejumo A, Szabo G. Circulating and exosome-packaged hepatitis C single-stranded RNA induce monocyte differentiation via TLR7/8 to polarized macrophages and fibrocytes. *J Immunol*. 2017; 198: 1974–1984. <https://doi.org/10.4049/jimmunol.1600797> PMID: 28122964
20. Zitzmann C, Kaderali L. Mathematical analysis of viral replication dynamics and antiviral treatment strategies: From basic models to age-based multi-scale modeling. *Front Microbiol*. *Frontiers*; 2018. p. 1546. <https://doi.org/10.3389/fmicb.2018.01546> PMID: 30050523
21. Neumann AU, Lam NP, Dahari H, Gretch DR, Wiley TE, Layden TJ, et al. Hepatitis C viral dynamics in vivo and the antiviral efficacy of interferon- $\alpha$  therapy. *Science*. 1998; 282:103–107. <https://doi.org/10.1126/science.282.5386.103> PMID: 9756471
22. Perelson AS. Modelling viral and immune system dynamics. *Nat Rev Immunol*. 2002; 2:28–36. <https://doi.org/10.1038/nri700> PMID: 11905835
23. Perelson AS, Neumann AU, Markowitz M, Leonard JM, Ho DD. HIV-1 dynamics in vivo: virion clearance rate, infected cell life-span, and viral generation time. *Science*. 1996; 271:1582–1586. <https://doi.org/10.1126/science.271.5255.1582> PMID: 8599114
24. Baccam P, Beauchemin C, Macken CA, Hayden FG, Perelson AS. Kinetics of influenza A virus infection in humans. *J Virol*. 2006; 80:7590–9. <https://doi.org/10.1128/JVI.01623-05> PMID: 16840338

25. Ke R, Li H, Wang S, Ding W, Ribeiro RM, Giorgi EE, et al. Superinfection and cure of infected cells as mechanisms for hepatitis C virus adaptation and persistence. *Proc Natl Acad Sci U S A*. 2018; 115: E7139–E7148. <https://doi.org/10.1073/pnas.1805267115> PMID: 29987026
26. Bonhoeffer S, May RM, Shaw GM, Nowak MA. Virus dynamics and drug therapy. *Proc Natl Acad Sci U S A*. 1997; 94:6971–6976. <https://doi.org/10.1073/pnas.94.13.6971> PMID: 9192676
27. Rong L, Perelson AS. Modeling HIV persistence, the latent reservoir, and viral blips. *J Theor Biol*. 2009; 260:308–331. <https://doi.org/10.1016/j.jtbi.2009.06.011> PMID: 19539630
28. Perelson AS, Ribeiro RM. Modeling the within-host dynamics of HIV infection. *BMC Biol*. 2013; 11:96. <https://doi.org/10.1186/1741-7007-11-96> PMID: 24020860
29. Boianelli A, Nguyen VK, Ebsensen T, Schulze K, Wilk E, Sharma N, et al. Modeling influenza virus infection: A roadmap for influenza research. *Viruses*. 2015; 7:5274–5304. <https://doi.org/10.3390/v7102875> PMID: 26473911
30. Quintela B de M, Conway JM, Hyman JM, Guedj J, dos Santos RW, Lobosco M, et al. A new age-structured multiscale model of the hepatitis C virus life-cycle during infection and therapy with direct-acting antiviral agents. *Front Microbiol*. 2018; 9:601. <https://doi.org/10.3389/fmicb.2018.00601> PMID: 29670586
31. Benzine T, Brandt R, Lovell WC, Yamane D, Neddermann P, De Francesco R, et al. NS5A inhibitors unmask differences in functional replicase complex half-life between different hepatitis C virus strains. Randall G, editor. *PLOS Pathog*. 2017; 13:e1006343. <https://doi.org/10.1371/journal.ppat.1006343> PMID: 28594932
32. Raue A, Steiert B, Schelker M, Kreutz C, Maiwald T, Hass H, et al. Data2Dynamics: a modeling environment tailored to parameter estimation in dynamical systems. *Bioinformatics*. 2015; 31:3558–3560. <https://doi.org/10.1093/bioinformatics/btv405> PMID: 26142188
33. Raue A, Schilling M, Bachmann J, Matteson A, Schelker M, Schelke M, et al. Lessons learned from quantitative dynamical modeling in systems biology. *PLoS One*. 2013; 8:e74335. <https://doi.org/10.1371/journal.pone.0074335> PMID: 24098642
34. Raue A, Kreutz C, Maiwald T, Bachmann J, Schilling M, Klingmüller U, et al. Structural and practical identifiability analysis of partially observed dynamical models by exploiting the profile likelihood. *Bioinformatics*. 2009; 25:1923–1929. <https://doi.org/10.1093/bioinformatics/btp358> PMID: 19505944
35. Keum SJ, Park SM, Park JH, Jung JH, Shin EJ, Jang SK. The specific infectivity of hepatitis C virus changes through its life cycle. *Virology*. 2012; 433:462–470. <https://doi.org/10.1016/j.virol.2012.08.046> PMID: 22999258
36. Rohatgi A. WebPlotDigitizer—Web based tool to extract data from plots, images, and maps. Arohathgi. 2010. Available from: <https://automeris.io/WebPlotDigitizer/>.
37. Burnham KP, Anderson DR. Model selection and multimodel inference: A practical information-theoretic approach. Springer. 2002; 488. <https://doi.org/10.2307/3802723>
38. Burnham KP, Anderson DR. Multimodel inference: Understanding AIC and BIC in model selection. *Sociological Methods and Research*. 261 Sociological Methods Research; 2004. pp. 261–304. <https://doi.org/10.1177/0049124104268644>
39. Marino S, Hogue IB, Ray CJ, Kirschner DE. A methodology for performing global uncertainty and sensitivity analysis in systems biology. *J Theor Biol*. 2008; 254:178–96. <https://doi.org/10.1016/j.jtbi.2008.04.011> PMID: 18572196
40. Grünvogel O, Colasanti O, Lee JY, Klöss V, Belouzard S, Reustle A, et al. Secretion of hepatitis C virus replication intermediates reduces activation of toll-like receptor 3 in hepatocytes. *Gastroenterology*. 2018; 154:2237–2251.e16. <https://doi.org/10.1053/j.gastro.2018.03.020> PMID: 29535029
41. Lee J-Y, Cortese M, Haselmann U, Tabata K, Romero-Brey I, Funaya C, et al. Spatiotemporal coupling of the hepatitis C virus replication cycle by creating a lipid droplet- proximal membranous replication compartment. *Cell Rep*. 2019; 27:3602–3617.e5. <https://doi.org/10.1016/j.celrep.2019.05.063> PMID: 31216478
42. Guedj J, Dahari H, Rong L, Sansone ND, Nettles RE, Cotler SJ, et al. Modeling shows that the NS5A inhibitor daclatasvir has two modes of action and yields a shorter estimate of the hepatitis C virus half-life. *Proc Natl Acad Sci U S A*. 2013; 110:3991–6. <https://doi.org/10.1073/pnas.1203110110> PMID: 23431163
43. Paul D, Hoppe S, Saher G, Krijnse-Locker J, Bartenschlager R. Morphological and biochemical characterization of the membranous hepatitis C virus replication compartment. *J Virol*. 2013; 87:10612–27. <https://doi.org/10.1128/JVI.01370-13> PMID: 23885072
44. Perelson AS, Guedj J. Modelling hepatitis C therapy-predicting effects of treatment. *Nat Rev Gastroenterol Hepatol*. 2015; 12:437–445. <https://doi.org/10.1038/nrgastro.2015.97> PMID: 26122475

45. Gao M, Nettles RE, Belema M, Snyder LB, Nguyen VN, Fridell RA, et al. Chemical genetics strategy identifies an HCV NS5A inhibitor with a potent clinical effect. *Nature*. 2010; 465:96–100. <https://doi.org/10.1038/nature08960> PMID: 20410884
46. Layden TJ, Layden JE, Ribeiro RM, Perelson AS. Mathematical modeling of viral kinetics: A tool to understand and optimize therapy. *Clin Liver Dis*. 2003; 7:163–178. [https://doi.org/10.1016/s1089-3261\(02\)00063-6](https://doi.org/10.1016/s1089-3261(02)00063-6) PMID: 12691465
47. Dahari H, Lo A, Ribeiro RM, Perelson AS. Modeling hepatitis C virus dynamics: Liver regeneration and critical drug efficacy. *J Theor Biol*. 2007; 247:371–381. <https://doi.org/10.1016/j.jtbi.2007.03.006> PMID: 17451750
48. Canini L, Perelson AS. Viral kinetic modeling: State of the art. *J Pharmacokinet Pharmacodyn*. 2014; 41:431–443. <https://doi.org/10.1007/s10928-014-9363-3> PMID: 24961742
49. Graw F, Perelson AS. Modeling viral spread. *Annu Rev Virol*. 2016; 3:555–572. <https://doi.org/10.1146/annurev-virology-110615-042249> PMID: 27618637
50. Chatterjee A, Guedj J, Perelson AS. Mathematical modelling of HCV infection: What can it teach us in the era of direct-acting antiviral agents? *Antivir Ther*. 2012; 17:1171–1182. <https://doi.org/10.3851/IMP2428> PMID: 23186606
51. Dahari H, Ribeiro RM, Rice CM, Perelson AS. Mathematical modeling of subgenomic hepatitis C virus replication in Huh-7 cells. *J Virol*. 2007; 81:750–60. <https://doi.org/10.1128/JVI.01304-06> PMID: 17035310
52. Binder M, Sulaimanov N, Clausznitzer D, Schulze M, Hüber CM, Lenz SM, et al. Replication vesicles are load- and choke-points in the hepatitis C virus lifecycle. *PLoS Pathog*. 2013; 9:e1003561. <https://doi.org/10.1371/journal.ppat.1003561> PMID: 23990783
53. Clausznitzer D, Harnisch J, Kaderali L. Multi-scale model for hepatitis C viral load kinetics under treatment with direct acting antivirals. *Virus Res*. 2015; 218:96–101. <https://doi.org/10.1016/j.virusres.2015.09.011> PMID: 26409026
54. Dreux M, Garaigorta U, Boyd B, Décembre E, Chung J, Whitten-Bauer C, et al. Short-range exosomal transfer of viral RNA from infected cells to plasmacytoid dendritic cells triggers innate immunity. *Cell Host Microbe*. 2012; 12:558–70. <https://doi.org/10.1016/j.chom.2012.08.010> PMID: 23084922
55. Pearson JE, Krapivsky P, Perelson AS. Stochastic theory of early viral infection: Continuous versus burst production of virions. *PLoS Comput Biol*. 2011; 7:e1001058. <https://doi.org/10.1371/journal.pcbi.1001058> PMID: 21304934
56. Quinkert D, Bartenschlager R, Lohmann V. Quantitative analysis of the hepatitis C virus replication complex. *J Virol*. 2005; 79:13594–13605. <https://doi.org/10.1128/JVI.79.21.13594-13605.2005> PMID: 16227280
57. Bartenschlager R, Penin F, Lohmann V, André P. Assembly of infectious hepatitis C virus particles. *Trends Microbiol*. 2011; 19:95–103. <https://doi.org/10.1016/j.tim.2010.11.005> PMID: 21146993
58. Catanese MT, Uryu K, Kopp M, Edwards TJ, Andrus L, Rice WJ, et al. Ultrastructural analysis of hepatitis C virus particles. *Proc Natl Acad Sci U S A*. 2013; 110:9505–10. <https://doi.org/10.1073/pnas.1307527110> PMID: 23690609
59. Deng L, Jiang W, Wang X, Merz A, Hiet MS, Chen Y, et al. Syntenin regulates hepatitis C virus sensitivity to neutralizing antibody by promoting E2 secretion through exosomes. *J Hepatol*. 2019; 71:52–61. <https://doi.org/10.1016/j.jhep.2019.03.006> PMID: 30880226
60. Chatel-Chaix L, Melançon P, Racine M-È, Baril M, Lamarre D. Y-box-binding protein 1 interacts with hepatitis C virus NS3/4A and influences the equilibrium between viral RNA replication and infectious particle production. *J Virol*. 2011; 85:11022–37. <https://doi.org/10.1128/JVI.00719-11> PMID: 21849455
61. Masaki T, Arend KC, Li Y, Yamane D, McGivern DR, Kato T, et al. MiR-122 stimulates hepatitis C virus RNA synthesis by altering the balance of viral RNAs engaged in replication versus translation. *Cell Host Microbe*. 2015; 17:217–228. <https://doi.org/10.1016/j.chom.2014.12.014> PMID: 25662750
62. Heldt FS, Frensing T, Reichl U. Modeling the intracellular dynamics of influenza virus replication to understand the control of viral RNA synthesis. *J Virol*. 2012; 86:7806–17. <https://doi.org/10.1128/JVI.00080-12> PMID: 22593159
63. Appel N, Zayas M, Miller S, Krijnse-Locker J, Schaller T, Friebe P, et al. Essential role of domain III of nonstructural protein 5A for hepatitis C virus infectious particle assembly. *PLoS Pathog*. 2008; 4:e1000035. <https://doi.org/10.1371/journal.ppat.1000035> PMID: 18369481
64. Zeisel MB, Lupberger J, Fofana I, Baumert TF. Host-targeting agents for prevention and treatment of chronic hepatitis C—Perspectives and challenges. *J Hepatol*. 2013; 58:375–384. <https://doi.org/10.1016/j.jhep.2012.09.022> PMID: 23041307

65. van Dongen HM, Masoumi N, Witwer KW, Pegtel DM. Extracellular vesicles exploit viral entry routes for cargo delivery. *Microbiol Mol Biol Rev.* 2016; 80:369–386. <https://doi.org/10.1128/MMBR.00063-15> PMID: 26935137
66. Broering TJ, Garrity KA, Boatright NK, Sloan SE, Sandor F, Thomas WD, et al. Identification and characterization of broadly neutralizing human monoclonal antibodies directed against the E2 envelope glycoprotein of hepatitis C virus. *J Virol.* 2009; 83:12473–12482. <https://doi.org/10.1128/JVI.01138-09> PMID: 19759151
67. Meuleman P, Hesselgesser J, Paulson M, Vanwolleghem T, Desombere I, Reiser H, et al. Anti-CD81 antibodies can prevent a hepatitis C virus infection in vivo. *Hepatology.* 2008; 48:1761–1768. <https://doi.org/10.1002/hep.22547> PMID: 19030166
68. Morin TJ, Broering TJ, Leav BA, Blair BM, Rowley KJ. Human monoclonal antibody HCV1 effectively prevents and treats HCV infection in chimpanzees. *PLoS Pathog.* 2012; 8:1002895. <https://doi.org/10.1371/journal.ppat.1002895> PMID: 22952447
69. Lindenbach BD, Evans MJ, Syder AJ, Wölk B, Tellinghuisen TL, Liu CC, et al. Complete replication of hepatitis C virus in cell culture. *Science (80-).* 2005; 309:623–626. <https://doi.org/10.1126/science.1114016> PMID: 15947137
70. Owsianka AM, Tarr AW, Keck ZY, Li TK, Witteveldt J, Adair R, et al. Broadly neutralizing human monoclonal antibodies to the hepatitis C virus E2 glycoprotein. *J Gen Virol.* 2008; 89:653–659. <https://doi.org/10.1099/vir.0.83386-0> PMID: 18272755
71. Timpe JM, Stamatakis Z, Jennings A, Hu K, Farquhar MJ, Harris HJ, et al. Hepatitis C virus cell-cell transmission in hepatoma cells in the presence of neutralizing antibodies. *Hepatology.* 2007; 47:17–24. <https://doi.org/10.1002/hep.21959> PMID: 17941058
72. Witteveldt J, Evans MJ, Bitzegeio J, Koutsoudakis G, Owsianka AM, Angus AGN, et al. CD81 is dispensable for hepatitis C virus cell-to-cell transmission in hepatoma cells. *J Gen Virol.* 2009; 90:48–58. <https://doi.org/10.1099/vir.0.006700-0> PMID: 19088272
73. Brimacombe CL, Grove J, Meredith LW, Hu K, Syder AJ, Flores M V., et al. Neutralizing antibody-resistant hepatitis C virus cell-to-cell transmission. *J Virol.* 2011; 85:596–605. <https://doi.org/10.1128/JVI.01592-10> PMID: 20962076
74. Wang L, Cao D, Wang L, Zhao J, Nguyen LN, Dang X, et al. HCV-associated exosomes promote myeloid-derived suppressor cell expansion via inhibiting miR-124 to regulate T follicular cell differentiation and function. *Cell Discov.* 2018; 4:51. <https://doi.org/10.1038/s41421-018-0052-z> PMID: 30210805
75. Welker MW, Reichert D, Susser S, Sarrazin C, Martinez Y, Herrmann E, et al. Soluble serum CD81 is elevated in patients with chronic hepatitis C and correlates with alanine aminotransferase serum activity. *PLoS One.* 2012; 7:30796. <https://doi.org/10.1371/journal.pone.0030796> PMID: 22355327
76. Fritzsche B, Schwer B, Kartenbeck J, Pedal A, Horejsi V, Ott M. Release and intercellular transfer of cell surface CD81 via microparticles. *J Immunol.* 2002; 169:5531–5537. <https://doi.org/10.4049/jimmunol.169.10.5531> PMID: 12421929
77. Afdhal N, Zeuzem S, Kwo P, Chojkier M, Gitlin N, Puoti M, et al. Ledipasvir and sofosbuvir for untreated HCV genotype 1 infection. *N Engl J Med.* 2014; 370:1889–1898. <https://doi.org/10.1056/NEJMoa1402454> PMID: 24725239
78. Cosset F-L, Turlure F, Denolly S, Boson B, Dreux M, Chamot C. Daclatasvir prevents hepatitis C virus infectivity by blocking transfer of the viral genome to assembly sites. *Gastroenterology.* 2016; 152:895–907.e14. <https://doi.org/10.1053/j.gastro.2016.11.047> PMID: 27932311
79. Nguyen THT, Guedj J, Uprichard SL, Kohli A, Kottillil S, Perelson AS. The paradox of highly effective sofosbuvir-based combination therapy despite slow viral decline: can we still rely on viral kinetics? *Sci Rep.* 2017; 7:10233. <https://doi.org/10.1038/s41598-017-09776-z> PMID: 28860456
80. Hezode C, Chevaliez S, Scoazec G, Bouvier-Alias M, Ruiz I, Francois M, et al. P0843: On-treatment viral kinetics do not predict SVR in patients with advanced liver disease receiving sofosbuvir in combination with daclatasvir or simeprevir for 12 weeks. *J Hepatol.* 2015; 62:S654–S655. [https://doi.org/10.1016/S0168-8278\(15\)31045-X](https://doi.org/10.1016/S0168-8278(15)31045-X)



# APPENDIX

## Supplementary material

The supplementary material for all three publications is published and can be found online.

## **Eidesstattliche Erklärung**

Hiermit erkläre ich, dass ich die vorliegende Dissertation selbständig verfasst und keine anderen als die angegebenen Hilfsmittel benutzt habe.

Die Dissertation ist bisher keiner anderen Fakultät, keiner anderen wissenschaftlichen Einrichtung vorgelegt worden.

Ich erkläre, dass ich bisher kein Promotionsverfahren erfolglos beendet habe und dass eine Aberkennung eines bereits erworbenen Doktorgrades nicht vorliegt.

---

Datum

---

Unterschrift

# REFERENCES

- [1] Mark J Abzug, Marian G Michaels, Ellen Wald, Richard F Jacobs, José R Romero, Pablo J Sánchez, Gregory Wilson, Paul Krogstad, Gregory A Storch, Robert Lawrence, et al. A randomized, double-blind, placebo-controlled trial of pleconaril for the treatment of neonates with enterovirus sepsis. *Journal of the Pediatric Infectious Diseases Society*, 5(1):53–62, 2016. doi: 10.1093/jpids/piv015.
- [2] Eliana G Acosta and Ralf Bartenschlager. The quest for host targets to combat dengue virus infections. *Current Opinion in Virology*, 20:47–54, 2016. doi: 10.1016/j.coviro.2016.09.003.
- [3] JC Adkins and AJ Wagstaff. Recombinant hepatitis b vaccine: a review of its immunogenicity and protective efficacy against hepatitis b. *BioDrugs: clinical immunotherapeutics, biopharmaceuticals and gene therapy*, 10:137–158, 1998. doi: 10.2165/00063030-199810020-00005.
- [4] Mukhtar Ahmed, Muhammad Ali Raza, and Taimoor Hussain. Dynamic modeling, 2020. URL [http://link.springer.com/10.1007/978-981-15-4728-7\\_4](http://link.springer.com/10.1007/978-981-15-4728-7_4).
- [5] Philipp M. Altrock, Lin L. Liu, and Franziska Michor. The mathematics of cancer: integrating quantitative models. *Nature Reviews Cancer*, 15:730–745, 2015. doi: 10.1038/nrc4029.
- [6] Takayuki Amemiya, M. Michael Gromiha, Katsuhisa Horimoto, and Kazuhiko Fukui. Drug repositioning for dengue haemorrhagic fever by integrating multiple omics analyses. *Scientific Reports* 2019 9:1, 9:1–13, 2019. doi: 10.1038/s41598-018-36636-1.
- [7] Masashi Arakawa and Eiji Morita. Flavivirus replication organelle biogenesis in the endoplasmic reticulum: Comparison with other single-stranded positive-sense rna viruses. *International Journal of Molecular Sciences*, 20:2336, 2019. doi: 10.3390/ijms20092336.
- [8] Esam I. Azhar, Sherif A. El-Kafrawy, Suha A. Farraj, Ahmed M. Hassan, Muneera S. Al-Saeed, Anwar M. Hashem, and Tariq A. Madani. Evidence for camel-to-human transmission of mers coronavirus. *New England Journal of Medicine*, 370:2499–2505, 2014. doi: 10.1056/NEJMoa1401505.
- [9] Alexandre Balaphas, Jeremy Meyer, Rémy Sadoul, Philippe Morel, Carmen Gonelle-Gispert, and Leo Hans Bühler. Extracellular vesicles: Future diagnostic and therapeutic tools for liver disease and regeneration. *Liver International*, page liv.14189, 2019. doi: 10.1111/liv.14189.
- [10] Bas W.M. Van Balkom, Almut S. Eisele, D. Michiel Pegtel, Sander Bervoets, and Marianne C. Verhaar. Quantitative and qualitative analysis of small rnas in human endothelial cells and exosomes provides insights into localized rna processing, degradation and sorting. *Journal of Extracellular Vesicles*, 4:1–14, 2015. doi: 10.3402/jev.v4.26760.
- [11] Rodolphe Barrangou, Amanda Birmingham, Stefan Wiemann, Roderick L. Beijersbergen, Veit Hornung, and Anja van Brabant Smith. Advances in crispr-cas9 genome engineering: lessons learned from rna interference. *Nucleic Acids Research*, 43:3407–3419, 2015. doi: 10.1093/NAR/GKV226.
- [12] Ralf Bartenschlager, Thomas F. Baumert, Jens Bukh, Michael Houghton, Stanley M. Lemon, Brett D. Lindenbach, Volker Lohmann, Darius Moradpour, Thomas Pietschmann, Charles M. Rice, Robert Thimme, and Takaji Wakita. Critical challenges and emerging opportunities in hepatitis c virus research in an era of potent antiviral therapy: Considerations for scientists and funding agencies. *Virus research*, 248:53–62, 2018. doi: 10.1016/J.VIRUSRES.2018.02.016.
- [13] Amy L Bauer, Catherine A.A. Beauchemin, and Alan S Perelson. Agent-based modeling of host-pathogen systems: The successes and challenges. *Information Sciences*, 179:1379–1389, 2009. doi: 10.1016/j.ins.2008.11.012.
- [14] Lisa Bauer, Heyrhyoung Lyoo, Hilde M van der Schaar, Jeroen RPM Strating, and Frank JM van Kuppeveld. Direct-acting antivirals and host-targeting strategies to combat enterovirus infections. *Current Opinion in Virology*, 24:1–8, 2017. ISSN 1879-6257. doi: <https://doi.org/10.1016/j.coviro.2017.03.009>.

- [15] George A Belov and Frank JM van Kuppeveld. (+)rna viruses rewire cellular pathways to build replication organelles. *Current Opinion in Virology*, 2:740–747, 2012. doi: 10.1016/j.coviro.2012.09.006.
- [16] Marco Binder, Georg Kochs, Ralf Bartenschlager, and Volker Lohmann. Hepatitis c virus escape from the interferon regulatory factor 3 pathway by a passive and active evasion strategy. *Hepatology*, 46:1365–1374, 2007. doi: 10.1002/hep.21829.
- [17] Marco Binder, Nurgazy Sulaimanov, Diana Clausnitzer, Manuel Schulze, Christian M. Hüber, Simon M. Lenz, Johannes P. Schlöder, Martin Trippler, Ralf Bartenschlager, Volker Lohmann, and Lars Kaderali. Replication vesicles are load- and choke-points in the hepatitis c virus lifecycle. *PLoS Pathogens*, 9:e1003561, 2013. doi: 10.1371/journal.ppat.1003561.
- [18] Michael Boutros and Julie Ahringer. The art and design of genetic screens: Rna interference. *Nature Reviews Genetics*, 9:554–566, 2008. doi: 10.1038/nrg2364.
- [19] Terence N. Bukong, Fatemeh Momen-Heravi, Karen Kodys, Shashi Bala, and Gyongyi Szabo. Exosomes from hepatitis c infected patients transmit hcv infection and contain replication competent viral rna in complex with ago2-mir122-hsp90. *PLoS Pathogens*, 10:e1004424, 2014. doi: 10.1371/journal.ppat.1004424.
- [20] Laura A Byk, Néstor G Iglesias, Federico A De Maio, Leopoldo G Gebhard, Mario Rossi, and Andrea V Gamarnik. Dengue virus genome uncoating requires ubiquitination. *mBio*, 7:e00804–16, 2016. doi: 10.1128/mBio.00804-16.
- [21] MT Catanese, K Uryu, M Kopp, TJ Edwards, L Andrus, WJ Rice, M Silvestry, RJ Kuhn, and SM Rice. Ultrastructural analysis of hepatitis c virus particles. *Proceedings of the National Academy of Sciences of the United States of America*, 110:9505–9510, 2013. doi: 10.1073/PNAS.1307527110.
- [22] Harendra Singh Chahar, Xiaoyong Bao, and Antonella Casola. Exosomes and their role in the life cycle and pathogenesis of rna viruses. *Viruses*, 7:3204–3225, 2015. doi: 10.3390/v7062770.
- [23] Paul K.S. Chan and Martin C.W. Chan. Tracing the sars-coronavirus. *Journal of Thoracic Disease*, 5: S118, 2013. doi: 10.3978/j.issn.2072-1439.2013.06.19.
- [24] Takol Chareonsirisuthigul, Siripen Kalayanarooj, and Sukathida Ubol. Dengue virus (denv) antibody-dependent enhancement of infection upregulates the production of anti-inflammatory cytokines, but suppresses anti-denv free radical and pro-inflammatory cytokine production, in thp-1 cells. *Journal of General Virology*, 88:365–375, 2007. doi: 10.1099/vir.0.82537-0.
- [25] Laurent Chatel-Chaix and Ralf Bartenschlager. Dengue virus- and hepatitis c virus-induced replication. *Journal of Virology*, 88:5907 – 5911, 2014. doi: <https://doi.org/10.1128/JVI.03404-13>.
- [26] Laurent Chatel-Chaix, Pierre Melançon, Marie Ève Racine, Martin Baril, and Daniel Lamarre. Y-box-binding protein 1 interacts with hepatitis c virus ns3/4a and influences the equilibrium between viral rna replication and infectious particle production. *Journal of virology*, 85:11022–37, 2011. doi: 10.1128/JVI.00719-11.
- [27] Laurent Chatel-Chaix, Marie-Anne Germain, Alena Motorina, Éric Bonneil, Pierre Thibault, Martin Baril, and Daniel Lamarre. A host yb-1 ribonucleoprotein complex is hijacked by hepatitis c virus for the control of ns3-dependent particle production. *Journal of virology*, 87:11704–20, 2013. doi: 10.1128/JVI.01474-13.
- [28] Francesco Checchi, Michelle Gayer, Rebecca Freeman Grais, and Edward J Mills. *Public health in crisis-affected populations: A practical guide for decision-makers*. 2007. ISBN 9780850038552.
- [29] Sun Ku Chung, Joo Young Kim, In Beom Kim, Sang Ick Park, Kyung Hee Paek, and Jae Hwan Nam. Internalization and trafficking mechanisms of coxsackievirus b3 in hela cells. *Virology*, 333:31–40, 2005. doi: 10.1016/J.VIROL.2004.12.010.
- [30] Che C. Colpitts, Pei-Ling Tsai, and Mirjam B. Zeisel. Hepatitis c virus entry: An intriguingly complex and highly regulated process. *International Journal of Molecular Sciences 2020, Vol. 21, Page 2091*, 21:2091, 2020. doi: 10.3390/IJMS21062091.
- [31] Emery D. Conrad and John J. Tyson. Modeling molecular interaction networks with nonlinear ordinary differential equations, 2013.
- [32] Brennetta J Crenshaw, Linlin Gu, Brian Sims, and Qiana L Matthews. Exosome biogenesis and biological function in response to viral infections. *The Open Virology Journal*, 12:134–148, 2018. doi: 10.2174/1874357901812010134.

- [33] Christine Cruz-Oliveira, João Miguel Freire, Thaís M. Conceição, Luiza M. Higa, Miguel A.R.B. Castanho, and Andrea T. Da Poian. Receptors and routes of dengue virus entry into the host cells. *FEMS Microbiology Reviews*, 39:155–170, 2015. doi: 10.1093/femsre/fuu004.
- [34] David Cyranoski. Did pangolins spread the china coronavirus to people? *Nature*, 2020. doi: 10.1038/d41586-020-00364-2.
- [35] Leen Delang, Jan Paeshuyse, and Johan Neyts. The role of phosphatidylinositol 4-kinases and phosphatidylinositol 4-phosphate during viral replication. *Biochemical Pharmacology*, 84:1400, 2012. doi: 10.1016/J.BCP.2012.07.034.
- [36] Kylie H. Van der Hoek, Nicholas S. Eyre, Byron Shue, Onruedee Khantisitthiporn, Kittirat Glab-Ampi, Jillian M. Carr, Matthew J. Gartner, Lachlan A. Jolly, Paul Q. Thomas, Fatwa Adikusuma, Tanja Jankovic-Karasoulos, Claire T. Roberts, Karla J. Helbig, and Michael R. Beard. Viperin is an important host restriction factor in control of zika virus infection. *Scientific Reports* 2017 7:1, 7:1–14, 2017. doi: 10.1038/s41598-017-04138-1.
- [37] Mayra Diosa-Toro, Berit Troost, Denise van de Pol, Alexander Martin Heberle, Silvio Urcuqui-Inchima, Kathrin Thedieck, and Jolanda M. Smit. Tomatidine, a novel antiviral compound towards dengue virus. *Antiviral Research*, 161:90–99, 2019. doi: 10.1016/j.antiviral.2018.11.011.
- [38] Ensheng Dong, Hongru Du, and Lauren Gardner. An interactive web-based dashboard to track covid-19 in real time. *The Lancet Infectious Diseases*, 3099:19–20, 2020. doi: 10.1016/S1473-3099(20)30120-1.
- [39] Jennifer K. Dowling and Ashley Mansell. Toll-like receptors: The swiss army knife of immunity and vaccine development. *Clinical and Translational Immunology*, 5:e85, 2016. doi: 10.1038/cti.2016.22.
- [40] Lynn B. Dustin. Innate and adaptive immune responses in chronic hcv infection. *Current Drug Targets*, 18:826–843, 2015. doi: 10.2174/1389450116666150825110532.
- [41] Christopher Dächert, Evgeny Gladilin, and Marco Binder. Gene expression profiling of different huh7 variants reveals novel hepatitis c virus host factors. *Viruses*, 12:36, 2019. doi: 10.3390/v12010036.
- [42] James R. Edgar. Qa: What are exosomes, exactly? *BMC Biology*, 14:46, 2016. doi: 10.1186/s12915-016-0268-z.
- [43] Raluca Eftimie, Joseph J Gillard, and Doreen A Cantrell. Mathematical models for immunology: Current state of the art and future research directions. *Bull Math Biol*, 78:2091–2134, 2016. doi: 10.1007/s11538-016-0214-9.
- [44] Ahmed El-Shamy, Andrea D. Branch, Thomas D. Schiano, and Peter D. Gorevic. The complement system and c1q in chronic hepatitis c virus infection and mixed cryoglobulinemia. *Frontiers in Immunology*, 9, 2018. doi: 10.3389/fimmu.2018.01001.
- [45] Enyue Fang, Xiaohui Liu, Miao Li, Zelun Zhang, Lifang Song, Baiyu Zhu, Xiaohong Wu, Jingjing Liu, Danhua Zhao, and Yuhua Li. Advances in covid-19 mrna vaccine development. *Signal Transduction and Targeted Therapy*, 7(1):1–31, 2022. doi: 10.1038/s41392-022-00950-y.
- [46] Zongdi Feng, Lucinda Hensley, Kevin L. McKnight, Fengyu Hu, Victoria Madden, Lifang Ping, Sook Hyang Jeong, Christopher Walker, Robert E. Lanford, and Stanley M. Lemon. A pathogenic picornavirus acquires an envelope by hijacking cellular membranes. *Nature*, 496:367–371, 2013. doi: 10.1038/nature12029.
- [47] Bernard N. Fields, David M. (David Mahan) Knipe, and Peter M. Howley. *Fields virology*. Wolters Kluwer Health/Lippincott Williams and Wilkins, 2013. ISBN 1451105630, 9781451105636.
- [48] Katherine A Fitzgerald and Jonathan C Kagan. Toll-like receptors and the control of immunity. *Cell*, 180:1044–1066, 2020. doi: 10.1016/j.cell.2020.02.041.
- [49] S J Flint, L W Enquist, V R Racaniello, and A M Skalka. *Principles of virology : molecular biology, pathogenesis and control of animal viruses*. ASM Press, 2009. ISBN 9781555816308.
- [50] Centers for Disease Control and Prevention. Nitazoxanide | cryptosporidium | parasites | cdc, 2021. URL <https://www.cdc.gov/parasites/crypto/nitazoxanide.html>.
- [51] PLISA Health Information Platform for the Americas. Pan american health organization/world health organization data, 2022. URL [http://www.paho.org/data/index.php/en/?option=com\\_content&view=article&id=524&Itemid=](http://www.paho.org/data/index.php/en/?option=com_content&view=article&id=524&Itemid=).

- [52] Haydar Frangoul, David Altshuler, M. Domenica Cappellini, Yi-Shan Chen, Jennifer Domm, Brenda K. Eustace, Juergen Foell, Josu de la Fuente, Stephan Grupp, Rupert Handgretinger, Tony W. Ho, Antonis Kattamis, Andrew Kernytsky, Julie Lekstrom-Himes, Amanda M. Li, Franco Locatelli, Markus Y. Mapara, Mariane de Montalembert, Damiano Rondelli, Akshay Sharma, Sujit Sheth, Sandeep Soni, Martin H. Steinberg, Donna Wall, Angela Yen, and Selim Corbacioglu. Crispr-cas9 gene editing for sickle cell disease and  $\beta$ -thalassemia. *New England Journal of Medicine*, 384:252–260, 2021. doi: 10.1056/nejmoa2031054.
- [53] Farshid S Garmaroudi, David Marchant, Reid Hendry, Honglin Luo, Decheng Yang, Xin Ye, Junyan Shi, and Bruce M Mcmanus. Coxsackievirus b3 replication and pathogenesis. 10:629–652, 2015.
- [54] THEMIS Bioscience GmbH. Vaccines and related biological products advisory committee, 2019. URL <https://www.fda.gov/media/132288/download>.
- [55] Belinda J. Goldie, Matthew D. Dun, Minjie Lin, Nathan D. Smith, Nicole M. Verrills, Christopher V. Dayas, and Murray J. Cairns. Activity-associated mirna are packaged in map1b-enriched exosomes released from depolarized neurons. *Nucleic Acids Research*, 42:9195–9208, 2014. doi: 10.1093/nar/gku594.
- [56] Delphine Goubau, Safia Deddouche, and Caetano Reis e Sousa. Cytosolic sensing of viruses. *Immunity*, 38:855–869, 2013. doi: 10.1016/j.immuni.2013.05.007.
- [57] Elizabeth A. Grice and Julia A. Segre. The skin microbiome. *Nature Reviews Microbiology*, 9:244–253, 2011. doi: 10.1038/nrmicro2537.
- [58] Jasenka Guduric-Fuchs, Anna O'Connor, Bailey Camp, Christina L. O'Neill, Reinhold J. Medina, and David A. Simpson. Selective extracellular vesicle-mediated export of an overlapping set of micrnas from multiple cell types. *BMC Genomics*, 13, 2012. doi: 10.1186/1471-2164-13-357.
- [59] Sangiliyandi Gurunathan, Min Hee Kang, and Jin-Hoi Kim. Diverse effects of exosomes on covid-19: a perspective of progress from transmission to therapeutic developments. *Frontiers in Immunology*, 12, 2021. doi: <https://doi.org/10.3389/fimmu.2021.716407>.
- [60] Maria G. Guzman, Duane J. Gubler, Alienys Izquierdo, Eric Martinez, and Scott B. Halstead. Dengue infection. *Nature Reviews Disease Primers*, 2, 2016. doi: 10.1038/nrdp.2016.55.
- [61] Eric J Haas, Frederick J Angulo, John M McLaughlin, Emilia Anis, Shepherd R Singer, Farid Khan, Nati Brooks, Meir Smaja, Gabriel Mircus, Kaijie Pan, Jo Southern, David L Swerdlow, Luis Jodar, Yeheskel Levy, and Sharon Alroy-Preis. Impact and effectiveness of mrna bnt162b2 vaccine against sars-cov-2 infections and covid-19 cases, hospitalisations, and deaths following a nationwide vaccination campaign in israel: an observational study using national surveillance data. *The Lancet*, 397:1819–1829, 2021. doi: 10.1016/S0140-6736(21)00947-8.
- [62] Mohamed Lamine Hafirassou, Laurent Meertens, Claudia Umaña-Díaz, Athena Labeau, Ophelie Dejarnac, Lucie Bonnet-Madin, Beate M. Kümmerer, Constance Delaugerre, Philippe Roingard, Pierre Olivier Vidalain, and Ali Amara. A global interactome map of the dengue virus ns1 identifies virus restriction and dependency host factors. *Cell Reports*, 21:3900–3913, 2017. doi: 10.1016/j.celrep.2017.11.094.
- [63] S. B. Halstead and E. J. O'Rourke. Antibody-enhanced dengue virus infection in primate leukocytes. *Nature*, 265:739–741, 1977. doi: 10.1038/265739a0.
- [64] Gregory J. Hannon. Rna interference. *Nature*, 418:244–251, 2002. doi: 10.1038/418244a.
- [65] Christian Harak and Volker Lohmann. Ultrastructure of the replication sites of positive-strand rna viruses. *Virology*, 479-480:418–433, 2015. doi: 10.1016/J.VIROL.2015.02.029.
- [66] Lei Hei and Jin Zhong. Laboratory of genetics and physiology 2 (lgp2) plays an essential role in hepatitis c virus infection-induced interferon responses. *Hepatology*, 65:1478–1491, 2017. doi: 10.1002/HEP.29050.
- [67] Markus H. Heim. Innate immunity and hcv. *Journal of Hepatology*, 58:564–574, 2013. doi: 10.1016/j.jhep.2012.10.005.
- [68] Markus H. Heim and Robert Thimme. Innate and adaptive immune responses in hcv infections. *Journal of Hepatology*, 61:S14–S25, 2014. doi: 10.1016/j.jhep.2014.06.035.

- [69] Karla J. Helbig, Jillian M. Carr, Julie K. Calvert, Satiya Wati, Jennifer N. Clarke, Nicholas S. Eyre, Sumudu K. Narayana, Guillaume N. Fiches, Erin M. McCartney, and Michael R. Beard. Viperin is induced following dengue virus type-2 (denv-2) infection and has anti-viral actions requiring the c-terminal end of viperin. *PLoS Neglected Tropical Diseases*, 7:e2178, 2013. doi: 10.1371/journal.pntd.0002178.
- [70] C. Hezode, S. Chevaliez, G. Scoazec, M. Bouvier-Alias, I. Ruiz, M. Francois, A. Mallat, C. Feray, and J.-M. Pawlotsky. P0843: On-treatment viral kinetics do not predict svr in patients with advanced liver disease receiving sofosbuvir in combination with daclatasvir or simeprevir for 12 weeks. *Journal of Hepatology*, 62:S654–S655, 2015. doi: 10.1016/S0168-8278(15)31045-X.
- [71] Alison L. Hill, Daniel I.S. Rosenbloom, Martin A. Nowak, and Robert F. Siliciano. Insight into treatment of hiv infection from viral dynamics models. *Immunological Reviews*, 285:9–25, 2018. doi: 10.1111/imr.12698.
- [72] Ryohei Hirose, Hiroshi Ikegaya, Yuji Naito, Naoto Watanabe, Takuma Yoshida, Risa Bandou, Tomo Daidoji, Yoshito Itoh, and Takaaki Nakaya. Survival of sars-cov-2 and influenza virus on the human skin: Importance of hand hygiene in covid-19. *Clinical Infectious Diseases*, 2020. doi: 10.1093/cid/ciaa1517.
- [73] Bing Ching Ho, Sung Liang Yu, Jeremy J.W. Chen, Sui Yuan Chang, Bo Shiun Yan, Qi Sheng Hong, Sher Singh, Chuan Liang Kao, Hsuan Yu Chen, Kang Yi Su, Ker Chau Li, Chiou Ling Cheng, Hao Wei Cheng, Jen Yi Lee, Chun Nan Lee, and Pan Chyr Yang. Enterovirus-induced mir-141 contributes to shutoff of host protein translation by targeting the translation initiation factor eif4e. *Cell Host and Microbe*, 9:58–69, 2011. doi: 10.1016/J.CHOM.2010.12.001.
- [74] James M. Hogle. Poliovirus cell entry: Common structural themes in viral cell entry pathways. *Annual review of microbiology*, 56:677, 2002. doi: 10.1146/ANNUREV.MICRO.56.012302.160757.
- [75] Nai Yun Hsu, Olha Ilnytska, Georgiy Belov, Marianita Santiana, Ying Han Chen, Peter M. Takvorian, Cyrilla Pau, Hilde van der Schaar, Neerja Kaushik-Basu, Tamas Balla, Craig E. Cameron, Elie Ehrenfeld, Frank J.M. van Kuppeveld, and Nihal Altan-Bonnet. Viral reorganization of the secretory pathway generates distinct organelles for rna replication. *Cell*, 141:799–811, 2010. doi: 10.1016/j.cell.2010.03.050.
- [76] Jennifer L. Hyde and Michael S. Diamond. Innate immune restriction and antagonism of viral rna lacking 2'-o methylation. *Virology*, 479-480:66–74, 2015. doi: 10.1016/j.virol.2015.01.019.
- [77] Brian P. Ingalls. *Mathematical modeling in systems biology: an introduction*, volume 51. The MIT Press, 2014. ISBN 0262018888. doi: 10.5860/choice.51-3830.
- [78] Benjamin Israelow, Christopher M. Narbus, Marion Sourisseau, and Matthew J. Evans. Hepg2 cells mount an effective antiviral interferon-lambda based innate immune response to hepatitis c virus infection. *Hepatology*, 60:1170–1179, 2014. doi: 10.1002/hep.27227.
- [79] Søren Jensen and Allan Randrup Thomsen. Sensing of rna viruses: A review of innate immune receptors involved in recognizing rna virus invasion. 2012. doi: 10.1128/JVI.05738-11.
- [80] Xingyue Ji and Zhuorong Li. Medicinal chemistry strategies toward host targeting antiviral agents. *Medicinal Research Reviews*, 40:1519–1557, 2020. doi: 10.1002/MED.21664.
- [81] Dong Jiang, Jessica M. Weidner, Min Qing, Xiao-Ben Pan, Haitao Guo, Chunxiao Xu, Xianchao Zhang, Alex Birk, Jinhong Chang, Pei-Yong Shi, Timothy M. Block, and Ju-Tao Guo. Identification of five interferon-induced cellular proteins that inhibit west nile virus and dengue virus infections. *Journal of Virology*, 84:8332–8341, 2010. doi: 10.1128/jvi.02199-09.
- [82] Martin Jinek, Krzysztof Chylinski, Ines Fonfara, Michael Hauer, Jennifer A. Doudna, and Emmanuelle Charpentier. A programmable dual-rna-guided dna endonuclease in adaptive bacterial immunity. *Science*, 337:816–821, 2012. doi: 10.1126/SCIENCE.1225829.
- [83] Kenneth A. Johnson and Roger S. Goody. The original michaelis constant: Translation of the 1913 michaelis-menten paper. *Biochemistry*, 50:8264–8269, 2011. doi: 10.1021/bi201284u.
- [84] Raghu Kalluri and Valerie S. LeBleu. The biology, function, and biomedical applications of exosomes. *Science*, 367, 2020. doi: 10.1126/science.aau6977.
- [85] Rafal Kaminski, Yilan Chen, Tracy Fischer, Ellen Tedaldi, Alessandro Napoli, Yonggang Zhang, Jonathan Karn, Wenhui Hu, and Kamel Khalili. Elimination of hiv-1 genomes from human t-lymphoid cells by crispr/cas9 geneediting. *Scientific Reports 2016 6:1*, 6:1–15, 2016. doi: 10.1038/srep22555.

- [86] Stefan H.E. Kaufmann, Anca Dorhoi, Richard S. Hotchkiss, and Ralf Bartenschlager. Host-directed therapies for bacterial and viral infections. *Nature Reviews Drug Discovery*, 17:35–56, 2018. doi: 10.1038/nrd.2017.162.
- [87] Shivakumar Keerthikumar, David Chisanga, Dinuka Ariyaratne, Haidar Al Saffar, Sushma Anand, Kening Zhao, Monisha Samuel, Mohashin Pathan, Markandeya Jois, Naveen Chilamkurti, Lahiru Gangoda, and Suresh Mathivanan. Exocarta: A web-based compendium of exosomal cargo. *Journal of Molecular Biology*, 428:688–692, 2016. doi: 10.1016/j.jmb.2015.09.019.
- [88] Sun Ju Keum, Sung Mi Park, Ji Hoon Park, Jong Ha Jung, Eun Ji Shin, and Sung Key Jang. The specific infectivity of hepatitis c virus changes through its life cycle. *Virology*, 433:462–470, 2012. doi: 10.1016/j.virol.2012.08.046.
- [89] Dae-Kyum Kim, Jaewook Lee, Sae Rom Kim, Dong-Sic Choi, Yae Jin Yoon, Ji Hyun Kim, Gyeongyun Go, Dinh Nhung, Kahye Hong, Su Chul Jang, et al. Evpedia: A community web portal for extracellular vesicles research. *Bioinformatics*, 31:933–939, 2015. doi: 10.1093/bioinformatics/btu741.
- [90] Heon Seok Kim, Kyungjin Lee, Seong-Jun Kim, Sungchan Cho, Hye Jin Shin, Chonsaeng Kim, and Jin-Soo Kim. Arrayed crispr screen with image-based assay reliably uncovers host genes required for coxsackievirus infection. *Genome Research*, 28:859–868, 2018. doi: 10.1101/GR.230250.117.
- [91] Volker Kinast, Agnieszka Plociennikowska, Anggakusuma, Thilo Bracht, Daniel Todt, Richard JP. Brown, Tujana Boldanova, Yudi Zhang, Yannick Brueggemann, Martina Friesland, Michael Engelmann, Gabrielle Vieyres, Ruth Broering, Florian W.R. Vondran, Markus H. Heim, Barbara Sitek, Ralf Bartenschlager, Thomas Pietschmann, and Eike Steinmann. C19orf66 is an interferon-induced inhibitor of hcv replication that restricts formation of the viral replication organelle. *Journal of Hepatology*, 2020. doi: 10.1016/j.jhep.2020.03.047.
- [92] Edda Klipp, Wolfram Liebermeister, Christoph Wierling, Axel Kowald, Hans Lehrach, and Ralf Herwig. *Systems biology: A textbook*. 2016. ISBN 978-3-527-31874.
- [93] A. Knijnenburg and U. Kreischer. A new aspect of the rna bacteriophages translation control mechanism. *BioSystems*, 7:245–249, 1975. doi: 10.1016/0303-2647(75)90031-3.
- [94] Helen M. Lazear, Timothy J. Nice, and Michael S. Diamond. Interferon- $\lambda$ : Immune functions at barrier surfaces and beyond. *Immunity*, 43:15–28, 2015. doi: 10.1016/j.immuni.2015.07.001.
- [95] Ji-Young Lee, Mirko Cortese, Uta Haselmann, Keisuke Tabata, Inés Romero-Brey, Charlotta Funaya, Nicole L. Schieber, Yu Qiang, Marie Bartenschlager, Stephanie Kallis, Christian Ritter, Karl Rohr, Yannick Schwab, Alessia Ruggieri, and Ralf Bartenschlager. Spatiotemporal coupling of the hepatitis c virus replication cycle by creating a lipid droplet- proximal membranous replication compartment. *Cell Reports*, 27:3602–3617.e5, 2019. doi: 10.1016/j.celrep.2019.05.063.
- [96] Jin Ching Lee, Chin Kai Tseng, Yu Hsuan Wu, Neerja Kaushik-Basu, Chun Kuang Lin, Wei Chun Chen, and Huey Nan Wu. Characterization of the activity of 2'-c-methylcytidine against dengue virus replication. *Antiviral Research*, 116:1–9, 2015. doi: 10.1016/j.antiviral.2015.01.002.
- [97] David E. Levy and Adolfo García-Sastre. The virus battles: I $\beta$ n induction of the antiviral state and mechanisms of viral evasion. *Cytokine and Growth Factor Reviews*, 12:143–156, 2001. doi: 10.1016/S1359-6101(00)00027-7.
- [98] Qisheng Li, Abraham L. Brass, Aylwin Ng, Zongyi Hu, Ramnik J. Xavier, T. Jake Liang, and Stephen J. Elledge. A genome-wide genetic screen for host factors required for hepatitis c virus propagation. *Proceedings of the National Academy of Sciences*, 106:16410–16415, 2009. doi: 10.1073/PNAS.0907439106.
- [99] Qisheng Li, Yong-Yuan Zhang, Stephan Chiu, Zongyi Hu, Keng-Hsin Lan, Helen Cha, Catherine Sordroski, Fang Zhang, Ching-Sheng Hsu, Emmanuel Thomas, and T. Jake Liang. Integrative functional genomics of hepatitis c virus infection identifies host dependencies in complete viral replication cycle. *PLOS Pathogens*, 10:e1004163, 2014. doi: 10.1371/JOURNAL.PPAT.1004163.
- [100] Shuo Li. Regulation of ribosomal proteins on viral infection. *Cells*, 8:508, 2019. doi: 10.3390/CELLS8050508.
- [101] Yating Liao, Dan Luo, Kailan Peng, and Yanhua Zeng. Cyclophilin a: a key player for etiological agent infection. *Applied Microbiology and Biotechnology* 2021 105:4, 105:1365–1377, 2021. doi: 10.1007/S00253-021-11115-2.
- [102] Ren-Jye Lin, Han-Pang Yu, Bi-Lan Chang, Wei-Chun Tang, Ching-Len Liao, and Yi-Ling Lin. Distinct antiviral roles for human 2',5'-oligoadenylate synthetase family members against dengue virus infection. *The Journal of Immunology*, 183:8035–8043, 2009. doi: 10.4049/JIMMUNOL.0902728.



- [103] BD Lindenbach and CM Rice. The ins and outs of hepatitis c virus entry and assembly. *Nature reviews. Microbiology*, 11:688–700, 2013. doi: 10.1038/NRMICRO3098.
- [104] Ding Xiang Liu, To Sing Fung, Kelvin Kian-Long Chong, Aditi Shukla, and Rolf Hilgenfeld. Accessory proteins of sars-cov and other coronaviruses. *Antiviral Research*, 109:97–109, 2014. doi: 10.1016/J.ANTIVIRAL.2014.06.013.
- [105] Volker Lohmann and Ralf Bartenschlager. On the history of hepatitis c virus cell culture systems. *Journal of medicinal chemistry*, 57:1627–1642, 2014. doi: 10.1021/JM401401N.
- [106] Andrea Longatti, Bryan Boyd, and Francis V. Chisari. Virion-independent transfer of replication-competent hepatitis c virus rna between permissive cells. *Journal of Virology*, 89:2956–2961, 2014. doi: 10.1128/jvi.02721-14.
- [107] Dina B. Mahmoud, Zayyanu Shitu, and Ahmed Mostafa. Drug repurposing of nitazoxanide: can it be an effective therapy for covid-19? *Journal of Genetic Engineering and Biotechnology* 2020 18:1, 18:1–10, 2020. doi: 10.1186/S43141-020-00055-5.
- [108] Dumrong Mairiang, Huamei Zhang, Ann Sodja, Thilakam Murali, Prapat Suriyaphol, Prida Malasit, Thawornchai Limjindaporn, and Russell L. Finley Jr. Identification of new protein interactions between dengue fever virus and its hosts, human and mosquito. *PLOS ONE*, 8:e53535, 2013. doi: 10.1371/JOURNAL.PONE.0053535.
- [109] Michael P. Manns, Maria Buti, Ed Gane, Jean-Michel Pawlotsky, Homie Razavi, Norah Terrault, and Zobair Younossi. Hepatitis c virus infection. *Nature Reviews Disease Primers*, 3:17006, 2017. doi: 10.1038/nrdp.2017.6.
- [110] Roberto Mateo, Lisa C Lindesmith, Shaily J Garg, Keith Gottlieb, Karen Lin, Sara Said, Juan S Leon, Amy C Sims, David J Weber, Ralph S Baric, Sean N Tucker, and David N Taylor. Production and clinical evaluation of norwalk gi.1 virus lot 001-09nv in norovirus vaccine development. *The Journal of Infectious Diseases*, 2019. doi: 10.1093/infdis/jiz540.
- [111] Finlay McNab, Katrin Mayer-Barber, Alan Sher, Andreas Wack, and Anne O’Garra. Type i interferons in infectious disease. *Nature Reviews Immunology*, 15:87–103, 2015. doi: 10.1038/nri3787.
- [112] Charlotte E. Melia, Christopher J. Peddie, Anja W. M. de Jong, Eric J. Snijder, Lucy M. Collinson, Abraham J. Koster, Hilde M. van der Schaar, Frank J. M. van Kuppeveld, and Montserrat Bárcena. Origins of enterovirus replication organelles established by whole-cell electron microscopy. *mBio*, 10, 2019. doi: 10.1128/mbio.00951-19.
- [113] Ritu Mishra, Sneha Lata, Amjad Ali, and Akhil C. Banerjee. Dengue haemorrhagic fever: a job done via exosomes? *Emerging Microbes and Infections*, 8:1626–1635, 2019. doi: 10.1080/22221751.2019.1685913.
- [114] Naphak Modhiran, Sirsipen Kalayanaroj, and Sukathida Ubol. Subversion of innate defenses by the interplay between dengv and pre-existing enhancing antibodies: Tlr3 signaling collapse. *PLoS Neglected Tropical Diseases*, 4:1–12, 2010. doi: 10.1371/journal.pntd.0000924.
- [115] Susanne Modrow, Dietrich Falke, Uwe Truyen, and Hermann Schätzl. Viruses with single-stranded, positive-sense rna genomes, 2013.
- [116] Jorge L. Muñoz-Jordán and Brenda L. Fredericksen. How flaviviruses activate and suppress the interferon response. *Viruses*, 2:676–691, 2010. doi: 10.3390/v2020676.
- [117] Peter D. Nagy and Judit Pogany. Host factors promoting viral rna replication, 2009.
- [118] Peter D. Nagy and Judit Pogany. The dependence of viral rna replication on co-opted host factors. *Nature Reviews Microbiology*, 10:137–149, 2012. doi: 10.1038/nrmicro2692.
- [119] Peter D. Nagy and Judit Pogany. The dependence of viral rna replication on co-opted host factors. *Nature Reviews Microbiology*, 10:137–149, 2012. doi: 10.1038/nrmicro2692.
- [120] Christopher J. Neufeldt, Mirko Cortese, Eliana G. Acosta, and Ralf Bartenschlager. Rewiring cellular networks by members of the flaviviridae family. *Nature Reviews Microbiology*, 16:125–142, 2018. doi: 10.1038/nrmicro.2017.170.
- [121] Annie Elong Ngonu and Sujana Shrestha. Immune response to dengue and zika. *Annual Review of Immunology*, 36, 2018. doi: 10.1146/annurev-immunol-042617-053142.

- [122] Nguyet Minh Nguyen, Chau Nguyen Bich Tran, Lam Khanh Phung, Kien Thi Hue Duong, Huy Le Anh Huynh, Jeremy Farrar, Quyen Than Ha Nguyen, Hien Tinh Tran, Chau Van Vinh Nguyen, Laura Merson, Long Truong Hoang, Martin L. Hibberd, Pauline P.K. Aw, Andreas Wilm, Niranjan Nagarajan, Dung Thi Nguyen, Mai Phuong Pham, Truong Thanh Nguyen, Hassan Javanbakht, Klaus Klumpp, Janet Hammond, Rosemary Petric, Marcel Wolbers, Chinh Tran Nguyen, and Cameron P. Simmons. A randomized, double-blind placebo controlled trial of balapiravir, a polymerase inhibitor, in adult dengue patients. *Journal of Infectious Diseases*, 207:1442–1450, 2013. doi: 10.1093/infdis/jis470.
- [123] Thi Huyen Tram Nguyen, Jérémie Guedj, Susan L Uprichard, Anita Kohli, Shyam Kottlilil, and Alan S Perelson. The paradox of highly effective sofosbuvir-based combination therapy despite slow viral decline: can we still rely on viral kinetics? *Scientific reports*, 7:10233, 2017. doi: 10.1038/s41598-017-09776-z.
- [124] Centers of Disease Control and Prevention. What is polio?, 2022. URL <https://www.cdc.gov/polio/what-is-polio/index.htm>.
- [125] World Health Organization. Weekly epidemiological record: Polio vaccines: Who position paper – march, 2016. *World Health Organization*, 91:145–168, 2016. doi: 10.5025/hansen.85.157. URL <https://www.who.int/publications/i/item/WHO-WER9112>.
- [126] World Health Organization. Dengue vaccine: Who position paper – july 2016. *Wkly Epidemiol Rec.*, 91:349–64, 2016. URL <https://doi.org/10.1016/j.vaccine.2016.10.070>.
- [127] World Health Organization. *Guidelines for the care and treatment of persons diagnosed with chronic hepatitis C virus infection*. 2018. ISBN 9789241550345. URL <https://apps.who.int/iris/bitstream/handle/10665/273174/9789241550345-eng.pdf?ua=1>.
- [128] World Health Organization. Zika virus, 2018. URL <https://www.who.int/news-room/fact-sheets/detail/zika-virus>.
- [129] World Health Organization. Progress report on access to hepatitis c treatment: focus on overcoming barriers in low- and middle-income countries, march 2018. *Who*, page 49, 2018.
- [130] World Health Organization. Hepatitis c, 2019. URL <https://www.who.int/news-room/fact-sheets/detail/hepatitis-c>.
- [131] World Health Organization. Two out of three wild poliovirus strains eradicated, 2019. URL <https://www.who.int/news-room/feature-stories/detail/two-out-of-three-wild-poliovirus-strains-eradicated>.
- [132] World Health Organization. Who vaccine position papers. WHO, 2022. URL <https://www.who.int/teams/immunization-vaccines-and-biologicals/policies/position-papers>.
- [133] World Health Organization and Global Hepatitis Programme. *Global hepatitis report, 2017*. WHO, 2017. ISBN 9789241565455.
- [134] CO Owino and JJH Chu. Recent advances on the role of host factors during non-poliovirus enteroviral infections. *Journal of biomedical science*, 26, 2019. doi: 10.1186/S12929-019-0540-Y.
- [135] Mohashin Pathan, Pamali Fonseka, Sai V Chitti, Taeyoung Kang, Rahul Sanwani, Jan Van Deun, An Hendrix, and Suresh Mathivanan. Vesiclepedia 2019: A compendium of rna, proteins, lipids and metabolites in extracellular vesicles. *Nucleic Acids Research*, 47, 2019. doi: 10.1093/nar/gky1029.
- [136] Tapas Patra, Ratna Ray, and Ranjit Ray. Strategies to circumvent host innate immune response by hepatitis c virus. *Cells*, 8:274, 2019. doi: 10.3390/cells8030274.
- [137] David Paul and Ralf Bartenschlager. Flaviviridae replication organelles: Oh, what a tangled web we weave. *Annual review of virology*, 2:289–310, 2015. doi: 10.1146/annurev-virology-100114-055007.
- [138] Stefan Peischard, Huyen Tran Ho, Carsten Theiss, Nathalie Strutz-Seebohm, and Guiscard Seebohm. A kidnapping story: How coxsackievirus b3 and its host cell interact. *Cellular Physiology and Biochemistry*, 53:121–140, 2019. doi: 10.33594/000000125.
- [139] Stanley Perlman and Jason Netland. Coronaviruses post-sars: update on replication and pathogenesis. *Nature Reviews Microbiology*, 7:439–450, 2009. doi: 10.1038/nrmicro2147.
- [140] Lucy Pigati, Sree C.S. Yaddanapudi, Ravi Iyengar, Dong Ja Kim, Steven A. Hearn, David Danforth, Michelle L. Hastings, and Dominik M. Duelli. Selective release of microRNA species from normal and malignant mammary epithelial cells. *PLoS ONE*, 5, 2010. doi: 10.1371/journal.pone.0013515.

- [141] Josilene Ramos Pinheiro-Michelsen, Rayane da Silva Oliveira Souza, Itana Vivian Rocha Santana, Patrícia de Souza da Silva, Erick Carvalho Mendez, Wilson Barros Luiz, and Jaime Henrique Amorim. Anti-dengue vaccines: From development to clinical trials. *Frontiers in Immunology*, 11:1252, 2020. doi: 10.3389/fimmu.2020.01252.
- [142] Jie Qing, Yaxin Wang, Yuna Sun, Jiaoyan Huang, Wenzhong Yan, Jinglan Wang, Dan Su, Cheng Ni, Jian Li, Zihao Rao, Lei Liu, and Zhiyong Lou. Cyclophilin a associates with enterovirus-71 virus capsid and plays an essential role in viral infection as an uncoating regulator. *PLOS Pathogens*, 10:e1004422, 2014. doi: 10.1371/JOURNAL.PPAT.1004422.
- [143] Holly R. Ramage, G. Renuka Kumar, Erik Verschueren, Jeffrey R. Johnson, John Von Dollen, Tasha Johnson, Billy Newton, Priya Shah, Julie Horner, Nevan J. Krogan, and Melanie Ott. A combined proteomics/genomics approach links hepatitis c virus infection with nonsense-mediated mrna decay. *Molecular Cell*, 57:329–340, 2015. doi: 10.1016/J.MOLCEL.2014.12.028.
- [144] Jorge Andrés Castillo Ramirez and Silvio Urcuqui-Inchima. Dengue virus control of type i ifn responses: A history of manipulation and control. *Journal of Interferon and Cytokine Research*, 35:421–430, 2015. doi: 10.1089/jir.2014.0129.
- [145] Suchitra Ranjit and Niranjana Kissoon. Dengue hemorrhagic fever and shock syndromes\*. *Pediatric Critical Care Medicine*, 12:90–100, 2011. doi: 10.1097/PCC.0b013e3181e911a7.
- [146] Zarifah Reed and Mary Jane Cardoso. Status of research and development of vaccines for enterovirus 71. *Vaccine*, 34:2967–2970, 2016. doi: 10.1016/j.vaccine.2016.02.077.
- [147] K. N. Reetoo, S. A. Osman, S. J. Illavia, C. L. Cameron-Wilson, J. E. Banatvala, and P. Muir. Quantitative analysis of viral rna kinetics in coxsackievirus b3-induced murine myocarditis: Biphasic pattern of clearance following acute infection, with persistence of residual viral rna throughout and beyond the inflammatory phase of disease. *Journal of General Virology*, 81:2755–2762, 2000. doi: 10.1099/0022-1317-81-11-2755.
- [148] Jean-François Rossignol and Christian Bréchet. A pilot clinical trial of nitazoxanide in the treatment of chronic hepatitis b. *Hepatology Communications*, 3:744, 2019. doi: 10.1002/HEP4.1339.
- [149] Henrik Salje, Derek A.T. Cummings, Isabel Rodriguez-Barraquer, Leah C. Katzelnick, Justin Lessler, Chonticha Klungthong, Buntsaya Thaisomboonsuk, Ananda Nisalak, Alden Weg, Damon Ellison, Louis Macareo, In Kyu Yoon, Richard Jarman, Stephen Thomas, Alan L. Rothman, Timothy Endy, and Simon Cauchemez. Reconstruction of antibody dynamics and infection histories to evaluate dengue risk. *Nature*, 557:719–723, 2018. doi: 10.1038/s41586-018-0157-4.
- [150] Christoph Sarrazin. Treatment failure with daa therapy: Importance of resistance. *Journal of Hepatology*, 74:1472–1482, 2021. doi: 10.1016/J.JHEP.2021.03.004.
- [151] Troels K H Scheel and Charles M Rice. Understanding the hepatitis c virus life cycle paves the way for highly effective therapies. *Nature Medicine*, 19:837–849, 2013. doi: 10.1038/nm.3248.
- [152] William M. Schneider, Meike Dittmann Chevillotte, and Charles M. Rice. Interferon-stimulated genes: A complex web of host defenses. *Annual Review of Immunology*, 32:513–545, 2014. doi: 10.1146/annurev-immunol-032713-120231.
- [153] John W Schoggins and Charles M Rice. Interferon-stimulated genes and their antiviral effector functions. *Current Opinion in Virology*, 1:519–525, 2011. doi: 10.1016/j.coviro.2011.10.008.
- [154] Mohamed Shahren, Zihu Guo, Akhtar Hussain Shar, Reham Ebaid, Qin Tao, Wenjuan Zhang, Ziyin Wu, Yaofei Bai, Yingxue Fu, Chunli Zheng, He Wang, Piar Ali Shar, Jianling Liu, Zhenzhong Wang, Wei Xiao, and Yonghua Wan. Dengue virus causes changes of micrornagenes regulatory network revealing potential targets for antiviral drugs. *BMC Systems Biology*, 12:2, 2018. doi: 10.1186/s12918-017-0518-x.
- [155] Geetika Sharma, Harsha Raheja, and Saumitra Das. Hepatitis c virus: Enslavement of host factors. *IUBMB Life*, 70:41–49, 2018. doi: 10.1002/IUB.1702.
- [156] Kristin L. Shingler, Jennifer L. Yoder, Michael S. Carnegie, Robert E. Ashley, Alexander M. Makhov, James F. Conway, and Susan Hafenstein. The enterovirus 71 a-particle forms a gateway to allow genome release: A cryoem study of picornavirus uncoating. *PLOS Pathogens*, 9(3):1–10, 2013. doi: 10.1371/journal.ppat.1003240.
- [157] Ana Shulla and Glenn Randall. (+) rna virus replication compartments: a safe home for (most) viral replication. *Current Opinion in Microbiology*, 32:82–88, 2016. doi: 10.1016/J.MIB.2016.05.003.

- [158] Jayne Smith-Palmer, Karin Cerri, and William Valentine. Achieving sustained virologic response in hepatitis c: a systematic review of the clinical, economic and quality of life benefits. *BMC Infectious Diseases*, 15:1–19, 2015. doi: 10.1186/S12879-015-0748-8.
- [159] Mohammad Soheilypour and Mohammad R.K. Mofrad. Agent-based modeling in molecular systems biology. *BioEssays*, 40:1800020, 2018. doi: 10.1002/bies.201800020.
- [160] Megan L Stanifer, Kalliopi Pervolaraki, and Steeve Boulant. Molecular sciences differential regulation of type i and type iii interferon signaling. doi: 10.3390/ijms20061445.
- [161] Xiaoqiang Sun and Bin Hu. Mathematical modeling and computational prediction of cancer drug resistance. *Briefings in Bioinformatics*, 19:1382–1399, 2018. doi: 10.1093/bib/bbx065.
- [162] Kiyoshi Takeda and Shizuo Akira. Toll-like receptors. *Current Protocols in Immunology*, 77, 2007. doi: 10.1002/0471142735.im1412s77.
- [163] Robert Thimme, Marco Binder, and Ralf Bartenschlager. Failure of innate and adaptive immune responses in controlling hepatitis c virus infection. *FEMS Microbiology Reviews*, 36:663–683, 2012. doi: 10.1111/j.1574-6976.2011.00319.x.
- [164] Emmanuel Thomas, Marc G Ghany, and T Jake Liang. The application and mechanism of action of ribavirin in therapy of hepatitis c. *Antiviral chemistry and chemotherapy*, 23:1, 2012. doi: 10.3851/IMP2125.
- [165] Silvia Torres, Juan Carlos Hernández, Diana Giraldo, Margarita Arboleda, Mauricio Rojas, Jolanda M. Smit, and Silvio Urcuqui-Inchima. Differential expression of toll-like receptors in dendritic cells of patients with dengue during early and late acute phases of the disease. *PLoS Neglected Tropical Diseases*, 7, 2013. doi: 10.1371/journal.pntd.0002060.
- [166] Nicolas Tremblay, Wesley Freppel, Aïssatou Aïcha Sow, and Laurent Chatel-Chaix. The interplay between dengue virus and the human innate immune system: A game of hide and seek. *Vaccines*, 7:145, 2019. doi: 10.3390/vaccines7040145.
- [167] Mark D. Turner, Belinda Nedjai, Tara Hurst, and Daniel J. Pennington. Cytokines and chemokines: At the crossroads of cell signalling and inflammatory disease. *Biochimica et Biophysica Acta - Molecular Cell Research*, 1843:2563–2582, 2014. doi: 10.1016/j.bbamcr.2014.05.014.
- [168] Sukathida Ubol, Weerawat Phuklia, Siripen Kalayanarooj, and Naphak Modhiran. Mechanisms of immune evasion induced by a complex of dengue virus and preexisting enhancing antibodies. *The Journal of Infectious Diseases*, 201:923–935, 2010. doi: 10.1086/651018.
- [169] John Hopkins University and Medicine. Covid-19 map - johns hopkins coronavirus resource center, 2020. URL <https://coronavirus.jhu.edu/map.html>.
- [170] Naoko Uno and Ted M Ross. Dengue virus and the host innate immune response. *Emerging microbes and infections*, 7:167, 2018. doi: 10.1038/s41426-018-0168-0.
- [171] Susanne G. van der Grein, Kyra A. Y. Defourny, Huib H. Rabouw, Chenna R. Galiveti, Martijn A. Langereis, Marca H. M. Wauben, Ger J. A. Arkesteijn, Frank J. M. van Kuppeveld, and Esther N. M. Nolte-'t Hoen. Picornavirus infection induces temporal release of multiple extracellular vesicle subsets that differ in molecular composition and infectious potential. *PLOS Pathogens*, 15(2):1–22, 2019. doi: 10.1371/journal.ppat.1007594. URL <https://doi.org/10.1371/journal.ppat.1007594>.
- [172] Yoram Vodovotz, Ashley Xia, Elizabeth L. Read, Josep Bassaganya-Riera, David A. Hafler, Eduardo Sontag, Jin Wang, John S. Tsang, Judy D. Day, Steven H. Kleinstein, Atul J. Butte, Matthew C. Altman, Ross Hammond, and Stuart C. Sealfon. Solving immunology? *Trends in Immunology*, 38:116–127, 2017. doi: 10.1016/J.IT.2016.11.006.
- [173] Ashish Vora, Wenshuo Zhou, Berlin Londono-Renteria, Michael Woodson, Michael B. Sherman, Tonya M. Colpitts, Girish Neelakanta, and Hameeda Sultana. Arthropod evs mediate dengue virus transmission through interaction with a tetraspanin domain containing glycoprotein tsp29fb. *Proceedings of the National Academy of Sciences of the United States of America*, 115:E6604–E6613, 2018. doi: 10.1073/pnas.1720125115.
- [174] Supaporn Wacharapluesadee, Chee Wah Tan, Patarapol Maneeorn, Prateep Duengkae, Feng Zhu, Yutthana Joyjinda, Thongchai Kaewpom, Wan Ni Chia, Weenassarin Ampoot, Beng Lee Lim, Kanthita Worachotsueptrakun, Vivian Chih Wei Chen, Nutthinee Sirichan, Chanida Ruchisrisarod, Apaporn Rodpan, Kirana Noradechanon, Thanawadee Phaichana, Niran Jantararat, Boonchu Thongnumchaima, Changchun Tu, Gary Cramer, Martha M. Stokes, Thiravat Hemachudha, and Lin Fa Wang. Evidence for sars-cov-2 related coronaviruses circulating in bats and pangolins in southeast asia. *Nature Communications*, 12:1–9, 2021. doi: 10.1038/s41467-021-21240-1.

- [175] S. N. Waggoner, C. H. T. Hall, and Y. S. Hahn. Hcv core protein interaction with gc1q receptor inhibits th1 differentiation of cd4+ t cells via suppression of dendritic cell il-12 production. *Journal of Leukocyte Biology*, 82:1407–1419, 2007. doi: 10.1189/jlb.0507268.
- [176] Gary Walsh and Gary Walsh. Interferons, interleukins and tumour necrosis factors, 6 2015.
- [177] Chen Wang, Peter W Horby, Frederick G Hayden, and George F Gao. A novel coronavirus outbreak of global health concern. 2020. doi: 10.1016/S0140-6736(20)30154-9.
- [178] Kezhen Wang, Chunling Zou, Xiujuan Wang, Chenxiao Huang, Tingting Feng, Wen Pan, Qihan Wu, Penghua Wang, and Jianfeng Dai. Interferon-stimulated trim69 interrupts dengue virus replication by ubiquitinating viral nonstructural protein 3. *PLoS Pathogens*, 14, 2018. doi: 10.1371/JOURNAL.PPAT.1007287.
- [179] Peter J Wangersky. Lotka-volterra population models. *Annual Review of Ecology and Systematics*, 9: 189–218, 1978.
- [180] Stephen S. Whitehead, Joseph E. Blaney, Anna P. Durbin, and Brian R. Murphy. Prospects for a dengue virus vaccine. *Nature Reviews Microbiology*, 5:518–528, 2007. doi: 10.1038/nrmicro1690.
- [181] Annelies Wilder-Smith. Dengue vaccine development: status and future. *Bundesgesundheitsblatt - Gesundheitsforschung - Gesundheitsschutz*, 63:40–44, 2020. doi: 10.1007/s00103-019-03060-3.
- [182] Annelies Wilder-Smith, Eng Eong Ooi, Olaf Horstick, and Bridget Wills. Dengue. *The Lancet*, 393: 350–363, 2019. doi: 10.1016/S0140-6736(18)32560-1.
- [183] Georg Wolff, Charlotte E. Melia, Eric J. Snijder, and Montserrat Bárcena. Double-membrane vesicles as platforms for viral replication. *Trends in Microbiology*, 28:1022–1033, 2020. doi: 10.1016/j.tim.2020.05.009.
- [184] Mun Teng Wong and Steve S.L. Chen. Emerging roles of interferon-stimulated genes in the innate immune response to hepatitis c virus infection. *Cellular and Molecular Immunology*, 13:11–35, 2016. doi: 10.1038/cmi.2014.127.
- [185] Florian Wrensch, Emilie Crouchet, Gaetan Ligat, Mirjam B. Zeisel, Zhen-Yong Keck, Steven K. H. Fong, Catherine Schuster, and Thomas F. Baumert. Hepatitis c virus (hcv)–apolipoprotein interactions and immune evasion and their impact on hcv vaccine design. *Frontiers in Immunology*, 9, 2018. doi: 10.3389/FIMMU.2018.01436.
- [186] Wenchao Zhang, Xiaofeng Jiang, Jinghui Bao, Yi Wang, Huixing Liu, and Lijun Tang. Exosomes in pathogen infections: A bridge to deliver molecules and link functions. *Front Immunol*, 9:90, 2018. doi: 10.3389/fimmu.2018.00090.
- [187] Li-Ya Zhou and Lei-Liang Zhang. Host restriction factors for hepatitis c virus. *World Journal of Gastroenterology*, 22:1477, 2016. doi: 10.3748/WJG.V22.I4.1477.
- [188] Carolin Zitzmann and Lars Kaderali. Mathematical analysis of viral replication dynamics and antiviral treatment strategies: From basic models to age-based multi-scale modeling. *Front Microbiol*, 9:1546, 2018. doi: 10.3389/fmicb.2018.01546.
- [189] Carolin Zitzmann, Lars Kaderali, and Alan S. Perelson. Mathematical modeling of hepatitis c rna replication, exosome secretion and virus release. *PLoS Computational Biology*, 16:e1008421, 2020. doi: 10.1371/journal.pcbi.1008421.
- [190] Carolin Zitzmann, Bianca Schmid, Alessia Ruggieri, Alan S. Perelson, Marco Binder, Ralf Bartenschlager, and Lars Kaderali. A coupled mathematical model of the intracellular replication of dengue virus and the host cell immune response to infection. *Frontiers in Microbiology*, 11:725, 2020. doi: 10.3389/fmicb.2020.00725.
- [191] Carolin Zitzmann, Christopher Dächert, Bianca Schmid, Hilde van der Schaar, Martijn van Hemert, Alan S Perelson, Frank J M van Kuppeveld, Ralf Bartenschlager, Marco Binder, and Lars Kaderali. Mathematical modeling of plus-strand rna virus replication to identify broad-spectrum antiviral treatment strategies. *PLOS Computational Biology*, 19:e1010423, 4 2023. doi: 10.1371/JOURNAL.PCBI.1010423.
- [192] Diego Alejandro Álvarez Díaz, Aimer Alonso Gutiérrez-Díaz, Elizabeth Orozco-García, Andrés Puerta-González, Clara Isabel Bermúdez-Santana, and Juan Carlos Gallego-Gómez. Dengue virus potentially promotes migratory responses on endothelial cells by enhancing pro-migratory soluble factors and mirnas. *Virus Research*, 259:68–76, 2019. doi: 10.1016/j.virusres.2018.10.018.